Exploring the Role of Pellino Proteins in Cells of the Adaptive Immune System

A thesis submitted to Maynooth University for the degree of Doctor of Philosophy

By

Sze Ying Tan, MPharm, M.Sc

Maynooth University
National University of Ireland Maynooth

Kathleen Lonsdale Institute for Human Health Research

November 2024

Supervisor: Professor Paul Moynagh

Head of Department: Professor Paul Moynagh

Declaration

This thesis has not been previously submitted to this or any other university for examination for a higher degree. The work presented here is entirely my own except where otherwise acknowledged. This thesis may be available for consultation within the university library. It may be copied or lent to other libraries for purposes of consultation.

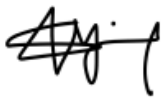

SZE YING TAN

Contents

Acknowledgements

Paul, I would like to thank you for the opportunity to work in your lab on a very meaningful project. Thank you for supporting my applications for John & Pat Hume Scholarship and Irish Research Council Postgraduate Scholarship, which funded my PhD. I appreciate all your guidance which has helped to direct my research project and consolidate my career development. Your generosity in sharing your knowledge, patience, and kindness created a very conducive learning environment for me to grow to become an independent researcher. It is a great honour to work with you and thank you for being a wonderful supervisor.

I would also like to thank everyone in the Molecular Immunology lab for welcoming me and making my 4-year PhD a very enjoyable time. Nezira, thank you for your genuine support and assistance from the smallest to the biggest thing in the lab. Ewa, thank you for co-supervising and teaching me when I first started my PhD. Your training forms a cornerstone of my PhD. Linan and Lu, thank you for your patience in answering all my questions and offering your valuable insight into my project. Aoife, thank you for your advice on both technical matters and personal development along my career path. Devlin, thank you for being a great senior and badminton partner. Wang and Jian, thank you for sharing your knowledge in research design. I really appreciate the entertaining chats and friendship that we have developed over these years. I hope we will continue to support each other in the future.

Andy, thank you for your willingness to recruit patient samples and share resources for my experiments. To my assessor Eoin, and advisor Emmanuelle, thank you for your guidance and encouragement during annual progress meetings. I want to especially thank the staff in Bioresource Unit – Deirdre, Gillian, and Dylan, you are very professional and helpful. It has always been a great pleasure working with all of you. To Ronan, Nidhi, and Fearon, many thanks for sharing your research experience with me and teaching me how to analyse and interpret some results.

To my PhD peers from the Department of Biology – Conor, Andrea, Ardena, Hazel, Laura, Ciara, Caoimhe, Catherine, Marwa, Maria, Marie, Aaron, Stephen, thank you for your help and mental support along the way. I would also like to thank my friends – Hui Han, Tracy, Joana, Ziba, Azeema, Muditha, Aparna, Kamal, Chloe for being lovely companions during my PhD journey. I enjoyed all our lunch time, coffee time, outings, and home meetings together. I will cherish the fond memories created with you inside and outside of Maynooth University.

To my beloved mom, thank you for your unwavering love and support. You have never failed to care for me despite the long distance and different time zone. To my beloved dad, thank you for everything. You live in my heart and I miss you dearly. My brother Darren, thank you for taking care of mom while I am away from home and managing things so well. Lastly, I want to specially thank my amazing husband, Mukgesh for joining me in Ireland to support me in every way he could. I know it is a big decision and all the struggles you face to start a new life with me here. I could not ask for a better husband! I love you to bits.

Glory be to God.

Abbreviations

AP-1	Activator protein-1
APCs	Antigen presenting cells
ASC	Apoptosis-associated speck-like protein containing a caspase activation and recruitment domain
ATP	Adenosine triphosphate
BATF	Basic leucine zipper ATF-like transcription factor
Bcl	B-cell lymphoma
BCR	B cell receptor
BMDC	Bone marrow derived dendritic cell
BMDM	Bone marrow-derived macrophage
BSA	Bovine serum albumin
Cbl	Casitas B cell lymphoma
CD	Cluster of differentiation
cDNA	Complementary deoxyribonucleic acid
CFSE	Carboxyfluorescein succinimidyl ester
CIA	Collagen-induced arthritis
CMC	Chronic mucocutaneous candidiasis
CpG	Cytosine-phosphate-guanine
CTL	Cytotoxic T lymphocyte
CTLA	Cytotoxic T lymphocyte-associated antigen
CXCL	Chemokine (C-X-C motif) ligand
CXCR	C-X-C motif receptor
c-IAP	Cellular inhibitor of apoptosis
DAMP	Danger associated molecular pattern
DCs	Dendritic cells
DISC	Death-inducing signalling complex
DN	Double negative
DP	Double positive
ds	Double stranded
EAE	Experimental autoimmune encephalomyelitis

EBV	Epstein-Barr gamma herpes virus
EDTA	Ethylenediaminetetraacetic acid
ELISA	Enzyme-linked immunosorbent assay
ERK	Extracellular signal-regulated kinase
Elk-1	Ets-like protein-1
EtOH	Ethanol
Ets-1	V-ets erythroblastosis virus E26 oncogene homolog 1
FACS	Fluorescence-activated cell sorting
FBS	Fetal bovine serum
FGF	Fibroblast growth factor
FHA	Forkhead-associated
FO	Follicular
FOXP	Forkhead transcription factor
FSC-A	Forward scatter area
FSC-H	Forward scatter height
GATA3	GATA-binding protein
GC	Germinal centre
G-CSF	Granulocyte colony-stimulating factor
GM-CSF	Granulocyte-macrophage colony-stimulating factor
H	Hour
Hp	*Helicobacter pylori*
HRP	Horseradish peroxidase
HSV	Herpes simplex virus
HVS13	Herpesvirus saimiri gene 13
IC	Intracellular
ICOS	Inducible T-cell costimulatory
IBD	Irritable bowel disease
IFN	Interferon
Ig	Immunoglobulin
IgH	Ig heavy chain
IKK	IκB kinase
IL	Interleukin
IL-17R	IL-17 receptor
IRAK	IL-1R associated kinase

IRF	Interferon regulatory factor
IκB-α	Inhibitor kappa B alpha
Jak	Janus kinase
JNK	c-Jun N-terminal kinases
KC	Keratinocytes-derived chemokine
kb	Kilobase
KLF	Kruppel-like factor
LCMV	Lymphocytic choriomeningitis virus
LDL	Low density lipoprotein
LPS	Lipopolysaccharides
Lys	Lysine
MACS	Magnetic activated cell sorting
Mal	MyD88-adapter-like
MAPK	Mitogen-activated protein kinase
MEF	Mouse embryonic fibroblast
MEM	Minimum essential medium
MHC	Major histocompatibility complex
MIP	Macrophage inflammatory protein
mRNA	Messenger ribonucleic acid
mTOR	Mammalian target of rapamycin
MZ	Marginal zone
MyD88	Myeloid differentiation primary response gene 88
NEMO	NF-κB essential modulator
NFAT	Nuclear factor of activated T cells
NF-κB	Nuclear factor kappa B
NIK	NF-κB inducing kinase
NK cell	Natural killer cell
NLRP	Nucleotide-binding domain, leucine-rich-containing family, pyrin domain-containing
NOD	Nucleotide-binding and oligomerization domain
OD	Optical density
Pam_2CSK4	Pam2CysSerLys4
Pam_3CSK4	Pam3CysSerLys4
PAMPs	Pathogen-associated molecular patterns

PBMC	Peripheral blood mononuclear cell
PBS	Phosphate-buffered saline
PD-1	Programmed cell death-1
Pgp	P-glycoprotein
PLN	Peripheral lymph node
PPARγ	Peroxisome proliferator-activated receptor γ
Pro-B	Progenitor B
PRRs	Pattern-recognition receptors
RBC	Red blood cell
RIG	Retinoic acid-inducible gene
RIP	Receptor interacting protein
ROCK	Rho-associated, coiled-coil-containing protein kinase
Rorc	RAR-related orphan receptor C
RORγt	Retinoic acid receptor-related orphan receptor gamma-T
RPMI	Roswell Park Memorial Institute
RT	Room temperature
RT-PCR	Reverse transcription polymerase chain reaction
Runx1	Runt-related transcription factor 1
SD	Standard deviation
SDS-PAGE	Sodium dodecyl sulfate - polyacrylamide gel electrophoresis
SEF	Similar expression to fibroblast growth factor genes
SEFIR	SEF and IL17R
SEM	Standard error of the mean
shRNA	Short hairpin ribonucleic acid
SHP2	Src homology 2 domain-containing tyrosine phosphatase
siRNA	small interfering ribonucleic acid
SLE	Systemic lupus erythematosus
SOCS3	Suppressor of cytokine signalling 3
SMAD	Sma- and Mad-related protein
SMD	Small molecule drug
SSC-A	Side scatter area
STAT	Signal transducer and activator of transcription
T-bet	T-box expressed in T cells
TAE	Tris-Acetate-EDTA

Tact	Activated T cell
TAB	TAK1-binding protein
TAK	Transforming growth factor β-activated kinase
TBK	TANK-binding kinase
TBS	Tris buffered saline
Tcm	Central memory $CD8^+$ T cell
TCR	T cell receptor
TD	T-dependent
Tem	Effector memory T cell
TEMED	Tetramethylethylenediamine
Tfh	T follicular helper
TGF-β	Transforming growth factor beta
Th	T helper
TI	T-independent
TIR	Toll/IL-1R
TLR	Toll like receptor
TMB	3,3',5,5'-tetramethylbenzidine
TNF	Tumour necrosis factor
TRAF	TNF receptor associated factor
TRAM	TRIF-related adaptor molecule
TRIF	TIR-domain-containing adapter-inducing interferon-β
Treg	Regulatory T cell
WT	Wild type
µg	Microgram
µl	Microlitre
µM	Micromolar

Abstract

The innate and adaptive immune systems intertwine in mounting an effective immune response against invading pathogens. The activation of innate immune components is often a prerequisite for the initiation of the adaptive immune response. The Pellino family consists of a 3-membered family of E3 ubiquitin ligases (Pellino 1, Pellino 2, and Pellino 3) that play important roles in immunity by catalysing post-translational modification of important signalling molecules. Pellino proteins have been widely studied for their roles in innate immunity. Nevertheless, emerging reports have highlighted the potential of Pellino proteins in regulating adaptive immune system. This thesis aims to further the knowledge in this area by performing the first systematic characterisation of the role of Pellino proteins in generating adaptive immune cell populations. To this end novel genetic models were generated resulting in mice that lack individual and combination of the Pellino family. Such models allowed for the first time to investigate potential functional interactions between the Pellino family members. While Pellino 3 does not mediate the production of various T and B cell subsets, Pellino 2 has a role in CD4 and CD8 T cell activation that is dependent on age. Importantly, the findings also highlight a selective role for Pellino 1 in negatively regulating the generation of activated CD4 and CD8 T cells, as well as germinal centre B cells and plasma cells in both young (10-12 weeks old) and aged (6 months old) mice. Interestingly, Pellino 1 and Pellino 2 exhibit distinctive functional roles in mediating CD8 T cell activation as individual deficiency of Pellino 1 and Pellino 2 favours its differentiation into $CD8^+$ effector memory (Tem) and central memory (Tcm) cells, respectively. This suggests that they might have different physiological roles in controlling cytotoxic functions of Tem cells or systemic infections through Tcm cells. It was also found that Pellino 1 negatively modulates IL-17 production in Th17 cells. The mechanistic basis to the role of Pellino 1 in controlling T cell activation and IL-17 production is also explored. The studies conclude that this regulatory function of Pellino 1 is intrinsic to T cells and not antigen presenting cells. Overall, this body of work provides novel insight into the role of Pellino proteins, particularly Pellino 1, in the adaptive immune system. It also forms a foundation for future research to elucidate the physiological role of Pellino 1 in Th17 cell differentiation and may represent a new pathway that may be open to therapeutic exploitation in the treatment of inflammatory diseases.

Chapter 1:
Introduction

1.1 The immune system

The immune system is a defence system that deploys intricate protective mechanisms against a wide array of pathogenic infections that challenge the host. The pool of immune cells that constitutes the immune system eliminates deleterious microbes via distinctive yet specific effector functions. Immune cells can be broadly grouped into two arms of the immune system, which are innate and adaptive immunity. Innate immune cells include granulocytes, monocytes, macrophages, dendritic cells, and natural killer (NK) cells; adaptive immune cells generally encompass T lymphocytes (also named T cells) and B lymphocytes (B cells).

Traditionally, innate and adaptive immunity have been distinguished based on several attributes. The first difference between these two arms of the immune systems is the degree of specificity to antigens. Innate immune responses are directed by germline-encoded, non-rearranging pattern-recognition receptors (PRRs), which sense pathogen-associated molecular patterns (PAMPs) that are shared by many pathogens (Kurtz, 2005). This leads to non-specific immune reactions. Unlike innate immunity, adaptive immune system exerts specificity in antigen recognition due to somatic rearrangement of gene elements encoding the highly diverse antigen receptors – T cell receptor (TCR) and immunoglobulin (Ig) (Lanier & Sun, 2009).

The second feature that differentiates innate and adaptive immunity is the speed of the response. Because PRRs are widely expressed on numerous cells, targeting a broad range of invading pathogens, the innate immunity is programmed to initiate rapid response and hence acts as the first line defence system (Chaplin, 2010). In contrary, the adaptive response occurs during the late stages of an immune response as it can take up to a week for naïve T cells and B cells to go through activation, differentiation, and clonal expansion to gain lymphocyte effector function (Bedoui *et al.*, 2016).

The generation of immunological memory is a key feature of adaptive immunity. Long-lived, antigen-specific adaptive immune cells generated following the initial encounter with an antigen, such as memory $CD8^+$ T cells, can provide quicker and

more robust immune response when they are re-challenged with the same antigen (Lertmemongkolchai *et al.*, 2001). Conversely, innate immune cells, such as neutrophils have a short lifespan of a few hours or days, restricting their ability to manifest immune memory (Lanier & Sun, 2009).

Taken together, immune cells have always been categorised based on the features of the two separate immune systems. Although NK cells are defined as lymphocytes, the lack of antigen-specific cell surface receptors leads them to be categorised as components of innate immunity. However, this remains debatable as NK cell memory has been unveiled in some studies (Vivier *et al.*, 2011). Emerging evidence has shown that the innate and adaptive immune cells display overlapping characteristics, leaving such classification in question (Lanier & Sun, 2009). Whether this branching system is ambiguous, it is more vital to learn more about the individual roles and interactions between these immune cells for better disease management and the development of novel therapeutic solutions.

1.2 The adaptive immune system

The adaptive immune system is a specialised system that orchestrates immune responses and maintains stability of immunity over a lifetime. Using chicken as a model, two lymphocyte lineages were first unearthed from thymus and avian bursa of Fabricius in 1965 (Cooper *et al.*, 1965). In addition, antibody-secreting cells were also derived from bone marrow, which coined the term B (for bursa or bone marrow origin) lymphocytes (Ivanyi *et al.*, 1972); similar nomenclature was adopted for T (for thymus origin) lymphocytes. T cells and B cells are two major components of the adaptive immune system that account for a specific immune response.

1.2.1 T cell development and its subsets

T cell development takes place in the thymus. Lymphoid progenitors that originate in the bone marrow migrate to the thymus via the blood. Here, the early T cells do not express TCR and are called double negative (DN; $CD3^-4^-8^-$) thymocytes based on the absence of expression of cluster of differentiation (CD) 4 or CD8. They develop into two mature T cell lineages – the main T cell population that expresses αβ TCR or the minor T cell population that expresses γδ TCR (Zhao *et al.*, 2018). Unlike γδ T cells, αβ T cells give rise to $CD4^+$ and $CD8^+$ immature thymocytes via a differentiation pathway. In the mouse thymic cortex, this differentiation occurs based on DN thymocytes' surface expression of CD44 and CD25 shows the following sequence of surface marker changes: $CD44^+CD25^-$ (DN1), $CD44^+CD25^+$ (DN2), $CD44^-CD25^+$ (DN3), and $CD44^-CD25^-$ (DN4) (Godfrey *et al.*, 1993). Following the transition from DN2 to DN4, these cells undergo TCR rearrangement to generate a αβ TCR (Godfrey *et al.*, 1993). This leads to the generation of small double positive (DP) thymocytes that co-express both $CD4^+$ and $CD8^+$.

Cortical thymic epithelial cells bear MHC molecules that present self-peptide to bind with αβ TCR on DP thymocytes. If the interaction is too weak to induce a viability signal, DP thymocytes experience death by neglect (Germain, 2002). The appropriate level of signalling is required for positive selection of DP thymocytes that will go through maturation to yield single positive $CD4^+$ or $CD8^+$ immature thymocytes. When DP thymocytes enter the medulla, they undergo negative selection where cells that interact strongly with the major histocompatibility complex (MHC)-self peptides complexes are eliminated via acute apoptosis (Germain, 2002). These cells are now ready to be distributed to peripheral lymphoid sites from the medulla.

Three theories have been proposed to explain the basis to single positive $CD4^+$ and $CD8^+$ lineage commitment. The first theory, known as the instruction model, implies that engagement between TCR and MHC ligands dictate the fate of DP thymocytes. $CD4^+CD8^+$ thymocytes which express TCR that binds to MHC class I results in $CD8^+$ expression, whereas interaction with MHC class II results in $CD4^+$ expression (Borgulya *et al.*, 1991). In contrast, the selection/stochastic model outlines a random

lineage occurrence followed by an appropriate pairing of TCR/MHC to achieve cell survival and maturation (Davis *et al.*, 1993). The third possible explanation for the mechanism of lineage commitment is the asymmetric model. This model suggests that CD8 commitment depends on MHC class I instructional signal, whereas CD4 lineage may be a default commitment independent of MHC signals (Suzuki *et al.*, 1995).

Naïve T cells can be distinguished from memory T cells based on their surface marker expression of different adhesion receptors. Two major T cell activation/memory markers that define subsets of $CD4^+$ and $CD8^+$ T cells in mice are CD62L (L-selectin; MEL-14; Leu-8) and CD44 (H-CAM; Pgp-1) (Mackay *et al.*, 1990; Gerberick *et al.*, 1997).

CD62L is the unique peripheral lymph node (PLN) homing receptor that regulates recirculation of naïve $CD4^+$ T cells to PLN (Bradley *et al.*, 1994). CD62L is also known as MEL-14 in mice (Gallatin *et al.*, 1983) and Leu-8 in humans (Berg & James, 1990). Memory $CD4^+$ T cells from murine spleen lack MEL-14 (Bradley *et al.*, 1992). Interestingly, CD62L expression can be influenced by microenvironmental conditions within PLN such that in-vitro cytokine stimulation of naïve $CD4^+$ T cells with interleukin-2 (IL-2) decreases CD62L expression, whereas stimulation with IL-6 and notably transforming growth factor beta 1 (TGF-β1) increases CD62L expression (Picker *et al.*, 1993).

CD44, also identified as P-glycoprotein 1 (Pgp-1)/Ly-24 in mice, is crucial for the generation of lymphoid progenitors within bone marrow (Miyake *et al.*, 1990). Uncommitted DN thymocytes in the thymus possess low CD44 expression, which is then lost for the initiation of TCRβ rearrangement, elevation of T-cell specific genes expression, and T cell development (Canté-Barrett *et al.*, 2017). Mature T cells regain CD44 expression. Furthermore, CD44 surface expression on $CD4^+$ and $CD8^+$ T cells is upregulated after antigenic encounter (Budd *et al.*, 1987; Butterfield *et al.*, 1989), revealing the function of CD44 as a marker for memory T cells.

The distinct expression of CD62L and CD44 in naïve and memory T cells suggests that they are likely to demonstrate distinct recirculation patterns to PLN. While naïve T cells migrate from blood to PLN via high endothelial venules, memory T cells travel from blood to peripheral tissues to PLN via afferent lymph (Mackay *et al.*, 1990). Collectively, naïve T cells are characterised by a $CD62L^{high}CD44^{low}$ expression, whereas effector memory T cells (Tem) are identified by a $CD62L^{low}CD44^{high}$ phenotype (Gerberick *et al.*, 1997). There is an additional subset of $CD8^+$ T cells – central memory $CD8^+$ T cells (Tcm), which exhibits a $CD62L^{high}CD44^{high}$ phenotype (Nakajima *et al.*, 2021). Tem cells move freely between secondary lymphoid organs and tissues to render immune surveillance and immediate effector functions, whereas Tcm cells are home to secondary lymphoid organs (Laidlaw *et al.*, 2016).

1.2.2 T cell activation and differentiation

Following T cell development in the thymus, naïve single positive T cells exit the thymus and enter secondary lymphoid organs, such as the lymph nodes and the spleen, where they encounter foreign antigens presented by MHC molecules of antigen-presenting cells (APCs), such as dendritic cells, macrophages, and B cells (Sallusto *et al.*, 2004). The interaction of antigenic peptide and TCR is the initial step to activate naïve T cells for optimal T cell responsiveness (Hochweller *et al.*, 2010). The TCR complex consists of two TCR chains in heterodimeric form (the typical TCRα/TCRβ or the small fraction of TCRγ/TCRδ) bonded with six CD3 chains (Shah *et al.*, 2021). Adjacent to the TCR complex are the CD4 or CD8 molecules expressed on the surface of T cells, acting as co-receptors to facilitate T cell development by engaging different classes of MHC molecules (Tikhonova *et al.*, 2012). Besides that, a co-stimulatory signal that involves the binding of CD28 on T cells with CD80 (B7-1) or CD86 (B7-2) on APCs is required to promote T cell proliferation and differentiation (Luckheeram *et al.*, 2012; Xia *et al.*, 2018). The co-stimulatory engagement is also vital to avoid cell death or anergy, a hyporesponsive state of T cells towards IL-2 restimulation, caused by weak TCR signals (Shah *et al.*,

2021). Collectively, two signals resulting from the bindings of TCR/peptide and CD28/CD80/86 are necessary for productive T cell activation.

Following the initial step of T cell activation, naïve $CD4^+$ T cells and naïve $CD8^+$ T cells undergo differentiation into effector cells with various functions. Effector $CD8^+$ T cells, also known as cytotoxic T lymphocytes (CTL), are responsible for clearing viral infections, such as Epstein-Barr gamma herpes virus (EBV), herpes simplex virus (HSV), lymphocytic choriomeningitis virus (LCMV), *Listeria*, and influenza (Zhang & Bevan, 2011). In addition, activated $CD8^+$ T cells also help to limit lung tissue injury by releasing immunosuppressive cytokine IL-10 (Palmer *et al.*, 2010).

On the other hand, lineage decision of activated $CD4^+$ T cells into distinct T helper cell subsets is mediated by cytokine polarisation (Figure 1.1). Five main T helper populations have been identified in chronological order: T helper 1 (Th1), T helper 2 (Th2), regulatory T cell (Treg), T helper 17 (Th17), and T follicular helper (Tfh) (Saravia *et al.*, 2019).

Th1 cell differentiation is driven by IL-12 and interferon (IFN)-γ (Shirota *et al.*, 2004). T-box expressed in T cells (T-bet) has been identified as the master transcription factor that dramatically upregulates IFN-γ production and IL-12Rβ2 expression (Lugo-Villarino *et al.*, 2003, Afkarian *et al.*, 2002). IFN-γ activates signal transducer and activator of transcription (STAT) 1, which increases T-bet expression and thus enhances IFN-γ generation (Afkarian *et al.*, 2002, Lighvani *et al.*, 2001). IL-12-induced STAT4 has also been demonstrated to act in a similar positive feedback loop that increases IFN-γ production and IL-12Rβ2 expression by elevation of IFN-γ secretion (Luckheeram *et al.*, 2012). In addition, T-bet also inhibits Th2 and Th17 lineage by interfering the function of the Th2 principal regulator, GATA-binding protein (GATA) 3 and forming linkage with Th17-committed RAR-related orphan receptor C (Rorc) promoter, respectively (Hwang *et al.*, 2005; Lazarevic *et al.*, 2011). Th1 cells generate effector cytokines IFN-γ and tumour necrosis factor (TNF) that are critical for intracellular antiviral and antibacterial responses (Saravia *et al.*, 2019; Laidlaw *et al.*, 2016; Du *et al.*, 2010).

Th2 lineage differentiation is initiated by IL-4, which is an inducer of STAT6, leading to the expression of the Th2 master transcription factor GATA3 (Zhu *et al.*, 2001). GATA3 is capable of suppressing Th1 development by diminishing STAT4 (Usui *et al.*, 2003). This is further supported by the finding that naïve CD4 T cells differentiate into Th1 cells, instead of Th2, in mice lacking GATA3 (Zhu *et al.*, 2004). It is reported that STAT3 and STAT5 play a role in assisting Th2 development. While STAT6 requires STAT3 coordination to engage with Th2 cell-related gene loci in the differentiation process (Stritesky *et al.*, 2011), GATA3 cooperates with STAT5 for complete differentiation of Th2 cells via interaction with different IL-4 loci (Zhu *et al.*, 2003). Interestingly, it has also been shown that STAT5 signalling can result in Th2 cell differentiation in the absence of IL-4 (Zhu *et al.*, 2006). Th2 cells produce cytokines IL-4, IL-5, and IL-13 that exert potent immunity against extracellular parasites, such as helminth infections (Saravia *et al.*, 2019).

Approximately a decade after the discovery of Th1 and Th2, Treg cells were designated with an immunosuppressive phenotype (Saravia *et al.*, 2019). The master regulators for Treg cells are IL-2 and TGF-β. TGF-β contributes to forkhead transcription factor (FOXP) 3 induction upon TCR engagement (Chen *et al.*, 2003). Activation of Sma- and Mad-related protein (Smad) 2 and Smad3 downstream to TGF-β signalling is also found to promote Treg cell differentiation by amplifying FOXP3 expression (Takimoto *et al.*, 2010). Furthermore, Smad3 suppresses Th17 differentiation by hindering transcription of the Th17-lineage principal regulator, retinoic acid receptor-related orphan receptor gamma-T (RORγt) (Martinez *et al.*, 2009). On the other hand, IL-2 signalling activates STAT5, which antagonises STAT3 function to bind to the IL-17 locus, resulting in a Treg lineage commitment that is favoured over Th17 cell development (Laurence *et al.*, 2007). Treg cells are defined by the expression of their signature cytokine IL-10 that is crucial for anti-inflammatory and prevention of autoimmune development (Luckheeram *et al.*, 2012). Treg cells have also been shown to control tissue damage by restraining host antiviral response in both chronic and acute viral infection (Swain *et al.*, 2012).

About two decades later, Th17 cells are identified partially from early research on the functions of IL-12 and IL-23 (Saravia *et al.*, 2019). Polarising cytokines for Th17 differentiation include IL-6, IL-21, IL-23, and TGF-β (Luckheeram *et al.*, 2012). The

principal transcription factor of Th17 differentiation is RORγt. Further details of Th17 cell differentiation are outlined in section 1.4. Signature effector cytokines of Th17 cells are IL-17A, IL-17F, and IL-22 (Saravia *et al.*, 2019). Th17 cells, though often associated with autoimmunity, are immunologically important against fungal and bacterial infections (Patel & Kuchroo, 2015).

Tfh cells are identified by the expression of C-X-C motif receptor-5 (CXCR5) and coexpression of programmed cell death-1 (PD-1) and/or inducible T-cell costimulator (ICOS), a member of CD28 family (Haynes *et al.*, 2007; Nurieva *et al.*, 2008). Situated in follicular regions of lymphoid tissue, Tfh cells are responsible for regulation of B-cell immunity (Breitfeld *et al.*, 2000). IL-6 and IL-21 have been elucidated to be the major cytokines participating in Tfh cell differentiation (Nurieva *et al.*, 2008). In contrast to Th17 cell development, Tfh cell differentiation *in vitro* is induced by IL-21 independent of TGF-β (Nurieva *et al.*, 2008). IL-6 and IL-21 signalling lead to the activation of B-cell lymphoma (Bcl)-6, the master transcription factor of Tfh cell, which drives Tfh differentiation and suppresses the development of other Th cell lineages (Nurieva *et al.*, 2009). Following Tfh cell differentiation, Tfh cells play an important role in driving B cell differentiation into Ig-secreting cells by IL-21 production (Bryant *et al.*, 2007) and assisting Ig class switching to define the antibody repertoire by IL-4 production (Reinhardt *et al.*, 2009).

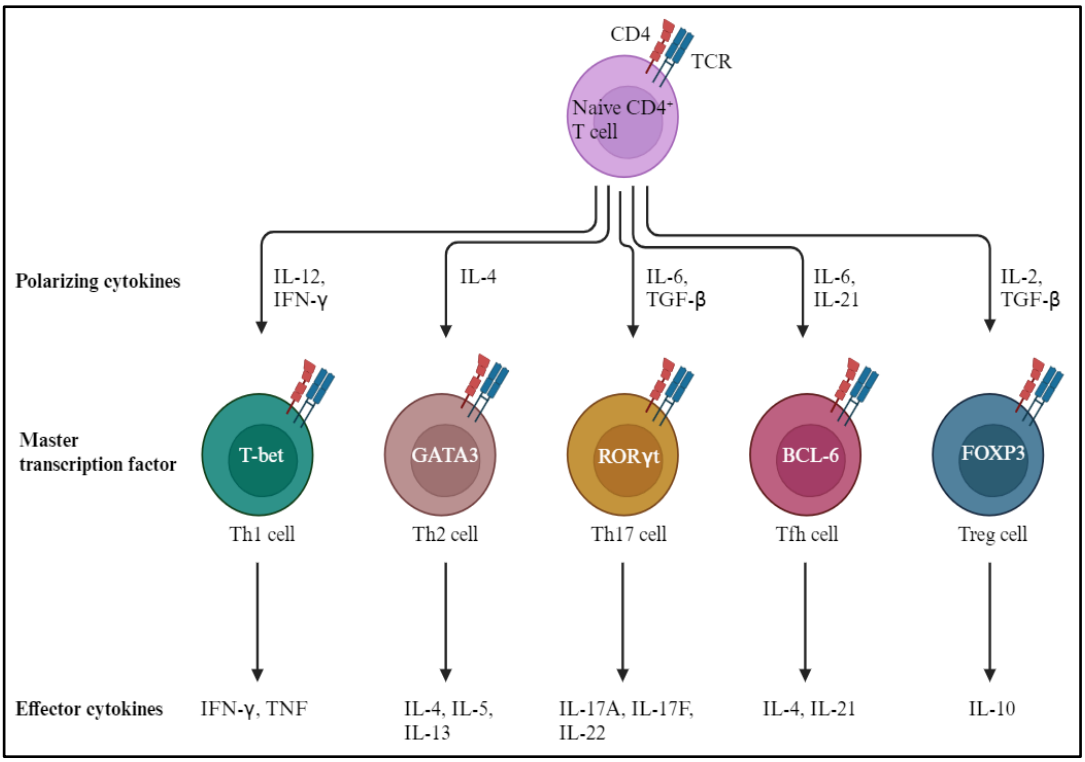

Figure 1.1 Th cell differentiation from naïve CD4⁺ T cells.

Described in detail in section 1.2.2. Th cell differentiation is dictated by polarising cytokines, giving rise to the expression of master transcription factor of different Th cell subsets. Figure created with BioRender.com.

1.2.3 B cell development and its subsets

B cells go through a series of developmental events in the bone marrow that are marked by immunoglobulin (Ig) rearrangement status and surface protein expression (Figure 1.2, Figure 1.3). Progenitor B (pro-B) cells that arise from the common lymphoid progenitors can be divided into three stages, namely fraction A, B, C (Hardy *et al.*, 1991). While the Ig genes of fraction A are in germline configuration, the Ig heavy chain (IgH), encoded by three genes (V, D, J) rearranges first in fraction B. D-J joining in fraction B precedes V-DJ gene recombination that occurs in fraction C (Hardy *et al.*, 1991). Pro-B cells are also recognised by the expression of CD43, IL-7 receptor, and BP-1 (Hardy *et al.*, 1991). The loss of these early B lineage surface markers and a successful VDJ rearrangement generate large pre-B cells expressing pre-B cell receptor (BCR), which encompasses two Ig μ-chains and two surrogate

light chains (λ5 and VpreB) together with two signalling subunits (Igα and Igβ) (Nishimoto *et al.*, 1991; Herzog *et al.*, 2009).

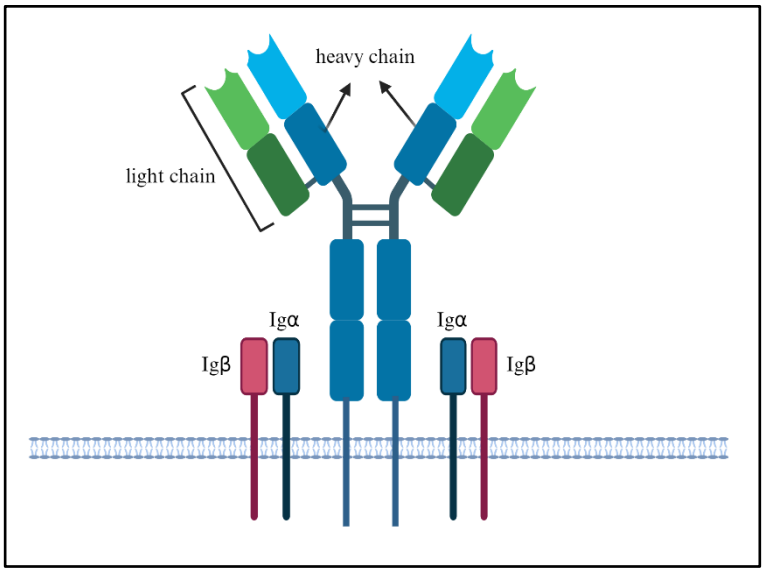

Figure 1.2 B cell receptor complex.
The B cell receptor complex consists of two light chains, two heavy chains, and two heterodimers of Igα and Igβ. Figure created with BioRender.com.

Subsequently, pre-BCR signalling induces large pre-B cell proliferation and differentiation into small pre-B cells that is accompanied by the transcriptional silencing of λ5 and VpreB (Parker *et al.*, 2005). The expression of intracellular Ig μ-chains in small pre-B cells also activates gene rearrangement of Ig light chain that comprises of the λ chain (Igλ) and the κ chain (Igκ) (Reth *et al.*, 1987). This leads to the formation of immature B cells that are marked by the expression of BCR, which consists of two Ig μ-chains and two Igλ or Igκ chains (Herzog *et al.*, 2009). Immature B cells also have a low expression of IgM molecules (IgM^{dull}) prior to their development into the highest IgM expression (IgM^{bright}) transitional B cells that are transported to the spleen by the bloodstream (Carsetti *et al.*, 1995). Here, transitional B cells become long lived mature B cells with a downregulated IgM expression and an enhanced expression of IgD (Loder *et al.*, 1999).

Specific pools of peripheral B cell subsets have been identified based on their receptor expression. B1 cells were first found primarily in the peritoneal cavities, express Ly-1 (also known as CD5) and constitute only 1-5% of total splenic B cells

in mice (Hayakawa *et al.*, 1985). The conventional B cells, B2 cells, were identified by a slightly lower CD19 and IgM expression in comparison to B1 cells (Wang *et al.*, 2012). Besides that, other surface markers that are used to differentiate B1 and B2 cells include $CD45RA^{lo}IgD^{lo}CD23^{-}CD43^{+}$ for B1 cells, and $CD45RA^{hi}IgD^{hi}CD23^{+}CD43^{-}$ for B2 cells (Prieto & Felippe, 2017). In mice, the CD45 isoform B220 was demonstrated to be a pan-B-cell marker (Bleesing & Fleisher, 2002). B1 cells play a role in front-line defence by secreting natural antibodies against infections. They also generate polyreactive IgM autoantibodies that can recognise both self and foreign antigens (Bhat *et al.*, 1992). In contrast, B2 cells are involved in mounting adaptive immune responses to pathogens and giving rise to memory B cells (Alter-Wolf *et al.*, 2009).

Transitional B cells in the spleen can develop either into marginal zone (MZ) B cells or follicular (FO) B cells, according to the signalling inputs they receive (Mebius & Kraal, 2005). Several theories have been proposed for this cell-fate decision of mature B cells, but more research is warranted to fully understand the mechanism. A signature surface protein used to distinguish MZ B cells and FO cells is CD23 (Waldschmidt *et al.*, 1988). $CD23^{+}$ FO B cells were discovered to dwell in the splenic follicle, whereas $CD23^{-}$ MZ B cells were found to reside in the splenic MZ (Figure 1.4). Furthermore, FO B cells, which are smaller in size than MZ B cells, express high levels of IgD and moderate levels of IgM, CD21, and CD38; the bigger MZ B cells express low levels of IgD and high levels of IgM, CD21, and CD38 (Kearney *et al.*, 1997).

Besides these phenotypic differences, MZ B cells and FO B cells also exhibit functional distinctions. Despite a slower proliferation rate of MZ B cells in comparison to FO B cells, MZ B cells are quicker in mounting an immune response through IgM antibodies secretion when treated with lipopolysaccharides (LPS) *in vitro* (Kearney *et al.*, 1997). MZ B cells provide a first-line protection against blood-borne T-independent (TI) antigens and encapsulated bacteria (Kruetzmann *et al.*, 2003; Weller *et al.*, 2004). Conversely, antigen-activated FO B cells require T cell help [T-dependent (TD)] to undergo differentiation predominantly into short-lived, low-affinity IgM plasma cells, while a small proportion instigate the formation of germinal centre (GC) (Roulland *et al.*, 2007). Rapid cell proliferation, clonal

expansion, and Ig class switching occur in GC for the generation of short-lived IgG-, IgE-, or IgA-secreting plasma cells as well as memory B cell (Roulland *et al.*, 2007). B cells that differentiate into GC B cells bear $CD95^{+}$ and $GL7^{+}$ surface markers (Hägglöf *et al.*, 2023; Martínez-Riaño *et al.*, 2023).

Plasma cells, as the final form of mature B cells, function as antibody-producing B cells to combat infection and disease. They can be generated by three major sources: (i) B1 cells producing IgM or IgA, (ii) germinal centre B cells giving rise to long-lived plasma cells, and (iii) plasmablasts in the extrafollicular zone in the spleen growing into short-lived, low-affinity plasma cells in both TI and TD response (MacLennan *et al.*, 2003). Plasma cells can be recognised by $B220^{-}$ and $CD138^{+}$ expression (Kumazaki *et al.*, 2007).

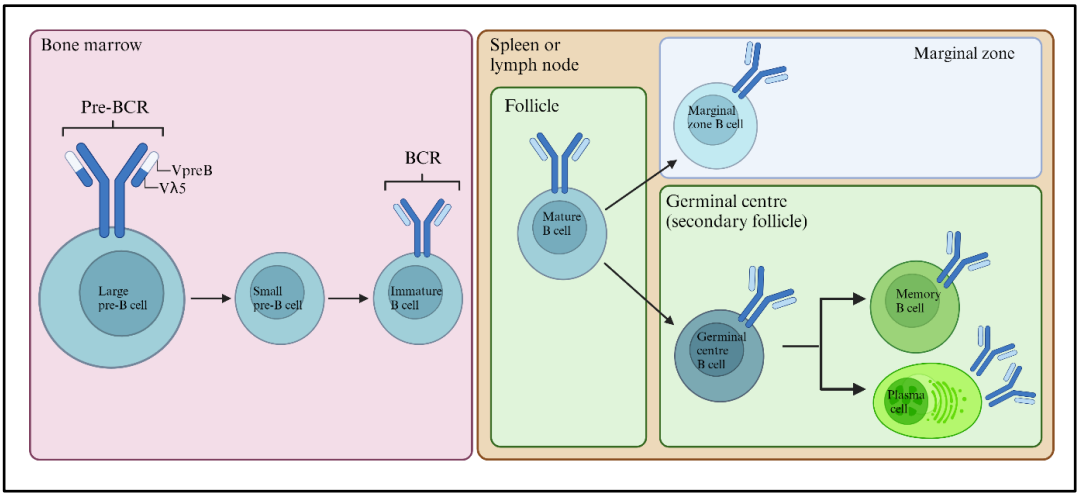

Figure 1.3 B cell development.

Described in detail in section 1.2.3. B cell development begins in bone marrow and continues to occur in the spleen or lymph node. Figure created with BioRender.com.

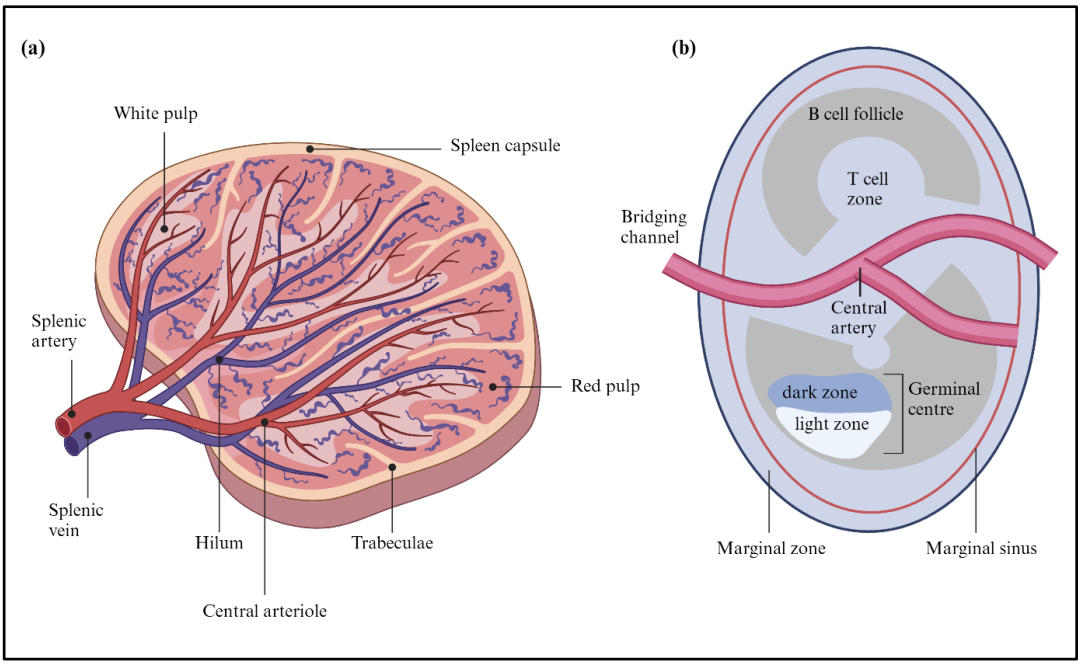

Figure 1.4 (a) Spleen anatomy and (b) the white pulp niche in mice.
The white pulp of the spleen contains a rich reservoir of T cells and B cells. Figure created with BioRender.com.

1.3 The IL-17 family cytokines and receptors

Cytotoxic T lymphocyte-associated antigen-8 (CTLA-8) was discovered via complementary deoxyribonucleic acid (cDNA) library screening of murine lymphoid cells in 1993 (Rouvier *et al*., 1993). It exhibits 57% homology to Herpesvirus saimiri gene 13 (HVS13), an open reading frame of a T cell-infecting virus HVS (Albrecht *et al*., 1992). CTLA-8 was then renamed as interleukin-17 (IL-17, also known as IL-17A) when a novel cytokine receptor, termed IL-17R was found to bind to both CTLA-8 and HVS13 (Yao *et al*., 1995a). In 1995, human IL-17 was identified to be 63% and 72% homologous to murine CTLA-8 and HVS13, respectively (Yao *et al*., 1995b). The function of IL-17 gathered substantial attention following the discovery of Th17 cells a decade later (Harrington *et al*., 2005).

New members of the IL-17 family, IL-17B through IL-17F were found based on structural homology with IL-17A (Li *et al*., 2000, Lee *et al*., 2001, Starnes *et al*., 2001, Starnes *et al*., 2002). Additionally, IL-17N was revealed from genome database

screening of Japanese pufferfish *Takifugu rubripes* (Korenaga *et al*., 2010). Among the IL-17 family members, IL-17F displays the highest degree of sequence overlap (55%) with IL-17A, followed by IL-17B, IL-17D, and IL-17C that share 29 to 23% homology with IL-17A; IL-17E is the least similar to IL-17A, sharing only 16% of sequence conservation (Brembilla *et al*., 2018).

The IL-17 receptor (IL-17R) family is characterised by a cytoplasmic domain, called SEFIR, that is common to both SEF [similar expression to fibroblast growth factor (FGF) genes] and IL-17Rs and is implicated in Toll like receptor (TLR)/IL-1R pathways (Novatchkova *et al*., 2003). It is believed that most IL-17 signalling transduces through IL-17Rs complexes encompass a shared IL-17RA chain and a second chain that confers specificity. However, the second chains of the IL-17Rs do not necessarily align with the reciprocal IL-17 binding in terms of nomenclature. For instance, IL-17A and IL-17F bind to IL-17RC, IL-17C binds to IL-17RE, and IL-17E binds to IL-17RB. These receptors are coupled with IL-17RA (Monin & Gaffen, 2018). An exception to this is the binding of IL-17B to IL-17RB, at a lower degree than IL-17E. It is also unclear whether IL-17RA is required for IL-17B signalling, while the receptor for IL-17D is yet to be determined (Monin & Gaffen, 2018).

1.4 The development of Th17 cells

A variety of cell types that contribute to the production of IL-17 has been identified: Th17 cells, $CD8^+$ cytotoxic T cells, γδ T cells, NK T cells (Monin & Gaffen, 2018), natural Th17 cells (Marks *et al*., 2009), type 3 innate lymphoid cells (Villanova *et al*., 2014), mucosal associated invariant T cells (Majumder & McGeachy, 2021), mast cells, and Paneth cells (Mills, 2023). Neutrophils have also been reported to serve as a source of IL-17 in the lung after LPS challenge (Ferretti *et al*., 2003). Nonetheless, this finding remains controversial as neutrophils do not release IL-17 during acute oropharyngeal candidiasis (Huppler *et al*., 2015).

The Th17 cell is a key contributor to IL-17 production and is one of the predominant $CD4^+$ T cells subsets that has been extensively studied. It is well known that IL-6 and

TGF-β work together to promote the differentiation of naïve $CD4^+$ T cells into Th17 cells (Bettelli *et al*., 2006). This is directed by the expression of RORγt, a transcription factor that determines the Th17 lineage (Ivanov *et al*., 2006). Besides that, IL-21 and IL-23 upregulate RORγt expression, promoting the generation of IL-17 (Zhou *et al*., 2007).

IL-23 is also indispensable for increased IL-17 levels produced by memory T cells (Aggarwal *et al*., 2003). This is further evidenced by the pathogenic development of inflammatory autoimmune diseases, such as experimental autoimmune encephalomyelitis (EAE), induced by Th17 cells via the IL-23-IL-17 pathway (Langrish *et al*., 2005). Although the IL-23 heterodimer consists of a p19 subunit and a shared p40 subunit with IL-12 (Oppmann *et al*., 2000), IL-12 is not related to IL-17 production (Aggarwal *et al*., 2003).

Interestingly, a diverse combination of cytokines that activate Th17 cells can lead to two different types of Th17 cells that differ in being pathogenic in inducing autoimmune disease or non-pathogenic in causing little or no autoimmune responses. TGF-β1 and IL-6 are demonstrated to be factors driving the non-pathogenic phenotype of Th17 cells, whereas IL-23 dependent TGF-β3 and IL-6 stimulation results in the more proinflammatory/pathogenic Th17 cells (Lee *et al*., 2012). Moreover, the presence of IL-23 without TGF-β is described to induce pathogenic Th17 cells (Ghoreschi *et al*., 2010).

In short, a paradigm involving three overlapping steps – differentiation, amplification, and stabilisation in Th17 cell development has been delineated. IL-6 and TGF-β are cytokines responsible for Th17 cell differentiation; IL-21 secreted by developing Th17 cells facilitates amplification; and IL-23 is essential for Th17 cell survival and stability to achieve their full functional capacity (Patel & Kuchroo, 2015).

1.5 Role of IL-17 and Th17 cell in infection and autoimmunity

Th17 cells do not produce IL-17A only, but also generate IL-17F (Harrington *et al*., 2005), IL-21 (Nurieva *et al*., 2007), IL-22 (Liang *et al*., 2006), granulocyte-macrophage colony-stimulating factor (GM-CSF), IFN-γ, and TNF (Mills, 2023). Based on this plethora of cytokines, there is evidence to support a function for Th17 cells in inducing a cytokine milieu that mediates the innate immune defence. This includes aiding the infiltration of neutrophils and macrophages to injured tissues via the induction of a variety of chemokines, such as chemokine (C-X-C motif) ligand (CXCL) 1, CXCL2, CXCL5, and CXCL8 (IL-8) by IL-17 (Onishi & Gaffen, 2010). Furthermore, IL-17 also induces granulocyte colony-stimulating factor (G-CSF) and GM-CSF that prolong neutrophil lifespan in inflamed rheumatoid arthritis synovium (Parsonage *et al*., 2008). IL-6, another product of the IL-17 pathway, acts in a positive feedback loop to sustain Th17 differentiation for acute responses (Ogura *et al*., 2008). IL-17 also triggers the production of pro-inflammatory cytokines, namely IL-1β, IL-6, TNF-α (Onishi & Gaffen, 2010).

The role of IL-17 in mitigating fungal and bacterial infections has been well implicated. Host defence in the kidney and survival of IL-17R-deficient mice were compromised upon *Candida albicans* systemic challenge, possibly due to impaired neutrophils peripheral circulation and recruitment to the infected organs (Huang *et al*., 2004). Mice lacking IL-17RA or Act1, an adaptor in IL-17 signalling, displayed highest susceptibility against oropharyngeal candidiasis compared with mice treated with antibody blockade of IL-17 or IL-17RA, and IL-17-deficient mice (Whibley *et al*., 2016). Chronic mucocutaneous candidiasis (CMC) is an infectious disease caused by *Candida albicans* and, in a lower degree, *Staphylococcus aureus* that affects the nails, skin, oral and genital mucosal layer. In humans, both IL-17 and IL-17F are crucial, even though they are redundant for eradicating CMC (Puel *et al*., 2011).

The secretion of IL-8, a cytokine that drives *Helicobacter pylori* (*Hp*)-related acute inflammatory response, is boosted by IL-17 in *Hp*-infected gastric mucosa. This observation was accompanied by consistent upregulated and downregulated IL-17 expression during *Hp* infection and after *Hp* elimination, respectively (Luzza *et al*.,

2000). *Klebsiella pneumoniae* challenge via intranasal causes 100% fatality in mice lacking IL-17R in comparison to control mice; this study also showed delayed neutrophil migration to the alveolar space associated with decreased mRNA and protein level of G-CSF and macrophage inflammatory protein (MIP)-2 in IL-17R-deficient mice (Ye *et al*., 2001). In addition, IL-17 contributed to activation and pneumococcal killing by neutrophils in response to intranasal immunisation with *Streptococcus pneumoniae* in humans (Lu *et al*., 2008). Overall, these findings corroborate the role of IL-17 in modulating antifungal and antibacterial immunity.

Autoimmunity develops when immune cells are chronically activated and improperly targeting host antigens, resulting in detrimental inflammation. The role of IL-17 as the hallmark of autoimmune diseases has been well documented. Increased IL-17 mRNA expression in immune cells was detected in the cerebrospinal fluid of multiple sclerosis patients (Matusevicius *et al*., 1999). Th17 cells also demonstrated the ability to cross the blood-brain barrier and participate in forming multiple sclerosis lesions (Kebir *et al*., 2007). In autoimmune arthritis, IL-17 promotes cartilage and bone destruction (Sato *et al*., 2006). Similarly, using IL-17-deficient mice, it has been depicted that IL-17 is critical for the development of collagen-induced arthritis (CIA), an animal model of rheumatoid arthritis, by triggering autoantigen-specific immune responses (Nakae *et al*., 2003).

Besides that, much attention has been paid to elucidate the role of IL-17 in the pathogenesis of psoriasis. A Spanish cross-sectional observation study has outlined a strong relevance between single nucleotide polymorphism in *IL17RA* and psoriasis (Batalla *et al*., 2015). Mice lacking IL-23 or IL-17R were found to be less prone to develop plaque type psoriasis caused by topical application of TLR7/TLR8 ligand, imiquimod (van der Fits *et al*., 2009). Th17 cells have been identified in the dermis of psoriatic skin, along with augmented IL-17 mRNA in parallel to psoriasis disease activity (Lowes *et al*., 2008). Like psoriasis, Crohn's disease, the more common form of irritable bowel disease (IBD), manifests an activated Th17 phenotype with increased IL-17 production (Kleinschek *et al*., 2009). It has been studied that IL-23 induced IL-17 drives chronic intestinal inflammation in IBD (Yen *et al*., 2006).

Nevertheless, IL-17 is indispensable to maintain healthy skin and mucosa. IL-17 enhances epithelial cell proliferation and wound healing after skin injury (McGeachy *et al*., 2019). Consistently in the gut, IL-17 is beneficial in preserving the epithelial integrity by mediating the tight junction protein occludin in a dextran sodium sulphate model of acute IBD (Lee *et al*., 2015). While IL-17 is necessary to provide anti-microbial responses and restore barrier function, excessive IL-17 and Th17 cells can be potent inducers of autoimmunity. In short, these findings highlight the favourable and deleterious potential of IL-17 in containing infections and developing autoimmune diseases, respectively.

1.6 Regulation of IL-17 activity

Given that unrestrained production of IL-17 is a risk factor of chronic inflammation and autoimmune conditions, a tight regulation to maintain an appropriate balance is vital for health. The IL-17 signalling pathway is an intricate feedback loop and IL-17 itself promotes transmission of regulatory signals (McGeachy *et al*., 2019). Besides that, signals from other cytokines that interact with the target cell can also lead to either synergistic activation or dampening of IL-17 expression.

1.6.1 Positive regulators of IL-17

Molecules that promote the expression of IL-17 have been identified (Figure 1.5). It is well known that RORγt is the signature Th17 lineage transcription factor. This is further substantiated by inhibition of Th17 cell differentiation and imiquimod-induced psoriasis-like skin inflammation using a selective RORγt inverse agonist called TMP778 (Skepner *et al*., 2014). A second transcription factor that is essential for Th17 differentiation is Runt-related transcription factor 1 (Runx1); it induces RORγt expression and interacts directly with RORγt (Zhang *et al*., 2008).

In addition, STAT3 has been found to influence Th17 differentiation through its binding to the promoter regions of IL-17A and IL-17F (Chen *et al*., 2006). IL-17

induction is also controlled by the IL-6-mediated Janus Kinase (JAK) 2/STAT3 pathway. Phosphorylated STAT3 in $CD4^+$ T cells and proinflammatory cytokines, such as IL-17, IL-1β, and IL-6 are diminished when mice with CIA are treated with JAK2 inhibitor, AG490 (Park *et al*., 2014). The role of nuclear factor kappa B (NF-κB) as a positive regulator of IL-17 has been described. IL-17 secretion is halted when NF-κB activation is suppressed by BAY11-7082, a synthetic inhibitor of inhibitor kappa B alpha (IκB-α) phosphorylation (Huang *et al*., 2008). Furthermore, two family members of NF-κB, RelA/p65 and c-Rel bind to RORγ and RORγt promoters, respectively to increase their expression, which leads to Th17 differentiation (Ruan *et al*., 2011).

Interferon regulatory factor (IRF) 4 also contributes to Th17 differentiation. Mice lacking IRF4 are resistant to EAE due to impeded Th17 differentiation, decreased RORγt expression, and elevated Foxp3 expression (Brüstle *et al*., 2007). Rho-associated, coiled-coil-containing protein kinase (ROCK) 2-induced phosphorylation of IRF4 is indispensable for IL-17 and IL-21 production (Biswas *et al*., 2010). Additionally, Kruppel-like factor (KLF) 4 mediates IL-17 production through direct interaction with IL-17 promoter without affecting RORγt expression (Lebson *et al*., 2010). Basic leucine zipper ATF-like transcription factor (BATF) has also been shown to induce IL-17 expression and Th17 differentiation (Jordan-Williams *et al*., 2013).

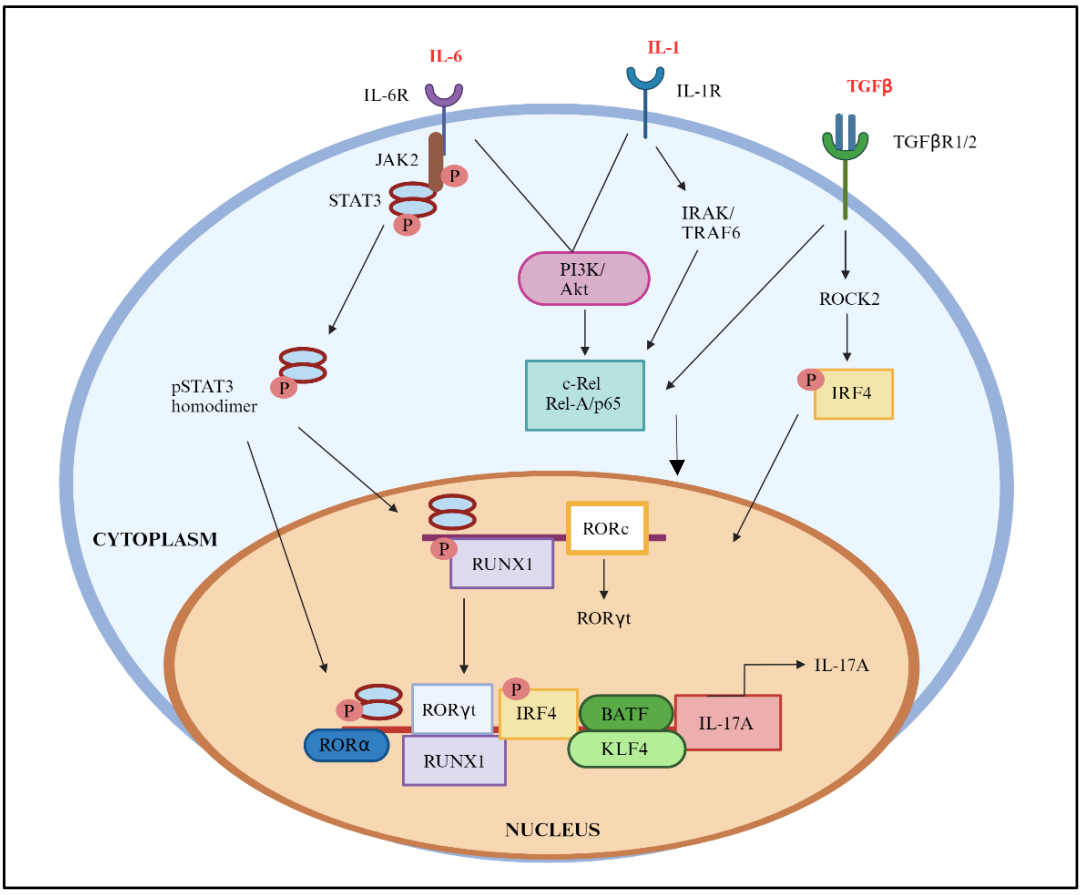

Figure 1.5 Positive regulators of IL-17.

Described in detail in section 1.6.1. A myriad of cytokines and molecules are involved in different signaling pathways that induce (black arrows and lines) the expression of *RORc* and consequently *il17* gene. Figure created with BioRender.com.

1.6.2 Negative regulators of IL-17

Molecules that negatively modulate IL-17 expression have been studied (Figure 1.6). Differentiation of Th17 is blunted by the presence of IFN-γ and IL-4 (Harrington *et al*., 2005). IL-27 is important to control EAE by inhibiting Th17 development, thus decreasing IL-17 production (Batten *et al*., 2006). Suppressor of cytokine signalling 3 (SOCS3) also negatively impacts IL-23 signalling, leading to the suppression of Th17 differentiation (Chen *et al*., 2006). While interaction between Runx1 and RORγt results in IL-17 expression, Runx1-Foxp3 complex blocks Th17 differentiation (Zhang *et al*., 2008). Runx1-induced transactivation of *Rorc*, the gene encoding RORγt is stifled through its binding to tyrosine 304 of T-bet (Lazarevic *et*

al., 2011). Intriguingly, Foxp3 and IRF8 can interact with RORγt to hamper IL-17 promoter activation and reduce IL-17 transcription, respectively (Ichiyama *et al*., 2008; Ouyang *et al*., 2011). Peroxisome proliferator-activated receptor γ (PPARγ) has been depicted to repress human and mouse Th17 differentiation by obstructing RORγt transcription (Klotz *et al*., 2009). Unlike many regulators, v-ets erythroblastosis virus E26 oncogene homolog 1 (Ets-1) dampens Th17 differentiation without influencing RORγt (Moisan *et al*., 2007).

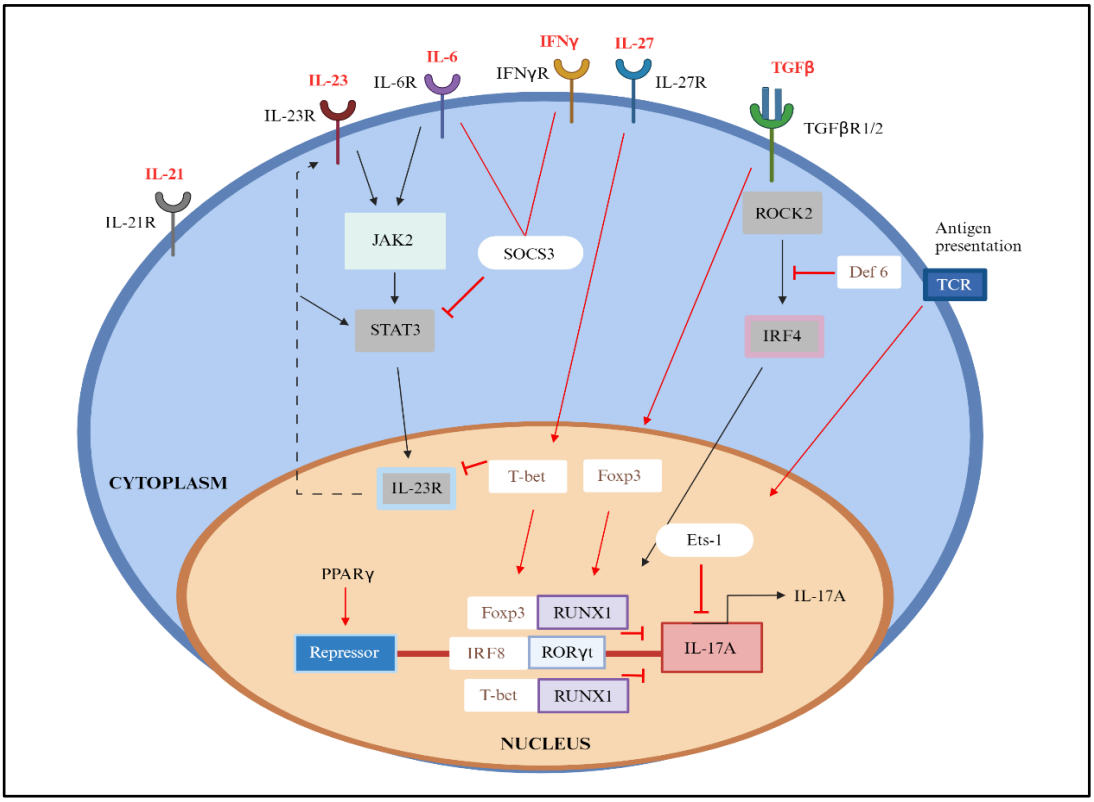

Figure 1.6 Negative regulators of IL-17.

Described in detail in section 1.6.2. A range of cytokines and molecules are involved in different signaling cascades that inhibit (red arrows and lines) the expression of *RORc* and consequently *il17* gene. Figure created with BioRender.com.

1.7 The Pellino family

The research described in this thesis describes investigation into the roles of the Pellino family proteins in adaptive immune cell populations. Pellino in *Drosophila melanogaster* was first discovered via binding to autophosphorylated and activated form of the serine/threonine protein kinase Pelle using the two-hybrid system (Groβhans *et al*., 1999). Pelle shares similarity in amino acid sequence with the mammalian kinase called IL-1R-associated kinase (IRAK) 1 (Cao *et al*., 1996). Genes for Pellino-like proteins were sequenced in *Caenorhabditis elegans* (Rich *et al*., 2000) and *Ciona intestinalis* (Hotta *et al*., 2000), indicating a cross-species conservation in Pellino proteins. Following that, three members of the mammalian Pellino family – Pellino 1, Pellino 2, and Pellino 3 were identified and genetically mapped (Jiang *et al*., 2003; Yu *et al*., 2002; Jensen and Whitehead, 2003a). Human Pellino 1 and Pellino 2 genes, namely PELI1 and PELI2 have six exons and are located on chromosome 2 and chromosome 14, respectively (Resch *et al*., 2001). The PELI3 gene that encodes Pellino 3 protein has eight exons and is mapped to chromosome 11 in humans. Unlike Pellino 1 and Pellino 2, Pellino 3 is expressed in two alternative spliced forms – the larger Pellino3a and the smaller Pellino3b (Jensen and Whitehead, 2003a).

Early reports established the role of Pellino family as scaffolding proteins: (i) Pellino 1 and Pellino 2 associates with IRAK1, IRAK4, TNF receptor associated factor (TRAF) 6, and transforming growth factor β-activated kinase (TAK)1 in the TLR signalling pathway that promotes activation of the transcription factor NF-κB (Jiang *et al*., 2003; Jensen and Whitehead, 2003b; Strelow *et al*., 2003), (ii) Pellino 3 acts as a positive regulator of mitogen-activated protein kinase (MAPK) pathway (Jensen and Whitehead, 2003a; Butler *et al*., 2005). All three Pellino proteins contain a CH2CH2 RING motif that is closely related to the structure of the C3HC4 RING domain, a classical feature found in E3 ubiquitin ligases (Saurin *et al.*, 1996; Schauvliege *et al.,* 2006). Such studies suggested that Pellino proteins may be capable of conferring E3 ligase activity (Schauvliege *et al.,* 2006). The latter study also inferred that IRAK1-mediated phosphorylation of Pellino proteins occur at the RING domain upon their association, which is required to promote stronger binding

to IRAK1 and in turn induce polyubiquitination of IRAK1 (Schauvliege *et al.*, 2006). The association between Pellino proteins and IRAK1 may not involve the RING domain of Pellino, but it requires IRAK1 kinase activity (Schauvliege *et al.*, 2006; Lin *et al.*, 2008). Despite that, some reports have illustrated that IRAK/Pellino interaction is independent of IRAK1 kinase activity (Butler *et al.*, 2007).

In relation to structure, all three Pellino proteins contain a RING motif and a forkhead-associated (FHA) domain, which is a recognised phosphothreonine-binding module (Figure 1.7). The C-terminal 140 amino acids across the Pellino family are dispensable for interaction with IRAK1, whereas the N-terminal domain of Pellino 1, 2, and 3b are shown to mediate this interaction (Lin *et al.*, 2008). The structure of the N-terminal region of Pellino 2 (amino acids 15-275) has been resolved through x-ray crystal structure (Lin *et al.*, 2008). Besides that, the unusual 'wing' or appendage adjacent to the FHA domain in Pellino 2 accounts for increased affinity and specificity in its binding to IRAK1 (Lin *et al.*, 2008). This likely explains variable affinity of the FHA domain for the target protein in different Pellino proteins. For instance, Pellino 1 displays high affinity for receptor interacting protein (RIP) 1 but not TRAF6, whereas Pellino 3 can bind strongly to TRAF6 (Huoh & Ferguson, 2014).

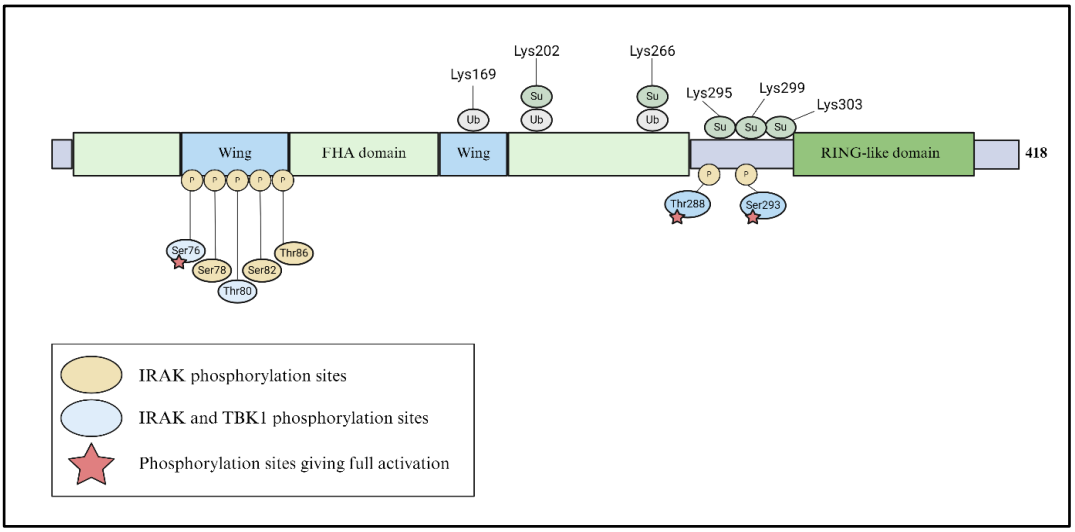

Figure 1.7 Molecular structures of Pellino proteins.

Pellino proteins contain an FHA domain in between two inserts that form a 'wing' and a RING-like domain. Figure created with BioRender.com.

Each of the Pellino proteins demonstrates E3 ubiquitin ligase activity in vitro (Butler *et al.,* 2007). Ubiquitination is a post-translational modification where ubiquitin (Ub) or small ubiquitin-like modifiers are covalently bound to the target proteins (Ohtake *et al.*, 2015). Ub is a small protein consisting of 76 amino acids (Chicooree *et al.*, 2013). This chemical reaction encompasses three steps that are catalysed by the sequential action of 3 enzymes: a ubiquitin activating E1 enzyme, followed by conjugation of ubiquitin to an E2 conjugating enzyme, and lastly transfer of the ubiquitin to the lysine residues of target proteins by E3 ubiquitin ligases (Figure 1.8; Hershko & Ciechanover, 1998). E3 ligase dictates substrate specificity for all E2 ubiquitin-conjugating enzymes. Seven lysine (K/Lys) residues have been identified as the coupling sites for ubiquitination; among them are K48 and K63 being the most well-documented residues and other lysine sites including K6, K11, K27, K29, and K33 (Peng *et al.*, 2003). Primarily, polyubiquitination at K48 is associated with proteosomal protein degradation, whereas K63-linked polyubiquitination leads to DNA repair and signal transduction by decorating surfaces of proteins with polyubiquitin chains that act as docking sites for signalling platforms (Ohtake *et al.*, 2015).

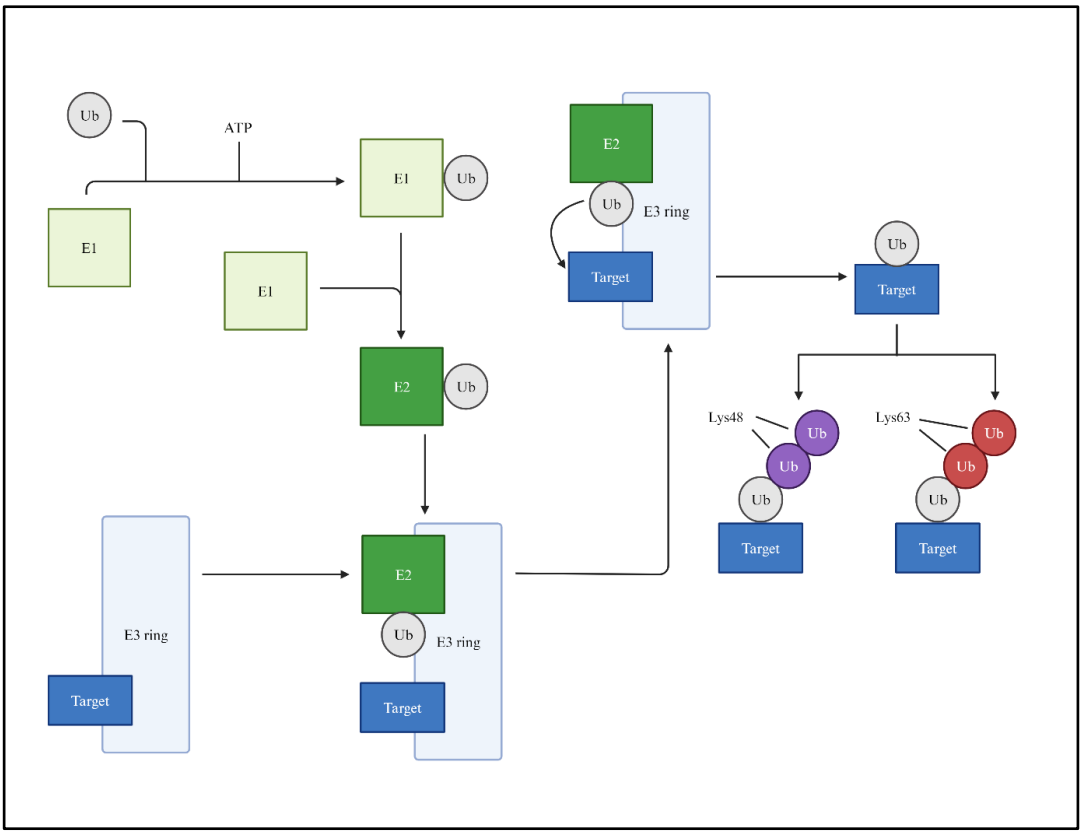

Figure 1.8 The three-step reaction of ubiquitination.

Described in detail in section 1.7. The ubiquitination pathway involves a sequential action of an E1 enzyme, an E2 enzyme, and an E3 ubiquitin ligase. Figure created with BioRender.com.

1.7.1. Pellino proteins and innate immune signalling

Despite the strong structural homology across the Pellino family, disparate functional roles of the individual members in the immune system have been demonstrated. To date the functional role of Pellino proteins has been mostly explored in innate immune signalling pathways. To this end an initial overview of innate immune signalling will be provided. Innate immune signalling is initiated by PRRs after recognition of PAMPs. Examples of PRRs are TLRs, nucleotide-binding and oligomerization domain (NOD)-like receptors, retinoic acid-inducible gene (RIG)-1-like receptor, and cytosolic nucleic acid-sensing receptors (Moynagh, 2014). TLRs form an important family of PPRs with TLR4 being the prototypical member of this family (Figure 1.9).

Activation of TLR4 leads to complex downstream signalling cascades (Fig 1.9). All TLRs and IL-1R harbour a common intracellular Toll/IL-1R (TIR) domain that recruits TIR adaptor proteins upon TLR/IL-1R activation (O'Neill *et al.*, 2013). When triggered by pathogens, such as LPS, a cell membrane component of gram-negative bacteria (Chow *et al.*, 1999), TLR4 interacts with either myeloid differentiation primary response gene 88 (MyD88) or TIR-domain-containing adapter-inducing interferon-β (TRIF, also known as TICAM1) and their respective bridging adapters, MyD88-adapter-like (Mal) and TRIF-related adaptor molecule (TRAM) (Fitzgerald *et al.*, 2001; Rowe *et al.*, 2006, Yamamoto *et al.*, 2003). MyD88 pathway leads to the hyper-phosphorylation and activation of IRAK1 and IRAK4, followed by their coupling with the E3 ubiquitin ligase TRAF6 (Li *et al.*, 2002; Suzuki *et al.*, 2002). TRAF6 then activates TAK1, resulting in downstream phosphorylation and proteasomal degradation of IκB kinase (IKK) α and IKKβ (Wang *et al.*, 2001). This abrogates the inhibitory effect of IKK complexes on NF-κB, enabling nuclear translocation of NF-κB and subsequent induction of pro-inflammatory gene expression (Moynagh, 2005).

Besides that, TLR4 can also deploy a MyD88-independent pathway to activate NF-κB. TRIF recruited by TRAM interacts with RIP1 and Pellino 1, which subsequently regulates K63-polyubiquitination of RIP1 (Cusson-Hermance *et al*., 2005; Chang *et al*., 2009). This allows for the recruitment of TAK1 and IKKα/IKKβ complex through their binding to TAK1-binding proteins (TABs) and NF-κB essential modulator (NEMO), respectively. These events stimulate the activation and transcription of NF-κB (Rahighi *et al*., 2009; Humphries & Moynagh, 2015). Moreover, TRIF pathway can also trigger the sequential activation of TRAF3, IKKε/IKK-related kinases TANK-binding kinase (TBK) 1 complex, and IRF3, resulting in the downstream production of type 1 IFNs (Fitzgerald *et al*., 2003; Sharma *et al*., 2003; Kagan *et al*., 2008).

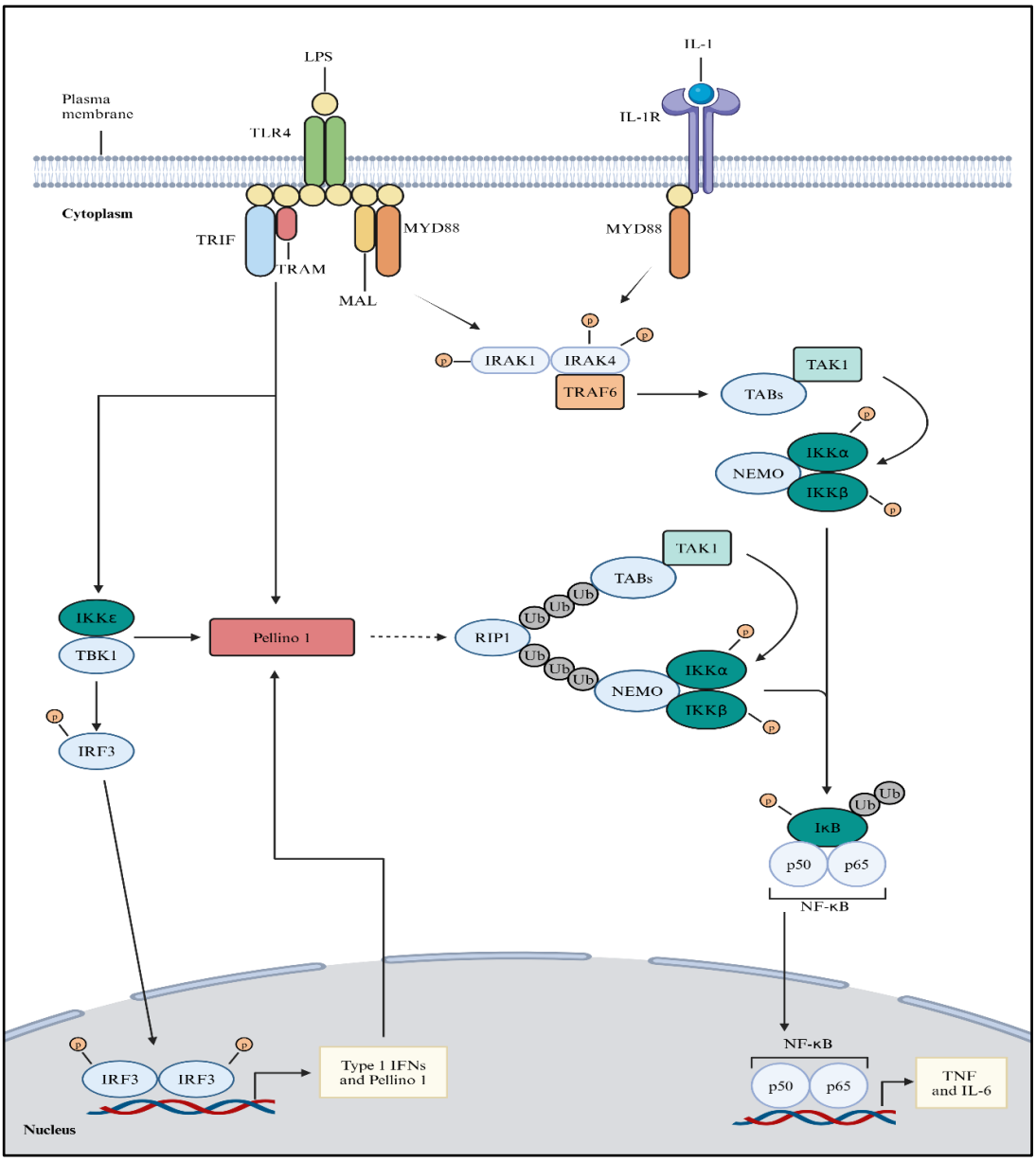

Figure 1.9 TLR4/IL-1R signalling pathway.

Described in detail in section 1.7.1. Pellino 1 contributes to the activation of TRIF-dependent NF-κB pathway by inducing RIP1 polyubiquitination upon stimulation of TLR4 with LPS. Figure created with BioRender.com.

Inflammasomes, multimeric protein complexes, activated by the interaction between PRRs and PAMPs, also play an important role in the generation of pro-inflammatory cytokines (Blevins *et al.*, 2022). To date, the nucleotide-binding domain, leucine-rich-containing family, pyrin domain-containing (NLRP) 3 is the most extensively studied inflammasome. The NLRP3 inflammasome encompasses a NLRP3 sensor

protein, an adaptor protein apoptosis-associated speck-like protein containing a caspase activation and recruitment domain (ASC), and an effector molecule caspase-1 (Schroder *et al*., 2010). The NLRP3 inflammasome is formed via a two-step process. Firstly, signal 1 or the priming signal triggered by an inflammatory stimulus (eg. TLR4 agonist) is necessary to upregulate the expression of NLRP3 and pro-inflammatory cytokines, such as pro-IL-1β and pro-IL-18 (Schroder *et al*., 2010). Secondly, signal 2 or the activation signal induced by a variety of stimuli including PAMPs, and danger associated molecular patterns (DAMPs), such as alum and extracellular adenosine triphosphate (ATP), is critical for NLRPs inflammasome assembly and a form of cell death called pyroptosis (Yang *et al*., 2019). The activation step is also required for the maturation of IL-1β and IL-18 (Yang *et al*., 2019).

1.7.2 The role of Pellino 1 in immunity

The mammalian counterpart of Pellino, named Pellino1 was first identified and shown to interact with IRAK1, IRAK4, TRAF6, and TAK1 in TLR and IL-1R signalling pathway for the activation of NF-κB (Jiang *et al*., 2003). Using protein overexpression and *in vitro* kinase assays, Pellino 1 did not affect the MAPK signalling pathway, implying a specific role in NF-κB activation (Jensen and Whitehead, 2003b). Smad6 is a negative regulator of NF-κB activation via TGF-β-induced association with Pellino 1, inhibiting the formation of IRAK4-IRAK1-Pellino-1-TRAF6 complex that leads to the expression of pro-inflammatory genes (Choi *et al*., 2006). Overall, these studies delineate that Pellino 1 modulates NF-κB activity.

The generation of a Pelino 1 knockout mouse has shed some light on the physiological functions of Pellino 1 in innate immune system. Pellino 1 deficiency impairs TLR3-induced RIP1 ubiquitination and IKK activation in the TRIF-dependent TLR pathway (Chang *et al*., 2009). Pellino 1 is partially required for TLR4 signalling (that involves both TRIF- and MyD88-dependent pathways) and dispensable for the signalling function of IL-1R, TLR2, and TLR9, suggesting that

Pellino 1 does not play a role in the transmission of MyD88-dependent signals (Chang *et al*., 2009). In addition, Pellino 1 does not affect TLR3-stimulated activation of IKKε, IRF3, and subsequent IFNβ expression, reinforcing the specific function of Pellino 1 in TRIF-dependent IKK-NF-κB signalling axis (Chang *et al*., 2009). Interestingly, Pellino 1-deficient B cells are partially defective in B cell survival and proliferation induced by cytosine-phosphate-guanine (CpG) (TLR9 ligand), consistent with the effect shown in RIP1-deficient B cells (Chang *et al*., 2009; Vivarelli *et al*., 2004).

However, there are distinct findings on the role of Pellino 1 in TLR3 signalling. Macrophages and dendritic cells from Pellino 1 [F397A] knock-in mutant mice with abolished E3 ligase activity demonstrated decreased IFNβ mRNA production and protein secretion when stimulated with LPS and polyinosinic-polycytidylic acid [Poly (I:C)]. Similar results were observed in mouse embryonic fibroblast (MEF) infected with Sendai virus (Enesa *et al*., 2012). Furthermore, poly (I:C)-stimulated RIP1 polyubiquitination, IKK complex activation, and MAPK activation were intact in bone marrow-derived macrophage (BMDM) from these mutant mice. The contrasting data between Pellino 1 knockout and knock-in mice needs to be addressed, but potentially elucidates that Pellino 1 acts devoid of its E3 ligase activity (Enesa *et al*., 2012). Normal IFNβ production in mice with complete loss of Pellino 1 may suggest compensation by other members of Pellino family or participation of additional E3 ligases in the signalling pathway (Enesa *et al*., 2012).

On the other hand, research on the functional relevance of Pellino 1 in adaptive immunity has produced some significant findings. Pellino 1 is an essential protein in regulating peripheral T cell tolerance by negatively regulating T cell activation (Chang *et al.*, 2011). Pellino 1 promotes K48 polyubiquitination of c-Rel, one of the five family members of NF-κB that results in its degradation and so represses NF-κB-driven activation of T cells (Chang *et al.*, 2011). Pellino 1-deficient mice are also more susceptible to autoimmunity as depicted by splenomegaly, increased immune cells infiltration in various tissues, increased serum antinuclear antibodies, and immune complexes deposition in kidney glomeruli (Chang *et al.*, 2011). Besides that, Pellino 1-deficient mice are resistant to EAE induction by inhibiting degradation of TRAF3, which is a negative regulator of MAPK activation (Xiao *et al.*, 2013). Pellino

1 is found abundantly present in microglia and facilitated K63 ubiquitination of cellular inhibitor of apoptosis (c-IAP) by being a downstream target of TRAF6 upon MyD88-dependent TLR activation. Activated c-IAP in turn regulates K48 ubiquitination of TRAF3, leading to MAPK signalling that produces proinflammatory cytokines and causes autoimmune neuroinflammation (Xiao *et al.*, 2013).

In addition, Pellino 1-deficient mice demonstrate enhanced IgG deposition in the kidney that is correlated with exacerbated lupus-like autoimmunity, accompanied by higher levels of plasma cells and GC B cells (Liu *et al.*, 2018). Pellino 1 mediates K48 ubiquitination and degradation of NF-κB inducing kinase (NIK), resulting in noncanonical NF-κB signalling that induces autoantibody production. In human peripheral blood mononuclear cells (PBMCs), PELI1 expression is negatively associated with systemic lupus erythematosus (SLE) severity and autoantibodies production (Liu *et al.*, 2018).

1.7.3 Pellino 2 and its role in the immune system

Pellino 2 was characterised and expressed as a tissue restricted protein in mice. Using Clustal W analysis, Drosophila Pellino was identified to be 53% identical to mouse Pellino 2, while mouse Pellino 1 was 75% identical to mouse Pellino 2 (Resch *et al*., 2001). Pellino 2 was capable of binding to IRAK1 when overexpressed and was required for LPS- and IL-1-induced activation of NF-κB-dependent gene promoters (Yu *et al*., 2002). Overexpression of Pellino 2 also enhances the expression of c-Jun and Ets-like protein-1 (Elk-1), which results in MAPK and NF-κB pathways activation (Jensen and Whitehead, 2003b). Pellino 2 has been demonstrated to associate with BCL10 during TLR4 signalling triggered by LPS, leading to downstream activation of NF-κB (Liu *et al*., 2004). The study also shows that SOCS3 acted as a negative regulator of this LPS signalling by inhibiting the interaction between BCL10 and Pellino 2 (Liu *et al*., 2004). The deployment of BCL10 to TLR4 signalling pathway was negatively impacted by SOCS3 in a feedback loop (Liu *et al*., 2004). Knockdown of Pellino 2 in cell lines using short hairpin ribonucleic acid

(shRNA) approach has suggested that Pellino 2 is indispensable for IL-1 and LPS-induced K63- and K-48-linked polyubiquitination of IRAK1 (Kim *et al*., 2012). Pellino 2 knockdown macrophages also reduced messenger ribonucleic acid (mRNA) stability of pro-inflammatory genes, including keratinocytes-derived chemokine (KC) (also known as CXCL1) and IL-6 when stimulated with LPS (Kim *et al*., 2012). Our research group generated Pellino 2-deficient mice to explore the physiological role of Pellino 2 and demonstrated a role for Pellino 2 in NLRP3 signalling by regulating K63-linked ubiquitination and hence priming of NLRP3 (Humphries *et al*., 2018). This results in the activation of NLRP3. The study also proposes a counter-regulatory relationship between IRAK1 and Pellino 2, whereby the inhibitory effect of IRAK1 on NLRP3 activation is terminated through Pellino 2-mediated ubiquitination of IRAK1 (Humphries *et al*., 2018).

1.7.4 Pellino 3 regulates innate immunity signalling

Pellino 3 was first highlighted as a pivotal scaffolding protein in IL-1 signalling (Jensen and Whitehead, 2003a). According to protein sequence alignment, Pellino 3 was found to share 84% and 85% similarity with Pellino 1 and Pellino 2, respectively (Jensen and Whitehead, 2003a). The regulatory role of Pellino 3 in activating p38 MAPK pathway was attributed to the additional 27-amino acid region at its N terminus, which was a unique characteristic in contrast to other Pellino members (Butler *et al*., 2005). This is further evidenced by its ability to activate c-Jun and Elk-1 in the MAPK pathway (Jensen and Whitehead, 2003a). Pellino3b, the shorter of the two alternatively spliced Pellino 3 mRNAs, induced Lys63-linked IRAK1 polyubiquitination, resulting in inhibition of both IL-1-triggered IRAK1 degradation and subsequent TAK1-dependent NF-κB activation (Xiao *et al*., 2008). Intriguingly, this negative modulation of downstream signalling from Lys63-linked IRAK1 polyubiquitination is contrary to the traditional view that it is associated with signalling transduction.

Pellino 3 plays a negative role in mediating type I IFN expression through TLR3 signalling pathway. Mice lacking Pellino 3 had greater protection against

encephalomyocarditis virus because of enhanced expression of *Ifnb* in response to TLR3 activation. This was implicated through Lys63-linked TRAF6 polyubiquitination by TLR3-induced Pellino 3, halting the interaction of TRAF6 with IRF7 and hence impaired nuclear translocation of IRF7 and downregulated *Ifnb* expression (Siednienko *et al*., 2012). Besides TLR3, Pellino 3 can also be activated by scavenger receptor-A1 in oxidised low density lipoproteins (LDL) signalling. TLR4-dependent IFNβ expression was diminished during the formation of foam cells by macrophages in atherosclerosis. This was due to mono-ubiquitination of TRAF family member-associated NF-κB activator by Pellino 3, which in turn blocked the recruitment of TBK1 to TRAF3 and subsequent IRF3 activation (Tzieply *et al*., 2012).

In addition to TLR signalling, Pellino 3 also regulates NOD2 signalling pathway, an intracellular receptor for the recognition of bacterial peptidoglycan (Rubino *et al*., 2012). Pellino 3-deficient mice involved in experimental colitis models displayed attenuated release of NOD2-induced proinflammatory cytokines and heightened intestinal inflammation, consistent with the pattern observed in patients with Crohn's disease where reduced Pellino 3 was found in their colons (Yang *et al*., 2013a). It was described that Pellino 3 was responsible for inducing Lys63-linked ubiquitination of RIP2, which assisted the recruitment of TAK1 and IKK complexes, leading to NF-κB and MAPKs activation (Yang *et al*., 2013a; Hasegawa *et al*., 2008). This finding indicates the importance of Pellino 3 in maintaining gut homeostasis. Upon TNF and cyclohexamide co-stimulation, Pellino 3 has been described to interact with RIP1, hindering the formation of death-inducing signalling complex (DISC) and suppressing TNF-induced apoptosis (Yang *et al*., 2013b). Intriguingly, this mechanism involving Pellino 3 was performed via its FHA domain instead of its RING-like domain, suggesting that certain Pellino functions may not require E3 ubiquitin ligase activity. Furthermore, Pellino 3 also contributed to protection against IL-1β-driven insulin resistance in obesity. Pellino 3 targeted TRAF6-mediated ubiquitination, disrupting stabilisation of HIF-1α, which in turn decreased HIF-1α-dependent IL-1 β expression and inflammation (Yang *et al*., 2014). Collectively, the evidence delineating Pellino 3 as a crucial regulator in immune signalling and disease control provides insight into the development of new therapeutic solutions.

1.8 Regulation of T cell signalling by ubiquitination

Although the regulatory role of Pellino proteins in T cell immunity has not been widely reported, ubiquitination is an important post-translational modification to regulate T cell signalling and deregulated actions of ubiquitin ligases can result in autoimmunity (Hu & Sun, 2016). It is well documented that the E3 ligase action of TRAF6 in inducing polyubiquitination of NEMO is required to activate NF-κB in T cells (Sun *et al*., 2004). Another E3 ubiquitin ligase, Itch promotes JunB polyubiquitination and expression of Th2 cytokine genes upon T cell activation (Gao *et al*., 2004). Moreover, Casitas B cell lymphoma (Cbl) induces ubiquitination of TCRζ chain, affecting T cell activation (Wang *et al*., 2001). Two members of the Cbl family, c-Cbl and Cbl-b, are found to regulate T cell function via termination of TCR signals (Naramura *et al*., 2002). The growing appreciation of the role of ubiquitination in adaptive immunity prompts an investigation into the role of other E3 ubiquitin ligases such as the Pellino family in regulating specific immunity.

1.9 Aims of project

Many studies have focused on elucidating the role of Pellino proteins in innate immune signalling. Nonetheless, emerging reports on the association of Pellino 1 with autoimmunity driven by T cell and B cell functions highlight the potential of Pellino proteins in mediating adaptive immune system. This thesis aims to perform a comprehensive characterisation of the roles of Pellino proteins in generating adaptive immune cell populations. The work was aided by the generating of mice lacking the different members of the Pellino family. The overarching aim was underpinned by 3 specific objectives:

- To explore the role of the individual Pellino family members in the generation of T and B cell populations

- To employ mice that are deficient in multiple Pellino family members in order to characterise functional interplay in the Pellino family

- To further explore the effect of Pellino 1 on T cell activation and differentiation

Chapter 2: Materials and Methods

2.1 Materials

2.1.1 Reagents

Reagents	Supplier	Catalogue #
Acetic acid 99-100% (glacial)	Sigma-Aldrich	27221
Agarose	Promega	V3125
B-mercaptoethanol	Gibco	21985023
Bovine serum albumin (BSA)	Sigma-Aldrich	A2153-100g
Bromophenol blue	Sigma-Aldrich	B0126
Carboxyfluorescein succinimidyl ester	eBioscience	65-0850-84
Chloroform	Sigma-Aldrich	C2432-1L
Cytosine-phosphate-guanine (CpG) 1826	Invivogen	tlrl-1826-1
DirectPCR lysis reagent (Tail)	Viagen Biotech	102-T
Dulbecco's modified eagle medium (DMEM)	Invitrogen	10103542
Ethylenediaminetetraacetic acid (EDTA) disodium salt dihydrate	Sigma-Aldrich	E5134-250G
Fetal bovine serum (FBS)	Sigma-Aldrich	F7524-500ml
Flagellin	Invivogen	tlrl-stfla
GelRed® Nucleic Acid Gel Stain	Biotium	41003
Glycine	Sigma-Aldrich	G8898-1kg
GSK805	MedChem	HY-12776
Intracellular (IC) Fixation buffer	Invitrogen	00-8222-49
Isopropanol	Fisher Scientific	11358461
Lipopolysaccharide (LPS)	Enzo Life Sciences	ALX-581-012-L002
Minimum essential medium (MEM) vitamin solution 100x	Sigma-Aldrich	M6895-100ML
Methanol	Sigma-Aldrich	322415-2L
Molecular biology grade water	Sigma-Aldrich	W4502-1L
Non-essential amino acid 100x	Sigma-Aldrich	M7145-100ML
OneComp eBeads™ compensation beads	Invitrogen	01-1111-42

Reagents	Supplier	Catalogue #
PageRuler™ Plus prestained protein ladder	Thermo Scientific™	26620
Pam2CysSerLys4 (Pam_2CSK4)	Invivogen	tlrl-pm2s-1
Pam3CysSerLys4 (Pam_3CSK4)	Invivogen	tlrl-pms
Phosphate-buffered saline (PBS)	Sigma-Aldrich	D8537-500ml
Penicillin Streptomycin	Gibco	15070-063
Polyinosinic-polycytidylic acid [Poly (I:C)]	Invivogen	tlrl-pic-5
Proteinase K	Qiagen	19131
Protogel	National Diagnostics	EC-890
RNase*ZAP*™	Ambion	R2020-250ML
Roswell Park Memorial Institute (RPMI) 1640 medium	Gibco	61870-044
SB-505124	Sigma-Aldrich	S4696-5MG
Sodium pyruvate 100 mM	Sigma-Aldrich	S8636-100ML
Tetramethylethylenediamine (TEMED)	Sigma-Aldrich	T9281 -100ml
3,3',5,5'-tetramethylbenzidine (TMB)	MOSS, Inc.	TMB-US-1L
Tris base	Sigma-Aldrich	T6066-5KG
Tris-HCl	Thermo Scientific™	15893661
Tween-20	Sigma-Aldrich	P1379-500ml
Zymosan	Invivogen	tlrl-zyn
1 kb DNA ladder	New England Biolabs	N3232S
1X red blood cell (RBC) lysis buffer	Invitrogen	00-4333-57
2X DreamTaq Green PCR Master Mix	Thermo Scientific™	K1082
2X PerfeCTa® SYBR® Green FastMixes™	Avantor	733-1386
(±)-ML 209	Tocris	5987

2.1.2 Kits

Kits	Supplier
Naïve $CD4^+$ T cell Isolation Kit	Miltenyi
Murine IL-1β ELISA Kit	R&D Systems
Murine IL-4 ELISA Kit	R&D Systems
Murine IL-6 ELISA Kit	R&D Systems
Murine IL-10 ELISA Kit	R&D Systems
Murine IL-17 ELISA Kit	R&D Systems
Murine TNF-α ELISA Kit	R&D Systems
Murine IFN-γ ELISA Kit	R&D Systems

2.1.3 Antibodies

2.1.3.1 Antibodies for immunoblotting

Primary Antibody	Supplier	Dilution	Diluent
Extracellular signal-regulated kinase (ERK)	Cell Signalling	1:1000	5% BSA TBST
IRF4	Cell Signalling	1:1000	5% BSA TBST
c-Jun N-terminal kinases (JNK)	Cell Signalling	1:1000	5% BSA TBST
Pellino 1/2	Santa Cruz	1:200	5% BSA TBST
Phospho-ERK	Cell Signalling	1:1000	5% BSA TBST
Phospho-JNK	Cell Signalling	1:1000	5% BSA TBST
Phospho-p38	Cell Signalling	1:1000	5% BSA TBST
p38	Cell Signalling	1:1000	5% BSA TBST
STAT3	Cell Signalling	1:1000	5% BSA TBST
β-actin	Sigma Aldrich	1:4000	5% BSA TBST

Secondary Antibody	Supplier	Dilution	Diluent
IRDye® 680RD Goat anti-Mouse	Li-cor	1:5000	5% BSA TBST
IRDye® 680RD Goat anti-Rabbit	Li-cor	1:5000	5% BSA TBST

2.1.3.2 Antibodies for IFN-β ELISA

Antibody	Supplier	Dilution	Diluent	Function
Rat anti-Mouse IFN- β	Santa Cruz	1:1000	1% BSA PBS	Capture
Rat anti-Mouse IFN- β	PBL	1:2000	1% BSA PBS	Detection
Anti-Rabbit HRP	Promega	1:2000	1% BSA PBS	Reporter

2.1.3.3 Antibodies for flow cytometry

Antibody	Clone	Target	Supplier	Dilution
Zombie NIR™ Dye	-	Cell viability	Biolegend	1:1000
Fc block	2.4G2	Fc receptor	BD Pharmingen	1:100
CD3 PE-Cy7	145-2C11	CD3 T cell	BD Pharmingen	1:100
CD4 PerCP	RM4-5	CD4 T cell	Biolegend	1:200
CD8 ef450	53-6.7	CD8 T cell	Invitrogen	1:200
γδTCR PE	eBioGL3	γδTCR T cell	Invitrogen	1:200
CD62L FITC	MEL-14	Naïve T cell	Biolegend	1:200
CD44 APC	IM7	Memory T cell	Invitrogen	1:200
B220 V500	RA3-6B2	B cell	BD Horizon	1:200
CD21 FITC	7E9	MZ B cell	Biolegend	1:200
CD138 PE	281-2	Plasma cell	Biolegend	1:200
CD23 PerCP	B3B4	Follicular B cell	Invitrogen	1:200
CD19 APC	eBio1D3	B1 and B2 cell	Invitrogen	1:200
CD95 PE-Cy7	Jo2	GC B cell	BD Pharmingen	1:200
GL-7 ef450	GL-7	GC B cell	Invitrogen	1:200

2.1.4 Primer Sequences

2.1.4.1 Real-time PCR primers

Gene	**Primer Sequence 5'-3'**
Murine HPRT	Forward: AGGGATTTGAATCACGTT
	Reverse: TTTACTGGCAACATCAACAG
Murine *Il17a*	Forward: TCCAGAAGGCCCTCAGACTA
	Reverse: TCAGGACCAGGATCTCTTGC
Murine *Il17f*	Forward: CCCCATGGGATTACAACATCAC
	Reverse: CATTGATGCAGCCTGAGTGTCT

2.1.4.2 DNA PCR primers

Allele	**Primer Sequence 5'-3'**
Murine *Peli1*	Forward: GCTGTTCTGGAGATGAGCACTT
	Reverse: CCTTGGCAGCCTGAGGAGTA
Murine *Peli2* (reaction 1)	Forward: GCCTCTACAGGATGCTCATTT
	Reverse: GGACAGTCATGCTAGTCTGAGG
Murine *Peli2* (reaction 2)	Forward: CGTGTCCATCACTCTTAAATGAA
	Reverse: GCACCATTGTACCTAAAGTAGAGAC
Murine *Peli3* (reaction 1)	Forward: GTGCATACACATTCATGCAAGC
	Reverse: CCCAACATAGGTGTTTCCTCTCC
Murine *Peli3* (reaction 2)	Forward: GACACGTGTGGAGATAATGAGG
	Reverse: ACCCAGGCACAAGTCAAGC
Housekeeping (control)	Forward: GAGACTCTGGCTACTCATCC
	Reverse: CCTTCAGCAAGAGCTGGGGAC

2.1.5 Buffers

Buffer	Ingredients
4X Laemmli sample buffer	0.25 M Tris-HCl, pH 6.8, 6% (w/v) SDS, 40% (w/v) glycerol, 0.04% (w/v) bromophenol blue, 20% (v/v) β-mercaptoethanol
4X Laemmli lower tris buffer	1.5M Tris, 0.4% (w/v) SDS, pH 8.8
4X Laemmli upper tris buffer	0.5M Tris, 0.4% (w/v) SDS, pH 6.8
SDS running buffer	25 mM Tris, 192 mM glycine, 0.1% (w/v) SDS, pH 8.3
Laemmli transfer buffer	25 mM Tris, 192 mM glycine, 15% (v/v) methanol
Tris-Acetate-EDTA (TAE) buffer	40 mM Tris base, 0.1% (v/v) glacial acetic acid, 1mM EDTA disodium salt dihydrate
Tris buffered saline (TBS)	25 mM Tris, 0.14 M NaCl, pH 7.4
Block buffer (Immunoblotting)	TBS, 0.1% (v/v) Tween-20, 5% (w/v) BSA or non-fat dry milk powder
Block buffer (ELISA)	PBS, 1% (w/v) BSA
Wash buffer (ELISA)	PBS, 0.05% (v/v) Tween-20
FACS buffer	PBS, 2% (w/v) HI-FBS
T cell media	RPMI 1640 containing L-Glutamine, 10% (v/v) FBS, 1% (v/v) 5000 units/ml penicillin 5000 μg/ml streptomycin, 0.4% (v/v) MEM Vitamin solution 100x, 1% (v/v) non-essential amino acid 100x, 0.1% (v/v) B-mercaptoethanol, 1% (v/v) sodium pyruvate

2.1.6 Gifts

Reagents below were gifted by Dr. Eoin McNamee (Maynooth University):

Reagents	Supplier	Catalogue Number
BAY-11-7085 (10mM)	Tocris	1743
JSH-23 (10mM)	Sigma-Aldrich	J4455
Ruxolitinib (10mM)	Selleck Chem	S1378
AMG 548 (10mM)	Tocris	3920
SP 600125 (10mM)	Tocris	1496
FR 180204 (10mM)	Tocris	3706
Everolimus (10mM)	Tocris	6188

Reagents below were gifted by Dr. Andrew Hogan (Maynooth University):

Reagents	Supplier	Catalogue #
autoMACS® running buffer [magnetic activated cell sorting (MACS) buffer]	Miltenyi	130-091-221

2.2 Methods

2.2.1 Mice

2.2.1.1 Generation of Pellino-knockout mice

C57BL/6 mice were used as wild type (WT) mice with intact Pellino proteins. Pellino 2-deficient (*Peli2*$^{-/-}$) and Pellino 3-deficient (*Peli3*$^{-/-}$) mice were created by Taconic Artemis using patented technology (Humphries *et al.*, 2018; Siednienko *et al.*, 2012). Heterozygous Pellino 1-deficient on a Pellino 2 & 3-double knockout background mice (*Peli1*$^{+/-}$*Peli2/3*$^{-/-}$) were generated by the Transgenics Facility in Trinity Biomedical Science Institute using clustered regularly interspaced short palindromic repeats (CRISPR). This procedure was performed with the approval of Animal Research Ethics Committee in Trinity College Dublin (Ref: 241109 and 111012).

Following that, *Peli2/3*$^{-/-}$ mice were mated with *Peli*$^{+/-}$*Peli2/3*$^{-/-}$ mice to generate Pellino triple-knockout (*Peli1/2/3*$^{-/-}$) mice (Figure 2.1). Subsequently, Pellino double-knockout (*Peli1/2*$^{-/-}$ and *Peli1/3*$^{-/-}$) mice were generated through the mating of *Peli1/2/3*$^{-/-}$ mice and *Peli2*$^{-/-}$ or *Peli3*$^{-/-}$ mice, leading to the establishment of double-knockout mice colony (Figure 2.2). A multi-step breeding has been deployed to generate Pellino 1-deficient (*Peli1*$^{-/-}$) mice (Figure 2.3). Firstly, *Peli1*$^{+/-}$*Peli2/3*$^{-/-}$ mice were mated with WT mice to produce *Peli1/2/3*$^{+/-}$ mice, which were crossed with the same genotype, yielding various combinations. By crossing two *Peli1*$^{+/-}$ offsprings, *Peli1*$^{-/-}$ mice were generated.

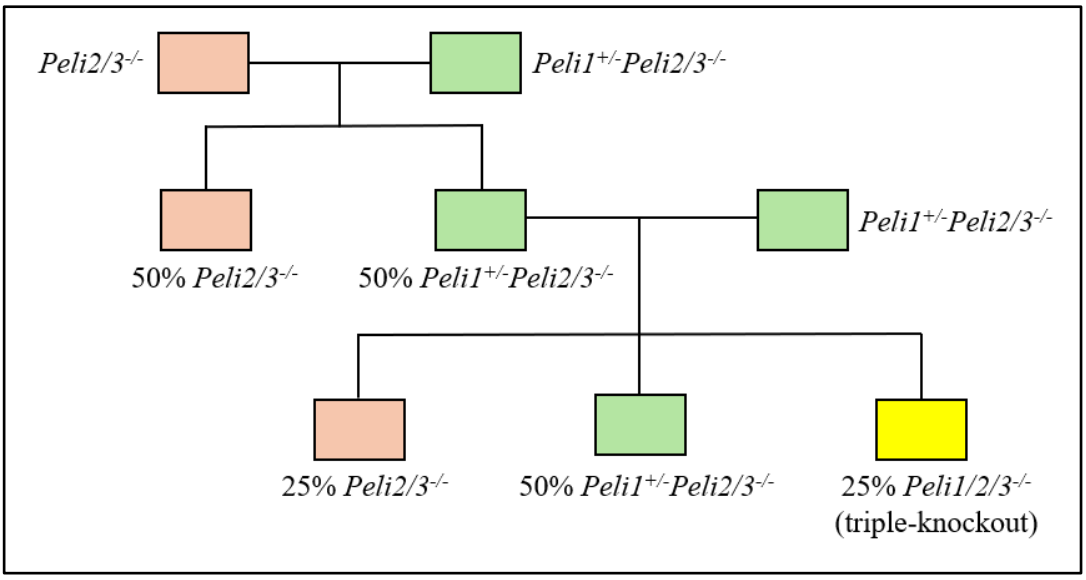

Figure 2.1 Breeding strategy of Pellino triple-knockout mice

Schematic figure showing the generation of Pellino triple-knockout offspring through two-step breeding, creating Pellino triple-knockout colony.

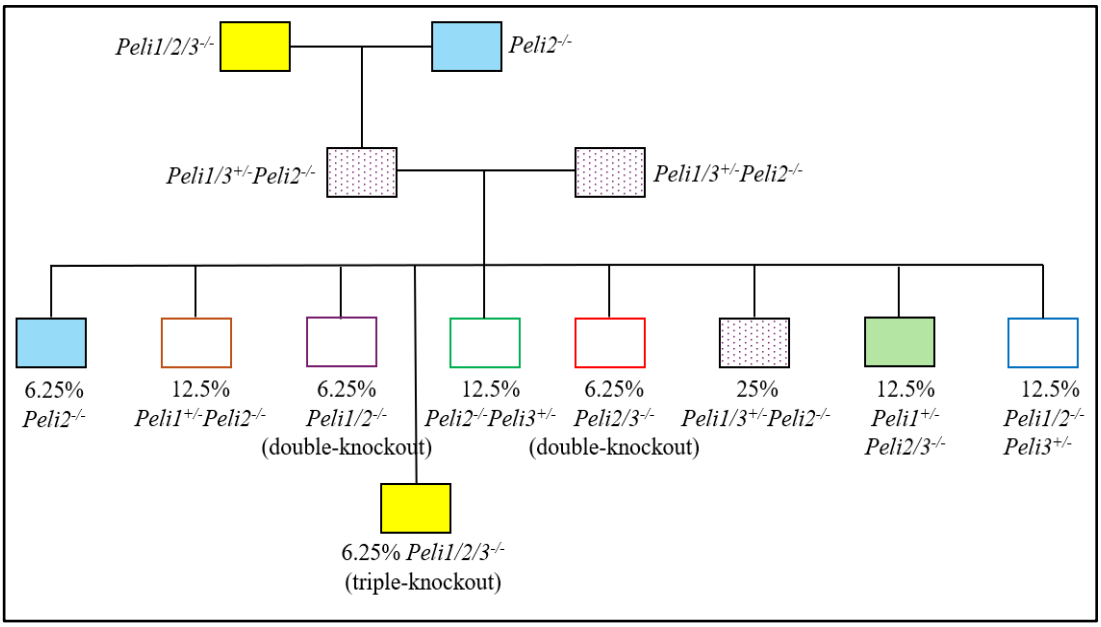

Figure 2.2 Breeding strategy of Pellino double-knockout mice

Representative schematic figure showing the generation of Pellino double-knockout offspring through two-step breeding, creating Pellino double-knockout colony.

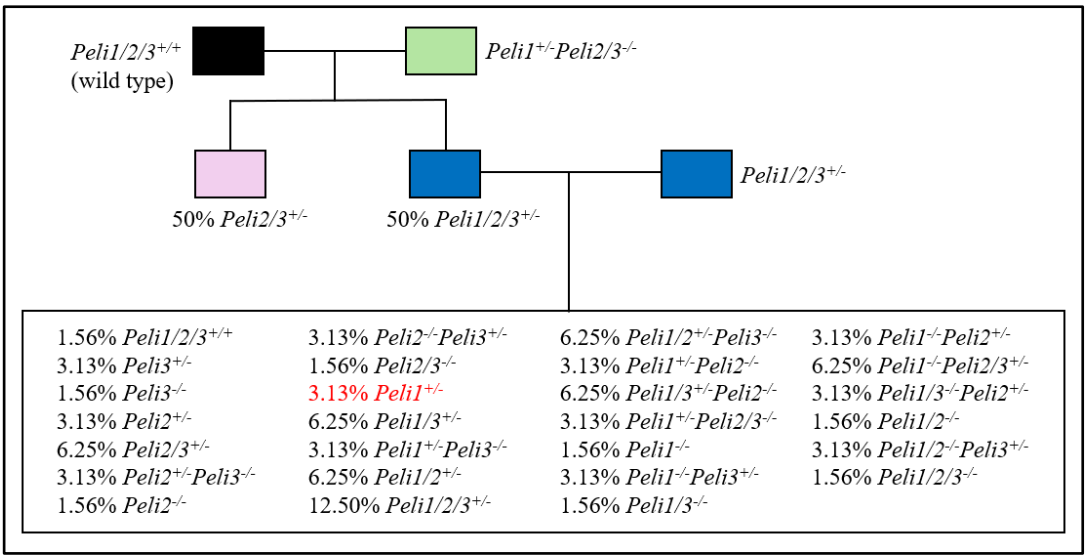

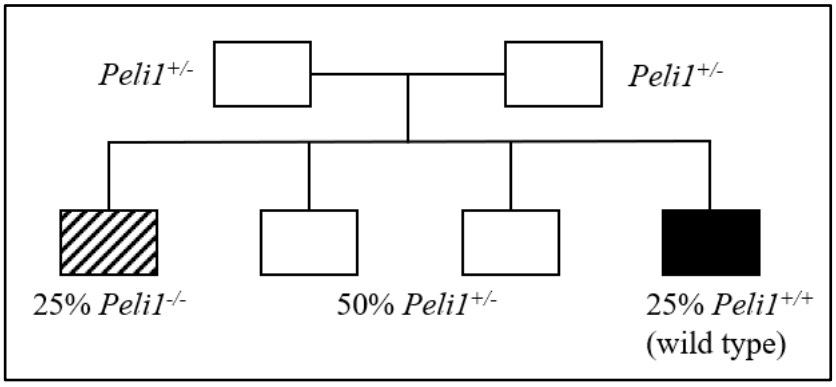

Figure 2.3 Breeding strategy of *Peli1*$^{-/-}$ mice

Representative schematic figure showing the generation of *Peli1*$^{+/-}$ mice (upper panel), which were heterozygous parents to *Peli1*$^{-/-}$ mice (lower panel).

All Pellino single-knockout (SKO) mice used for experiments in Chapter 3 and 4 were matched with littermate WT mice (labelled as WT x SKO in Chapter 3 figures) whenever possible. All Pellino double-knockout and triple-knockout mice used for experiments in Chapter 3 and 4 were matched with WT mice from the WT colony (labelled as WT colony in Chapter 3 figures) whenever possible. WT x SKO and WT colony mice were pooled together as WT for statistical analysis in Chapter 3. 10-12 weeks old mice were used as young mice, whereas 6 months old mice were used as old mice in Chapter 3. 8-10 weeks old mice were used in Chapter 4 if not otherwise specified.

2.2.1.2 Genotyping

3-week-old mice were earpunched by Bioresource Unit staff. 1.4 µl of Proteinase K (0.4 mg/ml) and 70 µl of DirectPCR lysis reagent (Tail) were added to the tissue samples stored in sterile 1.5 ml tubes. The samples were then lysed to generate crude DNA by incubating at 55 ^{o}C for a minimum of 3 hours or overnight. Samples were incubated for an additional 45 minutes at 85 ^{o}C to inactivate Proteinase K. Samples were vortexed briefly and subjected to short-spin centrifugation for 5 seconds to collect cell debris. 2 µl of supernatant was used as DNA template for PCR amplification. Predesigned DNA primers were used to facilitate amplification of DNA generated. Remaining DNA samples were stored at -20°C. The reagents that made up a final volume of 20 µl reaction mix prepared on ice were outlined as below:

Pellino 1

Reagent	**Volume (µl)**
2X DreamTaq Green PCR Master Mix	10
Forward Primers (100 µM)	0.5
Reverse Primers (100 µM)	0.5
DNA	2
Nuclease-free Water	7

Pellino 2 and Pellino 3 – reaction 1

Reagent	**Volume (µl)**
2X DreamTaq Green PCR Master Mix	10
Forward Primers (100 µM)	0.25
Reverse Primers (100 µM)	0.25
Housekeeping primer 1260-1 (100 µM)	0.2
Housekeeping primer 1260-2 (100 µM)	0.2
DNA	2
Nuclease-free Water	7.1

Pellino 2 and Pellino 3 – reaction 2

Reagent	Volume (µl)
2X DreamTaq Green PCR Master Mix	10
Forward Primers (100 µM)	0.25
Reverse Primers (100 µM)	0.25
DNA	2
Nuclease-free Water	7.5

Samples were amplified using an Applied Biosystems Step One™ real-time PCR instrument. DNA denaturation was initiated at 95°C for 5 minutes before samples were subjected to 30 cycles of 95°C for 30 seconds to denature DNA, 60°C for 30 seconds to anneal DNA, and 72°C for 1 minute to extend DNA. A final extension step was performed at 72°C for 10 minutes before the product was being incubated at 4°C. PCR products were stored at -20°C or immediately quantified by agarose gel electrophoresis.

Agarose gel was prepared by adding 2 g of agarose to 100 ml of Tris-Acetate-EDTA buffer. This solution was heated to fully dissolve agarose and allowed to cool to below 50°C. 10 µl of GelRed® Nucleic Acid Gel Stain (1:10000 dilution) was added to the solution and swirled to mix before it was poured into a pre-assembled gel tray with well combs. The solution was left at room temperature for at least 15 minutes to solidify into gel, which was then transferred to the electrophoresis rig filled with TAE buffer. 10 µl of amplified PCR mixture alongside a 1 kb DNA ladder was loaded to the gel and subjected to electrophoresis at 90 volts. DNA bands were visualized under ultraviolet light (254 nm) in a Syngene G:Box and images captured were printed for analysis and recording purposes.

2.2.2 Cell culture

2.2.2.1 Isolation and culture of primary bone marrow derived dendritic cells (BMDCs)

Age and gender matched WT and Peli1-/- mice were sacrificed by cervical dislocation. In a laminar flow hood, femurs and tibias of mice were removed after being sterilised with EtOH (70% (v/v)). 10 ml of media [RPMI supplemented with heat inactivated FBS (10% (v/v)), penicillin G (100 µg/ml) and streptomycin (100 µg/ml)] was used to flush the bone marrow into a 50ml tube with a 27-gauge needle. Cells were then centrifuged at 400 g for 5 minutes. Supernatant was discarded and the pellet was resuspended in 8 ml of media. 2ml of cells were added to a T175 cm^2 culture flask, and 30 ml of media containing 20 ng/ml (6 µl) GM-CSF (100 µg/ml) was then added. Cells were incubated at 37^oC in a humidified chamber conditioned with 5% CO_2 for 3 days before cells were fed with an additional pre-warmed 30 ml of media GM-CSF (20 ng/ml). Supernatant was removed from the flask 3 days later and replenished with 30 ml of media containing GM-CSF (20 ng/ml) before returning to culture. On the following day, 30 ml of RPMI, supplemented with GM-CSF, was gently added to cells which were cultured for a further 3 days. Differentiated non-adherent BMDCs were collected and pelleted by centrifugation at 400 g for 5 minutes. Cells were resuspended in 10 ml media and counted using a Countess counter. Cells were made up to 6.25 x 10^5 cells/ml and plated 200 µl in a 96-well U bottom plate for downstream cytokine analysis. Cells were cultured in a 37^oC humidified chamber under a 5% CO_2 atmosphere for at least 2 hours or overnight before being subjected to desired treatments. To investigate possible regulatory functions of Pellino 1 in antigen presenting cells, TLR ligands were added to the treated group (concentrations of ligands outlined in Figure 4.13). Cells were incubated in a 37°C humidified chamber under a 5% CO_2 atmosphere for 24 hours. After centrifuging samples at 800 g for 3 minutes, 200 µl of supernatant was stored at -20°C or immediately measured for levels of TNF-α, IL-6, IL-12 p40, IL-12 p70, and IFN-β by sandwich enzyme-linked immunosorbent assay.

2.2.2.2 Isolation and culture of splenocytes

Mice were sacrificed and weighed. Spleens were isolated under sterile environment in a laminar flow hood. Spleens were weighed and stored in 5 ml ice-cold media [RPMI supplemented with heat inactivated FBS (10% (v/v)), penicillin G (100 µg/ml) and streptomycin (100 µg/ml)]. Spleens were passed through 70 µm strainers and collected into 15 ml tubes by flushing the strainers twice with 2.5 ml of ice-cold media to obtain single cell suspension. Spleen cells were then subjected to centrifugation at 400 g for 5 minutes at room temperature (RT), followed by the removal of supernatant. Cell pellets were resuspended in 3 ml of 1X RBC lysis buffer and the suspensions were left at RT for 3 minutes. 12 ml of ice-cold media was added to each sample to stop the lysis before being centrifuged at 400 g for 5 minutes at RT. Supernatant was discarded and cell pellets were resuspended in 5 ml of ice-cold T cell media. Spleen cells were counted and seeded (2×10^6 cells/ml; 200 µl) in 96-well plates. 50 µl of anti-CD3 (0.5 µg/ml), diluted in cold sterile PBS, was added to wells of a 96-well plate prior to incubation at 4°C overnight. Plate bound anti-CD3 was washed with 200 µl of PBS twice to remove any unbound anti-CD3. 50 µl of T cell media and 50 µl of anti-CD28 (0.5 µg/ml) diluted in T cell media were added to untreated group and stimulated group, respectively. To investigate the potential pathway involved in IL-17 production, inhibitors were added to the treated group (indicated inhibitors outlined in figure 4.10). Cells were incubated in a 37°C humidified chamber under a 5% CO_2 atmosphere for 48 hours. After centrifuging samples at 800 g for 3 minutes, 200 µl of supernatant was stored at -20°C or immediately measured for levels of IL-4, IL-10, IL-17, IFN-γ, and TNF-α, by sandwich enzyme-linked immunosorbent assay.

2.2.2.3 Naïve $CD4^+$ T cell isolation

Spleen cells from an individual mouse or pooled from multiple mice were brought up to 10^8 total cells to ensure sufficient naive $CD4^+$ T cells yield. Splenocytes were centrifuged at 400 g for 5 minutes to generate cell pellets that were resuspended in 40 µl of ice cold magnetic activated cell sorting buffer per 10^7 total cells. Naive $CD4^+$

T cells were isolated from mouse splenocytes using the reagents in the naïve $CD4^+$ T cell isolation kit from Miltenyi. 10 µl of Biotin-Antibody Cocktail per 10^7 total cells was added to cells and mixed well for a 5-minute incubation in the refrigerator (2-8°C). Following that, 20 µl of MACS buffer per 10^7 total cells, 20 µl of Anti-Biotin Microbeads per 10^7 total cells, and 10 µl of CD44 Microbeads per 10^7 total cells were added to cells and mixed well for a 10-minute incubation in the refrigerator. Cells were washed with 100 µl of MACS buffer per 10^7 total cells before being subjected to centrifugation at 300 g for 10 minutes. LS column was setup in the magnetic field of a QuadroMACS™ Separator and rinsed with 3 ml of MACS buffer. Supernatant was completely removed using pipettes and cell pellets were resuspended in 550 µl MACS buffer to be passed through the LS column. By employing the negative cell isolation using this MACS technology, unlabelled cells in the flow through representing the enriched naive $CD4^+$ T cells were collected in a 15 ml tube together with the subsequent 3 ml of MACS buffer used to wash the column. Cells were centrifuged at 400 g for 5 minutes and resuspended in 1 ml T cell media for cell counting. 5×10^5 cells/ml of naive $CD4^+$ T cells were seeded 200 µl per well in 96-well plates for cytokine analysis, whereas naive $CD4^+$ T cells were seeded (1×10^6 cells/ml; 500 µl) in 24-well plates for protein analysis.

2.2.2.4 Th17 cell differentiation *in vitro*

Purified naive $CD4^+$ T cells from spleen cells were counted and seeded (5×10^5 cells/ml; 200 µl) in 96-well round-bottom plates. 50 µl of anti-CD3 (1 µg/ml), diluted in cold sterile PBS, was added to wells of a 96-well plate prior to incubation at 4°C overnight. Plate bound anti-CD3 was washed with 200 µl of PBS twice to remove any unbound anti-CD3. 50 µl of T cell media and 50 µl of anti-CD28 (5 µg/ml) diluted in T cell media were added to untreated group and stimulated group, respectively. In stimulated group for Th17 cell differentiation, naive $CD4^+$ T cells were also treated with polarising cytokines: (i) TGF-β (5 ng/ml) and IL-6 (20 ng/ml) or (ii) IL-1β (20 ng/ml) and IL-23 (20 ng/ml) in the presence of anti-IFN-γ (10 µg/ml) and anti-IL-4 (10 µg/ml). Cells were incubated in a 37°C humidified chamber under a 5% CO_2 atmosphere for 96 hours. After centrifuging samples at 800 g for 3 minutes,

200 µl of supernatant was stored at -20°C or immediately measured for levels of IL-17 by sandwich enzyme-linked immunosorbent assay.

2.2.3 Flow cytometry

2.2.3.1 Extracellular staining

$2x10^6$ spleen cells from WT and Peli1$^{-/-}$ mice were transferred to a V-bottom plate for extracellular staining. Cells were washed with 250 µl ice cold PBS and centrifuged at 400 g for 5 minutes. 100 µl of Fixable Viability Zombie NIR™ Dye (1000x dilution in PBS) was added to cells, whereas 100 µl of PBS was added to unstained controls. Cells were incubated at 4°C for 20 minutes in dark (plate covered with aluminium foil). CFSE-labelled cells were not stained with Fixable Viability Zombie NIR™ Dye to avoid interaction with CFSE within the cells. 150 µl of ice cold fluorescence-activated cell sorting (FACS) buffer (PBS containing 2% heat inactivated-FBS) was added to cells, followed by centrifugation at 400 g for 5 minutes. 50 µl of Fc block (100x dilution in FACS buffer) was added to all samples to prevent non-specific antibody binding. Cells were incubated at 4°C for 10 minutes in dark before adding 50 µl of T cell and B cell surface staining mastermix to cells (concentrations of antibodies outlined in section 2.1.3.3). Compensation samples were also prepared by mixing 1 drop of compensation beads and 1 µl of antibody in 50 µl of FACS buffer. Subsequently, cells and compensation samples were incubated at 4°C for 15 minutes in the dark. During this incubation, unstained control was incubated with 50 µl of FACS buffer only to be used as a negative control. Samples were centrifuged at 400 g for 5 minutes after 150 µl of FACS buffer was added to samples. Samples were resuspended in 100 µl of FACS buffer and 100 µl IC Fixation buffer before being transferred to 1.5 ml tubes for acquisition by Attune flow cytometry. Flow cytometry data was analysed using FlowJo software.

2.2.3.2 Carboxyfluorescein succinimidyl ester (CFSE) analysis

Single-cell suspension of splenocytes were washed twice with 5 ml of PBS and subjected to centrifugation at 400 g for 5 minutes. Cells were counted, diluted to 1 $x10^7$ splenocytes and 1 ml of this suspension was added to a 15 ml tube. The tube was laid horizontally. 110 µl of PBS was added to the top of the tube and 1.1 µl of the 5 mM stock of CFSE was added to the PBS. The tube was then securely capped and vortexed briefly. Splenocytes were labelled with CFSE (5 µM) by incubating for 5 minutes at RT in the dark (tube covered with aluminium foil). The reaction was halted by adding 10 ml of PBS containing 5% of heat inactivated FBS and the suspension was centrifuged at 300 g for 5 minutes. The cell pellet was washed in the same manner twice. CFSE-labelled spleen cells were counted and cultured ($2x10^6$ cells/ml; 200 µl) in 96-well plates in a 37°C humidified chamber under a 5% CO_2 atmosphere for 72 hours. Cells were either untreated or treated with plate bound anti-CD3 (1 µg/ml) and soluble anti-CD28 (1 µg/ml) diluted in T cell media. Non CFSE-labelled spleen cells were also cultured as a negative control.

2.2.3.3 Gating strategy

Lymphocytes were gated according to the forward scatter area (FSC-A) and side scatter area (SSC-A). To exclude doublets, cells were gated on forward scatter height (FSC-H) against FSC-A. The Zombie NIR™ dye-negative cells represents the live singlets. In this population, T cell and B cell subsets were selected using different cell surface markers (subset cell surface markers outlined in section 2.1.3.3) (Figure 2.4 and Figure 2.5). The purity of $CD11b^+$-depleted spleen cells and naïve $CD4^+$ T cells ($CD44^{low}$ and $CD62L^{hi}$) were also determined from live single cells using flow cytometry (Figure 2.6 and Figure 2.7).

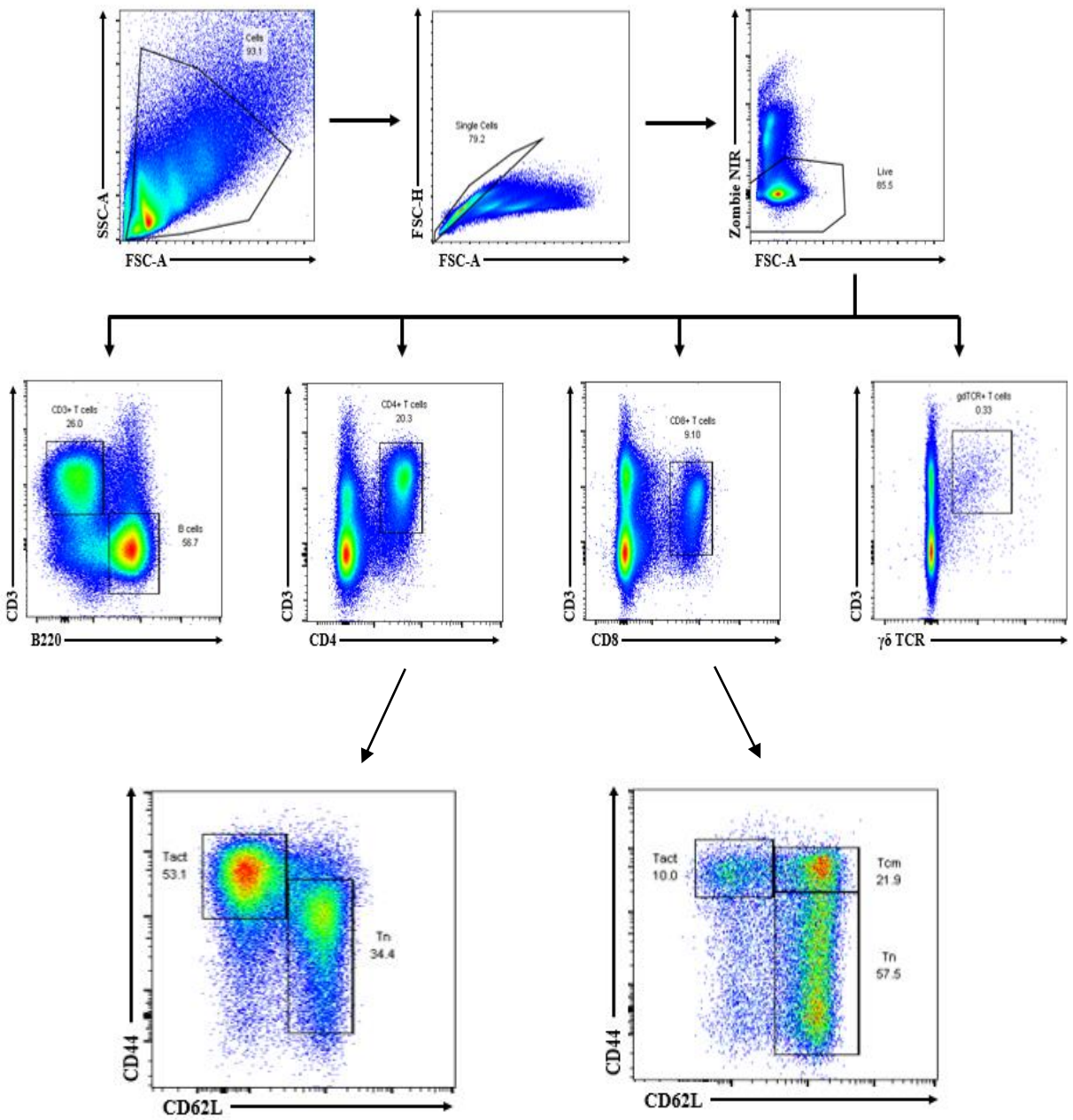

Figure 2.4 T cell subsets identification of a WT mouse using flow cytometric antibodies

Representative dot plots showing gating strategy of T cell subsets in the murine spleen by flow cytometry using extracellular antibodies against Zombie NIR, CD3, B220, CD4, CD8, γδTCR, CD44, and CD62L conjugated to appropriate fluorochromes.

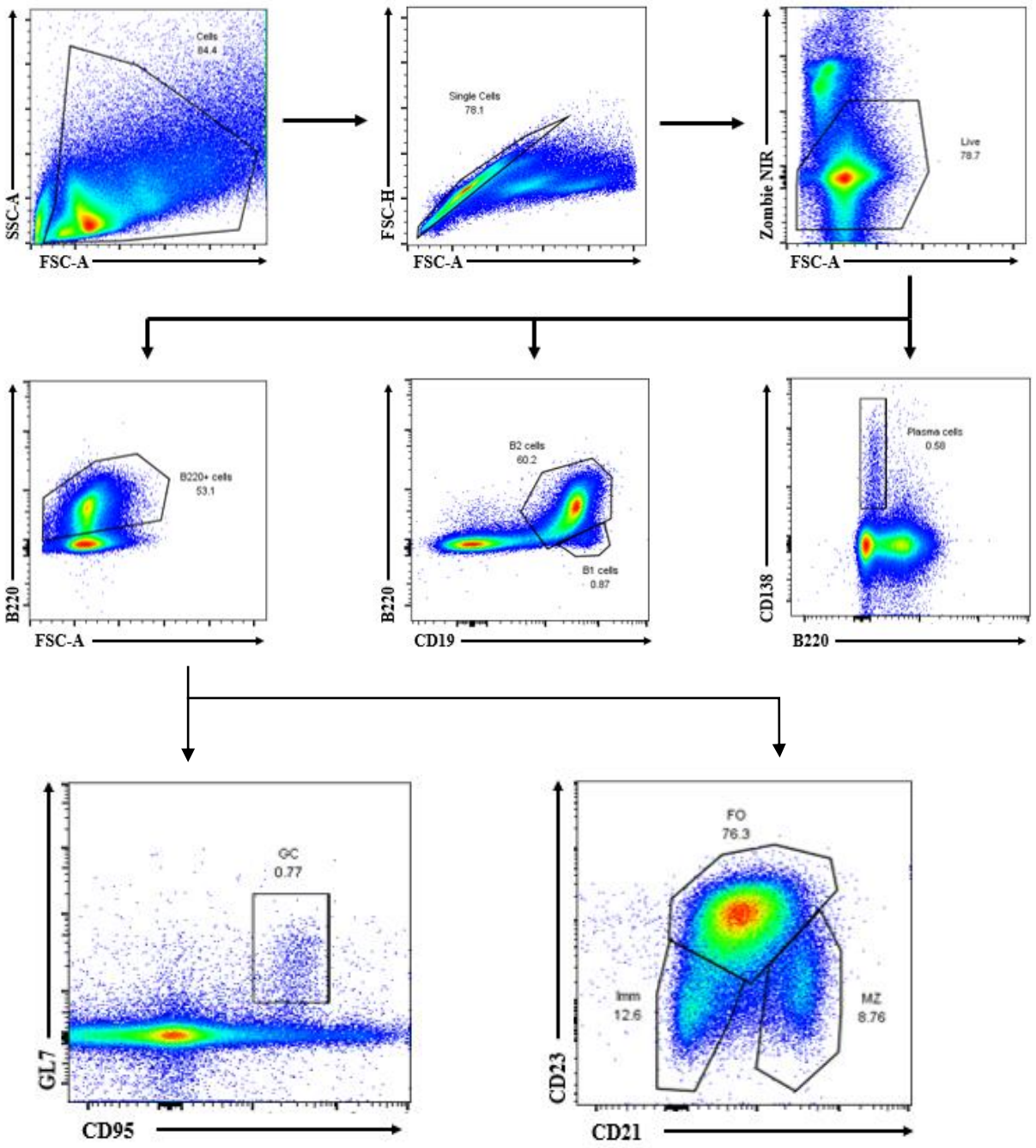

Figure 2.5 B cell subsets identification of a WT mouse using flow cytometric antibodies

Representative dot plots showing gating strategy of B cell subsets in the murine spleen by flow cytometry using extracellular antibodies against Zombie NIR, B220, CD19, CD138, GL7, CD95, CD23, and CD21 conjugated to appropriate fluorochromes.

(a)

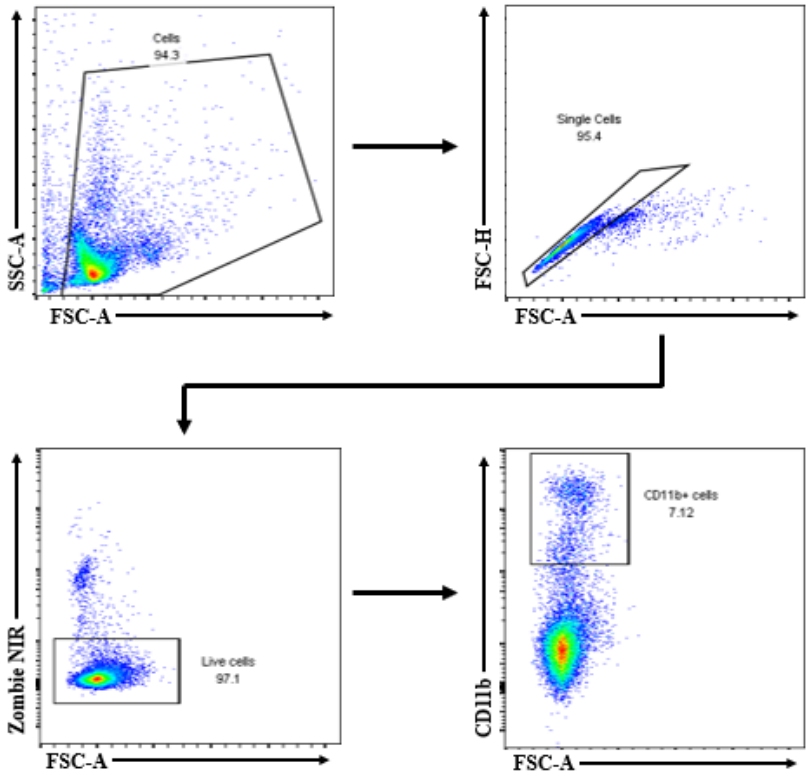

(b)

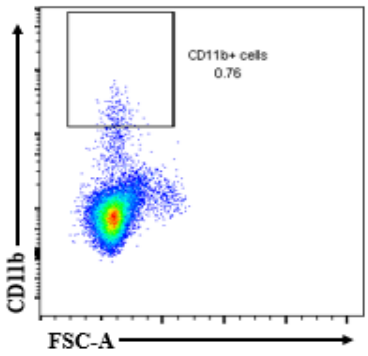

Figure 2.6 CD11b$^+$-depleted spleen cells isolated from a WT mouse confirmed using flow cytometric antibodies

Representative dot plots of (a) spleen cells without CD11b$^+$ depletion and (b) CD11b$^+$-depleted spleen cells were identified using extracellular antibodies against Zombie NIR and CD11b conjugated to appropriate fluorochromes. CD11b is a marker for myeloid cells.

(a)

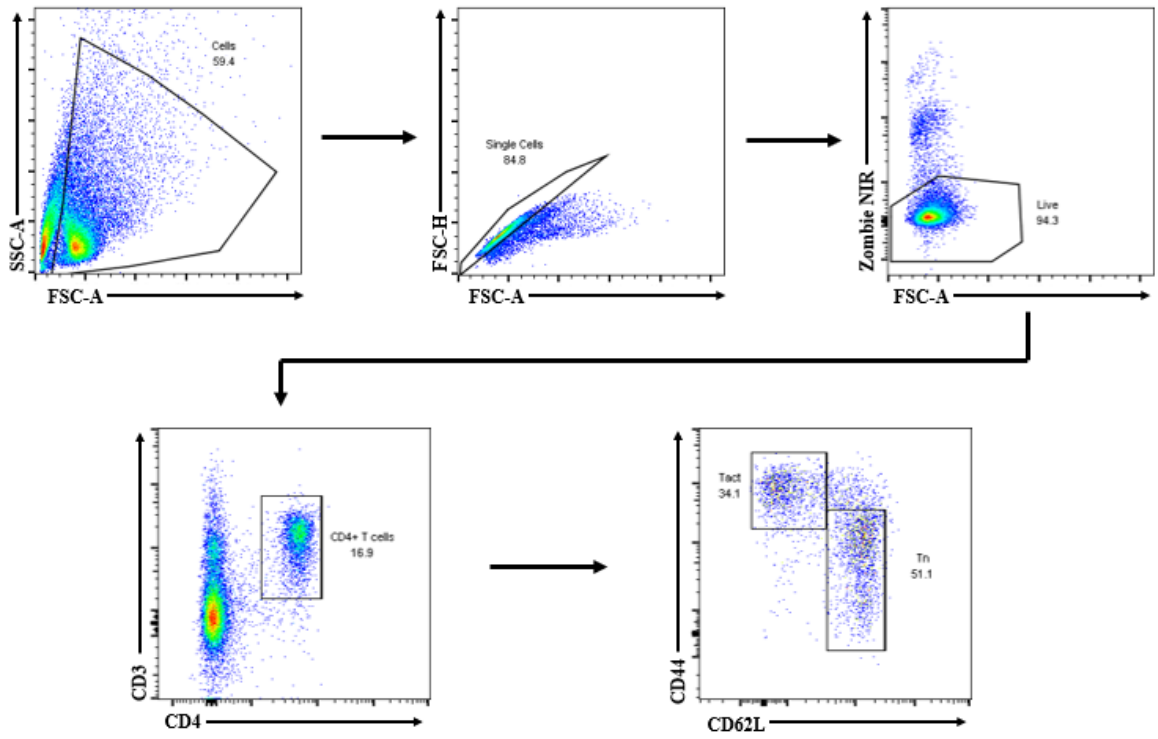

(b)

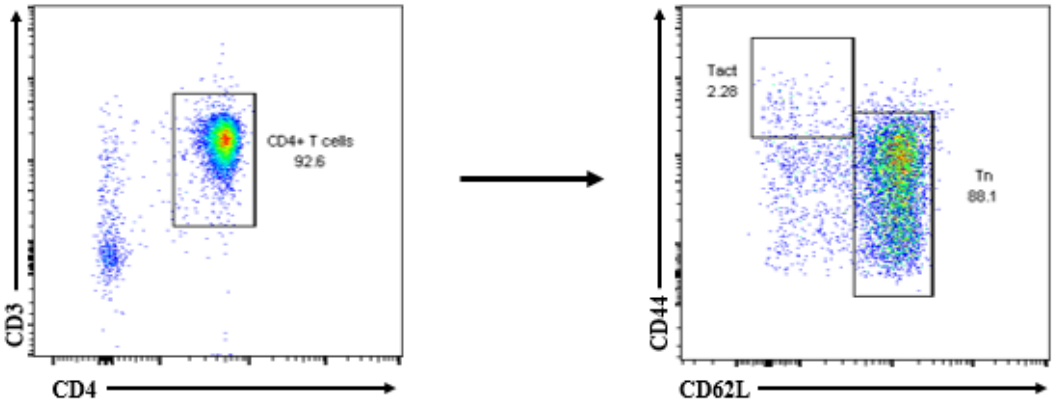

Figure 2.7 Enriched naïve CD4⁺ T cells isolated from a Pellino-1 deficient mouse confirmed using flow cytometric antibodies

Representative dot plots showing (a) gating strategy of spleen cells without naïve CD4⁺ T cells enrichment using extracellular antibodies against Zombie NIR, CD3, CD4, CD44, and CD62L conjugated to appropriate fluorochromes. (b) Purified naïve CD4⁺ T cells from spleen cells were confirmed after isolation using MACS technology.

2.2.4 Enzyme-linked immunosorbent assay (ELISA)

2.2.4.1 ELISA for IFN-γ, TNF-α, IL-4, IL-6, IL-10, IL-12 p40, IL-12 p70, IL-17

96-well assay plates (Costar®) were coated with 25 µl of 120-fold diluted capture antibody in PBS. Plates were covered with cling film to avoid evaporation and incubated overnight at 4°C. Plates were washed three times with a wash buffer (PBS-T). Plates with blocked with 100 µl diluent (1% (w/v) BSA in PBS) in each well at RT for a minimum of 1 hour. Plates were washed three times again with PBS-T. 25 µl of samples were added (neat or diluted in reagent diluent). Wells with standards were also coated with 25 µl of 2-fold serial diluted standards from a top working concentration. Plates were covered and incubated overnight at 4°C. Plates were washed three times with PBS-T. 25 µl of detection antibody diluted 60-fold in diluent was added to each well. Plates were incubated at RT for 2 hours and the wash step was repeated. 25 µl of Streptavidin-horseradish peroxidase (HRP) diluted 40-fold in diluent was added to every well followed by incubation at RT for 30 minutes. Plates were washed three times with PBS-T again. 25 µl of enzyme substrate (TMB) was added to every well and the plates were incubated in dark for 10 to 15 minutes. When the colour changed, 13 µl of 10% sulfuric acid was added to each well to halt the reaction. The optical density (OD) value of each well was measured at 450 nm and 590 nm by a microplate reader. Standards and samples were assayed in triplicate. A standard curve was generated from the standards to determine the sample concentrations. Data analysis was performed using GraphPad Prism 6 software.

2.2.4.2 ELISA for IFN-β

Plates were coated with 25 µl of 1000-fold diluted monoclonal rat anti-mouse IFN-β in PBS. Plates were covered with cling film and incubated on an orbital shaker at RT. Plates were washed three times with a wash buffer (PBS-T). Plates with blocked with 100 µl reagent diluent (1% (w/v) BSA in PBS) in each well at RT for 2 hours. Plates were washed three times again with PBS-T. 25 µl of samples were added either neat

or diluted in reagent diluent. Wells with standards were also coated with 25 µl of 2500-fold serial diluted standards from a top working concentration (2 ng/ml). Plates were covered and incubated overnight at 4°C. Plates were washed three times with PBS-T. 25 µl of polyclonal rabbit anti-mouse IFN-β diluted 2000-fold in reagent diluent was added to every well. Plates were incubated at RT for 2 hours and the wash step was repeated. 25 µl of anti-rabbit Streptavidin-HRP diluted 3000-fold in diluent was added to each well followed by incubation at RT for 30 minutes. Plates were washed six times with PBS-T again. 25 µl of enzyme substrate (TMB) was added to every well and the plates were incubated in dark for 10 to 15 minutes. When the colour changed, 13 µl of 10% sulfuric acid was added to each well to stop the reaction. The OD value of each well was measured at 450 nm and 590 nm by a microplate reader. Standards and samples were assayed in triplicate. A standard curve was generated from the standards to determine the sample concentrations. Data analysis was performed using GraphPad Prism 6 software.

2.2.5 Western blot analysis

2.2.5.1 Protein harvest

Cells were harvested after indicated stimulations in a 37°C humidified chamber under a 5% CO_2 atmosphere. Cells were transferred to 1.5 ml tubes and centrifuged at 400 g for 5 minutes. Supernatant was removed. 80 µl of 2x sample buffer was added to each well and combined with the cell pellets in 1.5 ml tubes. Samples were boiled at 95°C for 5 minutes and stored at -20°C for downstream application.

2.2.5.2 Sodium dodecyl sulfate - polyacrylamide gel electrophoresis (SDS-PAGE)

5% acrylamide stacking gel and 8-15% resolving gel were prepared according to the recipe by Laemmli (Laemmli, 1970). A higher percentage resolving gel was used to ensure better resolution of smaller sized target protein. 2 µl of pre-stained protein

ladder (10-180 kDa) and same volume of samples (10-15 µl) were loaded into each well. The amount of protein loading was determined by the loading control (eg. β-actin) expression. Electrophoresis was performed at 80 V for approximately 90 minutes, followed by 100 V for 1.5 – 2 hours.

2.2.5.3 Immunoblotting

After protein separation by electrophoresis was completed, the proteins were transferred by electrophoresis again to nitrocellulose membranes. Whatmann paper and nitrocellulose membranes were soaked in the transfer buffer for 5 minutes prior to use. Three Whatmann papers were positioned at the bottom, stacked with the resolving gel and then a single layer of nitrocellulose before three more Whatmann papers were added at the top surface in a closed transfer unit. Following the transfer, membranes were washed briefly in TBST buffer. Membranes were then blocked with TBST containing 5% (w/v) BSA at RT in an orbital shaker for 1 hour to inhibit non-specific antibody binding. Membranes were incubated at 4°C overnight on an orbital shaker with primary antibody in blocking reagent as per dilution below. Membranes were incubated at RT under constant agitation for one hour with a secondary antibody that can detect the corresponding host species of the primary antibody in blocking reagent after they were washed 3 times in TBST for 5 minutes each time. Protein bands were visualised using the Odyssey infrared imaging system from Licor Biosciences.

2.2.6 Quantitative real-time polymerase chain reaction (PCR)

2.2.6.1 RNA isolation from splenocytes

While conditioned media of treated splenocytes were used for cytokine analysis, cell pellets pooled from three wells were transferred to RNase free tubes for mRNA analysis. Cells were lysed in 500 µl Trizol. Samples were subjected to RNA isolation immediately or stored at -20°C. 200 µl of chloroform per 1 ml of Trizol used was

added to samples. Tubes were capped and inverted for vigorous mixing. The homogenous mixture was incubated at RT for 2 minutes. Samples were centrifuged at 12,000 g for 15 minutes at 4°C to allow separation. Approximately 200 µl of the colourless upper aqueous phase was transferred to new RNase free tubes without disturbing the interphase or the lower red phenol-chloroform phase. 500 µl of isopropanol per 1 ml of Trizol used was added to the aqueous phase to precipitate the RNA. The solution was mixed by pipetting up and down before being incubated at RT for 10 minutes. RNA was pelleted by centrifugation at 12,000 g for 10 minutes at 4°C. Supernatant was removed, followed by resuspension of pellet in 1 ml of 75% (v/v) ethanol per 1 ml of Trizol used to wash the RNA. The mixture was vortexed briefly and centrifuged at 7,500 g for 5 minutes at 4°C. Ethanol was removed and the RNA pellet was air dried for 10 minutes. The pellet was resuspended in 20 µl of RNase-free water and incubated in a heat block at 60 °C for 10 minutes. The RNA concentration of each sample was measured by a Nanodrop™ spectrophotometer. An absorbance at 260 nm over absorbance at 280 nm ratio of 1.8-2.0 indicated pure RNA. RNA was stored at -80 °C for downstream application.

2.2.6.2 Complementary DNA (cDNA) synthesis from RNA

To make a DNA copy from mRNA, a master mix consisting of 1 µl of 50X Qscript reverse transcriptase (enzyme) and 4 µl of 5X Qscript reaction mix (buffer) per sample was prepared on ice. 15 µl of nuclease-free water was added to RNase free tubes, followed by 5 µl nuclease-free water containing 1 µg of RNA and 5 µl of the master mix, bringing the mixture to a final volume of 20 µl. Remaining RNA samples were stored at -80°C. After giving the mixture a brief vortex, it was inserted into a thermal cycler for DNA synthesis. Samples were incubated at 22°C for 5 minutes, followed by 42°C for 30 minutes, then 85°C for 5 minutes, and were lastly held at 4°C. cDNA products were stored at -20°C or immediately analysed by RT-PCR.

2.2.6.3 Quantitative real-time PCR analysis

Predesigned DNA primers were used to target and amplify the region of interest on previously generated cDNA (outlined in section 2.2.5.2). Remaining cDNA samples were stored at -20°C. The reagents that made up a final volume of 20 µl reaction mix prepared on ice were outlined as below:

Reagent	**Volume (µl)**
2X PerfeCTa® SYBR® Green FastMixes™	10
Forward Primers (10 µM)	1
Reverse Primers (10 µM)	1
cDNA	2
Nuclease-free Water	6

Reaction mix of every target gene was added in triplicate wells on PCR plates to ensure reproducibility of assay. Samples were quantified using an Applied Biosystems Step One™ real-time PCR instrument. cDNA denaturation was initiated at 95°C for 10 minutes before samples were subjected to 30 cycles of 95°C for 15 seconds to denature DNA, 57°C for 30 seconds to anneal DNA, and 72°C for 45 seconds to extend DNA.

2.2.7 Statistical analysis

GraphPad Prism 6 was used to perform statistical analysis. For comparison of one grouping variable with more than one data set, one-way ANOVA test with a Tukey multiple comparison was used. For comparison of two grouping variables with more than one data set, two-way ANOVA test with a Sidak multiple comparison was used. In all figures, a p-value < 0.05 was regarded as statistically significant with asterisk marking for *$p \leq 0.05$, **$p \leq 0.01$, ***$p \leq 0.001$, and ****$p \leq 0.0001$.

Chapter 3: Exploring the Role of Pellino Proteins in the Generation of T and B Cell Populations

3.1 Introduction

It has been demonstrated that Pellino proteins play a role in mediating innate immune signalling. Over the last decade, there has been growing evidence on the regulatory function of Pellino proteins, in particular Pellino 1, in adaptive immunity. However, no systematic study has been performed to evaluate the potential role of Pellino proteins in the development and function of adaptive immune cells.

Immunophenotyping is a technique to identify immune cell type and their phenotype based on surface marker expression using flow cytometry. It has been widely used in clinical laboratory settings for diagnosis, prognosis, and treatment optimisation of many diseases (Mason *et al*., 2006; Overman *et al*., 2010). On the other hand, immunophenotyping is also a powerful tool in basic research to perform cell enumeration as well as providing information on their activation status and cellular function (Newton and Dobrovolskaia, 2022; Pockley *et al*., 2015).

The spleen is a secondary lymphoid tissue that contains a rich repertoire of immune cells. It is also a site for removal of damaged erythrocytes and initiation of immune responses against blood-born antigens (Cesta, 2006). Immune cell distribution in spleen tissue of mice was reported (Hensel *et al*., 2019), as summarised in table 3.1 below, making it an ideal immune organ for a comprehensive study of the adaptive immune system:

Cell type	Frequency in male (%) (n ≥ 6)	Frequency in female (%) (n ≥ 7)
T cells	42.32	38.76
B cells	18.01	21.36
Macrophages	4.58	3.60
Dendritic cells	3.95	2.23
NK cells	3.48	3.00
Neutrophils	3.45	2.15
Immature myeloid cells	1.99	2.32

Table 3.1 Cell type distribution in spleens of 8-week-old C57BL/6NCr mice
Distribution of various immune cell subtypes based on immunophenotypic analysis of splenocytes from C57BL/6NCr male mice (n ≥ 6) and female mice (n ≥ 7) (Hensel *et al*., 2019).

The generation of Pellino single-knockout (SKO) mice (*Peli1*$^{-/-}$, *Peli2*$^{-/-}$, and *Peli3*$^{-/-}$), double-knockout mice (*Peli1/2*$^{-/-}$, *Peli1/3*$^{-/-}$, and *Peli2/3*$^{-/-}$) and triple-knockout mice (*Peli1/2/3*$^{-/-}$) is described in section 2.2.6.1. In the figures of this chapter, WT controls to SKO mice have been identified by the name WT x SKO (white symbol). On the other hand, WT controls to double/triple-KO have been identified by the name WT colony with a different symbol colour (mustard symbol). Statistics were applied to combined WT group named WT (purple symbol) in comparison to Pellino single/double/triple-KO mice.

This project initially aimed to examine the role of Pellino proteins in adaptive immune cell development through *ex vivo* T cell and B cell immunophenotypic analysis of splenocytes from various Pellino knockout mice models. This study also explored the age and gender dimension of Pellino proteins in influencing T cell and B cell subset development and activation.

3.2 Results

3.2.1 Measurement of body and spleen weights in Pellino-deficient mice

Peli1, *Peli2*, and *Peli3* single-, double-, and triple-knockout mice were sex matched and categorised into two age groups: 10 to 12 weeks old (referenced as young) and 6 months old (referenced as aged/old). Body and spleen weights of these mice were recorded and also used to calculate spleen:body weight ratio. Male *Peli1/2*$^{-/-}$ mice showed reduced body weight in comparison to WT mice at both young (Fig. 3.1a) and old (Fig. 3.1b) age. Similarly, old male (Fig. 3.1b) and female (Fig. 3.2b) *Peli1/2/3*$^{-/-}$ mice also weighed less than WT mice.

Splenomegaly, a sign of autoimmunity has been reported in *Peli1*$^{-/-}$ mice (Chang *et al.*, 2011). Hence, it was intriguing to investigate this phenotype in mice that are deficient in other Pellino proteins. In comparison to WT mice, *Peli1*$^{-/-}$, *Peli1/2*$^{-/-}$, *Peli1/3*$^{-/-}$, and *Peli1/2/3*$^{-/-}$ mice of young female mice had increased spleen to body ratio, which was not demonstrated in the males (Fig. 3.1c and Fig. 3.2c). While old *Peli1*$^{-/-}$ and *Peli1/2*$^{-/-}$ male mice showed elevated spleen to body ratio relative to WT, only old *Peli1/2*$^{-/-}$ female mice portrayed the same effect (Fig. 3.1d and Fig. 3.2d). This finding reveals a Pellino1-driven impact in autoimmunity that is consistent with previous studies and is not affected by other Pellino proteins (Chang *et al.*, 2011; Liu *et al.*, 2018).

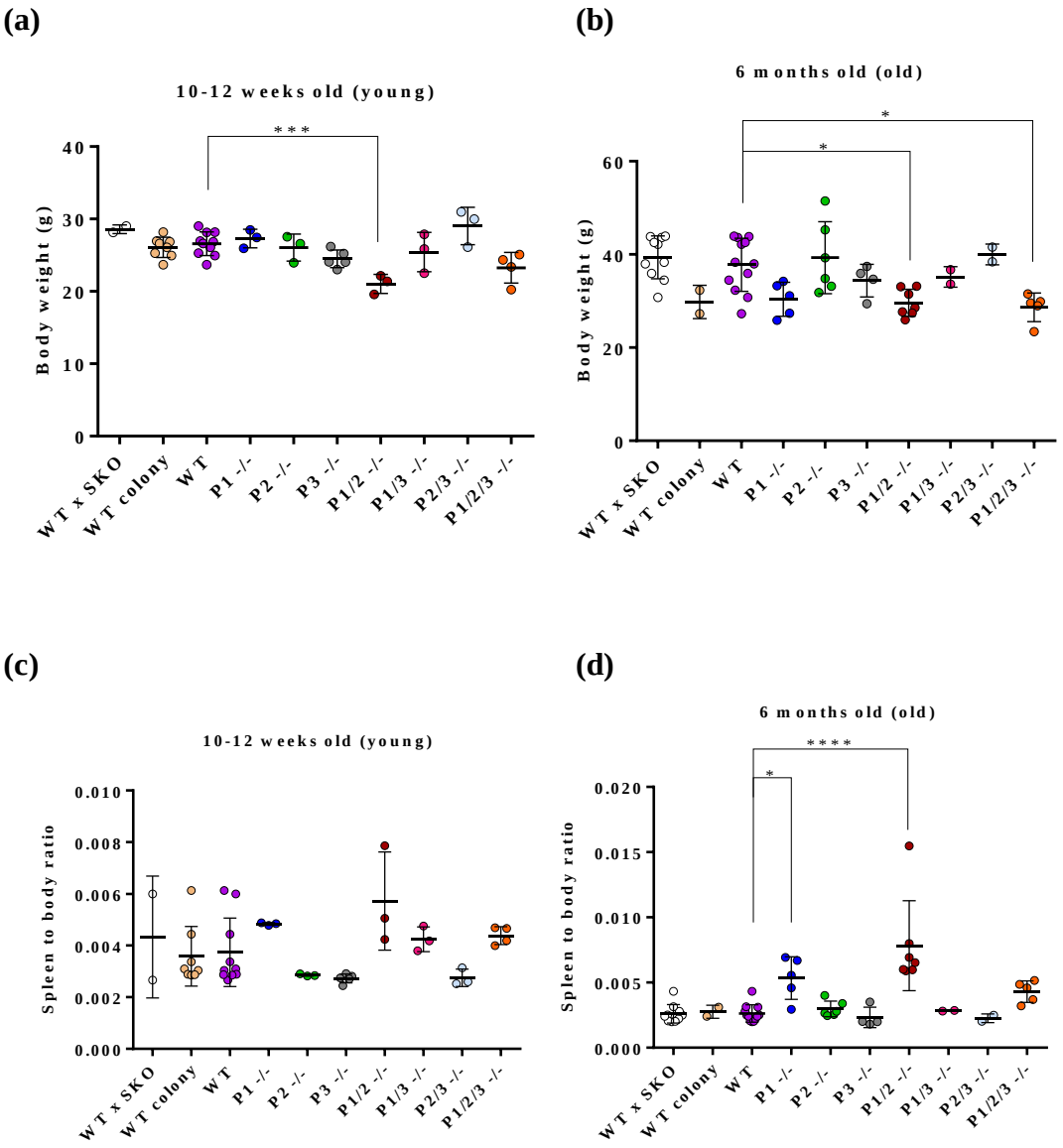

Figure 3.1 Measuring the effects of Pellino deficiency on body and spleen weights of male mice

Age matched wild type (WT) and Pellino-deficient male mice were monitored for variations in **(a, b)** body weight and **(c, d)** spleen:body ratios at **(a, c)** 10 to 12 weeks old and **(b, d)** 6 months old. Pellino-deficient mice were single-deficient in Pellino 1 ($P1^{-/-}$), Pellino 2 ($P2^{-/-}$) or Pellino 3 ($P3^{-/-}$); double-deficient in Pellino 1 and Pellino 2 ($P1/2^{-/-}$), Pellino 1 and Pellino 3 ($P1/3^{-/-}$) or Pellino 2 and Pellino 3 ($P2/3^{-/-}$); triple-deficient in Pellino 1, Pellino 2, and Pellino 3 ($P1/2/3^{-/-}$). All error bars are S.D. Statistical analysis was performed using one-way ANOVA.

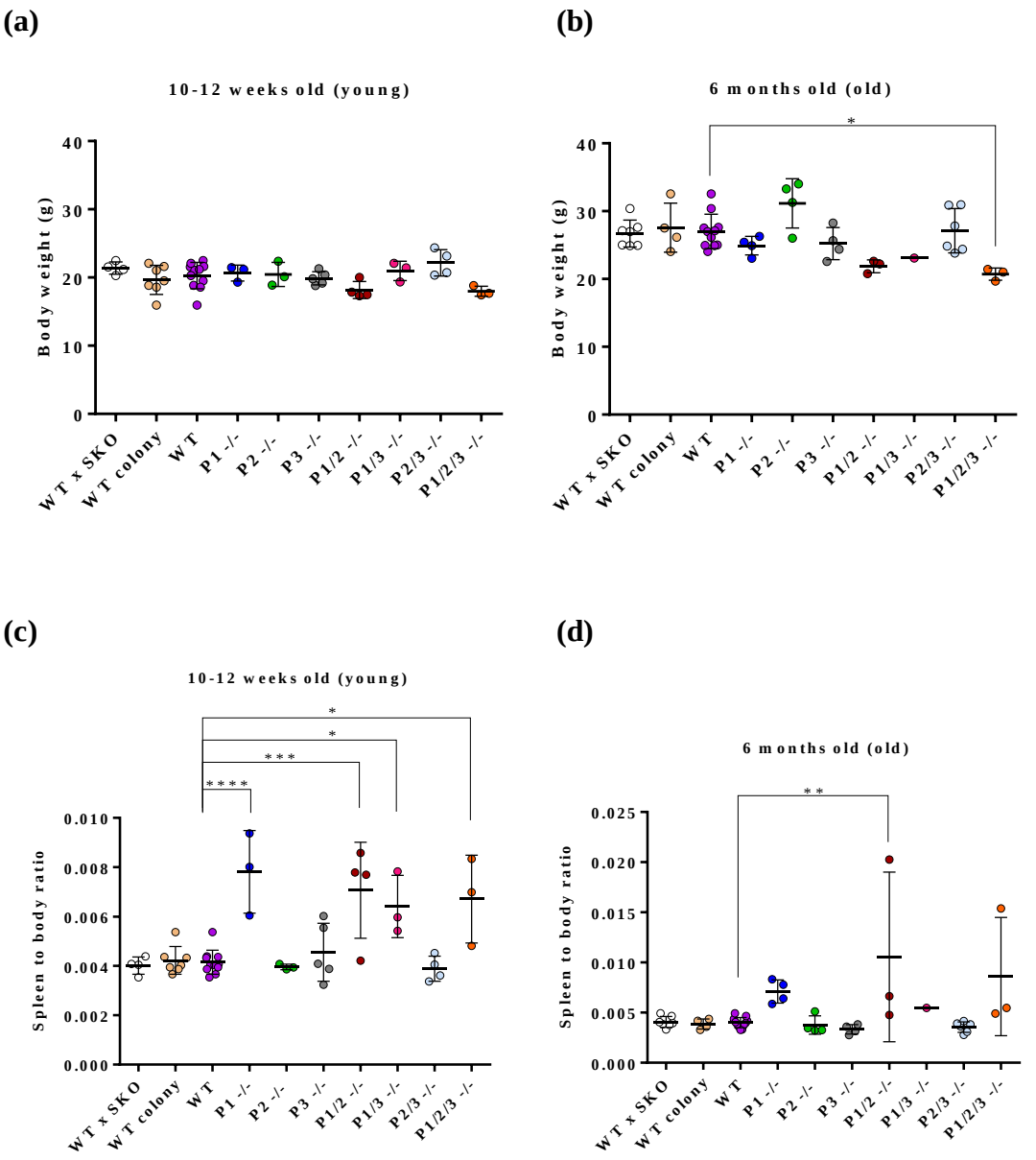

Figure 3.2 Measuring the effects of Pellino deficiency on body and spleen weights of female mice

Age matched WT and Pellino-deficient female mice were monitored for variations in **(a, b)** body weight and **(c, d)** spleen:body ratios at **(a, c)** 10 to 12 weeks old and **(b, d)** 6 months old. Pellino-deficient mice were single-deficient in Pellino 1 ($P1^{-/-}$), Pellino 2 ($P2^{-/-}$) or Pellino 3 ($P3^{-/-}$); double-deficient in Pellino 1 and Pellino 2 ($P1/2^{-/-}$), Pellino 1 and Pellino 3 ($P1/3^{-/-}$) or Pellino 2 and Pellino 3 ($P2/3^{-/-}$); triple-deficient in Pellino 1, Pellino 2, and Pellino 3 ($P1/2/3^{-/-}$). All error bars are S.D. Statistical analysis was performed using one-way ANOVA.

3.2.2 Measurement of splenocyte number in Pellino-deficient mice

Recording splenocyte number is useful to quantify the actual size of target immune cell populations within a spleen. For instance, the size of TCR-αβ repertoire was determined using total number of T cells derived from naïve mouse splenocytes (Casrouge *et al*., 2000). To generate a quantitative data on T and B cell enumeration, live splenocyte number was measured. It allows an accurate estimation of the size of various T and B cell subpopulations in the mouse spleen with different Pellino-deficiencies.

Live splenocytes generated from young *Peli1/2*$^{-/-}$ mice were significantly higher than WT mice, whereas the numbers of spleen cell in other mouse strains did not greatly vary with WT mice (Fig. 3.3a). There was no apparent difference between other genotypes with WT mice in old group (Fig. 3.3b). These data indicate that there may be infiltration of immune cells to the spleen in the absence of Pellino 1 and 2.

3.2.3 Immunophenotyping of T cell populations in Pellino-deficient mice

Given that Pellino 1 is a negative regulator of T cell activation (Chang *et al*., 2011), the impact of Pellino proteins on each T cell subset was further explored. T cells can be predominantly found in a mouse spleen. Single cell suspensions from spleens of sex and age matched mice lacking various Pellino proteins were generated. These spleen cells were then stained extracellularly with different cell surface markers to identify $CD3^+$ T cells, $CD4^+$ T cells, naïve $CD4^+$ T cells, activated $CD4^+$ T cells, $CD8^+$ T cells, naïve $CD8^+$ T cells, effector memory $CD8^+$ T cells, central memory $CD8^+$ T cells, and γδ T cells by flow cytometry. This quantitative study was presented in two parameters: live cell number and cell frequency/percentage. Live cell number of a particular population was calculated by multiplying the frequency of the indicated population with total live spleen cells. Data interpretation using both cell number and percentage helps to draw a more solid conclusion with a higher confidence.

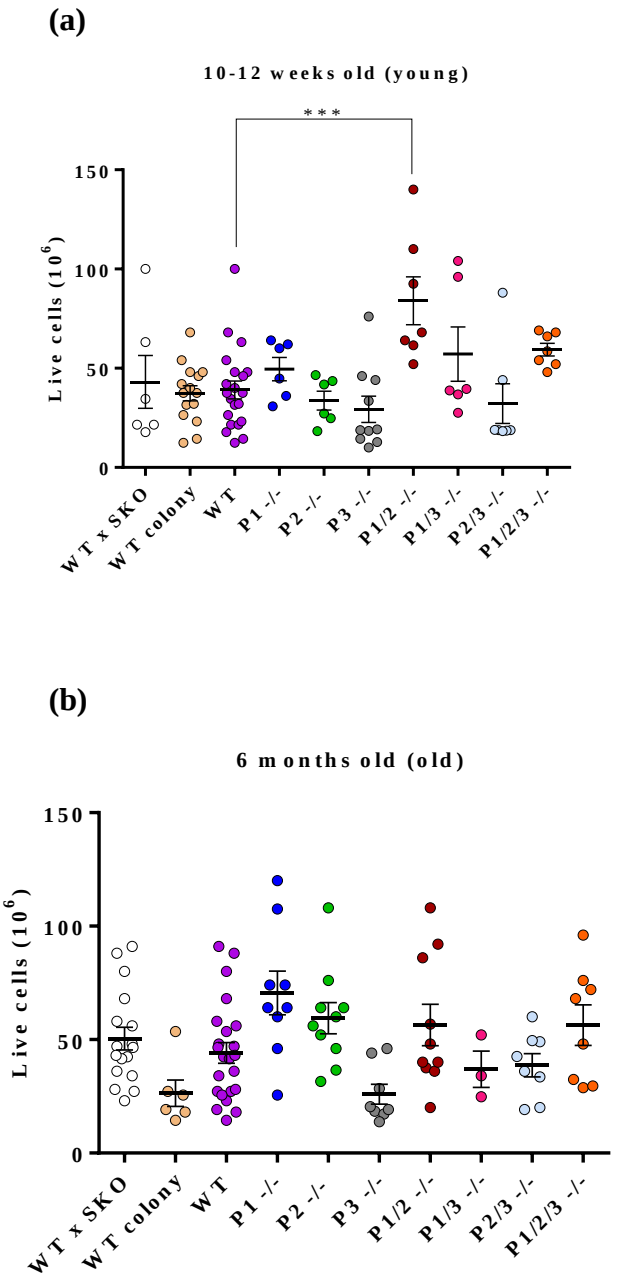

Figure 3.3 Splenocytes numbers in Pellino-deficient mice

Male and female mice were monitored for variations in splenocytes numbers at **(a)** 10 to 12 weeks old and **(b)** 6 months old. Pellino-deficient mice were single-deficient in Pellino 1 ($P1^{-/-}$), Pellino 2 ($P2^{-/-}$) or Pellino 3 ($P3^{-/-}$); double-deficient in Pellino 1 and Pellino 2 ($P1/2^{-/-}$), Pellino 1 and Pellino 3 ($P1/3^{-/-}$) or Pellino 2 and Pellino 3 ($P2/3^{-/-}$); triple-deficient in Pellino 1, Pellino 2, and Pellino 3 ($P1/2/3^{-/-}$). All error bars are S.E.M. Statistical analysis was performed using one-way ANOVA.

3.2.3.1 Enumeration of $CD3^+$ T cells in Pellino-deficient mice

CD3 chains bound to the TCR complex (Shah *et al.*, 2021) are a universal marker for T cells, hence all T cells are CD3 positive. They are further distinguished by a negative signal for B cell marker (B220) (Fig. 3.4a). Single Pellino-deficient mice exhibited comparable $CD3^+$ T cell count in comparison to WT mice regardless of age (Fig. 3.4b, c, d, e). This trend was replicated in double and triple Pellino-deficient mice with the exception of *Peli1/2*$^{-/-}$ mice (Fig. 3.4b, c, d, e).

With respect to age, there was a significantly higher number of $CD3^+$ T cells in young *Peli1/2*$^{-/-}$ mice (Fig. 3.4b), but the percentage dropped significantly as they became older when compared with WT mice (Fig. 3.4e). Generally, there were no statistical sex differences detected across WT and Pellino-deficient mice in both young and old mice group (Fig. 3.4f, g).

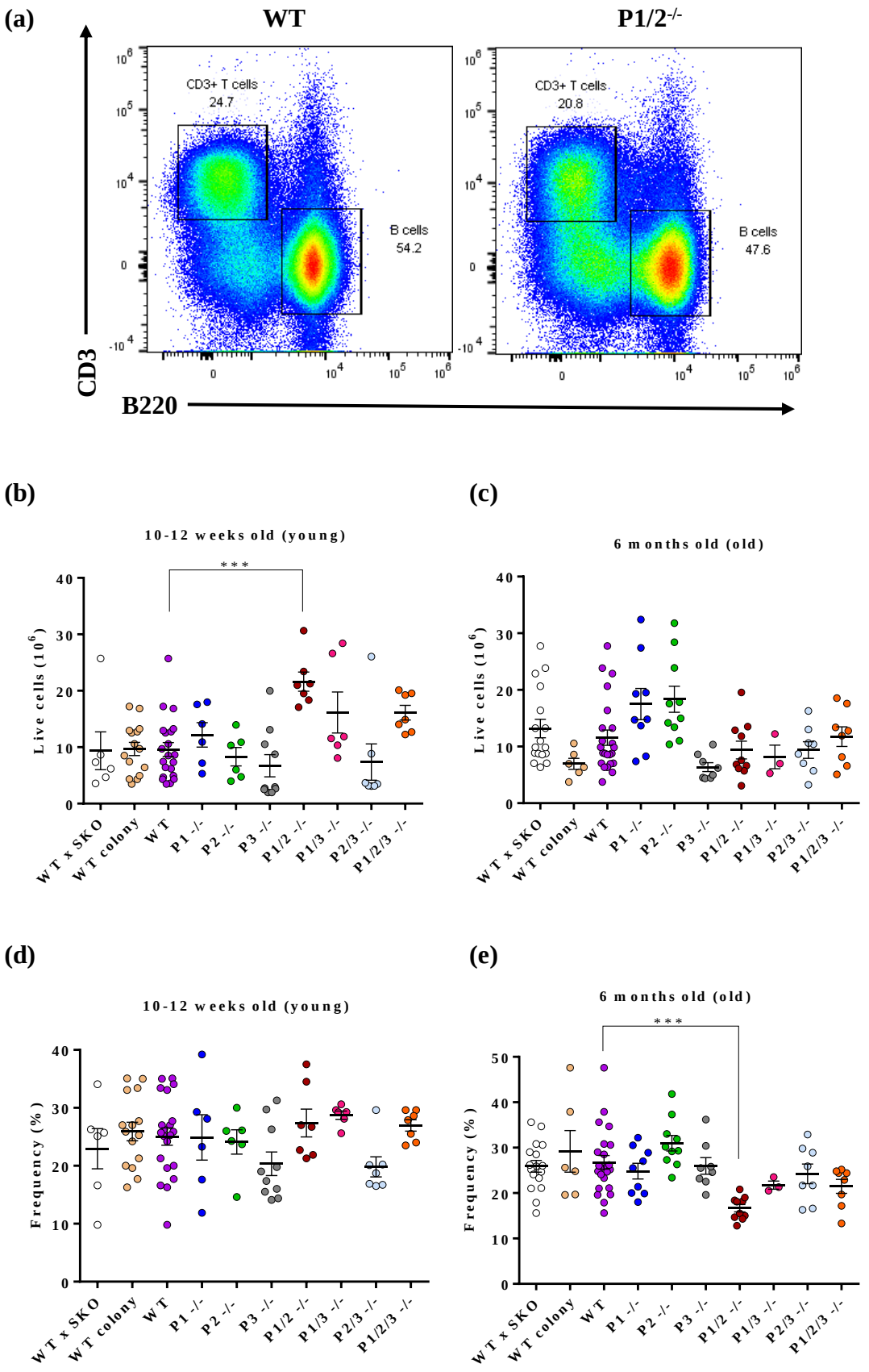
(a)
WT
P1/2-/-
CD3+ T cells
24.7
B cells
54.2
CD3+ T cells
20.8
B cells
47.6
CD3
B220
(b)
10-12 weeks old (young)
***
Live cells (10^6)
(c)
6 months old (old)
Live cells (10^6)
(d)
10-12 weeks old (young)
Frequency (%)
(e)
6 months old (old)
***
Frequency (%)
WT x SKO
WT colony
WT
P1 -/-
P2 -/-
P3 -/-
P1/2 -/-
P1/3 -/-
P2/3 -/-
P1/2/3 -/-

(f)

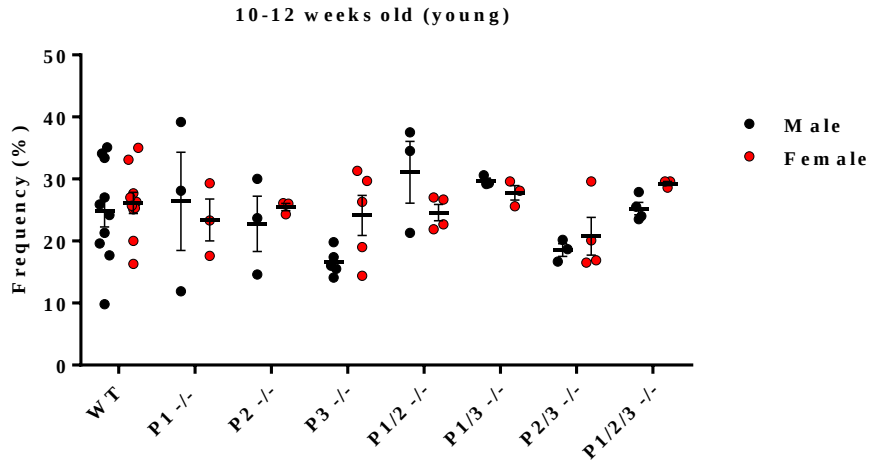

(g)

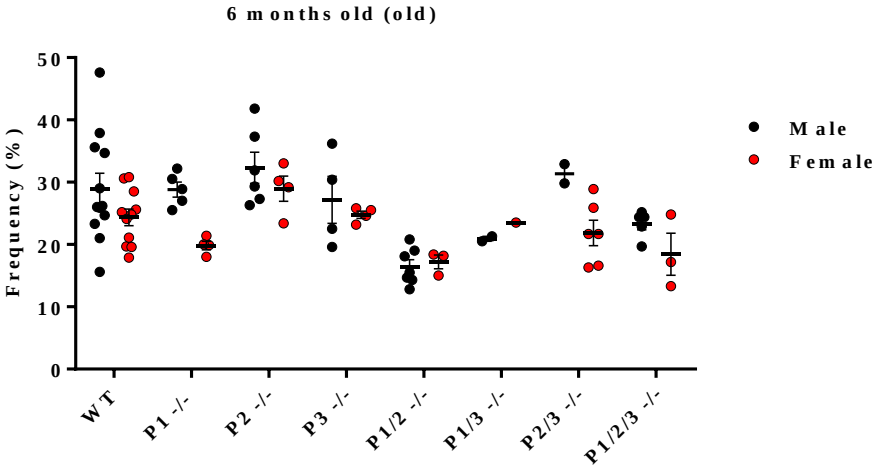

Figure 3.4 CD3$^+$ T cell enumeration in Pellino-deficient mice

Representative dot plots showing CD3$^+$ T cell frequencies of **(a)** a 6-month-old male WT mouse and a *Peli1/2*$^{-/-}$ mouse. Male and female mice were monitored for variations in **(b, c)** CD3$^+$ T cell numbers and **(d, e)** CD3$^+$ T cell frequencies at **(b, d)** 10 to 12 weeks old and **(c, e)** 6 months old. Age matched mice were monitored for gender variation in CD3$^+$ T cell frequencies at **(f)** 10 to 12 weeks old and **(g)** 6 months old. Pellino-deficient mice were single-deficient in Pellino 1 (P1$^{-/-}$), Pellino 2 (P2$^{-/-}$) or Pellino 3 (P3$^{-/-}$); double-deficient in Pellino 1 and Pellino 2 (P1/2$^{-/-}$), Pellino 1 and Pellino 3 (P1/3$^{-/-}$) or Pellino 2 and Pellino 3 (P2/3$^{-/-}$); triple-deficient in Pellino 1, Pellino 2, and Pellino 3 (P1/2/3$^{-/-}$). All error bars are S.E.M. Statistical analysis was performed using **(b, c, d, e)** one-way ANOVA and **(f, g)** two-way ANOVA.

3.2.3.2 Enumeration of $CD4^+$ T cells in Pellino-deficient mice

$CD4^+$ T cells are important mediators of adaptive immunity and differentiate into a specialised Th cell based on interactions with peptide-MHC complex in a particular cytokine milieu (Zhu *et al.*, 2009). $CD4^+$ T cells were identified as $CD3^+$ and $CD4^+$ populations by flow cytometry (Fig. 3.5a).

$CD4^+$ T cell enumeration demonstrated heterogeneity in cell numbers (Fig. 3.5b, c) and cell frequencies (Fig. 3.5d, e), but information could be gleaned from the consideration of age. $CD4^+$ T cell numbers were significantly enhanced in young *Peli1/2*$^{-/-}$ mice, but not in older mice (Fig. 3.5b, c) and it did not affect the population frequency (Fig. 3.5d, e). $CD4^+$ T cell numbers increased significantly in *Peli1*$^{-/-}$ and *Peli2*$^{-/-}$ mice in comparison with WT mice as they aged (Fig. 3.5b, c), but this trend was not observed when cell quantity is expressed as a percentage (Fig. 3.5d, e). On the other hand, $CD4^+$ T cell frequency in young *Peli2/3*$^{-/-}$ mice did not differ from WT mice (Fig. 3.5d), but old *Peli2/3*$^{-/-}$ mice had a significantly lower $CD4^+$ T cell frequency than WT mice (Fig. 3.5e). *Peli3*$^{-/-}$, *Peli1/3*$^{-/-}$, and *Peli1/2/3*$^{-/-}$ mice had mostly comparable $CD4^+$ T cell count with WT mice (Fig. 3.5b, c, d, e). From the perspective of gender differences, all groups had similar $CD4^+$ T cell frequency irrespective of age (Fig. 3.5f, g).

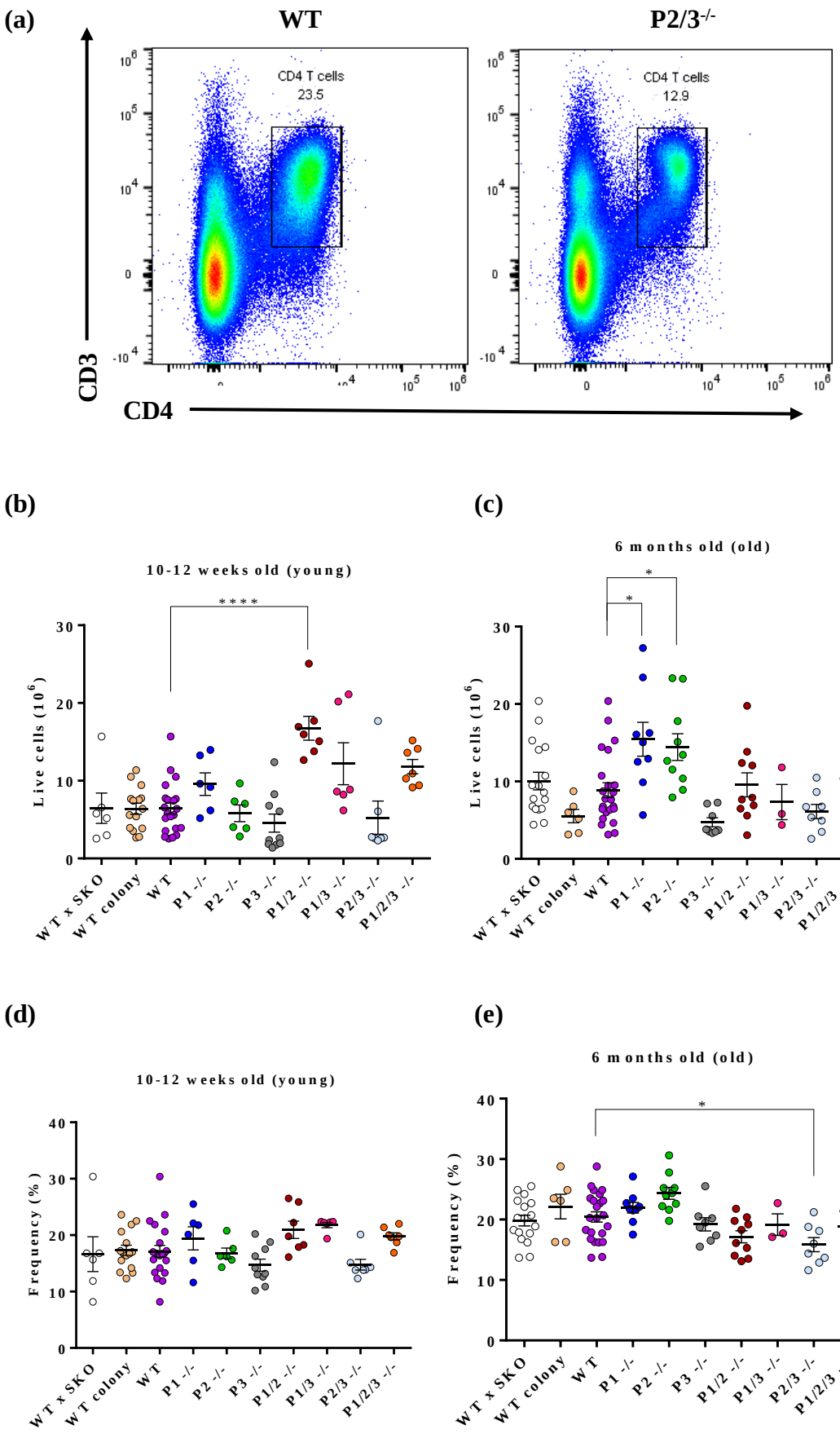
(a)
WT
P2/3-/-
CD4 T cells
23.5
CD4 T cells
12.9
CD3
CD4
(b)
10-12 weeks old (young)
****
Live cells (10^6)
(c)
6 months old (old)
*
*
Live cells (10^6)
WT x SKO
WT colony
WT
P1 -/-
P2 -/-
P3 -/-
P1/2 -/-
P1/3 -/-
P2/3 -/-
P1/2/3 -/-
(d)
10-12 weeks old (young)
Frequency (%)
(e)
6 months old (old)
*
Frequency (%)

(f)

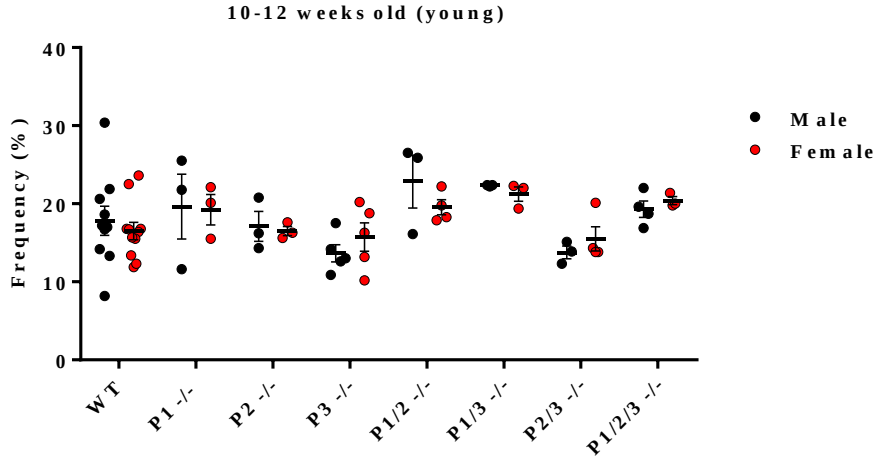

(g)

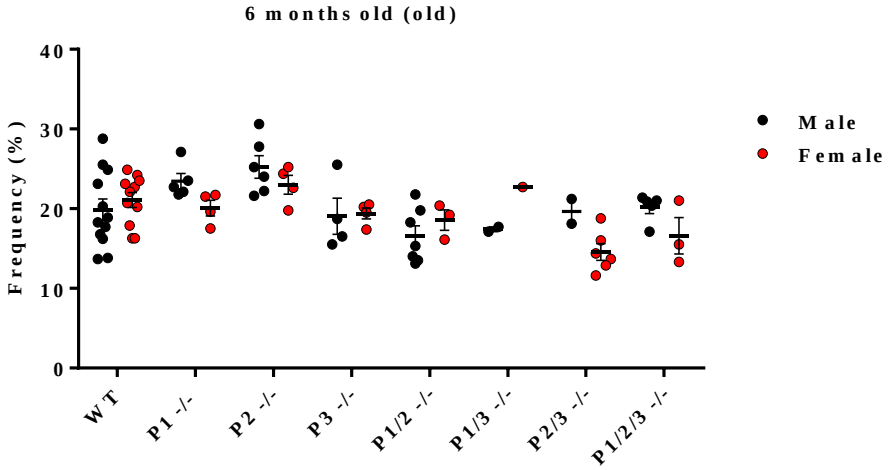

Figure 3.5 CD4$^+$ T cell enumeration in Pellino-deficient mice

Representative dot plots showing CD4$^+$ T cell frequencies of **(a)** a 6-month-old female WT mouse and a *Peli2/3*$^{-/-}$ mouse. Male and female mice were monitored for variations in **(b, c)** CD4$^+$ T cell numbers and **(d, e)** CD4$^+$ T cell frequencies at **(b, d)** 10 to 12 weeks old and **(c, e)** 6 months old. Age matched mice were monitored for gender variation in CD4$^+$ T cell frequencies at **(f)** 10 to 12 weeks old and **(g)** 6 months old. Pellino-deficient mice single-deficient in Pellino 1 (P1$^{-/-}$), Pellino 2 (P2$^{-/-}$) or Pellino 3 (P3$^{-/-}$); double-deficient in Pellino 1 and Pellino 2 (P1/2$^{-/-}$), Pellino 1 and Pellino 3 (P1/3$^{-/-}$) or Pellino 2 and Pellino 3 (P2/3$^{-/-}$); triple-deficient in Pellino 1, Pellino 2, and Pellino 3 (P1/2/3$^{-/-}$). All error bars are S.E.M. Statistical analysis was performed using **(b, c, d, e)** one-way ANOVA and **(f, g)** two-way ANOVA.

3.2.3.3 Enumeration of naïve CD4$^+$ T cells in Pellino-deficient mice

Naïve CD4$^+$ T cells arriving the spleen from the thymus are inert until the encounter of antigenic peptide (Hochweller *et al.*, 2010). They lack the memory T cell marker CD44 expression, but express CD62L that facilitates their recirculation to peripheral lymph nodes (Gerberick *et al.*, 1997; Bradley *et al.*, 1994). Therefore, naïve CD4$^+$ T cells were identified on the flow cytometer as CD44$^-$ and CD62L$^+$ subtype of total CD4$^+$ T cells (Fig. 3.6a).

Naïve CD4$^+$ T cell numbers and percentages were very dispersed in young mice, hence there was no statistical differences observed (Fig. 3.6b, d). Old *Peli1*$^{-/-}$ mice had similar naïve CD4$^+$ T cell numbers (Fig. 3.6c), but significantly lower frequency in comparison to WT mice (Fig. 3.6e). No pronounced differences were noticeable in old *Peli2*$^{-/-}$, *Peli3*$^{-/-}$, and *Peli2/3*$^{-/-}$ mice compared with WT mice (Fig. 3.6c, e). Old *Peli1/2*$^{-/-}$ mice had significantly lower naïve CD4$^+$ T cell numbers and percentages in parallel, emphasising a stark phenotype (Fig. 3.6c, e). There was also a significant reduction of naïve CD4$^+$ T cell frequency in old *Peli1/3*$^{-/-}$ and *Peli1/2/3*$^{-/-}$ mice (Fig. 3.6e).

From the age dimension, *Peli1/2*$^{-/-}$ mice lost naïve CD4$^+$ T cell numbers and frequency significantly as they became more mature (Fig. 3.6b, c, d, e). There was also a significant decrease in naïve CD4$^+$ T cell percentages for *Peli1*$^{-/-}$, *Peli1/3*$^{-/-}$, and *Peli1/2/3*$^{-/-}$ mice along the duration of aging (Fig. 3.6d, e). Together, the loss of naïve CD4$^+$ T cells was illustrated in a Pellino1-specific fashion over the maturation of mice. While there were no statistical differences between different genders in young mice (Fig. 3.6f), the frequency of naïve CD4$^+$ T cells in old WT female mice was significantly reduced in contrast to old WT male mice (Fig. 3.6g).

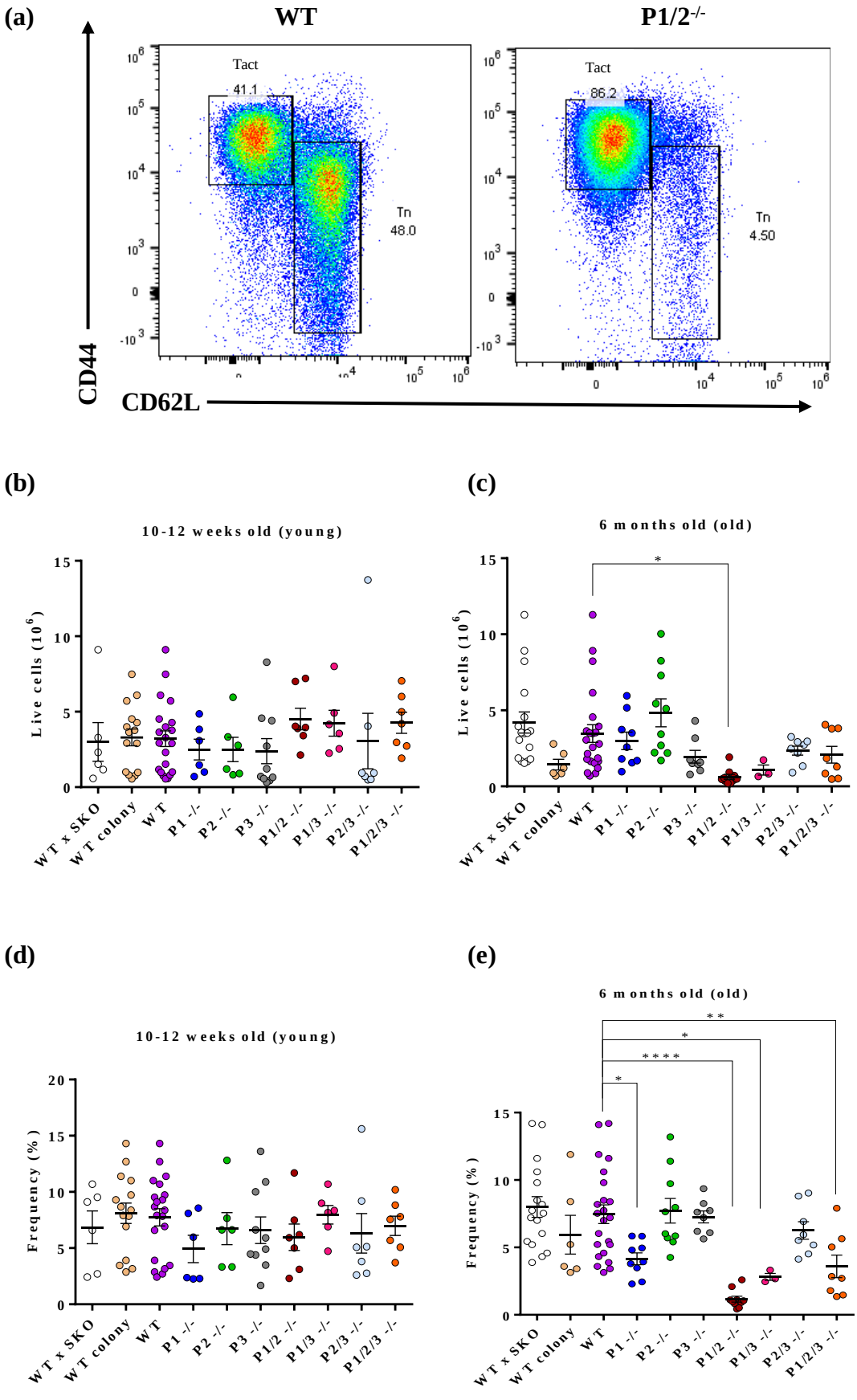
(a)
WT
P1/2-/-
Tact
41.1
Tn
48.0
Tact
86.2
Tn
4.50
CD44
CD62L
(b)
10-12 weeks old (young)
Live cells (10^6)
(c)
6 months old (old)
Live cells (10^6)
(d)
10-12 weeks old (young)
Frequency (%)
(e)
6 months old (old)
Frequency (%)
WT x SKO
WT colony
WT
P1 -/-
P2 -/-
P3 -/-
P1/2 -/-
P1/3 -/-
P2/3 -/-
P1/2/3 -/-

(f)

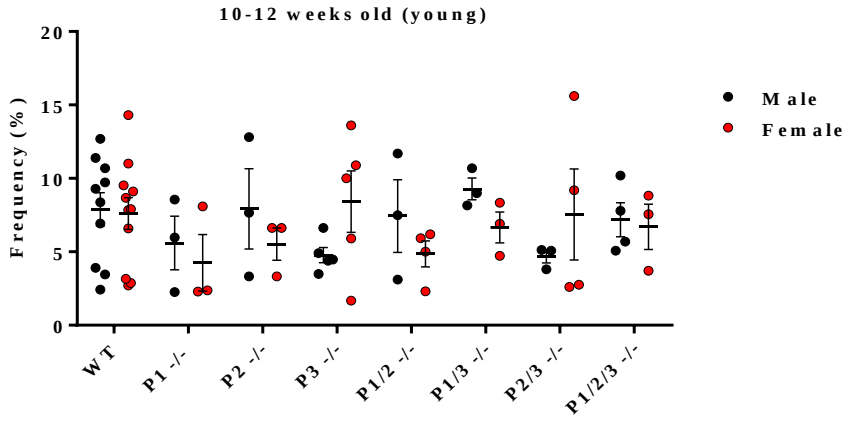

(g)

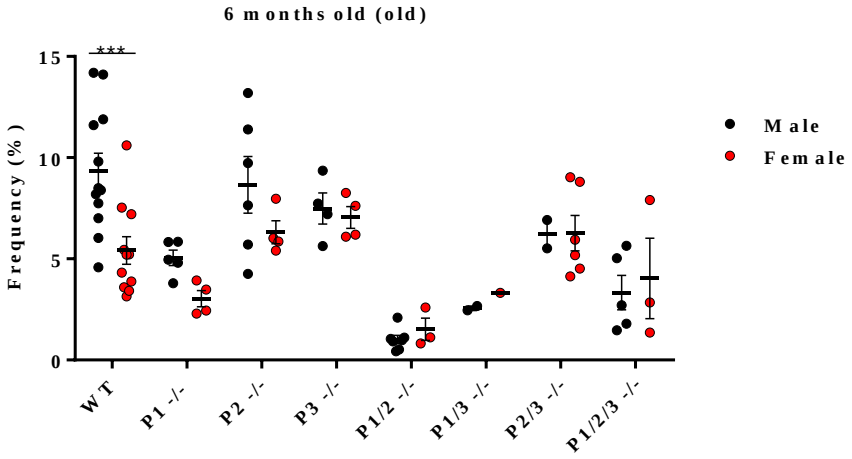

Figure 3.6 Naïve CD4$^+$ T cell enumeration in Pellino-deficient mice

Representative dot plots showing naïve CD4$^+$ T cell frequencies of **(a)** a 6-month-old male WT mouse and a *Peli1/2*$^{-/-}$ mouse. Male and female mice were monitored for variations in **(b, c)** naïve CD4$^+$ T cell numbers and **(d, e)** naïve CD4$^+$ T cell frequencies at **(b, d)** 10 to 12 weeks old and **(c, e)** 6 months old. Age matched mice were monitored for gender variation in naïve CD4$^+$ T cell frequencies at **(f)** 10 to 12 weeks old and **(g)** 6 months old. Pellino-deficient mice were single-deficient in Pellino 1 (P1$^{-/-}$), Pellino 2 (P2$^{-/-}$) or Pellino 3 (P3$^{-/-}$); double-deficient in Pellino 1 and Pellino 2 (P1/2$^{-/-}$), Pellino 1 and Pellino 3 (P1/3$^{-/-}$) or Pellino 2 and Pellino 3 (P2/3$^{-/-}$); triple-deficient in Pellino 1, Pellino 2, and Pellino 3 (P1/2/3$^{-/-}$). All error bars are S.E.M. Statistical analysis was performed using **(b, c, d, e)** one-way ANOVA and **(f, g)** two-way ANOVA.

3.2.3.4 Enumeration of activated CD4$^+$ T cells in Pellino-deficient mice

Upon engagement with peptide presented by APCs, naïve CD4$^+$ T cells become activated and harbour a CD62L^{low}CD44^{high} phenotype (Gerberick *et al.*, 1997). Thus, activated CD4$^+$ T cells were gated as CD44$^+$ and CD62L$^-$ subtype of total CD4$^+$ T cells by flow cytometry (Fig. 3.7a).

Young *Peli1*$^{-/-}$, *Peli1/2*$^{-/-}$, *Peli1/3*$^{-/-}$, and *Peli1/2/3*$^{-/-}$ mice had significantly increased activated CD4$^+$ T cell numbers and percentages as compared to WT mice, but the generation of this cell type was unaffected in young *Peli2*$^{-/-}$, *Peli3*$^{-/-}$, and *Peli2/3*$^{-/-}$ mice (Fig. 3.7b, d). There was also a significantly higher activated CD4$^+$ T cell numbers and frequency in old *Peli1*$^{-/-}$, *Peli2*$^{-/-}$, and *Peli1/2*$^{-/-}$ mice compared to WT mice (Fig. 3.7c, e). There were no differences in activated CD4$^+$ T cells numbers and frequency in old *Peli3*$^{-/-}$, *Peli1/3*$^{-/-}$, *Peli2/3*$^{-/-}$, and *Peli1/2/3*$^{-/-}$ mice, compared with WT controls (Fig. 3.7c, e).

It was obvious that *Peli2*$^{-/-}$ mice accumulated significantly more activated CD4$^+$ T cell numbers and frequency in the spleen as they aged (Fig. 3.7b, c, d, e). *Peli1*$^{-/-}$ and *Peli1/2*$^{-/-}$ mice had a significantly higher level of activated CD4$^+$ T cells in comparison to WT mice from young to old age (Fig. 3.7b, c, d, e). These data suggest that a strong activated CD4$^+$ T cells phenotype is driven by the absence of Pellino 1 irrespective of age. It also implies the Pellino 2 plays a role in maintaining the enhanced activated CD4$^+$ T cell phenotype in old age, but not during young age.

By taking sex differences into account, the young mice did not depict any statistical differences (Fig. 3.7f). In old mice, there was a significant increase of activated CD4$^+$ T cells in WT females in comparison to WT males (Fig. 3.7g).

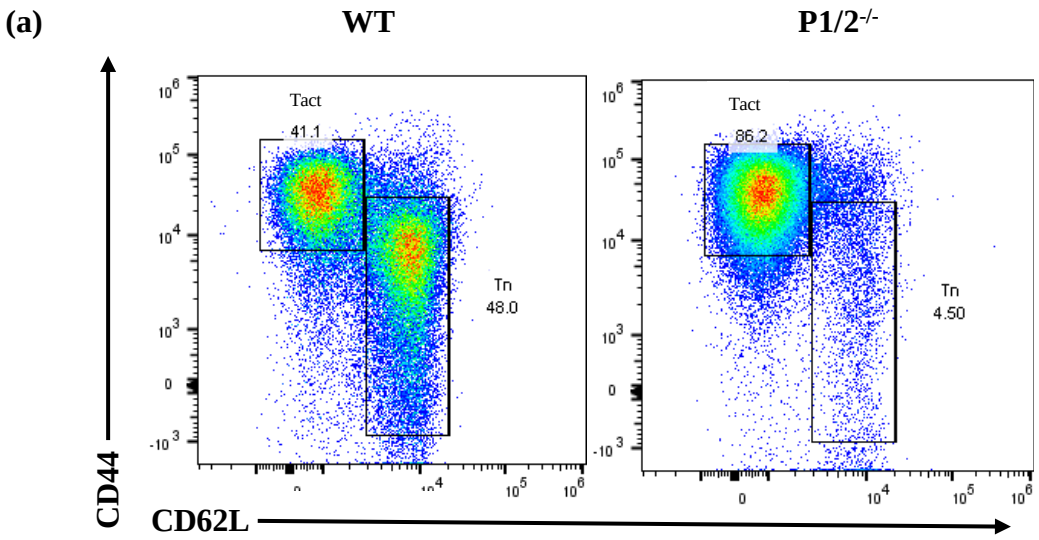
(a)
WT
P1/2-/-
Tact
41.1
Tn
48.0
Tact
86.2
Tn
4.50
CD44
CD62L

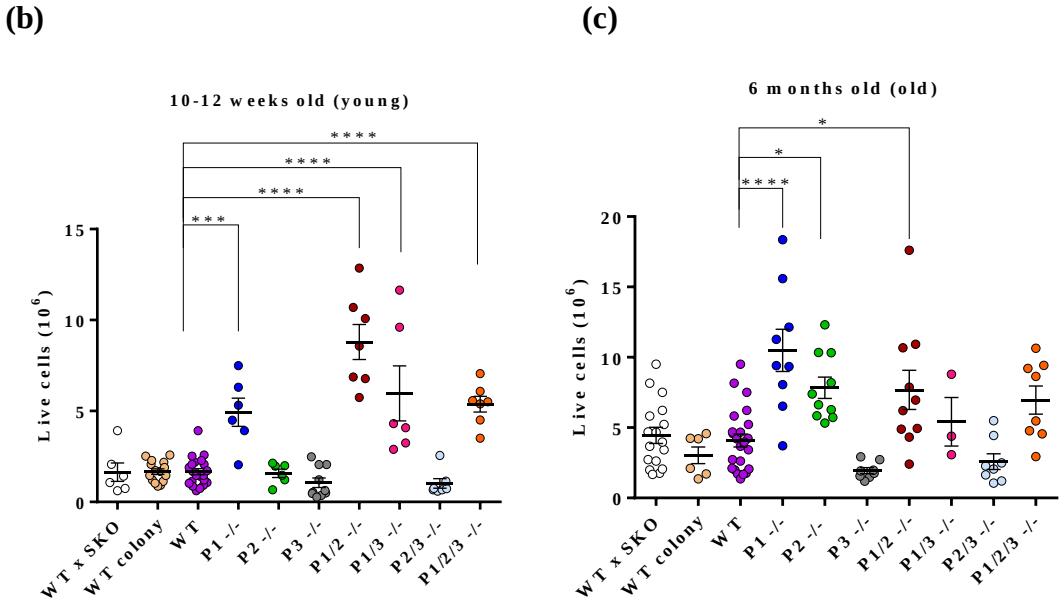
(b)
10-12 weeks old (young)
Live cells (10^6)
WT x SKO
WT colony
WT
P1 -/-
P2 -/-
P3 -/-
P1/2 -/-
P1/3 -/-
P2/3 -/-
P1/2/3 -/-
(c)
6 months old (old)
Live cells (10^6)
WT x SKO
WT colony
WT
P1 -/-
P2 -/-
P3 -/-
P1/2 -/-
P1/3 -/-
P2/3 -/-
P1/2/3 -/-

(d)

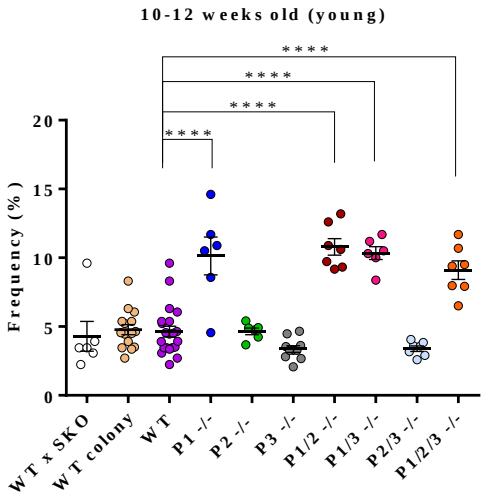
10-12 weeks old (young)
Frequency (%)
0
5
10
15
20
****
****
****
****
WT x SKO
WT colony
WT
P1 -/-
P2 -/-
P3 -/-
P1/2 -/-
P1/3 -/-
P2/3 -/-
P1/2/3 -/-

(e)

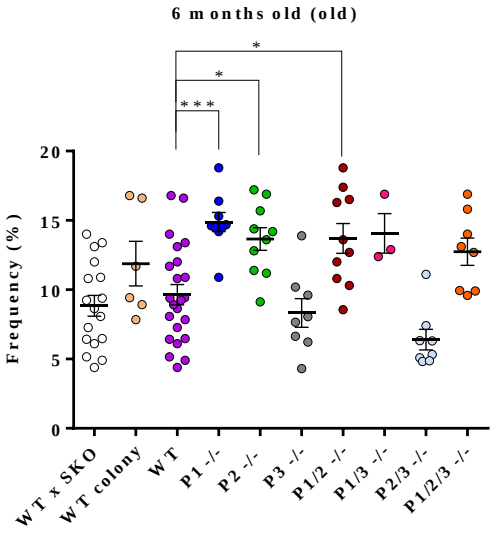
6 months old (old)
Frequency (%)
0
5
10
15
20
*
*
***
WT x SKO
WT colony
WT
P1 -/-
P2 -/-
P3 -/-
P1/2 -/-
P1/3 -/-
P2/3 -/-
P1/2/3 -/-

(f)

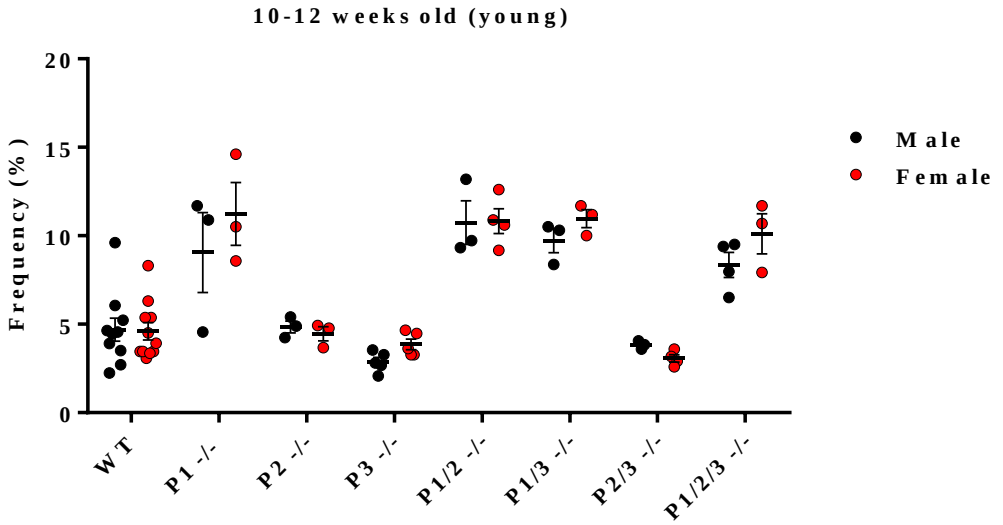
10-12 weeks old (young)
Frequency (%)
0
5
10
15
20
WT
P1 -/-
P2 -/-
P3 -/-
P1/2 -/-
P1/3 -/-
P2/3 -/-
P1/2/3 -/-
Male
Female

(g)

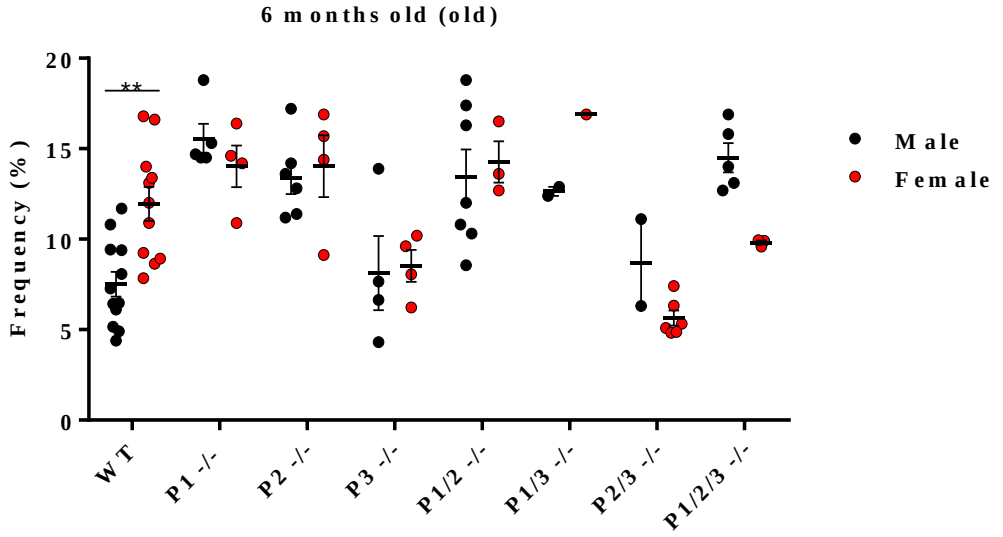

Figure 3.7 Activated CD4$^+$ T cell enumeration in Pellino-deficient mice

Representative dot plots showing activated CD4$^+$ T cell frequencies of **(a)** a 6-month-old male WT mouse and a *Peli1/2*$^{-/-}$ mouse. Male and female mice were monitored for variations in **(b, c)** activated CD4$^+$ T cell numbers and **(d, e)** activated CD4$^+$ T cell frequencies at **(b, d)** 10 to 12 weeks old and **(c, e)** 6 months old. Age matched mice were monitored for gender variation in activated CD4$^+$ T cell frequencies at **(f)** 10 to 12 weeks old and **(g)** 6 months old. Pellino-deficient mice were single-deficient in Pellino 1 (P1$^{-/-}$), Pellino 2 (P2$^{-/-}$) or Pellino 3 (P3$^{-/-}$); double-deficient in Pellino 1 and Pellino 2 (P1/2$^{-/-}$), Pellino 1 and Pellino 3 (P1/3$^{-/-}$) or Pellino 2 and Pellino 3 (P2/3$^{-/-}$); triple-deficient in Pellino 1, Pellino 2, and Pellino 3 (P1/2/3$^{-/-}$). All error bars are S.E.M. Statistical analysis was performed using **(b, c, d, e)** one-way ANOVA and **(f, g)** two-way ANOVA.

3.2.3.5 Enumeration of $CD8^+$ T cells in Pellino-deficient mice

To date, the role of Pellino proteins in regulating $CD8^+$ T cell function has not been published. Hence, this study also aimed to assess potential connection between Pellino proteins and $CD8^+$ T cell immunity. $CD8^+$ T cells, a subtype of $CD3^+$ T cells, are classified as cytotoxic T cells once they become activated. $CD8^+$ T cells express both CD3 and CD8 markers (Fig. 3.8a).

There were no remarkable differences of $CD8^+$ T cell count in young and old *Peli1*$^{-/-}$, *Peli2*$^{-/-}$, and *Peli3*$^{-/-}$ mice compared to WT mice (Fig. 3.8b, c, d, e). While young *Peli1/2*$^{-/-}$ mice did not show significant difference in $CD8^+$ T cell count in comparison to WT mice at young age (Fig. 3.8b, d), they lost $CD8^+$ T cell percentages significantly in comparison to WT mice at old age (Fig. 3.8e). Moreover, *Peli1/3*$^{-/-}$, *Peli2/3*$^{-/-}$, and *Peli1/2/3*$^{-/-}$ mice had comparable levels of $CD8^+$ T cells with WT mice (Fig. 3.8b).

In relation to age, no clear pattern was defined across Pellino-deficient mice (Fig. 3.8b, c, d, e); $CD8^+$ T cell frequency dropped significantly in old *Peli1/2*$^{-/-}$ mice only (Fig. 3.8e). Furthermore, no difference was detected when comparing $CD8^+$ T cells in young males and females of all genotypes (Fig. 3.8f). Similar to naïve $CD4^+$ T cells, there was a significantly lower $CD8^+$ T cell frequency in old WT female mice in contrast to old WT male mice (Fig. 3.8g).

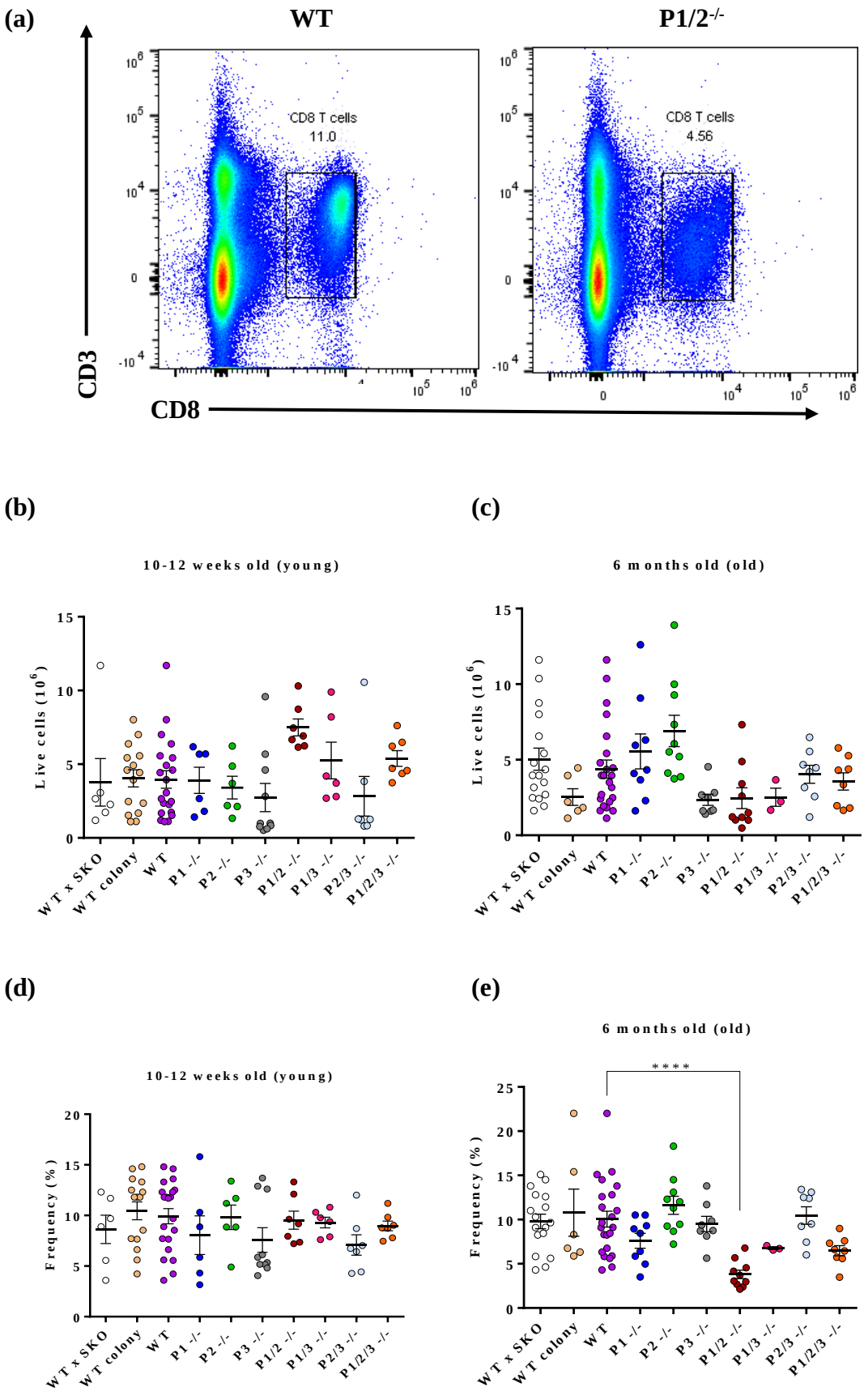
(a)
WT
P1/2-/-
CD8 T cells
11.0
CD8 T cells
4.56
CD3
CD8
(b)
10-12 weeks old (young)
Live cells (10^6)
(c)
6 months old (old)
Live cells (10^6)
(d)
10-12 weeks old (young)
Frequency (%)
(e)
6 months old (old)
****
Frequency (%)
WT x SKO
WT colony
WT
P1 -/-
P2 -/-
P3 -/-
P1/2 -/-
P1/3 -/-
P2/3 -/-
P1/2/3 -/-

(f)

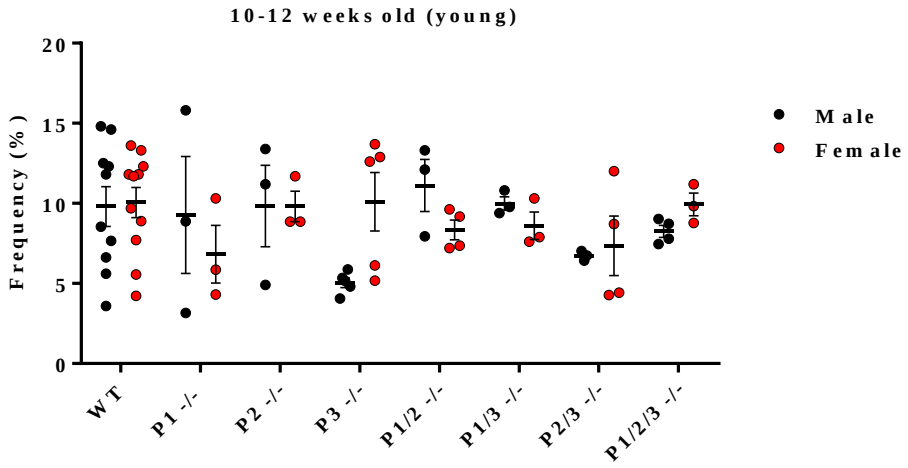

(g)

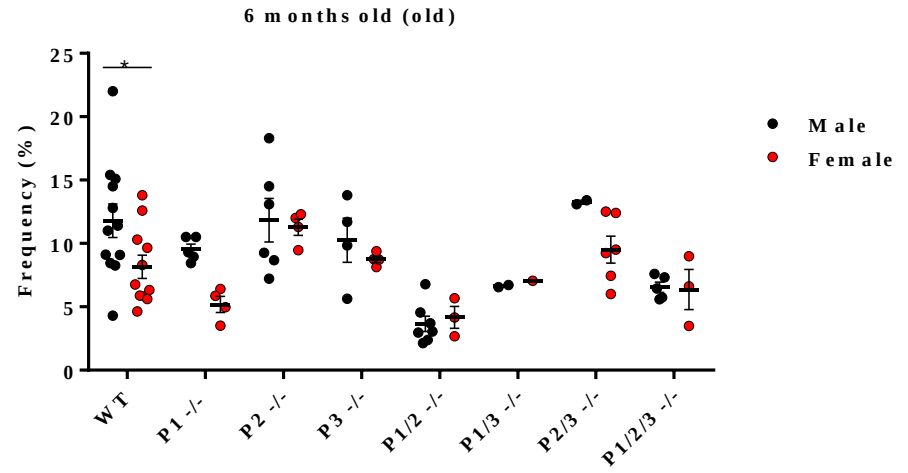

Figure 3.8 CD8$^+$ T cell enumeration in Pellino-deficient mice

Representative dot plots showing CD8$^+$ T cell frequencies of **(a)** a 6-month-old male WT mouse and a *Peli1/2*$^{-/-}$ mouse. Male and female mice were monitored for variations in **(b, c)** CD8$^+$ T cell numbers and **(d, e)** CD8$^+$ T cell frequencies at **(b, d)** 10 to 12 weeks old and **(c, e)** 6 months old. Age matched mice were monitored for gender variation in CD8$^+$ T cell frequencies at **(f)** 10 to 12 weeks old and **(g)** 6 months old. Pellino-deficient mice were single-deficient in Pellino 1 (P1$^{-/-}$), Pellino 2 (P2$^{-/-}$) or Pellino 3 (P3$^{-/-}$); double-deficient in Pellino 1 and Pellino 2 (P1/2$^{-/-}$), Pellino 1 and Pellino 3 (P1/3$^{-/-}$) or Pellino 2 and Pellino 3 (P2/3$^{-/-}$); triple-deficient in Pellino 1, Pellino 2, and Pellino 3 (P1/2/3$^{-/-}$). All error bars are S.E.M. Statistical analysis was performed using **(b, c, d, e)** one-way ANOVA and **(f, g)** two-way ANOVA.

3.2.3.6 Enumeration of naïve CD8$^+$ T cells in Pellino-deficient mice

Like naïve CD4$^+$ T cells, naïve CD8$^+$ T cells need to be activated via interaction with peptide presented by APCs to acquire effector functions (Hochweller *et al.*, 2010). Naïve CD8$^+$ T cells have a low CD44 expression and a high CD62L expression (Gerberick *et al.*, 1997). They were therefore characterised as CD44$^-$ and CD62L$^+$ subset of total CD4$^+$ T cells by flow cytometry (Fig. 3.9a).

There was no significant difference found in young mice across all genotypes (Fig. 3.9b, d). There was no difference in CD8$^+$ T cell numbers in old *Peli1*$^{-/-}$ mice relative to WT mice (Fig. 3.9c), but naïve CD8$^+$ T cell frequency decreased in *Peli1*$^{-/-}$ mice (Fig. 3.9e). Naïve CD8$^+$ T cells in old *Peli2*$^{-/-}$, *Peli3*$^{-/-}$, and *Peli2/3*$^{-/-}$ mice were closely matched with WT mice (Fig. 3.9c, e). However, naïve CD8$^+$ T cells were significantly decreased in aged *Peli1/2*$^{-/-}$ mice (Fig. 3.9c, e). Naïve CD8$^+$ T cell percentages were also significantly reduced in old *Peli1/2/3*$^{-/-}$ mice (Fig. 3.9e). Although a decrease of naïve CD8$^+$ T cells was shown in old *Peli1/3*$^{-/-}$ mice, its small sample size was likely account for its statistical insignificance (Fig. 3.9e). Collectively, this finding implies a common age-associated reduction in naïve CD8$^+$ T cells across all mice bearing Pellino1-deficiency.

When considering sex as a factor in young mice, there was no statistical difference across all groups (Fig. 3.9f). Similar to naïve CD4$^+$ T cells and CD8$^+$ T cells, there was a significantly lower naïve CD8$^+$ T cell frequency in old WT female mice in contrast to old WT male mice (Fig. 3.9g).

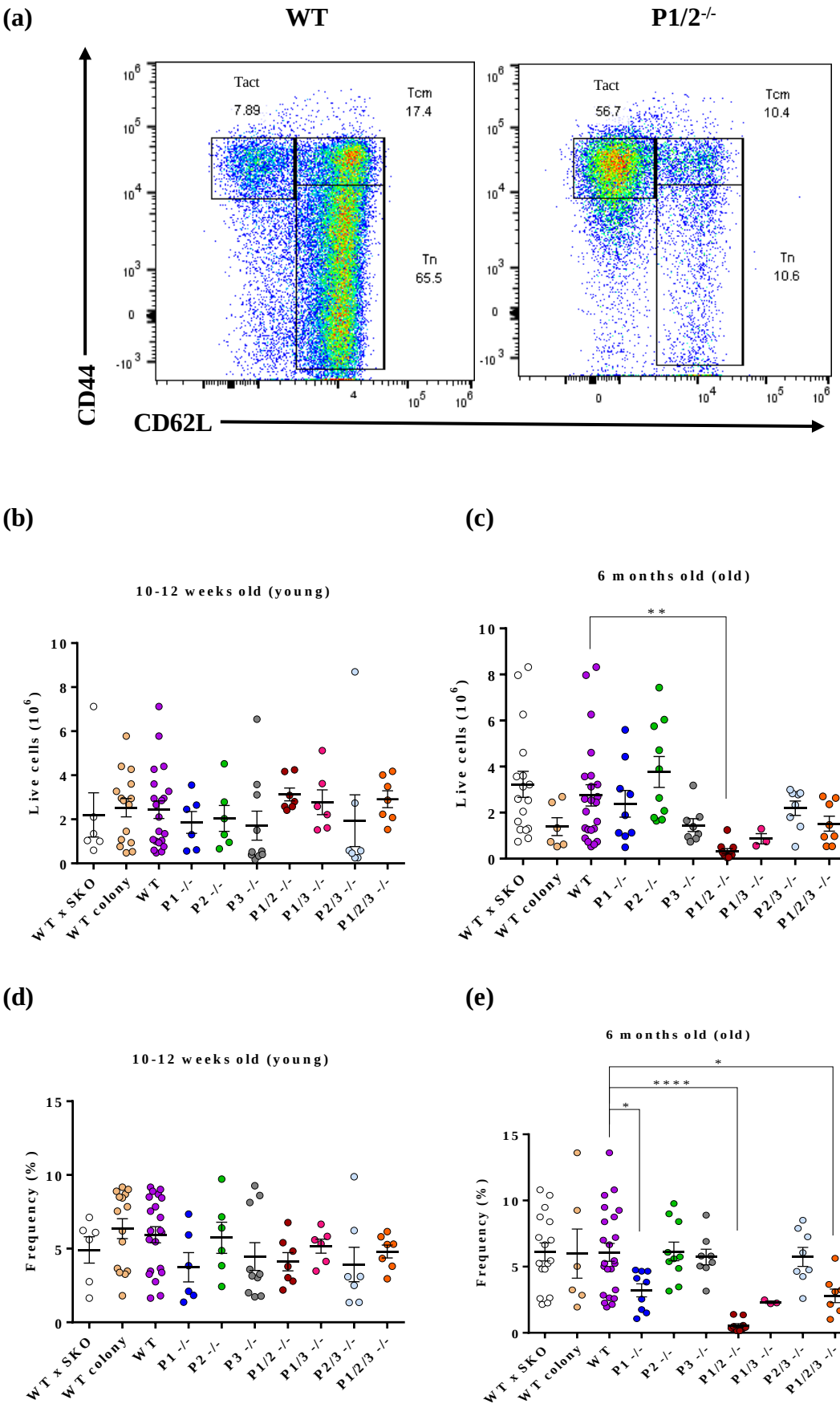
(a)
WT
P1/2-/-
Tact
7.89
Tcm
17.4
Tn
65.5
Tact
56.7
Tcm
10.4
Tn
10.6
CD44
CD62L
(b)
10-12 weeks old (young)
Live cells (10^6)
(c)
6 months old (old)
Live cells (10^6)
(d)
10-12 weeks old (young)
Frequency (%)
(e)
6 months old (old)
Frequency (%)
WT x SKO
WT colony
WT
P1 -/-
P2 -/-
P3 -/-
P1/2 -/-
P1/3 -/-
P2/3 -/-
P1/2/3 -/-

(f)

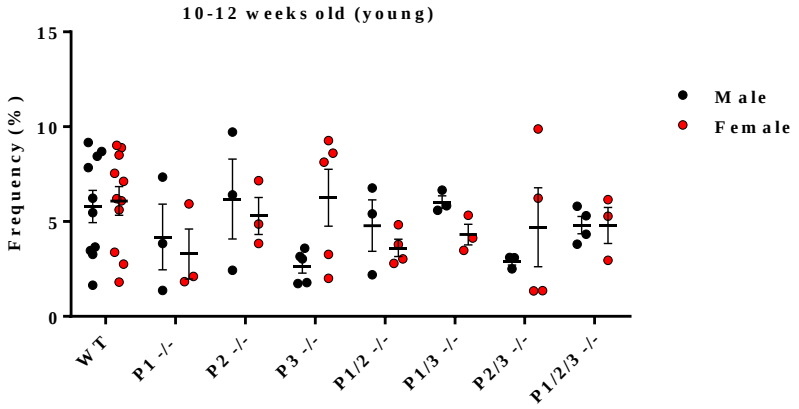

(g)

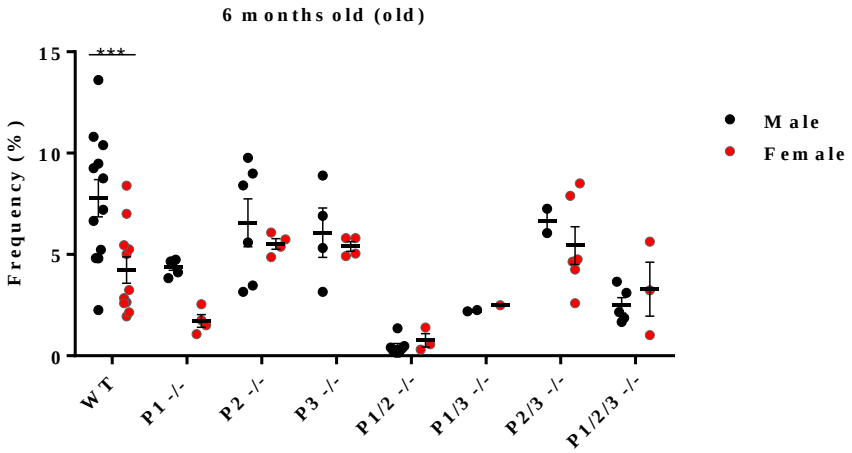

Figure 3.9 Naïve CD8$^+$ cell enumeration in Pellino-deficient mice

Representative dot plots showing naïve CD8$^+$ T cell frequencies of **(a)** a 6-month-old male WT mouse and a *Peli1/2*$^{-/-}$ mouse. Male and female mice were monitored for variations in **(b, c)** naïve CD8$^+$ T cell numbers and **(d, e)** naïve CD8$^+$ T cell frequencies at **(b, d)** 10 to 12 weeks old and **(c, e)** 6 months old. Age matched mice were monitored for gender variation in naïve CD8$^+$ T cell frequencies at **(f)** 10 to 12 weeks old and **(g)** 6 months old. Pellino-deficient mice were single-deficient in Pellino 1 (P1$^{-/-}$), Pellino 2 (P2$^{-/-}$) or Pellino 3 (P3$^{-/-}$); double-deficient in Pellino 1 and Pellino 2 (P1/2$^{-/-}$), Pellino 1 and Pellino 3 (P1/3$^{-/-}$) or Pellino 2 and Pellino 3 (P2/3$^{-/-}$); triple-deficient in Pellino 1, Pellino 2, and Pellino 3 (P1/2/3$^{-/-}$). All error bars are S.E.M. Statistical analysis was performed using **(b, c, d, e)** one-way ANOVA and **(f, g)** two-way ANOVA.

3.2.3.7 Enumeration of effector memory CD8$^+$ T cells in Pellino-deficient mice

Activated CD8$^+$ T cells orchestrate immune responses against neoplastic cells and viral infections (Raskov *et al.*, 2021; Zhang & Bevan., 2011). Memory CD8$^+$ T cells may be subdivided into effector memory (Tem) and central memory CD8$^+$ T cells (Tcm) based on their anatomical location. While CD8$^+$ Tem cells lacking PLN homing receptor CD62L expression are prevalent in nonlymphoid tissues, CD8$^+$ Tcm cells expressing CD62L tend to reside in secondary lymphoid organs (Laidlaw *et al.*, 2016). CD8$^+$ Tem cells confer protection against infections arising within peripheral organs due to their ability to migrate into tissues and exert cytotoxic functions (Martin & Badovinac, 2018). Based on the CD44^{high}CD62L^{low} phenotype of Tem, CD8$^+$ Tem cells were identified as CD44$^+$ and CD62L$^-$ subtype of total CD8$^+$ T cells by flow cytometry (Fig. 3.10a).

When examining the effect of Pellino proteins in CD8$^+$ T cell activation, significantly higher CD8$^+$ Tem cell numbers in young *Peli1/2*$^{-/-}$, *Peli1/3*$^{-/-}$, *Peli1/2/3*$^{-/-}$ mice and old *Peli1*$^{-/-}$ and *Peli1/2*$^{-/-}$ mice were exhibited (Fig. 3.10b, c). Furthermore, CD8$^+$ Tem cell frequency was also significantly elevated in both age groups of all genotypes that contain Pellino 1 deficiency, except old *Peli1/2/3*$^{-/-}$ mice which showed similar pattern without statistical significance (Fig. 3.10d, e). There was no difference in CD8$^+$ Tem cells in *Peli2*$^{-/-}$, *Peli3*$^{-/-}$ mice, and *Peli2/3*$^{-/-}$ mice relative to WT mice regardless of age (Fig. 3.10b, c, d, e). The greater production of CD8$^+$ Tem cells found in mice carrying Pellino 1-deficiency began from young age and remained until they aged; this is especially striking in *Peli1/2*$^{-/-}$ mice.

Gender exploration in young mice revealed no difference in CD8$^+$ Tem cells between males and females in all genotypes except a higher level in young *Peli1/2/3*$^{-/-}$ female mice than male mice (Fig. 3.10f). In old age group, no difference in CD8$^+$ Tem cells was observed between the two genders in all genotypes (Fig. 3.10g).

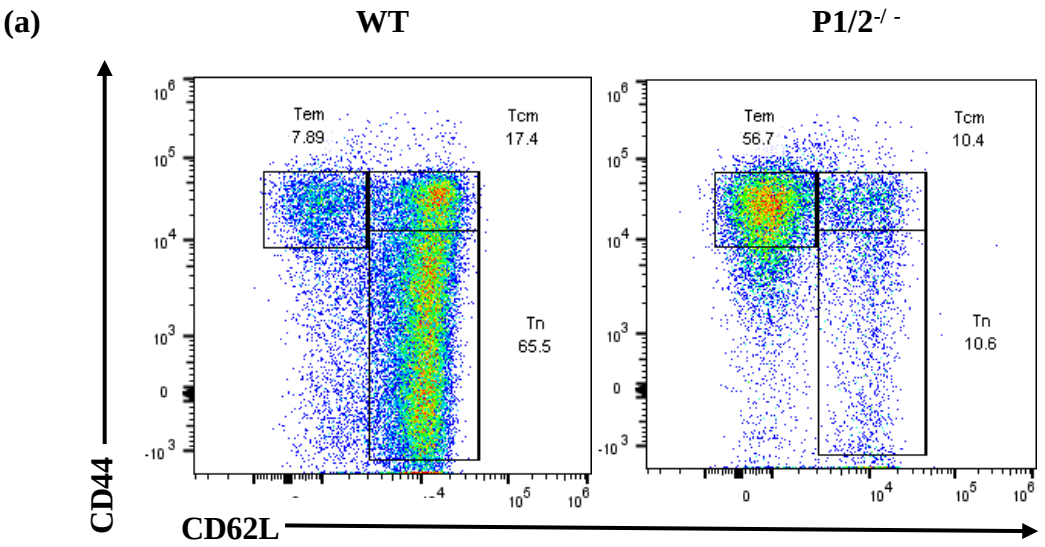
(a)
WT
P1/2-/-
Tem
7.89
Tcm
17.4
Tn
65.5
Tem
56.7
Tcm
10.4
Tn
10.6
CD44
CD62L

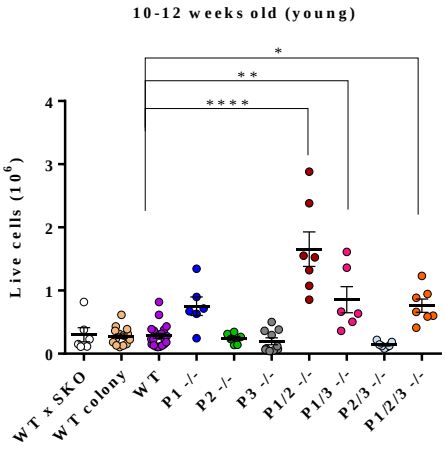
(b)
10-12 weeks old (young)
Live cells (10^6)
WT x SKO
WT colony
WT
P1 -/-
P2 -/-
P3 -/-
P1/2 -/-
P1/3 -/-
P2/3 -/-
P1/2/3 -/-

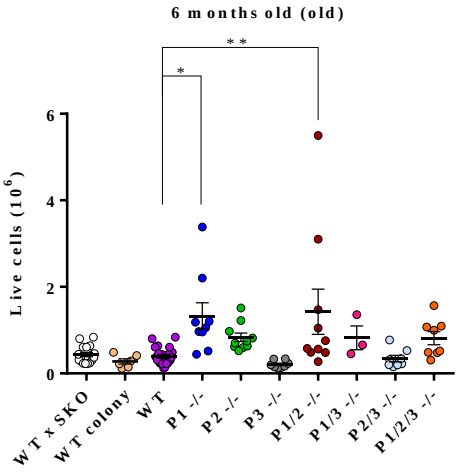
(c)
6 months old (old)
Live cells (10^6)
WT x SKO
WT colony
WT
P1 -/-
P2 -/-
P3 -/-
P1/2 -/-
P1/3 -/-
P2/3 -/-
P1/2/3 -/-

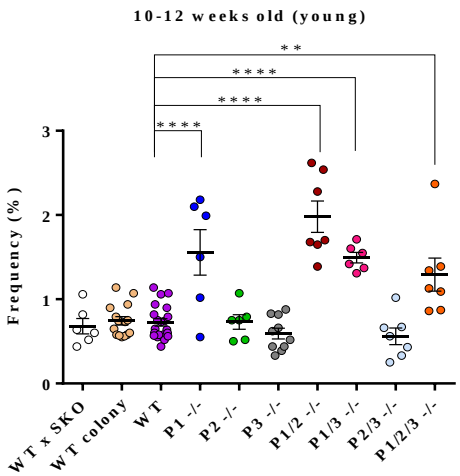
(d)
10-12 weeks old (young)
Frequency (%)
WT x SKO
WT colony
WT
P1 -/-
P2 -/-
P3 -/-
P1/2 -/-
P1/3 -/-
P2/3 -/-
P1/2/3 -/-

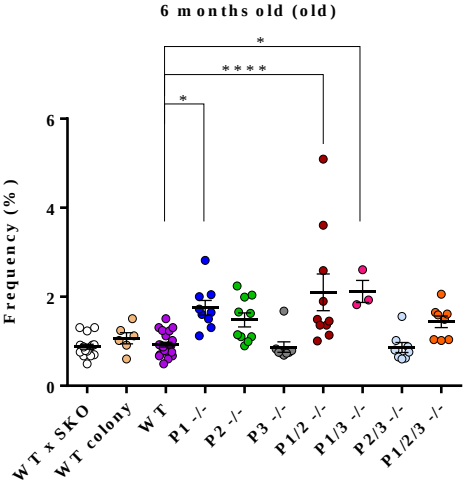
(e)
6 months old (old)
Frequency (%)
WT x SKO
WT colony
WT
P1 -/-
P2 -/-
P3 -/-
P1/2 -/-
P1/3 -/-
P2/3 -/-
P1/2/3 -/-

(f)

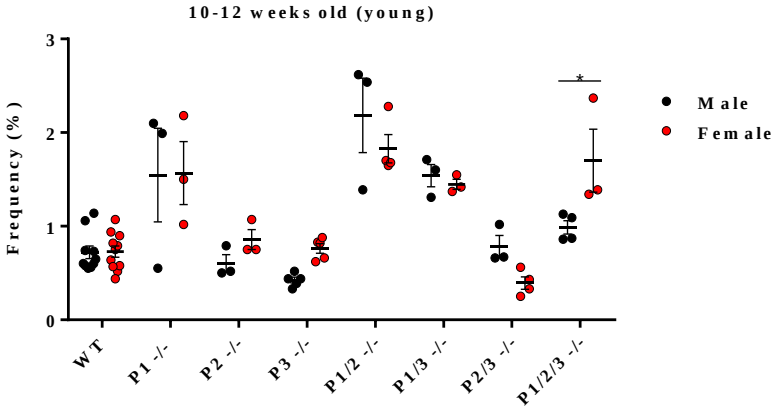

(g)

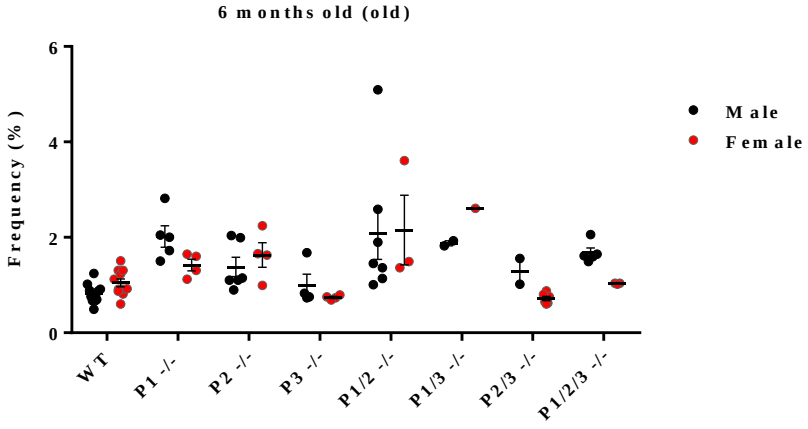

Figure 3.10 Effector memory CD8$^+$ T cell (Tem) enumeration in Pellino-deficient mice

Representative dot plots showing CD8$^+$ Tem cell frequencies of **(a)** a 6-month-old male WT mouse and a *Peli1/2*$^{-/-}$ mouse. Male and female mice were monitored for variations in **(b, c)** CD8$^+$ Tem cell numbers and **(d, e)** CD8$^+$ Tem cell frequencies at **(b, d)** 10 to 12 weeks old and **(c, e)** 6 months old. Age matched mice were monitored for gender variation in CD8$^+$ Tem cell frequencies at **(f)** 10 to 12 weeks old and **(g)** 6 months old. Pellino-deficient mice were single-deficient in Pellino 1 (P1$^{-/-}$), Pellino 2 (P2$^{-/-}$) or Pellino 3 (P3$^{-/-}$); double-deficient in Pellino 1 and Pellino 2 (P1/2$^{-/-}$), Pellino 1 and Pellino 3 (P1/3$^{-/-}$) or Pellino 2 and Pellino 3 (P2/3$^{-/-}$); triple-deficient in Pellino 1, Pellino 2, and Pellino 3 (P1/2/3$^{-/-}$). All error bars are S.E.M. Statistical analysis was performed using **(b, c, d, e)** one-way ANOVA and **(f, g)** two-way ANOVA.

3.2.3.8 Enumeration of central memory $CD8^+$ T cells in Pellino-deficient mice

It is reported that $CD8^+$ Tcm cells are responsible for clearing systemic infections due to their central location within secondary lymphoid organs and enhanced proliferative capability in response to antigens (Wherry *et al.*, 2003). They were characterised as $CD44^+$ and $CD62L^+$ population by flow cytometry (Fig. 3.11a).

Young mice of Pellino-deficient mice depicted comparable $CD8^+$ Tcm cells with WT mice except for a significant increase of $CD8^+$ Tcm cells found in young *Peli1/2*$^{-/-}$ (Fig. 3.11b, d). Old *Peli2*$^{-/-}$ mice also showed higher levels of $CD8^+$ Tcm cells compared with WT mice in terms of cell number and frequency (Fig. 3.11c, e). While $CD8^+$ Tcm cell frequency was primarily unaffected by the loss of Pellino proteins, there a significant reduction of $CD8^+$ Tcm cell frequency in old *Peli1/2*$^{-/-}$ mice (Fig. 3.11e).

Viewing from an age factor, *Peli2*$^{-/-}$ mice gained significantly greater $CD8^+$ Tcm cells than WT mice as they aged (Fig. 3.11b, c, d, e). Conversely, *Peli1/2*$^{-/-}$ mice had significantly higher $CD8^+$ Tcm cell count than WT mice at young age (Fig. 3.11b, d), which depleted significantly at old age (Fig. 3.11c, e). This suggests that $CD8^+$ Tcm cell generation was extensively impacted by aging process in *Peli1/2*$^{-/-}$ mice. Examination of gender dimension in both young and old mice revealed no difference in $CD8^+$ Tcm cells in female mice compared to their male counterparts across all genotypes (Fig. 3.11f, g).

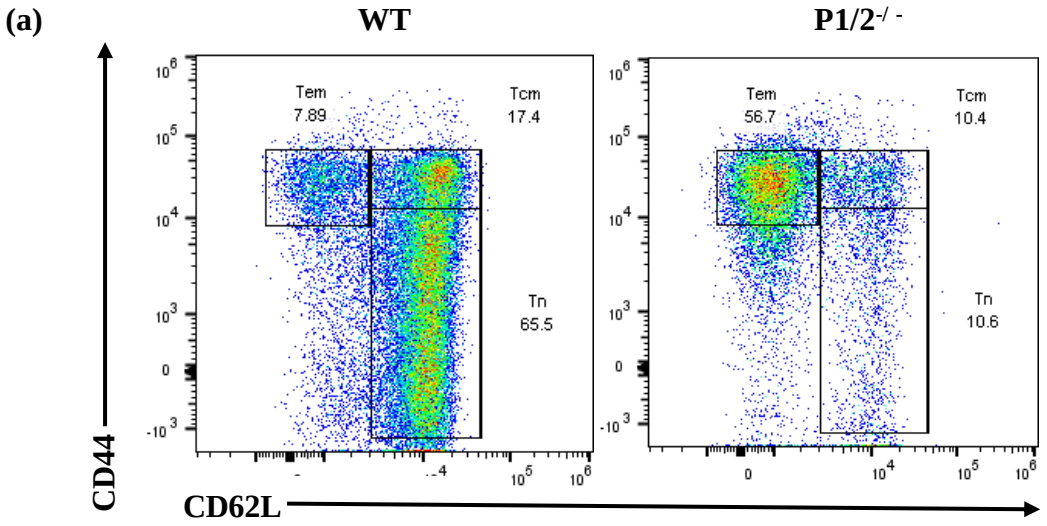
(a)
WT
P1/2-/-
Tem
7.89
Tcm
17.4
Tn
65.5
Tem
56.7
Tcm
10.4
Tn
10.6
CD44
CD62L

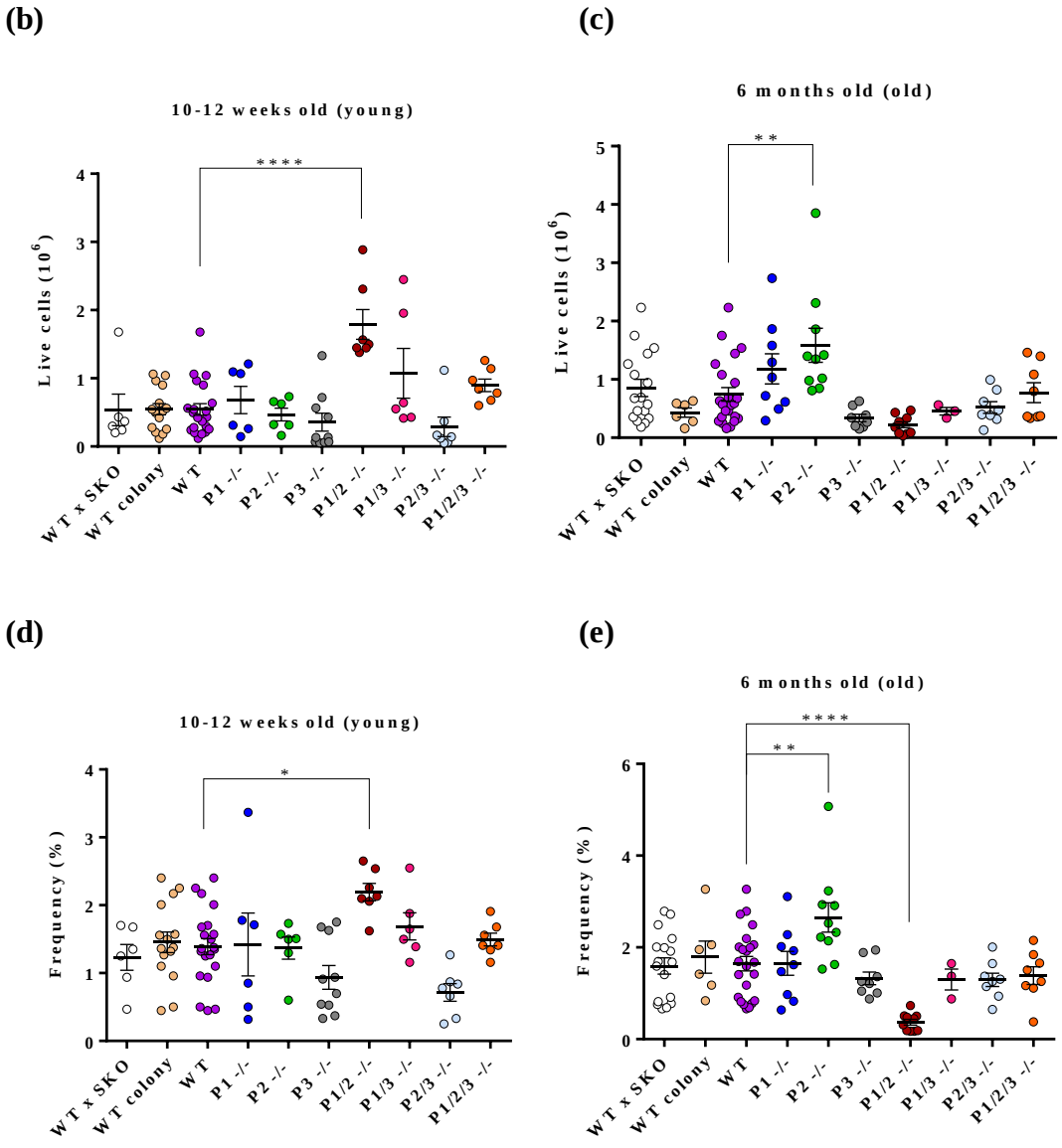
(b)
10-12 weeks old (young)
Live cells (10^6)
****
(c)
6 months old (old)
Live cells (10^6)
**
(d)
10-12 weeks old (young)
Frequency (%)
*
(e)
6 months old (old)
Frequency (%)
****
**
WT x SKO
WT colony
WT
P1 -/-
P2 -/-
P3 -/-
P1/2 -/-
P1/3 -/-
P2/3 -/-
P1/2/3 -/-

(f)

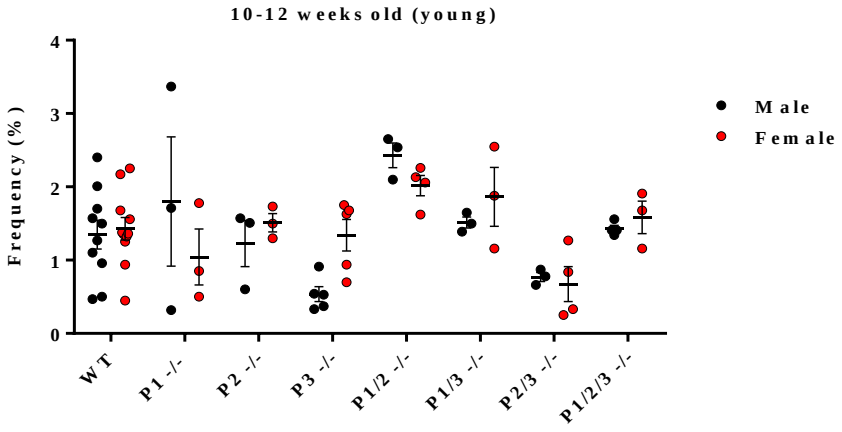

(g)

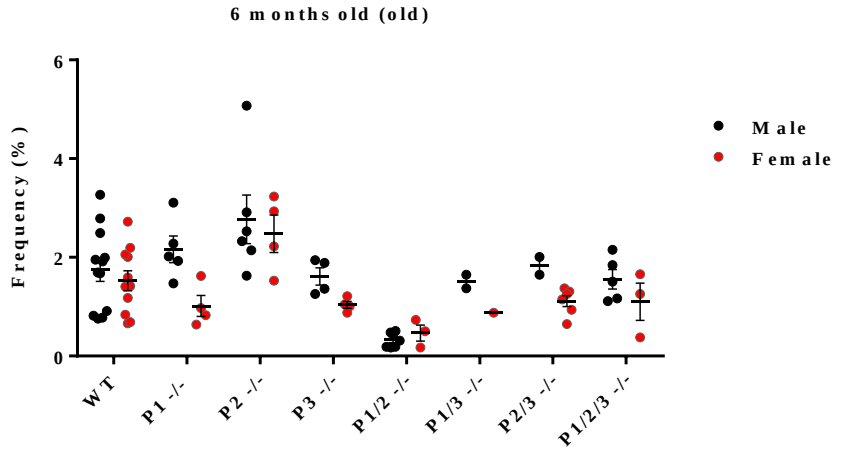

Figure 3.11 Central memory CD8$^+$ T cell (Tcm) enumeration in Pellino-deficient mice

Representative dot plots showing CD8$^+$ Tcm cell frequencies of **(a)** a 6-month-old male WT mouse and a *Peli1/2*$^{-/-}$ mouse. Male and female mice were monitored for variations in **(b, c)** CD8$^+$ Tcm cell numbers and **(d, e)** CD8$^+$ Tcm cell frequencies at **(b, d)** 10 to 12 weeks old and **(c, e)** 6 months old. Age matched mice were monitored for gender variation in CD8$^+$ Tcm cell frequencies at **(f)** 10 to 12 weeks old and **(g)** 6 months old. Pellino-deficient mice were single-deficient in Pellino 1 (P1$^{-/-}$), Pellino 2 (P2$^{-/-}$) or Pellino 3 (P3$^{-/-}$); double-deficient in Pellino 1 and Pellino 2 (P1/2$^{-/-}$), Pellino 1 and Pellino 3 (P1/3$^{-/-}$) or Pellino 2 and Pellino 3 (P2/3$^{-/-}$); triple-deficient in Pellino 1, Pellino 2, and Pellino 3 (P1/2/3$^{-/-}$). All error bars are S.E.M. Statistical analysis was performed using **(b, c, d, e)** one-way ANOVA and **(f, g)** two-way ANOVA.

3.2.3.9 Enumeration of γδ T cells in Pellino-deficient mice

γδ T cells are critical players in cancer immunity, tissue repair, and protection against pathogens (Silva-Santos *et al.*, 2015; Ribot *et al.*, 2021; Vantourout & Hayday, 2013). As a subset of T cells, γδ T cells express CD3 and γδTCR, hence they were identified as $CD3^+$ and $\gamma\delta TCR^+$ population by flow cytometry (Fig. 3.12a).

γδ T cell numbers in young *Peli1/2*$^{-/-}$ mice were significantly increased when compared to WT mice (Fig. 3.12b). There was no considerable difference detected between other young Pellino-deficient and WT mice with regards to γδ T cell numbers and frequencies (Fig. 3.12b, d). In aged mice, there was no difference in γδ T cell numbers and frequencies of old *Peli1*$^{-/-}$, *Peli2*$^{-/-}$, *Peli3*$^{-/-}$, and *Peli1/3*$^{-/-}$ mice relative to WT mice (Fig. 3.12c). γδ T cell percentages of old *Peli1/2*$^{-/-}$ and *Peli1/2/3*$^{-/-}$ mice were significantly decreased, whereas γδ T cell percentages were significantly elevated in old *Peli2/3*$^{-/-}$ mice compared with WT mice (Fig. 3.12e).

Age comparison in γδ T cell populations demonstrated declined production of these cells in *Peli1/2*$^{-/-}$, *Peli1/3*$^{-/-}$, and *Peli1/2/3*$^{-/-}$ mice as they grew older (Fig. 3.12b, c, d, e). On the other hand, this trend was reversed in *Peli2/3*$^{-/-}$ mice (Fig. 3.12b, c, d, e). Collectively, this implies the existence of intricate interactions among the Pellino family proteins when more than one member is simultaneously absent. By exploring gender dimension in young mice, there were significantly more γδ T cells in young WT females than WT males (Fig. 3.12f). Other young Pellino-deficient mice exhibited no difference in γδ T cells between genders (Fig. 3.12f). Furthermore, γδ T cell frequency in old females in contrast to their male counterparts was also similar (Fig. 3.12g).

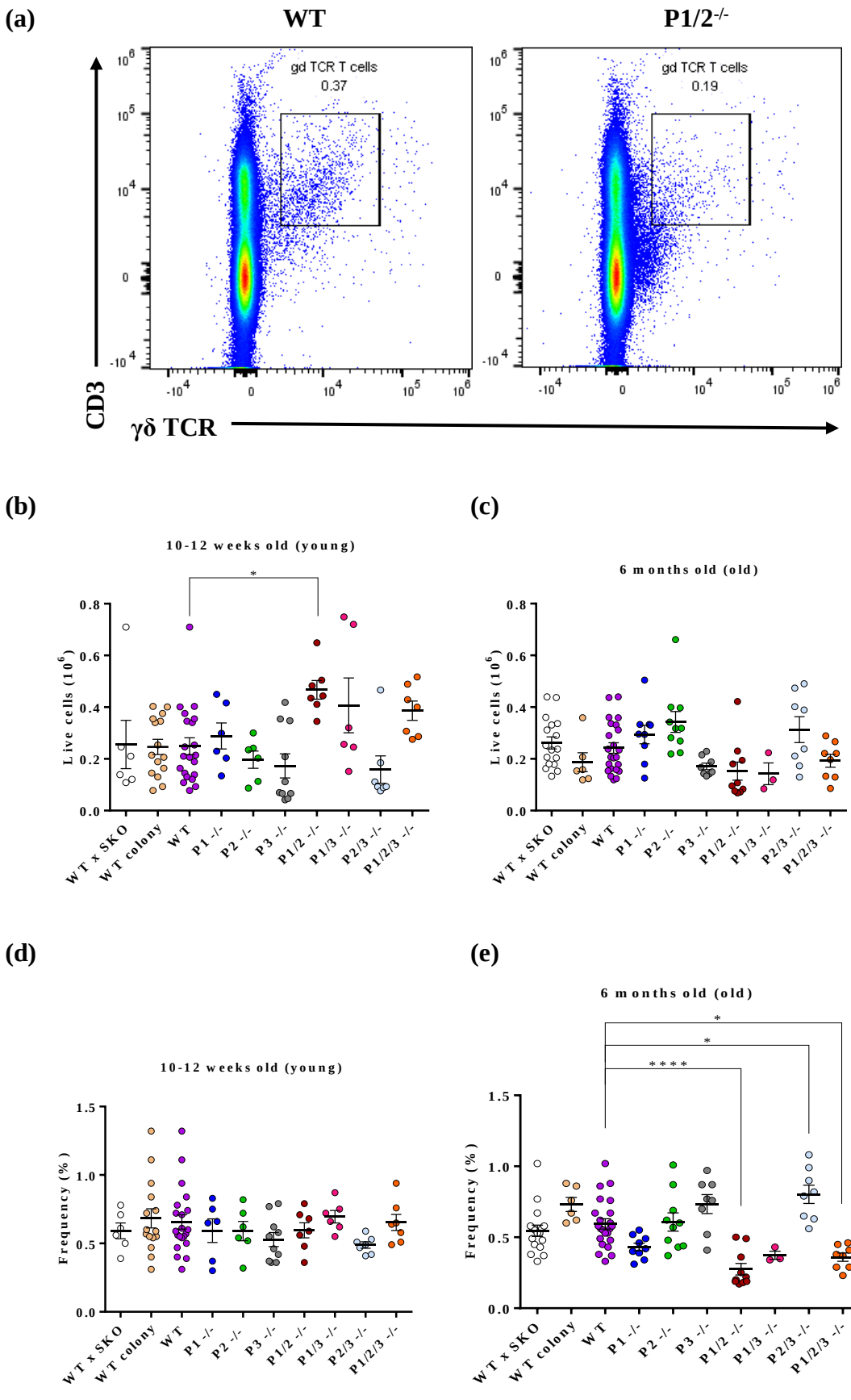
(a)
WT
P1/2-/-
gd TCR T cells
0.37
gd TCR T cells
0.19
CD3
γδ TCR
(b)
10-12 weeks old (young)
Live cells (10^6)
(c)
6 months old (old)
Live cells (10^6)
(d)
10-12 weeks old (young)
Frequency (%)
(e)
6 months old (old)
Frequency (%)
WT x SKO
WT colony
WT
P1 -/-
P2 -/-
P3 -/-
P1/2 -/-
P1/3 -/-
P2/3 -/-
P1/2/3 -/-

(f)

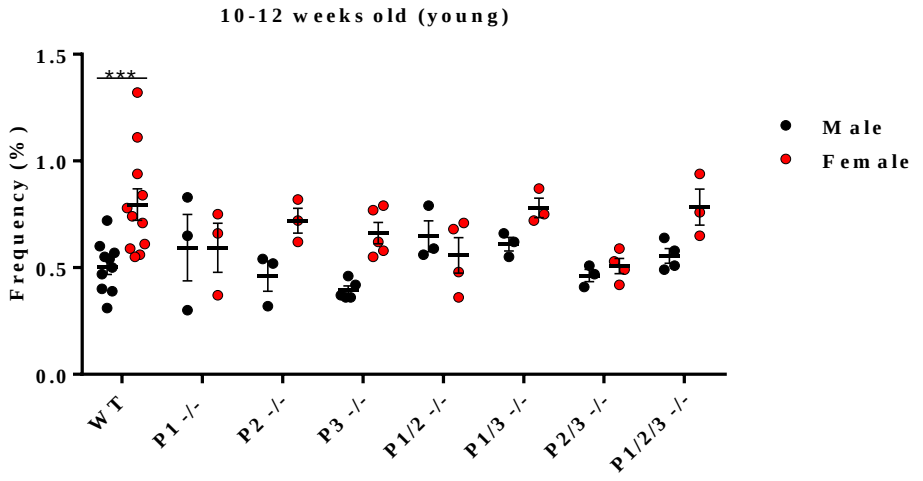

(g)

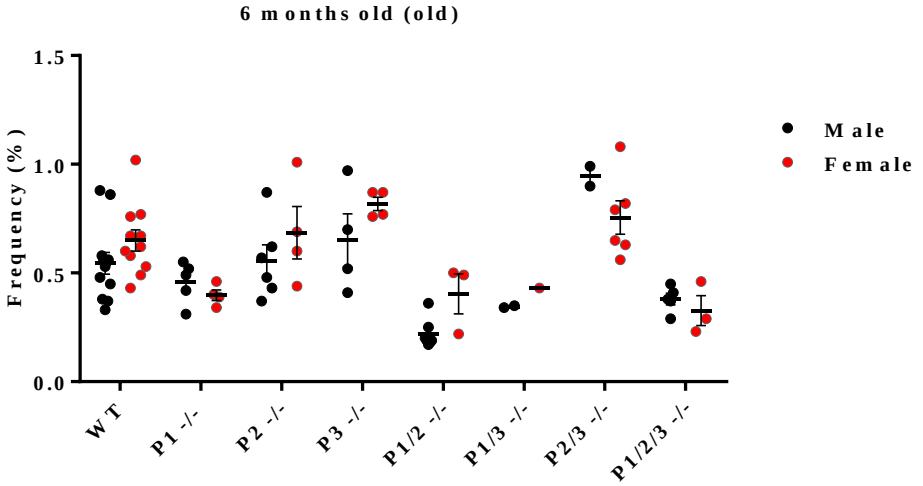

Figure 3.12 γδ T cell enumeration in Pellino-deficient mice

Representative dot plots showing γδ T cell frequencies of **(a)** a 6-month-old male WT mouse and a *Peli1/2*$^{-/-}$ mouse. Male and female mice were monitored for variations in **(b, c)** γδ T cell numbers and **(d, e)** γδ T cell frequencies at **(b, d)** 10 to 12 weeks old and **(c, e)** 6 months old. Age matched mice were monitored for gender variation in γδ T cell frequencies at **(f)** 10 to 12 weeks old and **(g)** 6 months old. Pellino-deficient mice single-deficient in Pellino 1 (P1$^{-/-}$), Pellino 2 (P2$^{-/-}$) or Pellino 3 (P3$^{-/-}$); double-deficient in Pellino 1 and Pellino 2 (P1/2$^{-/-}$), Pellino 1 and Pellino 3 (P1/3$^{-/-}$) or Pellino 2 and Pellino 3 (P2/3$^{-/-}$); triple-deficient in Pellino 1, Pellino 2, and

Pellino 3 (P1/2/3$^{-/-}$). All error bars are S.E.M. Statistical analysis was performed using **(b, c, d, e)** one-way ANOVA and **(f, g)** two-way ANOVA.

Genotypes		*Peli1*$^{-/-}$		*Peli1/2*$^{-/-}$		*Peli1/3*$^{-/-}$		*Peli1/2/3*$^{-/-}$		*Peli2*$^{-/-}$		*Peli3*$^{-/-}$		*Peli2/3*$^{-/-}$	
Cell types		Y	O	Y	O	Y	O	Y	O	Y	O	Y	O	Y	O
CD3$^+$ T cell	#														
	%														
CD4$^+$ T cell	#														
	%														
Naïve CD4$^+$ T cell	#														
	%														
Activated CD4$^+$ T cell	#														
	%														
CD8$^+$ T cell	#														
	%														
Naïve CD8$^+$ T cell	#														
	%														
CD8$^+$ Tem cell	#														
	%														
CD8$^+$ Tcm cell	#														
	%														
γδ T cell	#														
	%														

Table 3.2 Statistical significance relevance of splenic T cell subpopulations between WT and Pellino-deficient strains. Y = young mice, O = old mice, # = cell number, % = cell percentage/frequency, red column = statistical significant increase, blue column = statistical significant reduction, white column = no statistical significant changes.

3.2.4 Immunophenotyping of B cell populations in Pellino-deficient mice

Although Pellino 1 has been positively and negatively linked with B cell-related diseases (Park *et al.*, 2014; Liu *et al.*, 2018), the impact of Pellino proteins on each B cell subset remains to be fully investigated. B cells are the second most prevalent cell type in a mouse spleen. Single cell suspensions of sex and age matched mice lacking various Pellino proteins were generated from the spleen. These spleen cells were then stained extracellularly with different cell surface markers to identify B220$^+$ T cells, B1 cells, B2 cells, immature B cells, follicular B cells, marginal zone B cells, germinal centre B cells, and plasma cells by flow cytometry. This quantitative analysis was again presented in two parameters: live cell number and cell frequency/percentage.

3.2.4.1 Enumeration of B220^{+} B cells in Pellino-deficient mice

B cells are a component of the adaptive immune system that exert defensive mechanism against pathogens by releasing antibodies. B220 is the CD45 (leukocyte common antigen) isoform in mice that marks B lymphocytes (Bleesing & Fleisher, 2002). Therefore, B cells were detected as B220^{+} population by flow cytometry (Fig. 3.13a).

Young singly Pellino 1-, Pellino 2-, or Pellino 3-deficient mice had similar B cell numbers compared with WT mice (Fig. 3.13b), but *Peli2*$^{-/-}$ mice had enhanced frequency of B cells (Fig. 3.13d). The B cell numbers in young *Peli1/2*$^{-/-}$ mice were also markedly larger than that for WT mice of the same age (Fig. 3.13b), but this was not reflected in the population frequency (Fig. 3.13d). This implies that there may be a mild tendency towards B cell production in the absence of Pellino 2 that is related to Pellino 3 as this trend can be reversed by the loss of Pellino 3.

Moreover, the increase of B cell numbers and frequency observed in *Peli1/2*$^{-/-}$ and *Peli2*$^{-/-}$ mice, respectively was restricted in younger mice as there was no statistically meaningful sign of aberrant B cell expression in comparison with aged WT mice (Fig. 3.13c, d). When comparing between different genders of mice, females of young and old mice exhibited similar B cell frequency compared with the males (Fig. 3.13f, g). Taken together, this Pellino 2-associated B cell phenotype is age and sex specific.

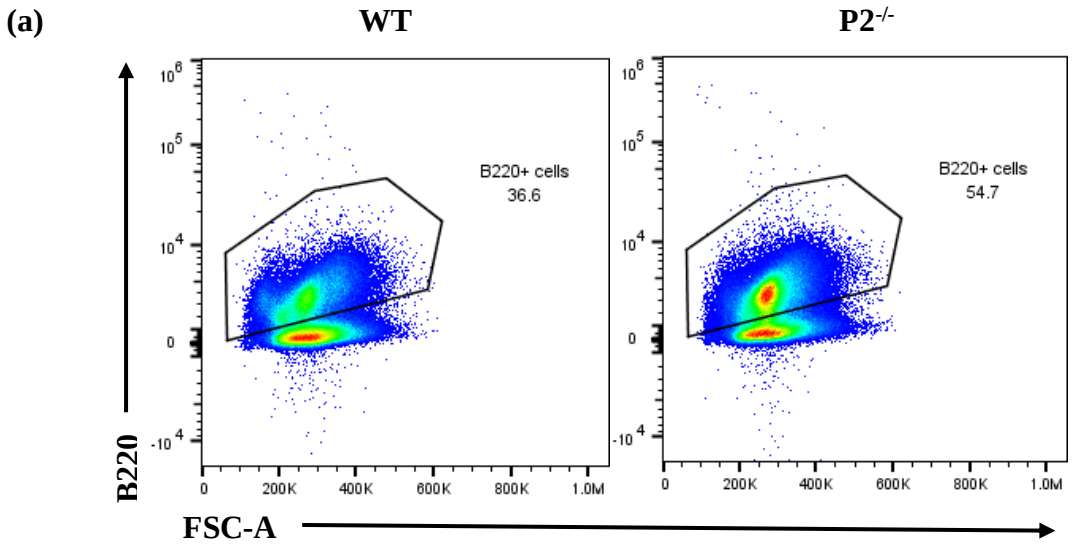
(a)
WT
P2-/-
B220+ cells
36.6
B220+ cells
54.7
B220
FSC-A

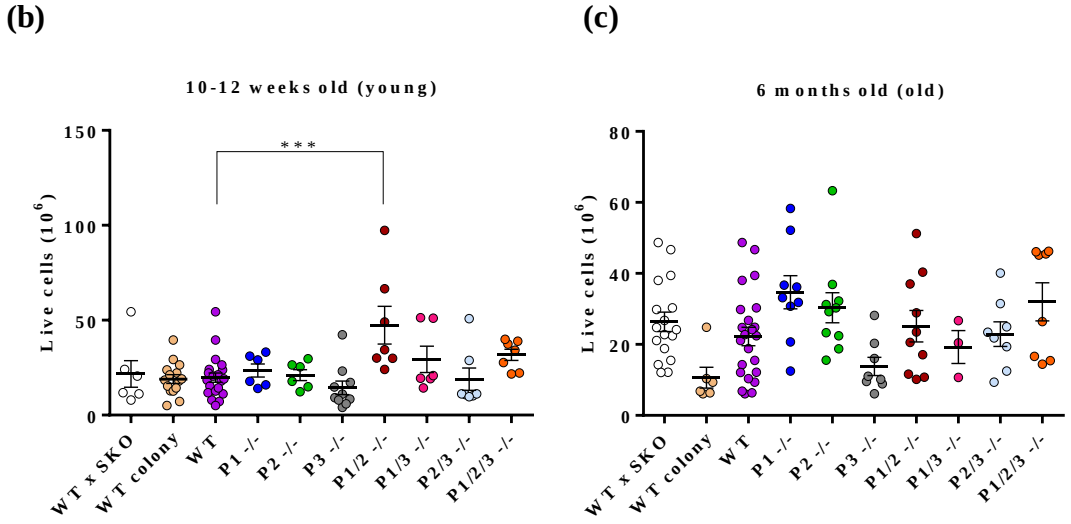
(b)
(c)
10-12 weeks old (young)
6 months old (old)
Live cells (10^6)
***
WT x SKO
WT colony
WT
P1 -/-
P2 -/-
P3 -/-
P1/2 -/-
P1/3 -/-
P2/3 -/-
P1/2/3 -/-

(d)

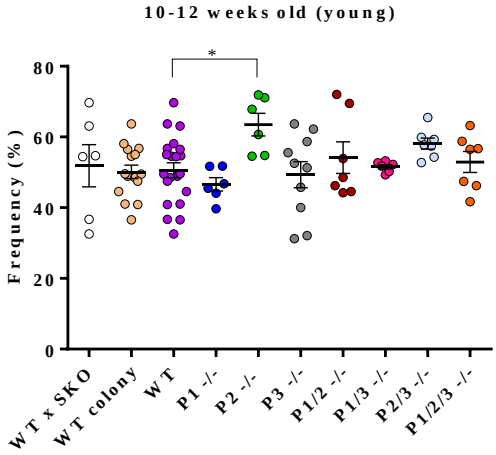
10-12 weeks old (young)
Frequency (%)
80
60
40
20
0
*
WT x SKO
WT colony
WT
P1 -/-
P2 -/-
P3 -/-
P1/2 -/-
P1/3 -/-
P2/3 -/-
P1/2/3 -/-

(e)

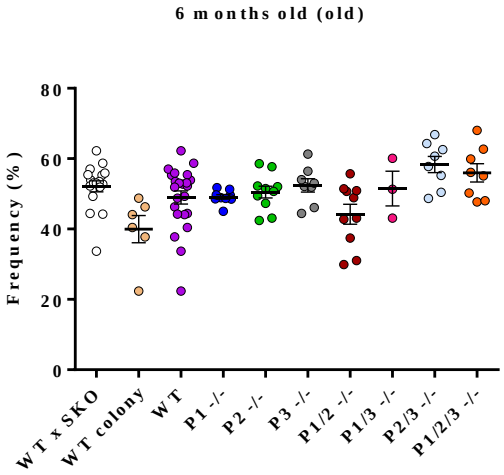
6 months old (old)
Frequency (%)
80
60
40
20
0
WT x SKO
WT colony
WT
P1 -/-
P2 -/-
P3 -/-
P1/2 -/-
P1/3 -/-
P2/3 -/-
P1/2/3 -/-

(f)

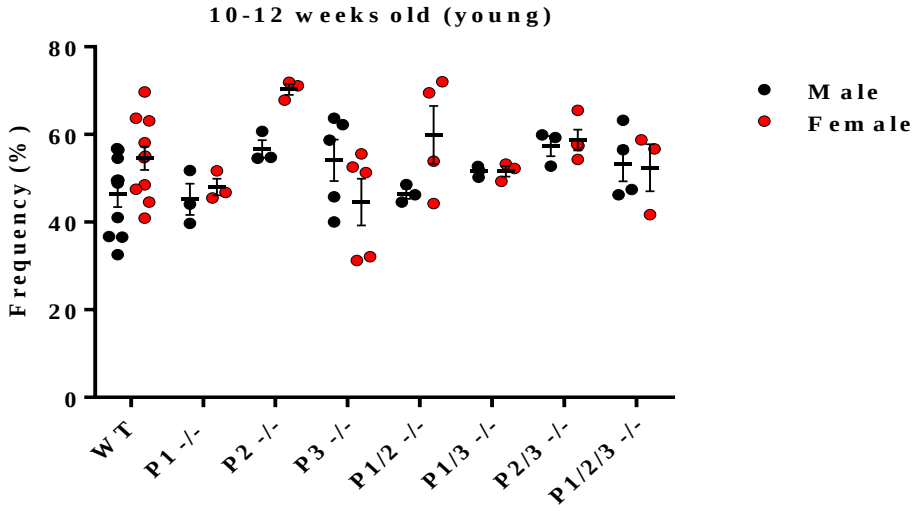
10-12 weeks old (young)
Frequency (%)
80
60
40
20
0
WT
P1 -/-
P2 -/-
P3 -/-
P1/2 -/-
P1/3 -/-
P2/3 -/-
P1/2/3 -/-
Male
Female

(g)

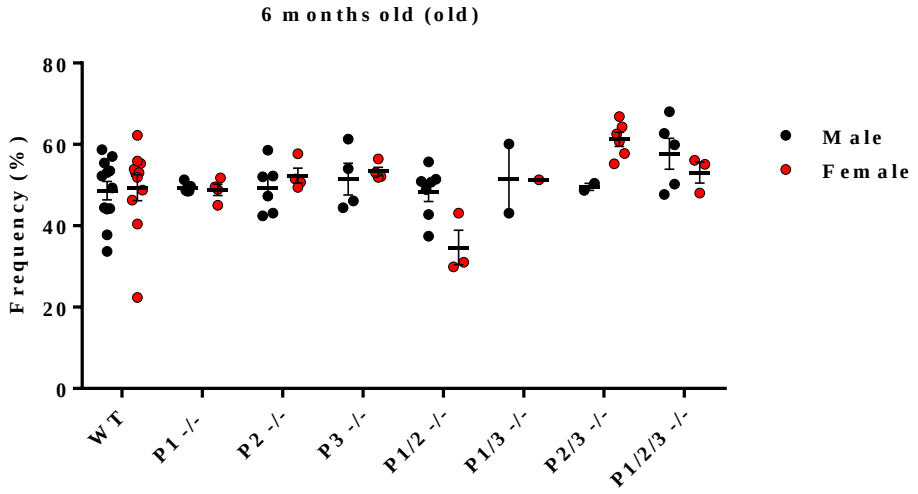

Figure 3.13 B220$^+$ cell enumeration in Pellino-deficient mice

Representative dot plots showing B220$^+$ cell frequencies of **(a)** a 10- to 12-week-old male WT mouse and a *Peli2*$^{-/-}$ mouse. Male and female mice were monitored for variations in **(b, c)** B220$^+$ cell numbers and **(d, e)** B220$^+$ cell frequencies at **(b, d)** 10 to 12 weeks old and **(c, e)** 6 months old. Age matched mice were monitored for gender variation in B220$^+$ cell frequencies at **(f)** 10 to 12 weeks old and **(g)** 6 months old. Pellino-deficient mice were single-deficient in Pellino 1 (P1$^{-/-}$), Pellino 2 (P2$^{-/-}$) or Pellino 3 (P3$^{-/-}$); double-deficient in Pellino 1 and Pellino 2 (P1/2$^{-/-}$), Pellino 1 and Pellino 3 (P1/3$^{-/-}$) or Pellino 2 and Pellino 3 (P2/3$^{-/-}$); triple-deficient in Pellino 1, Pellino 2, and Pellino 3 (P1/2/3$^{-/-}$). All error bars are S.E.M. Statistical analysis was performed using **(b, c, d, e)** one-way ANOVA and **(f, g)** two-way ANOVA.

3.2.4.2 Enumeration of B1 cells in Pellino-deficient mice

B1 cells are abundantly found in the peritoneal cavity, but constitute only a small fraction of the spleen of adult mice. B1 cells are crucial for first line defence by secreting natural antibodies against bacterial pathogens (Bhat *et al.*, 1992). B220 and CD19 were utilised as markers to identify B1 and B2 cell subtype. When B cells develop into B1 cells, unlike B2 cells, CD19 is expressed before B220 and CD43 (Ghosn *et al.*, 2011). As such, B1 cells harbour extracellular expression of $CD19^{+}$ and $B220^{low\text{-}negative}$ that can be identified by flow cytometry (Fig. 3.14a).

There was no discrete difference in B1 cell population illustrated between WT mice and Pellino protein-deficient mice (Fig. 3.14b, c, d, e), suggesting that Pellino proteins are not involved in the regulation of B1 cell production. There was also no considerable difference in B1 cell enumeration with regards to age in mice expressing Pellino proteins or not. Interestingly, the prevalence of B1 cell was significantly higher in young female *Peli2*$^{-/-}$ mice than that for male *Peli2*$^{-/-}$ mice (Fig. 3.14f). This explains the non-uniform spread of B1 cell frequency in young *Peli2*$^{-/-}$ mice (Fig. 3.14d). There was no difference between males and females of all groups in aged mice (Fig. 3.14g). Overall, Pellino 2 may have a gender-biased impact on B1 cell production.

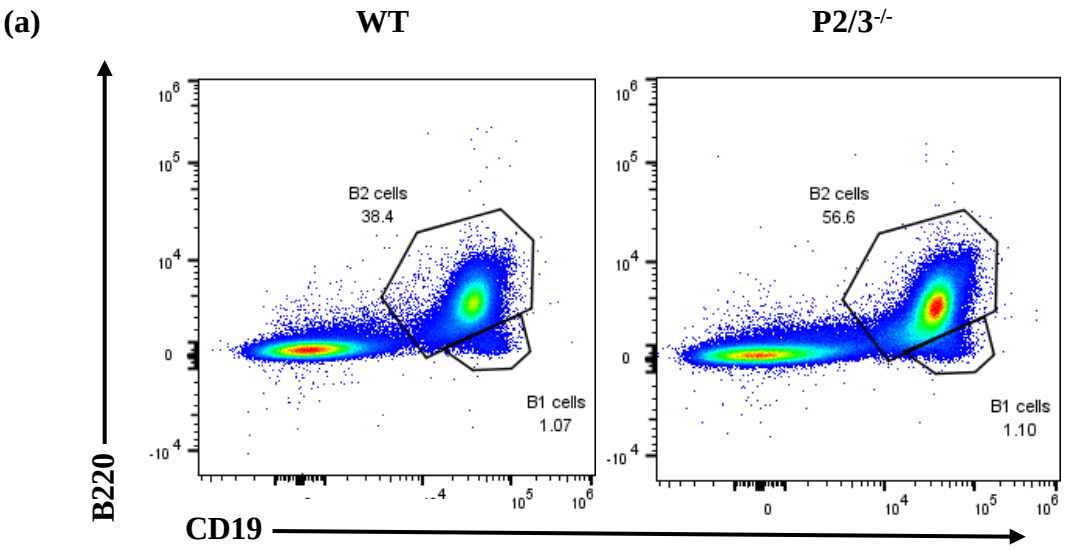
(a)
WT
P2/3-/-
B2 cells
38.4
B1 cells
1.07
B2 cells
56.6
B1 cells
1.10
B220
CD19

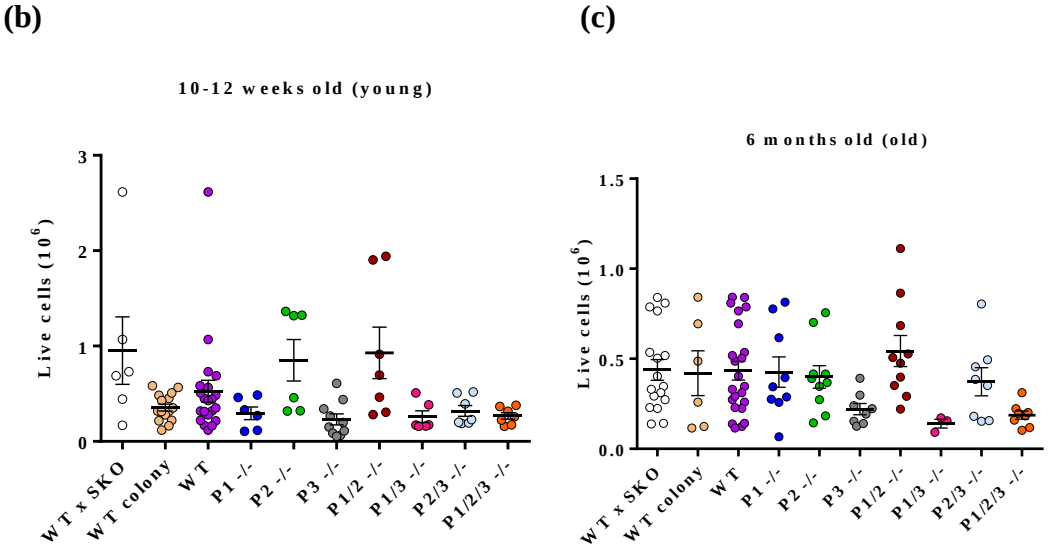
(b)
(c)
10-12 weeks old (young)
6 months old (old)
Live cells (10^6)
WT x SKO
WT colony
WT
P1 -/-
P2 -/-
P3 -/-
P1/2 -/-
P1/3 -/-
P2/3 -/-
P1/2/3 -/-

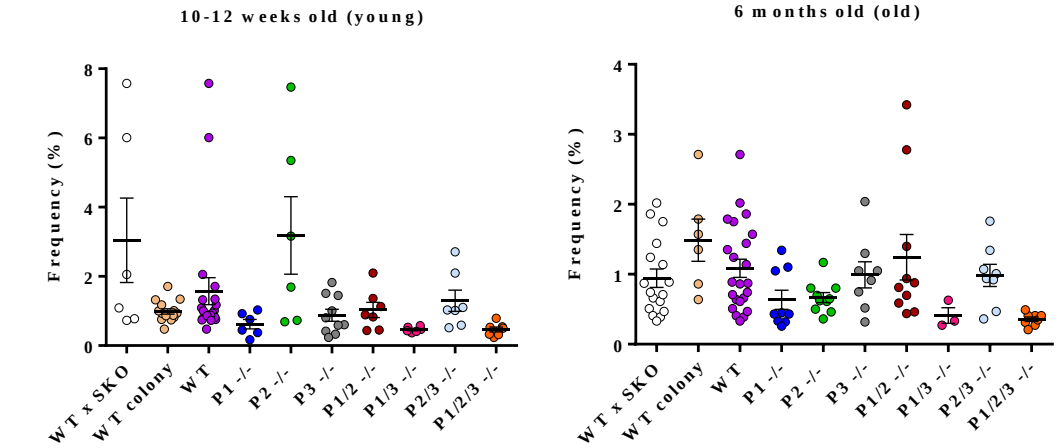
(d)
(e)
10-12 weeks old (young)
6 months old (old)
Frequency (%)
WT x SKO
WT colony
WT
P1 -/-
P2 -/-
P3 -/-
P1/2 -/-
P1/3 -/-
P2/3 -/-
P1/2/3 -/-

(f)

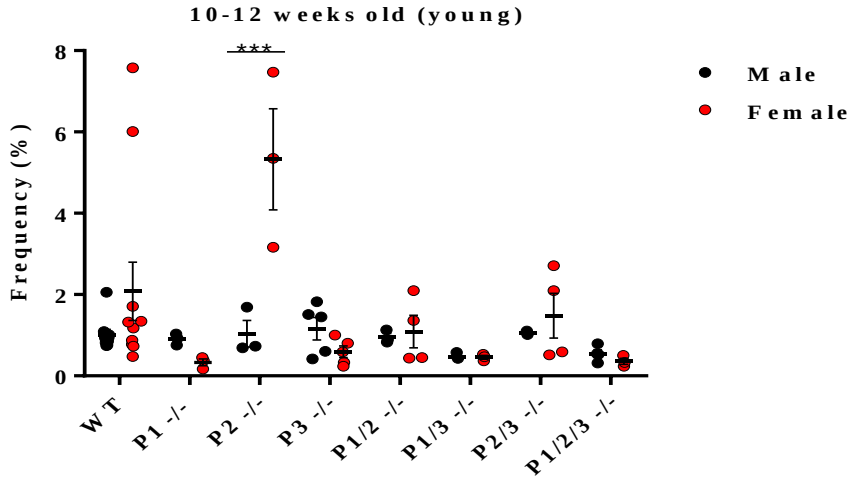

(g)

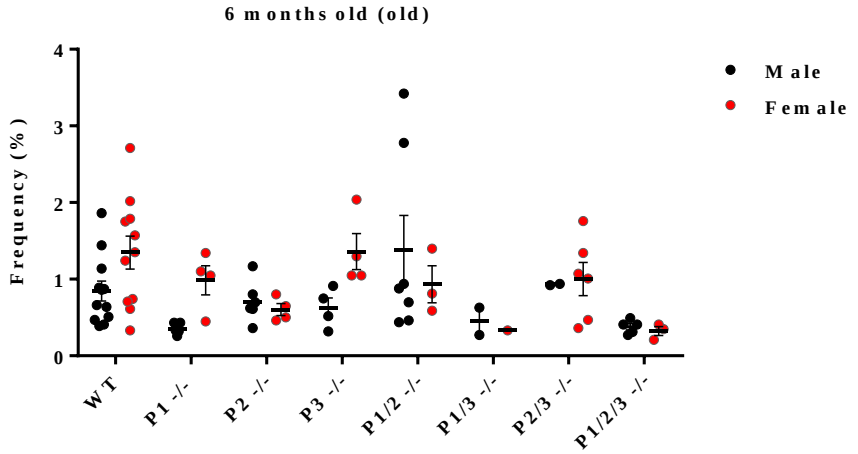

Figure 3.14 B1 cell enumeration in Pellino-deficient mice

Representative dot plots showing B1 cell frequencies of **(a)** a 10- to 12-week-old male WT mouse and a *Peli2/3*$^{-/-}$ mouse. Male and female mice were monitored for variations in **(b, c)** B1 cell numbers and **(d, e)** B1 cell frequencies at **(b, d)** 10 to 12 weeks old and **(c, e)** 6 months old. Age matched mice were monitored for gender variation in B1 cell frequencies at **(f)** 10 to 12 weeks old and **(g)** 6 months old. Pellino-deficient mice were single-deficient in Pellino 1 (P1$^{-/-}$), Pellino 2 (P2$^{-/-}$) or Pellino 3 (P3$^{-/-}$); double-deficient in Pellino 1 and Pellino 2 (P1/2$^{-/-}$), Pellino 1 and Pellino 3 (P1/3$^{-/-}$) or Pellino 2 and Pellino 3 (P2/3$^{-/-}$); triple-deficient in Pellino 1, Pellino 2, and Pellino 3 (P1/2/3$^{-/-}$). All error bars are S.E.M. Statistical analysis was performed using **(b, c, d, e)** one-way ANOVA and **(f, g)** two-way ANOVA.

3.2.4.3 Enumeration of B2 cells in Pellino-deficient mice

B2 cells are responsible for mounting adaptive immune responses and providing memory upon second encounter of pathogens (Alter-Wolf *et al.*, 2009). In contrast to B1 cells, B220 and CD43 are expressed before CD19 in B2 cells (Ghosn *et al.*, 2011), giving rise to their $CD19^{-}$ and $B220^{low\text{-}negative}$ expression that can be determined by flow cytometry (Fig. 3.15a).

Consistent with the literature (Alter-Wolf *et al.*, 2009), it was evident that majority of B cells in adult mice were B2 cells as outlined by the high frequency in the spleen (Fig. 3.15d, e). Single deficiency in any Pellino proteins did not affect B2 cell population at both young and old age (Fig. 3.15b, c, d, e). However, young *Peli1/2*$^{-/-}$ and *Peli2/3*$^{-/-}$ mice had significantly higher B2 cell numbers and frequency, respectively compared with WT mice without consistency of pattern in both parameters measured (Fig. 3.15b, d). This data rules out the potential of Pellino proteins in regulating B2 cell production. Age factor also did not significantly impact B2 cell expression (Fig. 3.15b, c, d, e). On the other hand, sex analysis showed bias towards lower percentages of B2 cells found in young females of *Peli3*$^{-/-}$ in comparison to the males (Fig. 3.15f). Nonetheless, gender difference did not contribute to disparate B2 cell enumeration in old mice (Fig. 3.15g).

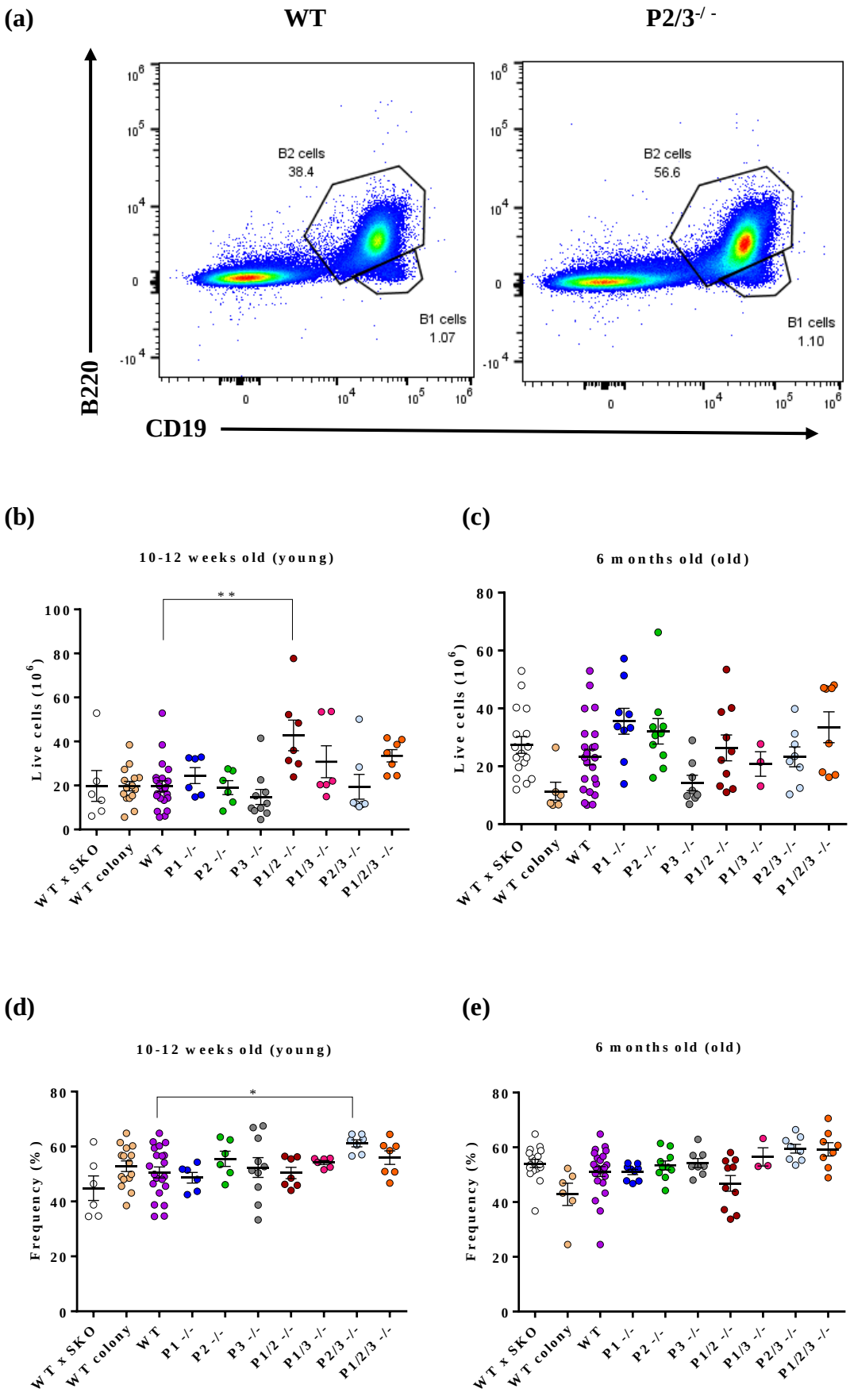
(a)
WT
P2/3-/-
B220
CD19
B2 cells
38.4
B1 cells
1.07
B2 cells
56.6
B1 cells
1.10
(b)
10-12 weeks old (young)
Live cells (10^6)
**
(c)
6 months old (old)
Live cells (10^6)
(d)
10-12 weeks old (young)
Frequency (%)
*
(e)
6 months old (old)
Frequency (%)
WT x SKO
WT colony
WT
P1 -/-
P2 -/-
P3 -/-
P1/2 -/-
P1/3 -/-
P2/3 -/-
P1/2/3 -/-

(f)

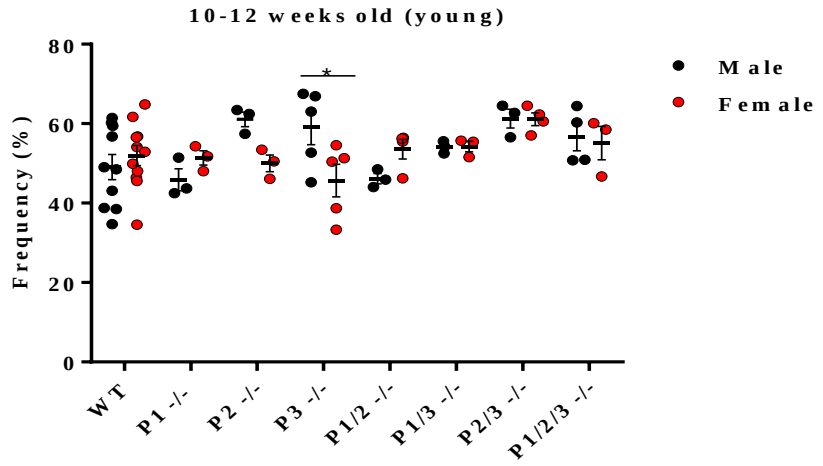

(g)

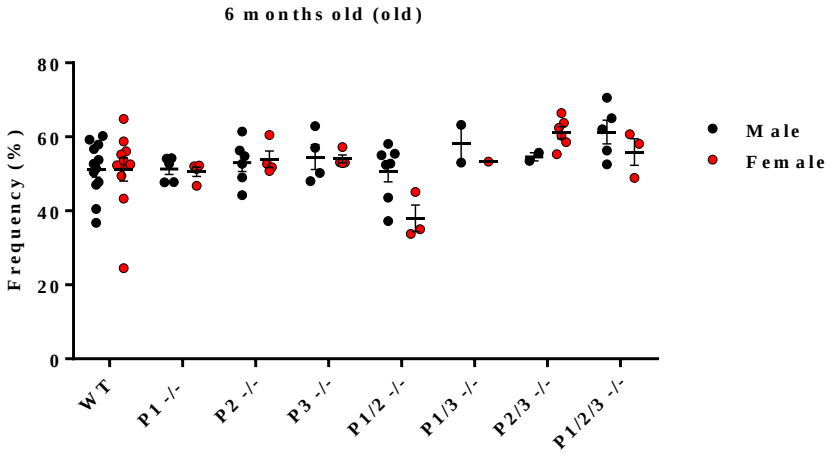

Figure 3.15 B2 cell enumeration in Pellino-deficient mice

Representative dot plots showing B2 cell frequencies of **(a)** a 10- to 12-week-old male WT mouse and a *Peli2/3*$^{-/-}$ mouse. Male and female mice were monitored for variations in **(b, c)** B2 cell numbers and **(d, e)** B2 cell frequencies at **(b, d)** 10 to 12 weeks old and **(c, e)** 6 months old. Age matched mice were monitored for gender variation in B2 cell frequencies at **(f)** 10 to 12 weeks old and **(g)** 6 months old. Pellino-deficient mice were single-deficient in Pellino 1 (P1$^{-/-}$), Pellino 2 (P2$^{-/-}$) or Pellino 3 (P3$^{-/-}$); double-deficient in Pellino 1 and Pellino 2 (P1/2$^{-/-}$), Pellino 1 and Pellino 3 (P1/3$^{-/-}$) or Pellino 2 and Pellino 3 (P2/3$^{-/-}$); triple-deficient in Pellino 1, Pellino 2, and Pellino 3 (P1/2/3$^{-/-}$). All error bars are S.E.M. Statistical analysis was performed using **(b, c, d, e)** one-way ANOVA and **(f, g)** two-way ANOVA.

3.2.4.4 Enumeration of immature B cells in Pellino-deficient mice

Murine B cell development begins in bone marrow where immature B cells are generated and marked by the expression of a functional BCR (Herzog *et al.*, 2009). Roughly 10% of immature transitional B cells overcome negative selection and successfully migrate to the spleen where they develop into mature B cells that are equipped with the ability to mount an efficient immune response (Sims *et al.*, 2005). Immature B cells are denoted as $B220^{+}$ cells that do not express CD23 or CD21 by flow cytometry (Fig. 3.16a).

There was a significant higher number of immature B cells in young *Peli1/2*$^{-/-}$ mice in comparison to WT mice (Fig. 3.16b). Immature B cell distribution in old mice was similar across all genotypes (Fig. 3.16c, e). On the other hand, gender analysis showed that immature B cells were significantly increased in young female WT mice compared with male WT mice (Fig. 3.16f). This pattern was replicated in young *Peli2*$^{-/-}$ mice (Fig. 3.16f). No obvious phenotype was detected between sexes in old mice (Fig. 3.16g), implying that Pellino 2 may manipulate B cell development differently between sexes during young age only.

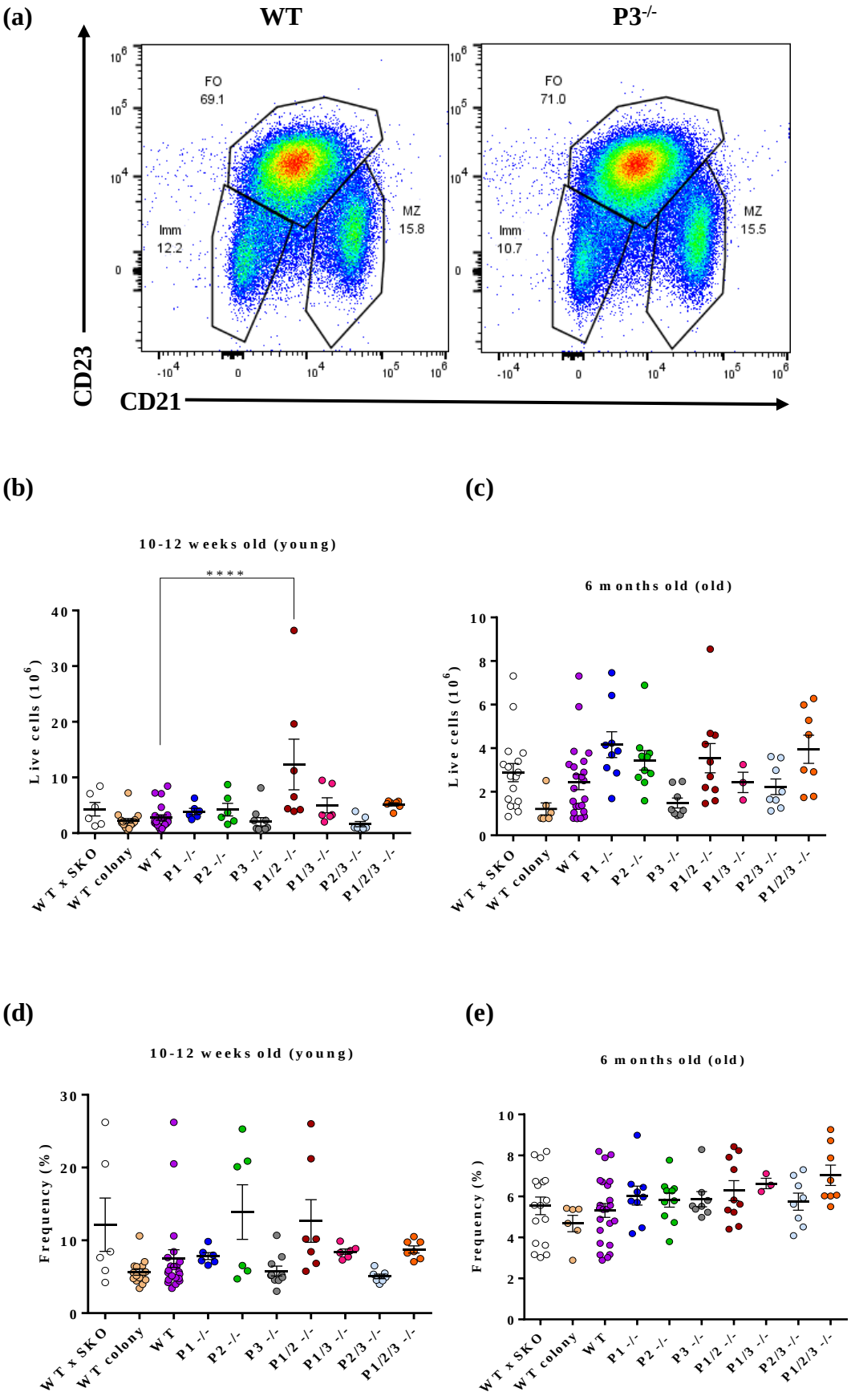
(a)
WT
P3-/-
FO
69.1
Imm
12.2
MZ
15.8
FO
71.0
Imm
10.7
MZ
15.5
CD23
CD21
(b)
(c)
10-12 weeks old (young)
6 months old (old)
Live cells (10^6)
****
WT x SKO
WT colony
WT
P1 -/-
P2 -/-
P3 -/-
P1/2 -/-
P1/3 -/-
P2/3 -/-
P1/2/3 -/-
(d)
(e)
10-12 weeks old (young)
6 months old (old)
Frequency (%)

(f)

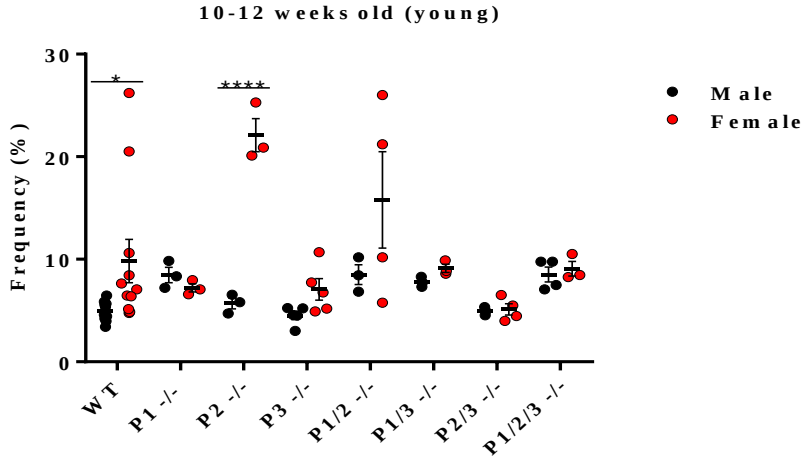

(g)

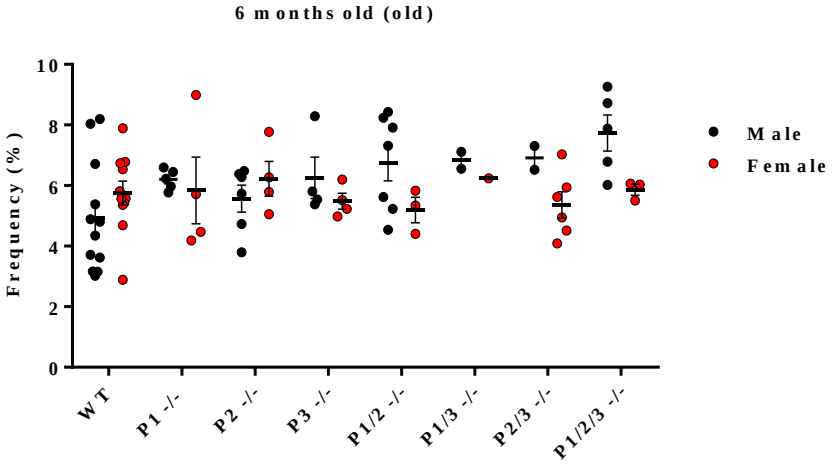

Figure 3.16 Immature B cell enumeration in Pellino-deficient mice

Representative dot plots showing immature B cell frequencies of **(a)** a 6-month-old male WT mouse and a *Peli3*$^{-/-}$ mouse. Male and female mice were monitored for variations in **(b, c)** immature B cell numbers and **(d, e)** immature B cell frequencies at **(b, d)** 10 to 12 weeks old and **(c, e)** 6 months old. Age matched mice were monitored for gender variation in immature B cell frequencies at **(f)** 10 to 12 weeks old and **(g)** 6 months old. Pellino-deficient mice were single-deficient in Pellino 1 (P1$^{-/-}$), Pellino 2 (P2$^{-/-}$) or Pellino 3 (P3$^{-/-}$); double-deficient in Pellino 1 and Pellino 2 (P1/2$^{-/-}$), Pellino 1 and Pellino 3 (P1/3$^{-/-}$) or Pellino 2 and Pellino 3 (P2/3$^{-/-}$); triple-deficient in Pellino 1, Pellino 2, and Pellino 3 (P1/2/3$^{-/-}$). All error bars are S.E.M. Statistical analysis was performed using **(b, c, d, e)** one-way ANOVA and **(f, g)** two-way ANOVA.

3.2.4.5 Enumeration of follicular B cells in Pellino-deficient mice

The maturation of splenic immature transitional B cells gives rise to follicular (FO) B cells or marginal zone (MZ) B cells (Mebius & Kraal, 2005). Subsequently, FO B cells can differentiate into plasma cells and induce germinal centre (GC) formation when they encounter antigens and undergo T cell-facilitated activation (Roulland *et al.*, 2007). FO B cells bear high and medium level of CD23 and CD21 surface markers, respectively (Fig. 3.17a).

Singly deficient Pellino mice did not illustrate different FO B cell enumeration in comparison to WT mice in both young and old age groups (Fig. 3.17b, c, d, e). The double or triple Pellino knockout mice also showed similar patterns (Fig. 3.17b, c, d, e) with the exception to young *Peli1/2*$^{-/-}$ mice, which had significantly greater FO B cell numbers compared to WT mice (Fig. 3.17b). In relation to gender differences, comparable FO B cell frequency was observed in both age groups (Fig. 3.17f, g). Taken together, Pellino proteins are not involved in the generation of FO B cells.

3.2.4.6 Enumeration of marginal zone B cells in Pellino-deficient mice

MZ B cells are splenic transitional B cells that act as first-line defence against blood-borne T-independent antigens and encapsulated bacteria (Kruetzmann *et al.*, 2003; Weller *et al.*, 2004). MZ B cells were marked by a low expression of CD21 and a high expression of CD23 (Fig. 3.18a).

There was no noticeable difference in MZ B cell population between WT mice and mice lacking Pellino proteins in both age groups (Fig. 3.18b, c, d, e). Different gender also did not bring about varying pattern across all genotypes (Fig. 3.18b, c, d, e). This finding reveals that Pellino proteins lack participation in MZ B cell production.

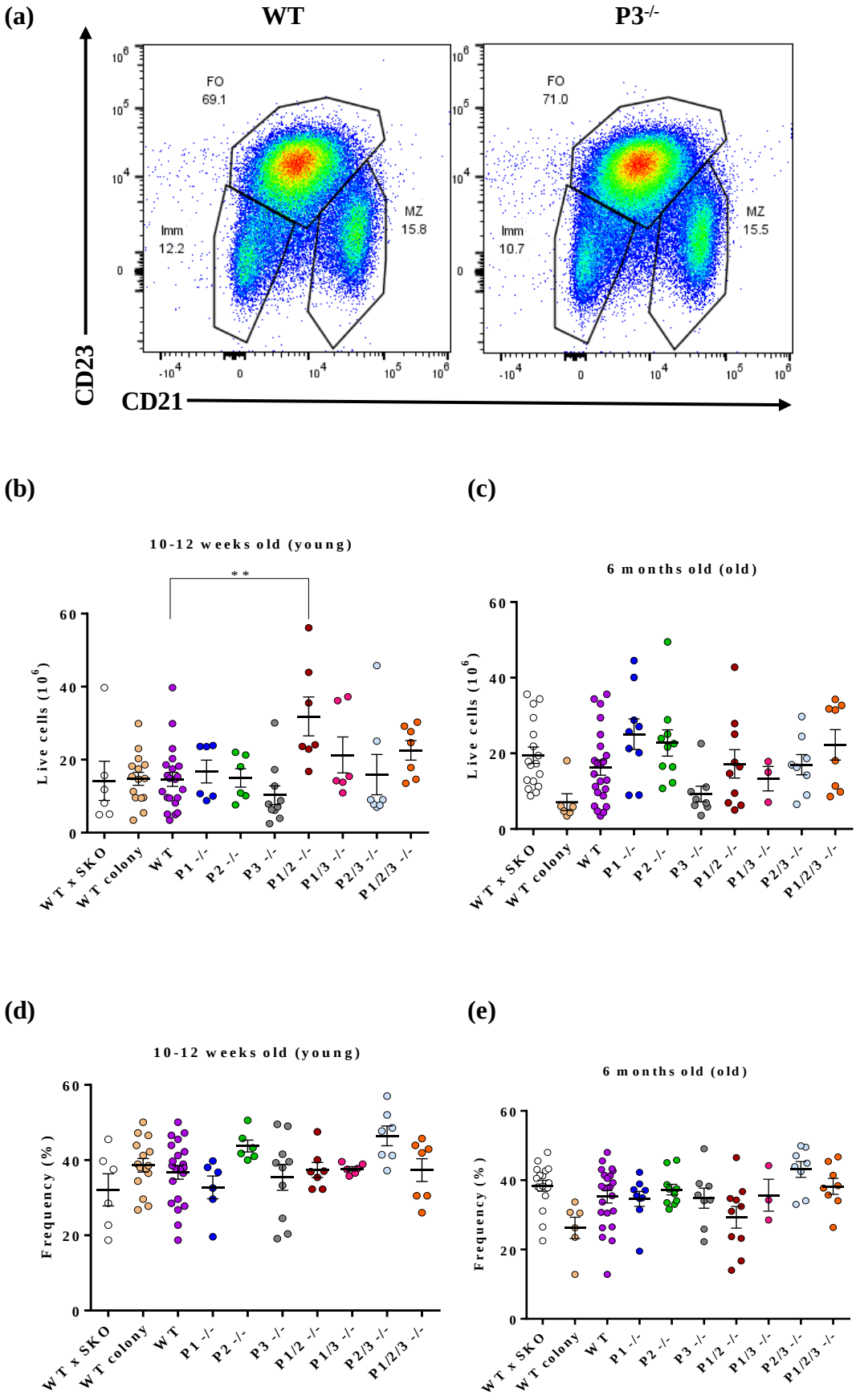
(a)
WT
P3-/-
FO
69.1
Imm
12.2
MZ
15.8
FO
71.0
Imm
10.7
MZ
15.5
CD23
CD21
(b)
10-12 weeks old (young)
**
Live cells (10^6)
(c)
6 months old (old)
Live cells (10^6)
(d)
10-12 weeks old (young)
Frequency (%)
(e)
6 months old (old)
Frequency (%)
WT x SKO
WT colony
WT
P1 -/-
P2 -/-
P3 -/-
P1/2 -/-
P1/3 -/-
P2/3 -/-
P1/2/3 -/-

(f)

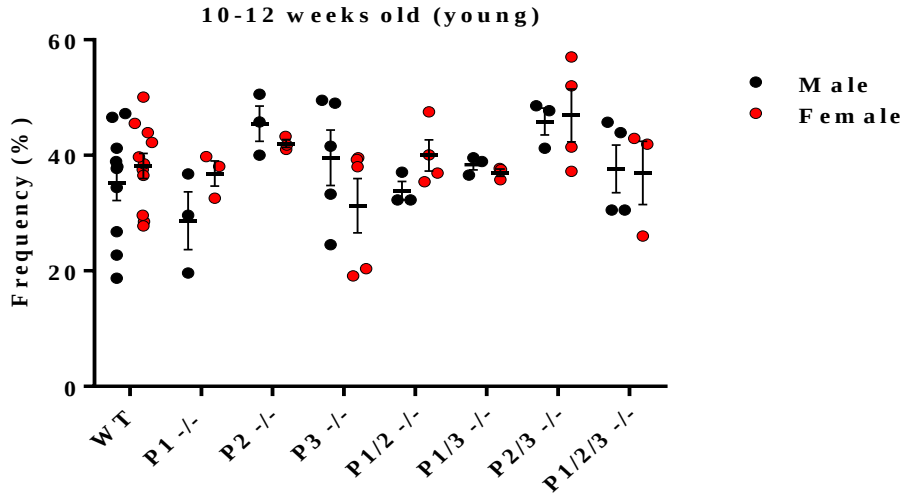

(g)

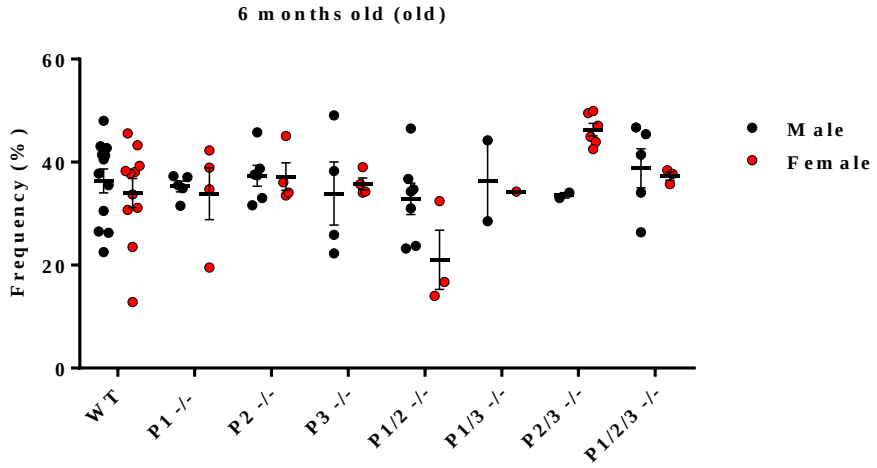

Figure 3.17 Follicular B cell enumeration in Pellino-deficient mice

Representative dot plots showing follicular B cell frequencies of **(a)** a 6-month-old male WT mouse and a *Peli3*$^{-/-}$ mouse. Male and female mice were monitored for variations in **(b, c)** follicular B cell numbers and **(d, e)** follicular B cell frequencies at **(b, d)** 10 to 12 weeks old and **(c, e)** 6 months old. Age matched mice were monitored for gender variation in follicular B cell frequencies at **(f)** 10 to 12 weeks old and **(g)** 6 months old. Pellino-deficient mice were single-deficient in Pellino 1 (P1$^{-/-}$), Pellino 2 (P2$^{-/-}$) or Pellino 3 (P3$^{-/-}$); double-deficient in Pellino 1 and Pellino 2 (P1/2$^{-/-}$), Pellino 1 and Pellino 3 (P1/3$^{-/-}$) or Pellino 2 and Pellino 3 (P2/3$^{-/-}$); triple-deficient in Pellino 1, Pellino 2, and Pellino 3 (P1/2/3$^{-/-}$). All error bars are S.E.M. Statistical analysis was performed using **(b, c, d, e)** one-way ANOVA and **(f, g)** two-way ANOVA.

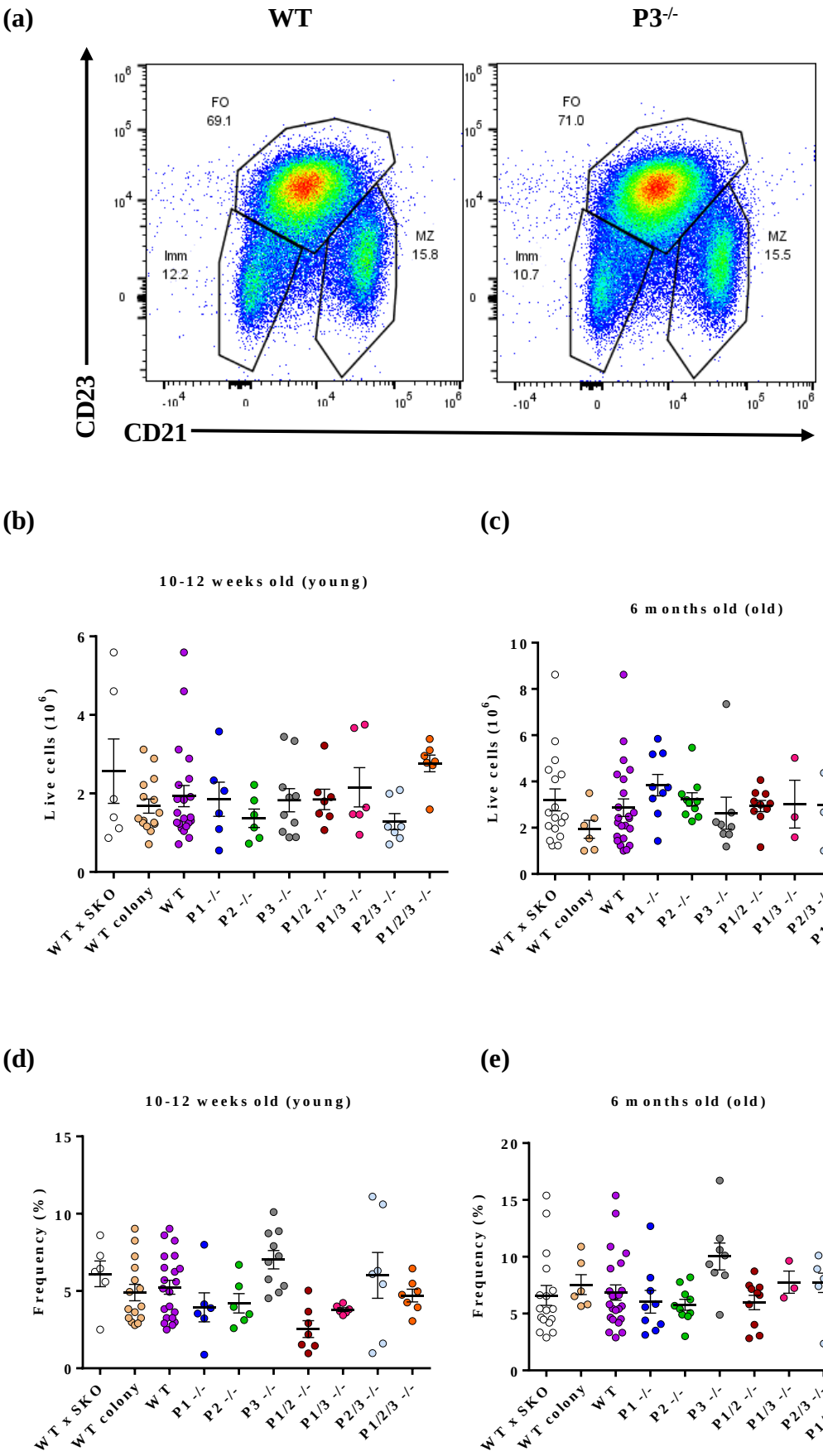
(a)
WT
P3-/-
FO
69.1
Imm
12.2
MZ
15.8
FO
71.0
Imm
10.7
MZ
15.5
CD23
CD21
(b)
(c)
10-12 weeks old (young)
6 months old (old)
Live cells (10^6)
WT x SKO
WT colony
WT
P1 -/-
P2 -/-
P3 -/-
P1/2 -/-
P1/3 -/-
P2/3 -/-
P1/2/3 -/-
(d)
(e)
Frequency (%)

(f)

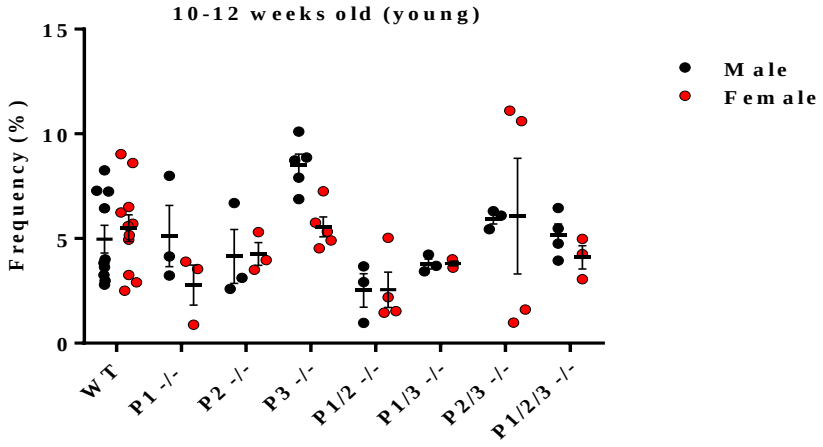

(g)

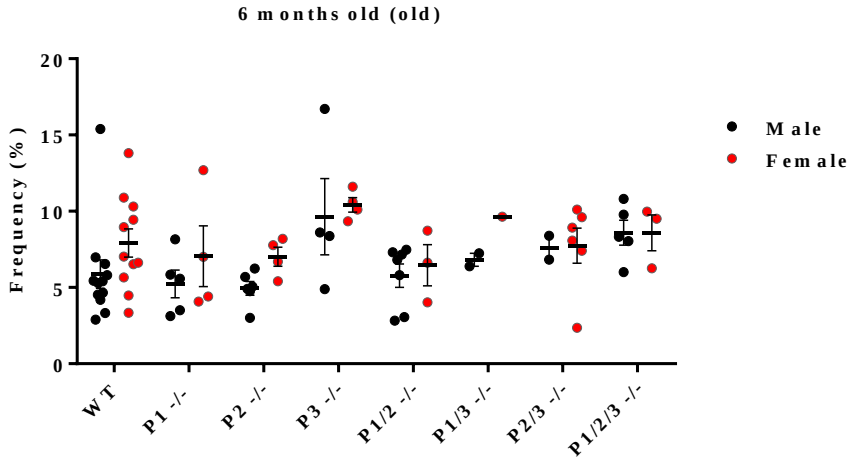

Figure 3.18 Marginal zone B cell enumeration in Pellino-deficient mice

Representative dot plots showing marginal zone B cell frequencies of **(a)** a 6-month-old male WT mouse and a *Peli3*$^{-/-}$ mouse. Male and female mice were monitored for variations in **(b, c)** marginal zone B cell numbers and **(d, e)** marginal zone B cell frequencies at **(b, d)** 10 to 12 weeks old and **(c, e)** 6 months old. Age matched mice were monitored for gender variation in marginal zone B cell frequencies at **(f)** 10 to 12 weeks old and **(g)** 6 months old. Pellino-deficient mice were single-deficient in Pellino 1 (P1$^{-/-}$), Pellino 2 (P2$^{-/-}$) or Pellino 3 (P3$^{-/-}$); double-deficient in Pellino 1 and Pellino 2 (P1/2$^{-/-}$), Pellino 1 and Pellino 3 (P1/3$^{-/-}$) or Pellino 2 and Pellino 3 (P2/3$^{-/-}$); triple-deficient in Pellino 1, Pellino 2, and Pellino 3 (P1/2/3$^{-/-}$). All error bars are S.E.M. Statistical analysis was performed using **(b, c, d, e)** one-way ANOVA and **(f, g)** two-way ANOVA.

3.2.4.7 Enumeration of germinal centre B cells in Pellino-deficient mice

Splenic B cells that reside in the germinal centre (GC) undergo proliferation, clonal expansion, and immunoglobulin class switching to generate antibody-secreting plasma cells and memory B cells (Roulland *et al.*, 2007). GC B cells are recognised by simultaneous expression of CD95 and GL7 ((Fig. 3.19a; Hägglöf *et al.*, 2023; Martínez-Riaño *et al.*, 2023).

At young age, GC B cells were significantly increased in *Peli1/2*$^{-/-}$, *Peli1/3*$^{-/-}$, and *Peli1/2/3*$^{-/-}$ mice compared to WT mice (Fig. 3.19b, d). Despite the lack of statistical significance, young *Peli1*$^{-/-}$ mice depicted a similar trend (Fig. 3.19b). It was supported by augmented percentage of GC B cells in young *Peli1*$^{-/-}$ mice that was statistically significant (Fig. 3.19d). These data provide strong evidence that GC B cell development is negatively mediated in a Pellino 1-specific manner. Interestingly, this pattern is also age dependent as old mice lost the phenotype, albeit a significant increase of GC B cell numbers was observed in *Peli1*$^{-/-}$ and *Peli1/2/3*$^{-/-}$ mice (Fig. 3.19c), but not in GC B cell percentages (Fig. 3.19e). There was a significant upregulation of GC B cells in young *Peli1/2*$^{-/-}$ and *Peli1/3*$^{-/-}$ female mice in comparison to their male counterparts (Fig. 3.19f). Conversely, old *Peli3*$^{-/-}$ female mice had a significantly lower percentage of GC B cells than the males (Fig. 3.19g). In short, Pellino 1 does not seem to functionally crosstalk with other Pellino family members in the context of GC B cell development.

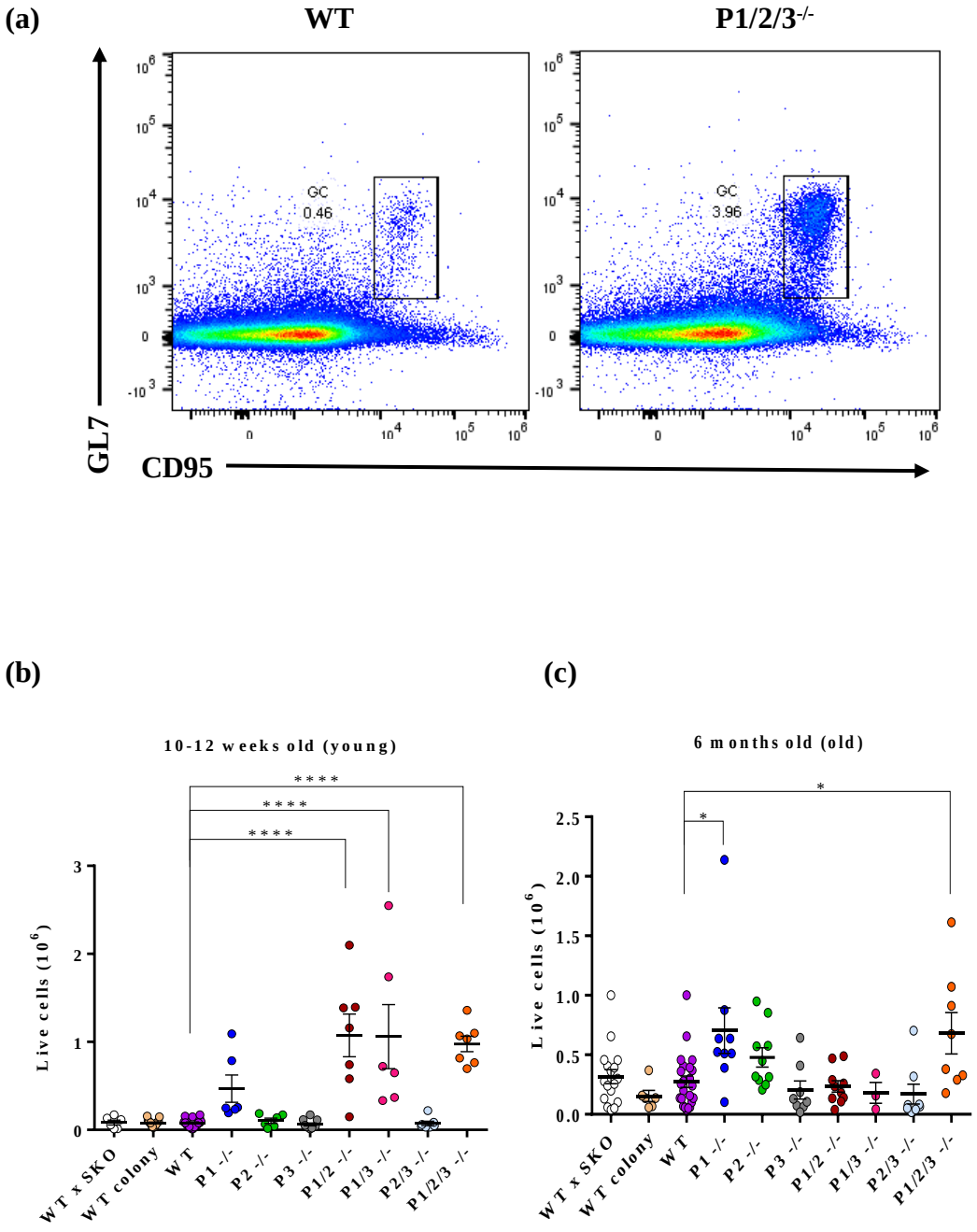
(a)
WT
P1/2/3-/-
GC
0.46
GC
3.96
GL7
CD95
(b)
10-12 weeks old (young)
Live cells (10^6)
WT x SKO
WT colony
WT
P1 -/-
P2 -/-
P3 -/-
P1/2 -/-
P1/3 -/-
P2/3 -/-
P1/2/3 -/-
(c)
6 months old (old)
Live cells (10^6)

(d)

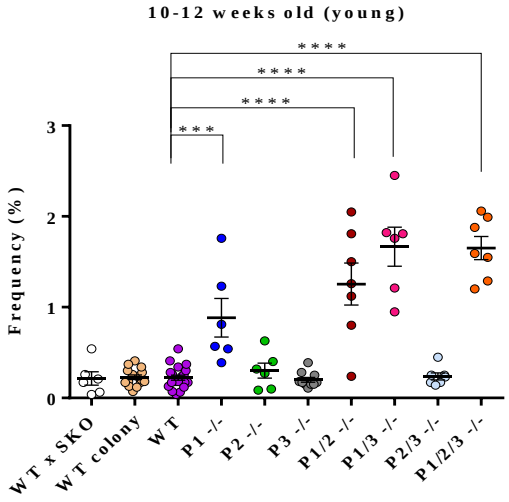
10-12 weeks old (young)
Frequency (%)
****
****
****
***
WT x SKO
WT colony
WT
P1 -/-
P2 -/-
P3 -/-
P1/2 -/-
P1/3 -/-
P2/3 -/-
P1/2/3 -/-

(e)

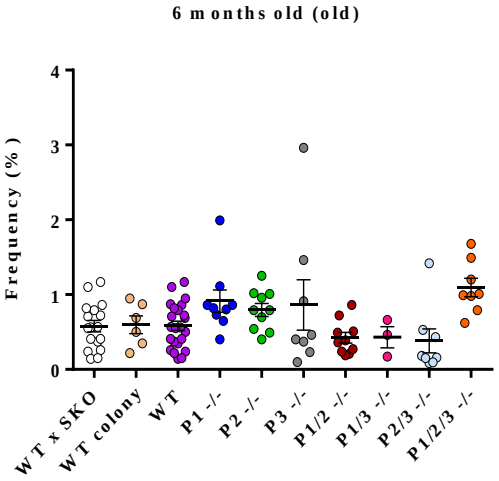
6 months old (old)
Frequency (%)
WT x SKO
WT colony
WT
P1 -/-
P2 -/-
P3 -/-
P1/2 -/-
P1/3 -/-
P2/3 -/-
P1/2/3 -/-

(f)

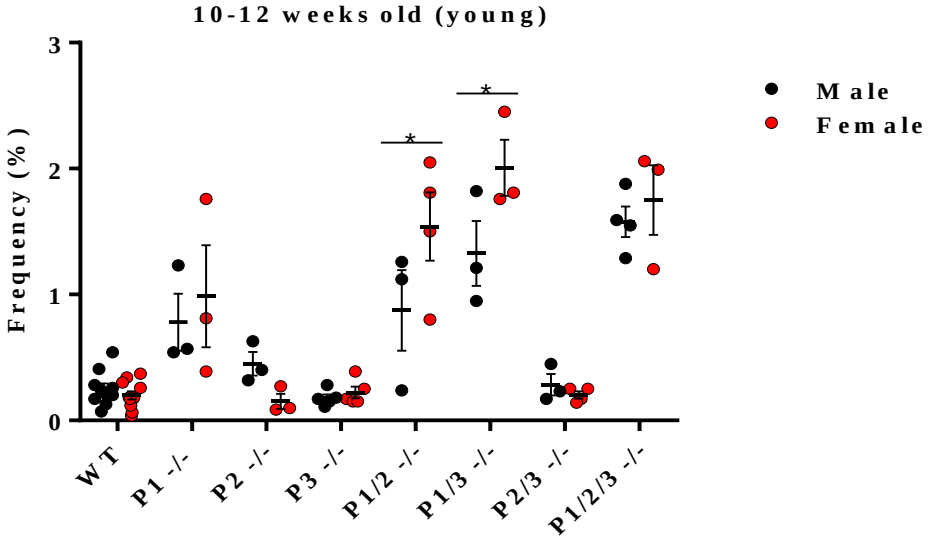
10-12 weeks old (young)
Frequency (%)
*
*
Male
Female
WT
P1 -/-
P2 -/-
P3 -/-
P1/2 -/-
P1/3 -/-
P2/3 -/-
P1/2/3 -/-

(g)

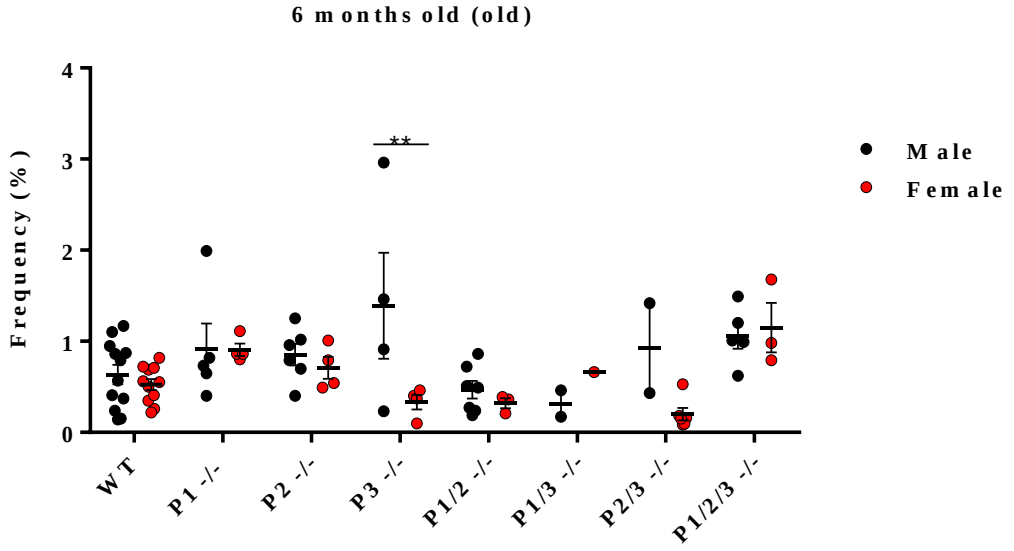

Figure 3.19 Germinal centre B cell enumeration in Pellino-deficient mice

Representative dot plots showing germinal centre B cell frequencies of **(a)** a 10- to 12-week-old male WT mouse and a *Peli1/2/3*$^{-/-}$ mouse. Male and female mice were monitored for variations in **(b, c)** germinal centre B cell number and **(d, e)** germinal centre B cell frequencies at **(b, d)** 10 to 12 weeks old and **(c, e)** 6 months old. Age matched mice were monitored for gender variation in germinal centre B cell frequencies at **(f)** 10 to 12 weeks old and **(g)** 6 months old. Pellino-deficient mice were single-deficient in Pellino 1 (P1$^{-/-}$), Pellino 2 (P2$^{-/-}$) or Pellino 3 (P3$^{-/-}$); double-deficient in Pellino 1 and Pellino 2 (P1/2$^{-/-}$), Pellino 1 and Pellino 3 (P1/3$^{-/-}$) or Pellino 2 and Pellino 3 (P2/3$^{-/-}$); triple-deficient in Pellino 1, Pellino 2, and Pellino 3 (P1/2/3$^{-/-}$). All error bars are S.E.M. Statistical analysis was performed using **(b, c, d, e)** one-way ANOVA and **(f, g)** two-way ANOVA.

3.2.4.8 Enumeration of plasma cells in Pellino-deficient mice

Plasma cells are terminally differentiated B cells that secrete antibodies to tackle foreign pathogens (D'Souza & Bhattacharya, 2019). Plasma cells harbour $B220^{-}$ and $CD138^{+}$ surface markers (Fig. 3.20a; Kumazaki *et al.*, 2007).

Similar to GC B cells, the numbers and frequency of plasma cells in young mice lacking Pellino 1 were significantly increased compared with WT mice (Fig. 3.20b, d). However, plasma cell enumeration was not impacted by the loss of Pellino 2 and/or Pellino 3 in both young and old mice (Fig. 3.20b, c, d, e), indicating a Pellino 1-specific role in regulating plasma cell production. In old mice, plasma cell numbers were significantly more abundant in *Peli1*$^{-/-}$ mice than WT mice (Fig. 3.20c), although this was not reflected in plasma cell frequency (Fig. 3.20e). Pellino 1-mediated plasma cell generation diminishes as aging takes place. When considering the gender profile, plasma cell production was significantly biased towards the young *Peli1*$^{-/-}$ female mice in contrast to the males (Fig. 3.20f). Aged female mice did not have varying levels of plasma cells in comparison to male mice (Fig. 3.20f, g).

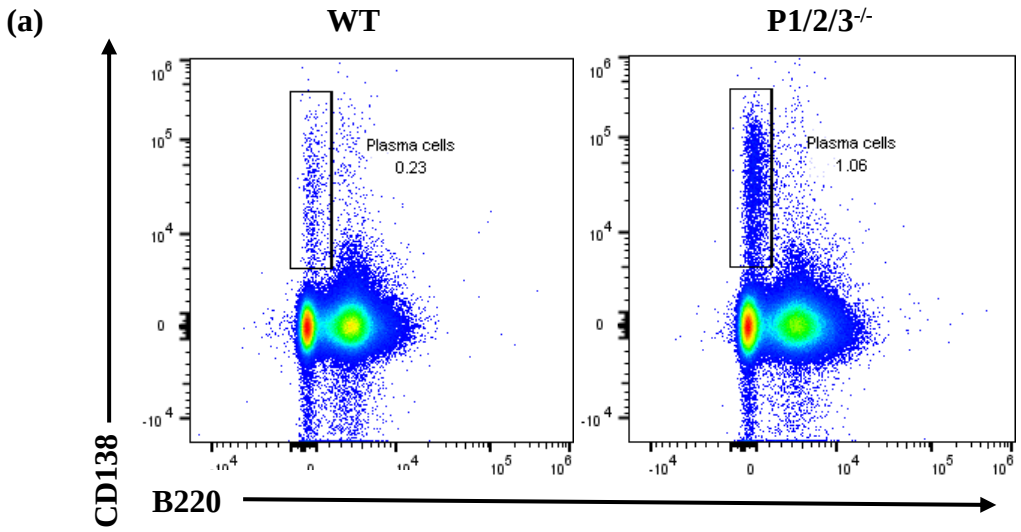
(a)
WT
P1/2/3-/-
Plasma cells
0.23
Plasma cells
1.06
CD138
B220

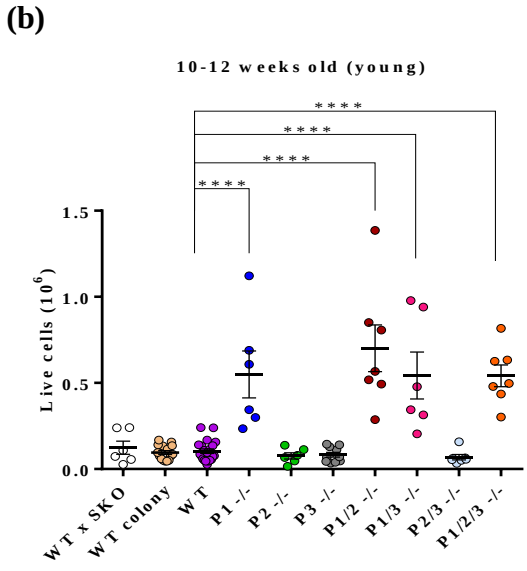
(b)
10-12 weeks old (young)
Live cells (10^6)
WT x SKO
WT colony
WT
P1 -/-
P2 -/-
P3 -/-
P1/2 -/-
P1/3 -/-
P2/3 -/-
P1/2/3 -/-

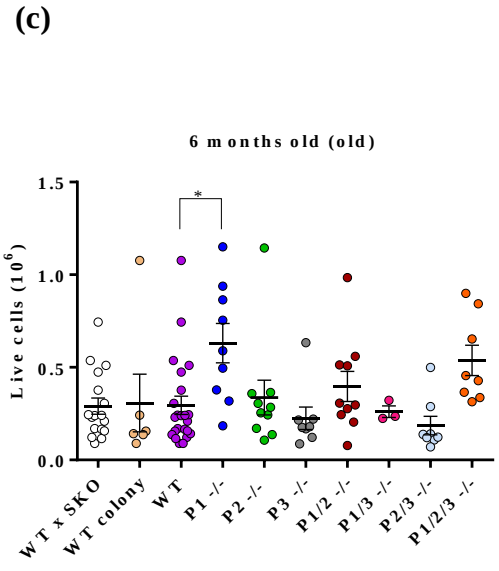
(c)
6 months old (old)
Live cells (10^6)
WT x SKO
WT colony
WT
P1 -/-
P2 -/-
P3 -/-
P1/2 -/-
P1/3 -/-
P2/3 -/-
P1/2/3 -/-

(d)

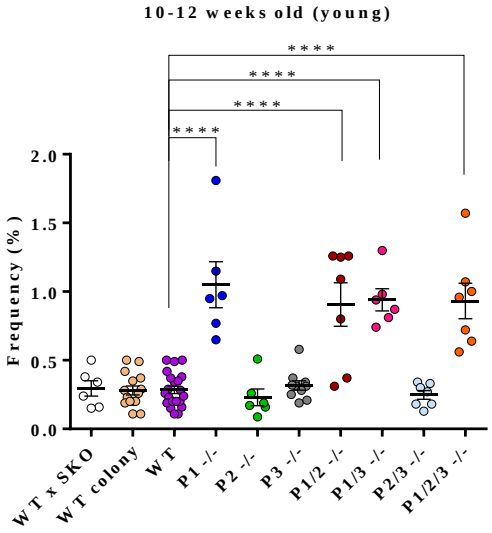
10-12 weeks old (young)
****
****
****
****
Frequency (%)
2.0
1.5
1.0
0.5
0.0
WT x SKO
WT colony
WT
P1 -/-
P2 -/-
P3 -/-
P1/2 -/-
P1/3 -/-
P2/3 -/-
P1/2/3 -/-

(e)

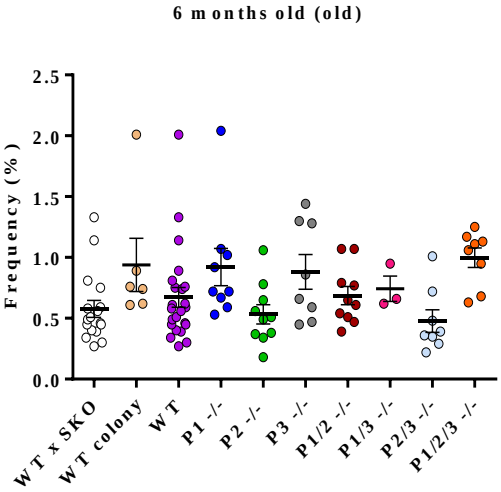
6 months old (old)
Frequency (%)
2.5
2.0
1.5
1.0
0.5
0.0
WT x SKO
WT colony
WT
P1 -/-
P2 -/-
P3 -/-
P1/2 -/-
P1/3 -/-
P2/3 -/-
P1/2/3 -/-

(f)

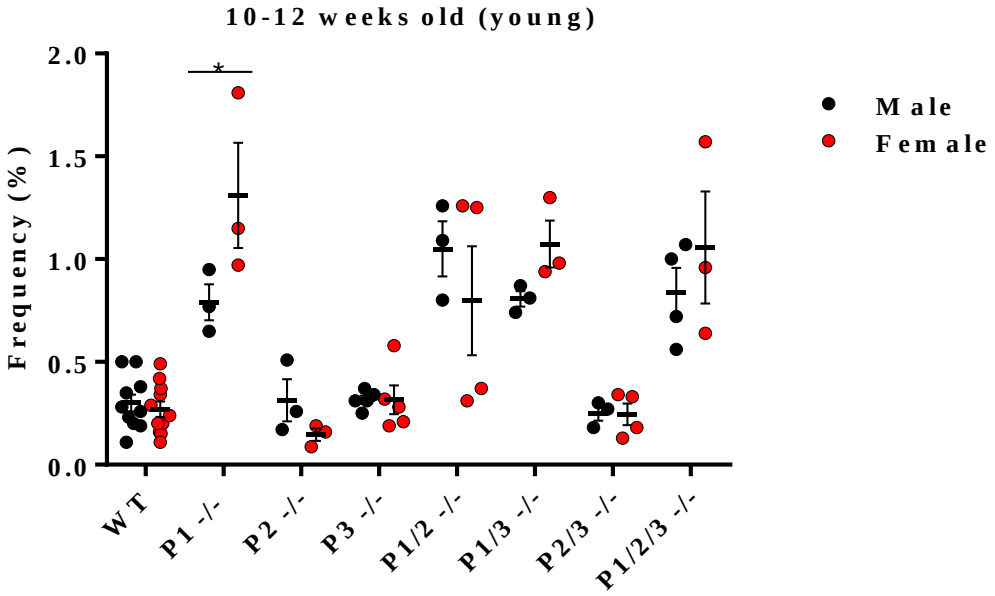
10-12 weeks old (young)
*
Frequency (%)
2.0
1.5
1.0
0.5
0.0
WT
P1 -/-
P2 -/-
P3 -/-
P1/2 -/-
P1/3 -/-
P2/3 -/-
P1/2/3 -/-
Male
Female

(g)

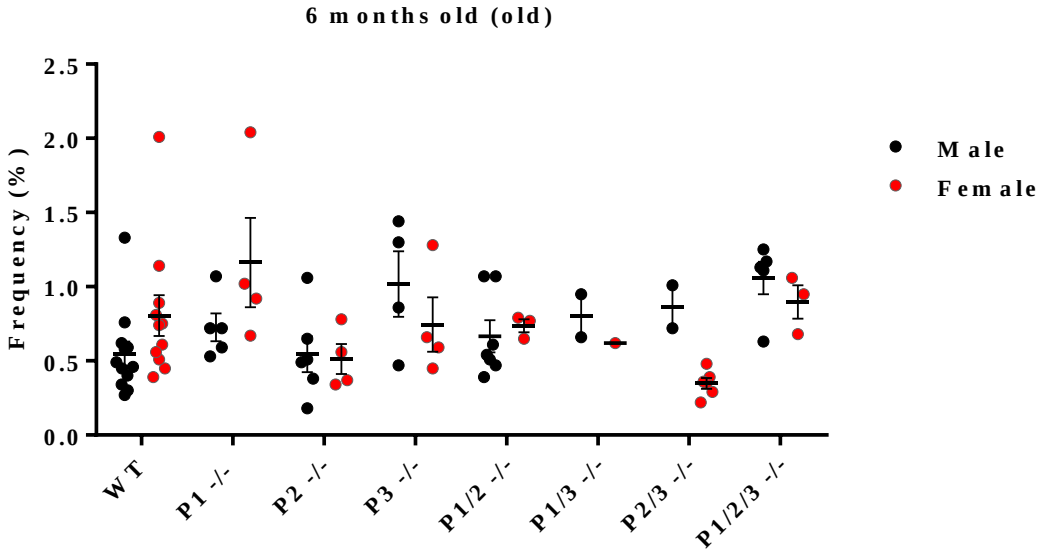

Figure 3.20 Plasma cell enumeration in Peli-deficient mice

Representative dot plots showing plasma cell frequencies of **(a)** a 10- to 12-week-old male WT mouse and a *Peli1/2/3*$^{-/-}$ mouse. Male and female mice were monitored for variations in **(b, c)** plasma cell numbers and **(d, e)** plasma cell frequencies at **(b, d)** 10 to 12 weeks old and **(c, e)** 6 months old. Age matched mice were monitored for gender variation in plasma cell frequencies at **(f)** 10 to 12 weeks old and **(g)** 6 months old. Pellino-deficient mice were single-deficient in Pellino 1 (P1$^{-/-}$), Pellino 2 (P2$^{-/-}$) or Pellino 3 (P3$^{-/-}$); double-deficient in Pellino 1 and Pellino 2 (P1/2$^{-/-}$), Pellino 1 and Pellino 3 (P1/3$^{-/-}$) or Pellino 2 and Pellino 3 (P2/3$^{-/-}$); triple-deficient in Pellino 1, Pellino 2, and Pellino 3 (P1/2/3$^{-/-}$). All error bars are S.E.M. Statistical analysis was performed using **(b, c, d, e)** one-way ANOVA and **(f, g)** two-way ANOVA.

The relevance of various Pellino-deficient mouse models on B cell populations are summarised in table 3.3 below.

Genotypes		*Peli1*$^{-/-}$		*Peli1/2*$^{-/-}$		*Peli1/3*$^{-/-}$		*Peli1/2/3*$^{-/-}$		*Peli2*$^{-/-}$		*Peli3*$^{-/-}$		*Peli2/3*$^{-/-}$	
Cell types		Y	O	Y	O	Y	O	Y	O	Y	O	Y	O	Y	O
B1 cell	#														
	%														
B2 cell	#														
	%														
B220^{+} cell	#														
	%														
Imm B cell	#														
	%														
FO B cell	#														
	%														
MZ B cell	#														
	%														
GC B cell	#														
	%														
Plasma cell	#														
	%														

Table 3.3 Statistical significance relevance of splenic B cell subpopulations between WT and Pellino-deficient strains. Y = young mice, O = old mice, # = cell number, % = cell percentage/frequency, red column = statistical significant increase, white column = no statistical significant changes.

3.3 Discussion

Research focusing on the functions of Pellino proteins has deepened our understanding of the regulatory roles of Pellino proteins in the immune system. To date, studies have predominantly demonstrated the functional role of Pellino proteins in innate immune signalling pathways. Whilst there are emerging studies unravelling the potential of Pellino proteins in regulating adaptive immunity, a comprehensive study on the role of Pellino family members in generating adaptive immune cell populations has yet to be carried out. This formed the basis for the initial studies in this body of work.

Single knockout (KO) mouse models of individual Pellino family members used in research have contributed to the advancement of knowledge in Pellino biology over the years. Utilising singly deficient mice in Pellino 1 (*Peli1*$^{-/-}$), Pellino 2 (*Peli1*$^{-/-}$) or Pellino 3 (*Peli1*$^{-/-}$), the work in this thesis aims to investigate the role of the individual Pellino proteins in the production of T cell and B cell subtypes. In addition, this thesis

also intends to examine functional crosstalk in the Pellino family for the first time using mice that are deficient in multiple Pellino family members. To date, only Pellino 1/Pellino 2 double-KO cells have been employed to study their E3 ligase activity in TAK1 activation (Strickson *et al*., 2017). Mice with multiple Pellino-deficiency are viable, although *Peli1/2*$^{-/-}$ and *Peli1/2/3*$^{-/-}$ mice are generally smaller in weight.

A mouse spleen is enriched with a variety of immune cells. Adaptive immune components – T and B cells constitute a high frequency of the immune cells in the spleen (Hensel *et al*., 2019). Therefore, the murine spleen is the secondary lymphoid tissue chosen to explore the effect of Pellino proteins in the generation of T and B cell populations. Enlarged spleen (splenomegaly) is often associated with autoimmune diseases (Viallard *et al*., 2024). By conducting physical examination and spleen weight measurement, mice that are deficient of Pellino 1 have splenomegaly, a sign of autoimmunity. This data corresponds to the observation in Pellino 1-KO mice (Chang *et al*., 2011), suggesting a protective role of Pellino 1 in autoimmunity. Moreover, this effect is specific to Pellino 1 as both the spleen weight and spleen:body ratio are unaffected in the absence of Pellino 2 and Pellino 3. The abundant presence of splenocytes in young *Peli1/2*$^{-/-}$ mice may indicate increased immune cells infiltration in the spleen, which is generally linked with cancer prognosis and characteristics of autoimmune diseases, such as lupus nephritis (Cao *et al*., 2019).

T cell immunophenotypic study in this thesis provides insight into the roles of Pellino proteins in T cell subtypes including $CD3^+$ T cells, $CD4^+$ T cells, naïve $CD4^+$ T cells, activated $CD4^+$ T cells, $CD8^+$ T cells, naïve $CD8^+$ T cells, effector memory $CD8^+$ T (Tem) cells, central memory $CD8^+$ T (Tcm) cells, and γδ T cell. In young mice, the high number of viable spleen cells in *Peli1/2*$^{-/-}$ mice give rise to significantly elevated number of $CD3^+$, $CD4^+$, and γδ T cell. However, this finding is not reflected by their corresponding percentage suggesting other cell types may also contribute to increase in overall numbers of spleen cells.

The present analysis also demonstrates a striking phenotype in which activated $CD4^+$ T cells and Tem cells are dramatically elevated in mice lacking Pellino 1 in

comparison to WT mice. The production of these cells is not affected by the absence of Pellino 2 or Pellino 3. The prevailing effect of Pellino 1-driven phenotype in activated $CD4^+$ and Tem cell populations of *Peli1/2*$^{-/-}$, *Peli1/3*$^{-/-}$, and *Peli1/2/3*$^{-/-}$ mice suggests that there is no functionality overlap among all Pellino members. This phenomenon implies a role solely for Pellino 1 in the Pellino family as a negative regulator of T cell activation. This is consistent with the negative impact of Pellino 1 on T cell activation that has been previously established (Chang *et al*., 2011). However, our studies provide the first insight that this function of Pellino1 does not extend to other Pellino family members.

Naïve $CD4^+$ and naïve $CD8^+$ T cell enumerations are similar across all genotypes at young age. However, as the mice age, there is an emerging pattern of losing naïve $CD4^+$ T cells and gaining activated $CD4^+$ T cells and this is further augmented in a Pellino 1-specific fashion. This is also evidenced in the reduction of naïve $CD8^+$ T cells and augmentation of Tem cells compared to WT mice that is apparent in the absence of Pellino 1 in aged mice. Notably, the aging process contributes to this phenotype. Under normal circumstances, memory T cell formation peaks during early childhood as they have many first interaction with new antigens; T cell compartment stabilises and produces less memory while it maintains immunosurveillance during adulthood (Kumar *et al*., 2018). Therefore, the age-related conversion of naïve $CD4^+$ and naïve $CD8^+$ T cell into respective activated $CD4^+$ T cells and Tem cells might underpin aberrant T cell activation in mice lacking Pellino 1 that progresses with time. This consolidates the role of Pellino 1 in modifying the molecular landscape of T cell activation.

There are several interesting observations depicted in the old age group. Firstly, $CD3^+$ T cell enumeration reveals a lower frequency of $CD3^+$ T cell in old *Peli1/2*$^{-/-}$ mice in comparison to WT mice. CD3 is a marker for all T cells, including $CD4^+$ and $CD8^+$ T cells. While $CD4^+$ T cell population in *Peli1/2*$^{-/-}$ mice is unaffected, there is a significantly reduced $CD8^+$ T cell population in these mice in contrast to WT mice, which may account for the overall $CD3^+$ T cell decrease. Because total $CD8^+$ T cell count is not affected in mice bearing individual Pellino 1 or Pellino 2 deficiency, it indicates an existing compensation between Pellino 1 and Pellino 2 to maintain total $CD8^+$ T cell homeostasis.

Secondly, there is a significant increase of total $CD4^+$ T cell number in old *Peli2*$^{-/-}$ mice in comparison to WT mice. This enhanced T cell count gives rise to significantly higher activated $CD4^+$ T cells in old *Peli2*$^{-/-}$ mice than WT mice without affecting naïve $CD4^+$ T cell population. It is also consistent with the influence of Pellino 2 on $CD8^+$ T cell compartment whereby old *Peli2*$^{-/-}$ mice had unchanging naïve $CD8^+$ T cells and significantly greater Tcm cells in contrast to WT mice. Since this phenotype is not illustrated in young mice lacking Pellino 2, $CD4^+$ and $CD8^+$ T cell activation mediated by Pellino 2 is age-associated.

Further exploration into $CD8^+$ T cell subsets delineates varying functions of different Pellino proteins. While Pellino 1 negatively mediates Tem cell production, it does not influence the Tcm subset. On the other hand, Pellino 2 is not involved in Tem cell production, but it appears to control Tcm cell generation in old age. However, there appears to be some functional and complex interplay between Pellino 1 and Pellino 2 in Tcm generation at a young age since young *Peli1/2*$^{-/-}$ mice show upregulated numbers of Tcm cells. However, in old mice, the loss of Pellino 1 and Pellino 2 results in a shift of naïve $CD8^+$ T cells into Tem cells, negatively impacting the expression of Tcm cells. This phenotype is likely due to the dominant effect of Pellino 1 over Pellino 2 in regulating Tem production. It would be interesting to explore this biology in the context of infection and assess the impact of Pellino 1 and Pellino 2 deficiency in Tem and Tcm-mediated protection against lymphocytic choriomeningitis virus or *Listeria monocytogenes* (Wherry *et al.*, 2003; Huster *et al.*, 2006). Taken together, Pellino 1 and Pellino 2 appear to negatively regulate the formation of Tem and Tcm cells, respectively.

In addition to T cell enumeration, B cell immunophenotypic study in this thesis sheds light on the role of Pellino proteins in B cell subsets including B1 cells, B2 cells, immature B cells, FO B cells, MZ B cells, GC B cells, and plasma cells. Pellino 1 plays a negative role in regulating GC B cells and plasma cells, whereas Pellino 2 and Pellino 3 do not contribute to the regulation of B cell subtypes. The regulatory impact of Pellino 1 on GC B cells and plasma cells diminishes with age; thus, it will be important to investigate the molecular mechanism related to age. In line with published findings, our data shows that Pellino 1 may have a protective role during

young age against B cell-mediated autoimmunity characterised by high prevalence of GC B cells and plasma cells (Liu *et al.*, 2018).

The impact of Pellino proteins on T cell and B cell subtypes was also evaluated from a sex/gender dimension. There are several phenomena displayed in this study that are female skewed, such as splenomegaly that links to autoimmunity in a Pellino 1-specific manner. Intriguingly, there is reduced naïve $CD4^+$ T cells and increased activated $CD4^+$ T cells in old WT female mice. Naïve $CD8^+$ T cells are generally less in old WT female mice that is represented by a reduction of total $CD8^+$ T cells. Young WT female mice also have a higher frequency of γδ T cells than the males. Furthermore, B cell immunophenotyping also reveals enhanced GC B cells in young *Peli1/2*$^{-/-}$ and *Peli1/3*$^{-/-}$ female mice, whereas young *Peli1*$^{-/-}$ female mice have elevated plasma cell population. The gender bias shown in these mice aligns with other research that show female are more prone to develop T cell and/or B-cell-driven autoimmune diseases, such as rheumatoid arthritis, Sjögren's syndrome, systemic lupus erythematosus, and Grave's disease (Xing *et al.*, 2022). Sex hormones, immune cells composition, and genetic factors are among factors that account for the higher risk to autoimmunity in female (Miquel *et al.*, 2023).

In short, these findings corroborate the role of Pellino 1 in negatively modulating T cell and B cell activation, as well as conferring protection against autoimmunity. Unlike Pellino 1, Pellino 2 does not affect naïve $CD4^+$ and naïve $CD8^+$ T cells while activating their counterparts, suggesting Pellino 2 regulates T cell activation via a different pathway. While Pellino 1 negatively impacts Tem cells, Pellino 2 imposes a greater influence on Tcm cells. This again highlights the different functional roles between Pellino 1 and Pellino 2 in mediating T cell activation. These studies form the basis for future studies to better understand these differences between Pellino 1 and Pellino 2 as well as to study the mechanism(s) used by Pellino 1 in controlling T cell and B cell activation.

Chapter 4: Exploring the Effect of Pellino 1 on T Cell Activation and Differentiation

4.1 Introduction

The immune system has 2 functional arms – the innate immune system and adaptive immune system. Although these two immune systems are commonly viewed as two separate entities, they are also interdependent. The discovery of PAMPs and PRRs has further refined the paradigm of interaction between innate immunity and adaptive immunity (Medzhitov & Janeway, 1997).

Recognition of PAMPs by PRRs activate APCs, such as macrophages and dendritic cells, producing the antigen-specific signals in the form of MHC-peptide complexes (Medzhitov & Janeway, 1997). This acts as a first signal that is critical for T cell activation through the engagement between peptide presented by MHC on the antigen presenting cell and the TCR on the T cell. The ligation of PAMPs to PRRs also leads to the expression of costimulatory molecules (B7.1 (CD80) and B7.2 (CD86)) on APCs. The binding of B7.1 or B7.2 to CD28 on T cells provides a second signal that is pivotal for clonal expansion of T cells, sustaining their proliferation and survival (June *et al*., 1994). In addition, encounter of pathogens by PRRs also results in the secretion of effector cytokines, which instructs the differentiation of activated T cells into a specific T helper subset, including Th1, Th2, Th17, Treg, and Tfh (Medzhitov & Janeway, 1997). Distinct effector T cells that form as an outcome of this process may then control the innate response. For instance, Th1 cells contribute to the activation of macrophage for antimicrobial activity through the production of IFN-γ (Dalton *et al*., 1993). IL-17 secreted by Th17 cells modulates the activation of neutrophils and their protection against pneumococcal (Lu *et al*., 2008).

The T cell response acts in an antigen-specific fashion but is also dependent on PRR activation by PAMPs. This entire mechanism ensures that a T cell that receives signal 1 and signal 2 derived from the same APC only elicits productive activation, preserving the specificity of T cell effector function (Liu & Janeway, 1992). It also prevents autoimmunity as PRRs do not generally recognise self-antigens and instead PAMPs from foreign organisms (Medzhitov & Janeway, 1997). In short, the interaction between PAMPS and PRRs, together with activation of the TCR and regulatory cytokines, gives rise to the 3 signals necessary to induce effector functions

of adaptive immune cells. It is apparent that the activation of innate immunity is required for the initiation of the adaptive immune response to an antigen, which may in turn facilitate target innate immune cells to mount an appropriate immune response.

The role of Pellino proteins in the innate immune system is being delineated over time. However, there is a gap of knowledge on the regulatory role of Pellino proteins in the adaptive immune system. Emerging reports on the involvement of Pellino proteins, particularly Pellino 1, in regulating T cell- and B cell-associated immunity are beginning to reveal its potential to control adaptive responses. It is suggested that Pellino 1 has a protective role against autoimmunity, such as SLE (Liu *et al.*, 2018). Despite that, Pellino 1 has also been recently linked with the production of IL-17A in psoriasis (Kim *et al.*, 2023). Among a myriad of cytokines, uncontrolled IL-17 production has been predominantly identified as a key factor for the development of autoimmune diseases, such as multiple sclerosis, rheumatoid arthritis, and psoriasis (Kebir *et al*., 2007; Sato *et al*., 2006; Batalla *et al*., 2015). Given that both Pellino 1 and IL-17 are correlated with autoimmunity, we were especially interested to further examine the relationship between Pellino 1 and IL-17.

The production of IL-17 is tightly regulated by different signalling pathways to maintain immune homeostasis (Fig. 4.1). Signalling through TCR and co-stimulation of CD28 leads to activation of NF-κB and nuclear factor of activated T cells (NFAT)-mediated AP-1 (Zhang *et al*., 2021). Differentiation of Th17 cells is mainly governed by IL-6, IL-21, IL-23, and TGF-β. IL-6 induces the expression of IL-21 in activated T cells and increases IL-23 receptor expression on Th17 cells (Nurieva *et al*., 2007; Yang *et al*., 2007). IL-21 and IL-23 have been reported to positively mediate the Th17-lineage transcription factor RORγt expression, which is encoded by *Rorc* (Zhou *et al*., 2007). The coupling of IL-6, IL-21, and IL-23 to their respective receptors activates JAK, leading to the activation of STAT3, which is vital for Th17 differentiation and development (Nishihara *et al*., 2007; Woś & Tabarkiewicz, 2021; Bloch *et al*., 2018).

On the other hand, the canonical TGF-β signalling pathway activates Smad2 and Smad3 by phosphorylation prior to the formation of a complex with Smad4 (Zhang *et al*., 2018). In the absence of TGF-β signalling, Smad4 recruits SKI and then engages with multiple loci of *Rorc* to suppresses RORγt transcription (Zhang *et al*., 2019). However, this effect is reversible by TGF-β-mediated degradation of SKI, allowing RORγt expression and Th17 differentiation (Zhang *et al*., 2017). It is postulated that the binding of TNF-α to TNF receptor 1 on Th17 cell membrane in an inflammatory environment is responsible for the activation of p38, JNK, and ERK, resulting in phosphorylation of STAT3; activated STAT3 triggers RORγt transcriptional activity and IL-17 secretion (Yang *et al*., 2018).

Furthermore, metabolic pathways can also influence the development of Th17 and hence IL-17 production. CD28 costimulatory signals activate mammalian target of rapamycin (mTOR), a serine/threonine kinase which regulates glycolysis to meet the metabolic need of effector T cells (Frauwirth *et al*., 2002; Maclver *et al*., 2013). Th17 cell regulation relies mainly on glycolysis as glucose-deprivation and blockade of mTOR activity with rapamycin restricts the production of Th17 cells (Cluxton *et al*., 2019). A glycolytic enzyme called pyruvate kinase M2 promotes Th17 cell differentiation by increasing phosphorylated STAT3 in the nucleus (Damasceno *et al*., 2020). Besides that, inhibition of glycolysis using 2-deoxyglucose limits Th17 cell production *in vitro* and confers resistance to the development of EAE (Shi *et al*., 2011).

Recent reports have shed light on the impact of Pellino 1 in mediating adaptive immune responses. Our comprehensive study of the roles of Pellino proteins in the generation of adaptive immune cell populations also emphasised a specified role for Pellino 1 in T cell development. Based on our understanding of how the innate immune response gives rise to T cell activation and differentiation, this part of the present study aimed to further investigate the role of Pellino 1 in mediating downstream T cell effector functions.

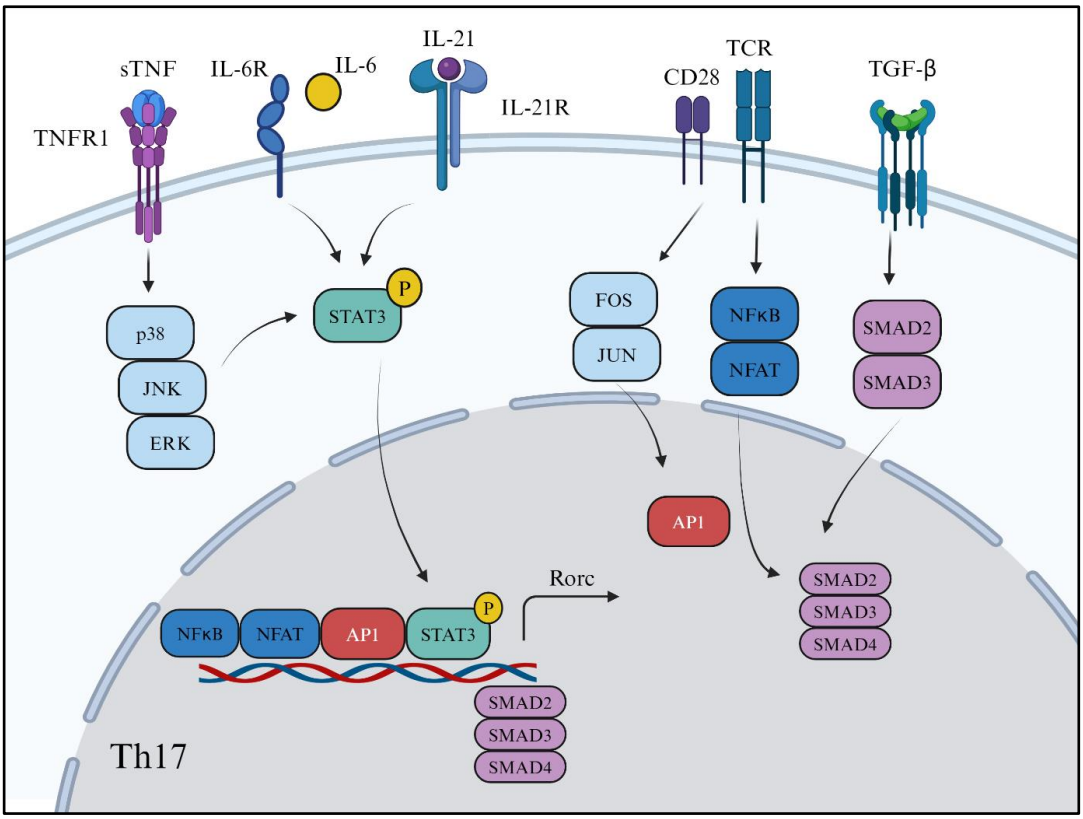

Figure 4.1 Th17 cell differentiation.

Described in detail in section 4.1. A wide range of molecules are involved in Th17 differentiation pathways that induce (black arrows) the expression of *RORc* and consequently *il17* gene. Figure created with BioRender.com.

4.2 Results

4.2.1 Proliferation of splenic CD4$^+$ T cells is unaltered by Pellino 1

Our immunophenotyping data, described in the previous chapter, highlighted a key role for Pellino1 in the control of T cell populations as evidenced by increased numbers of activated CD4$^+$ and CD8$^+$ T cell populations in Pellino 1 knockout mice. This prompted our interest to further investigate the role of Pellino 1 in its potential involvement in regulating T cell effector responses. Activated CD4$^+$ T cells that differentiate into different Th subtypes (Th1, Th2, Th17, Treg, and Tfh) produce lineage-committed effector cytokines (Swain *et al*., 2012) and so we investigated the effect of Pellino1 deficiency on T cell proliferation, differentiation, and effector cytokine production.

We first considered whether Pellino 1 influenced CD4$^+$ T cell proliferation rate. For this study, splenic T cells were primed for proliferation with TCR and CD28 stimulation or left unstimulated for 72 hours. Engagement of TCR and CD28 on CD4$^+$ T cells led to proliferation over the course of three days (Fig. 4.2a). Nevertheless, splenic CD4$^+$ T cell proliferation rate in *Peli1*$^{-/-}$ mice did not differ from WT mice when normalising to untreated cells of WT mice (Fig. 4.2b). Overall, this data shows that Pellino 1 does not have a role in CD4$^+$ T cell proliferation and we next assessed if Pellino 1 could affect T cell differentiation and T cell effector function.

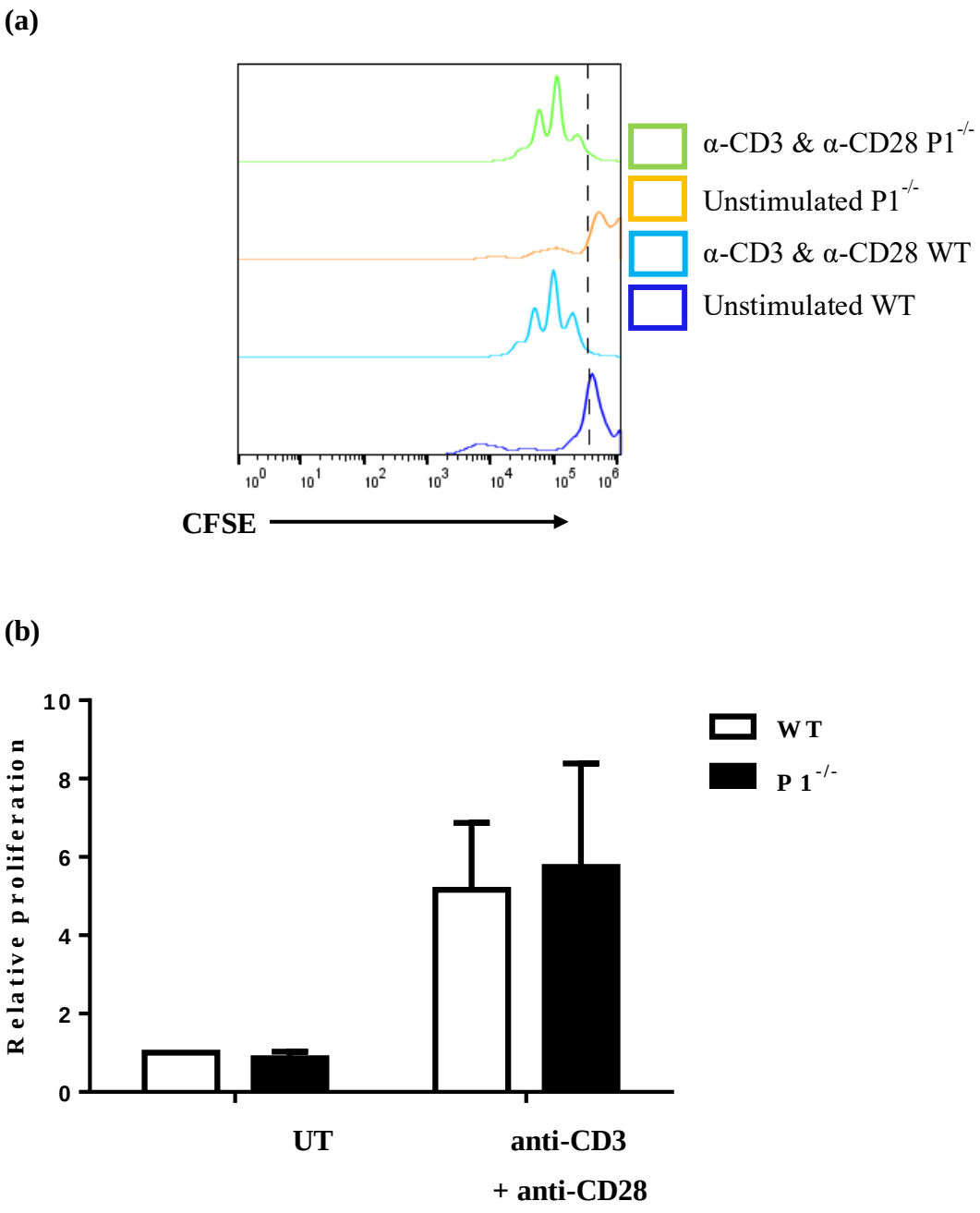

Figure 4.2 Effect of Pellino 1-deficiency on splenic CD4⁺ T cell proliferation

Spleen cells isolated from 8- to 10-week-old WT and Pellino 1-deficient ($P1^{-/-}$) mice were incubated with CFSE (5 μM) in dark at RT for 10 minutes prior to culture over 72 hours. **(a)** Splenic $CD4^+$ T cell proliferation was analysed by flow cytometry using CFSE dilution. **(b)** Pooled data is expressed relative to unstimulated splenic $CD4^+$ T cell in WT mouse as fold increase in proliferation. Data are representative of 3 independent experiments. All error bars are S.E.M. Statistical analysis was performed using two-way ANOVA.

4.2.2 Loss of Pellino affects the production of $CD4^+$ T cell differentiation-related cytokines

Spleen cells isolated from WT and *Peli1*$^{-/-}$ mice were cultured for 48 hours in the presence of anti-CD3 and anti-CD28 co-stimulation to activate Th cell effector responses that were assessed by measuring the protein secretion levels of Th cell lineage cytokines: IFN-γ and TNF-α (Th1 cells), IL-4 (Th2 and Tfh cells), IL-17 (Th17 cells), IL-10 (Treg cells). Cytokines were assayed by ELISA. There was a modest augmentation of levels of IFN-γ observed in stimulated *Peli1*$^{-/-}$ spleen cells relative to WT cells (Fig. 4.3a). Basal and stimulated-levels of TNF-α (Fig. 4.3b) and IL-4 (Fig. 4.3c) were not affected in *Peli1*$^{-/-}$ spleen cells. On the other hand, IL-17 (Fig. 4.3d) and IL-10 (Fig. 4.3e) levels were elevated significantly in *Peli1*$^{-/-}$ spleen cells, relative to WT cells, when co-stimulated with anti-CD3 and anti-CD28. TGF-β secretion was also examined, but its level was undetected by ELISA. These data suggest that Pellino 1 plays some role in mediating IFN-γ, IL-17 and IL-10 production in the process of T cell activation and differentiation.

(a)

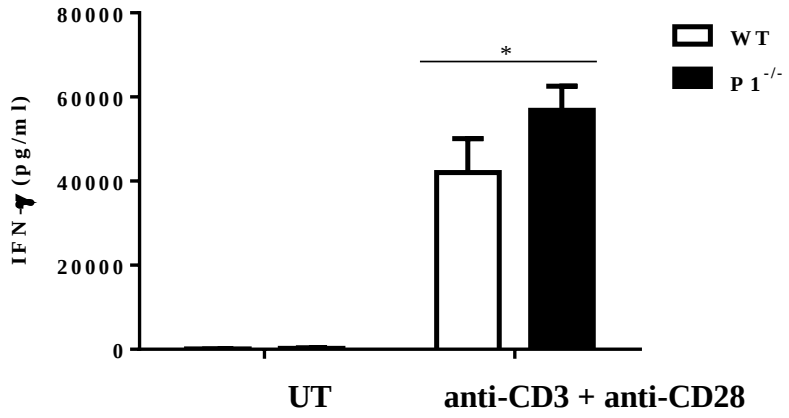
80000
60000
40000
20000
0
IFN-γ (pg/ml)
*
WT
P 1 -/-
UT
anti-CD3 + anti-CD28

(b)

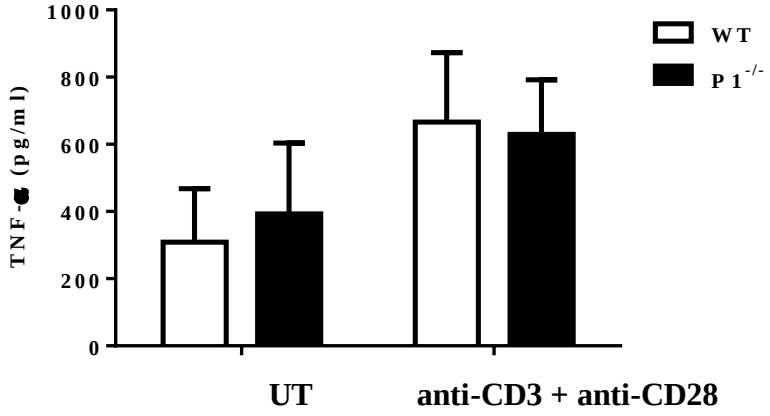
1000
800
600
400
200
0
TNF-α (pg/ml)
WT
P 1 -/-
UT
anti-CD3 + anti-CD28

(c)

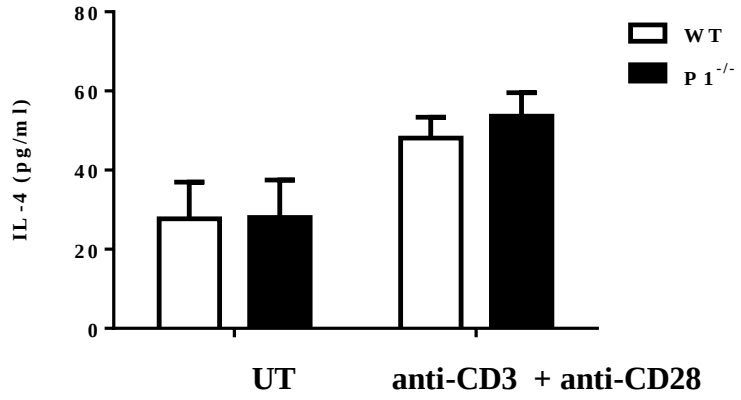
80
60
40
20
0
IL-4 (pg/ml)
WT
P 1 -/-
UT
anti-CD3 + anti-CD28

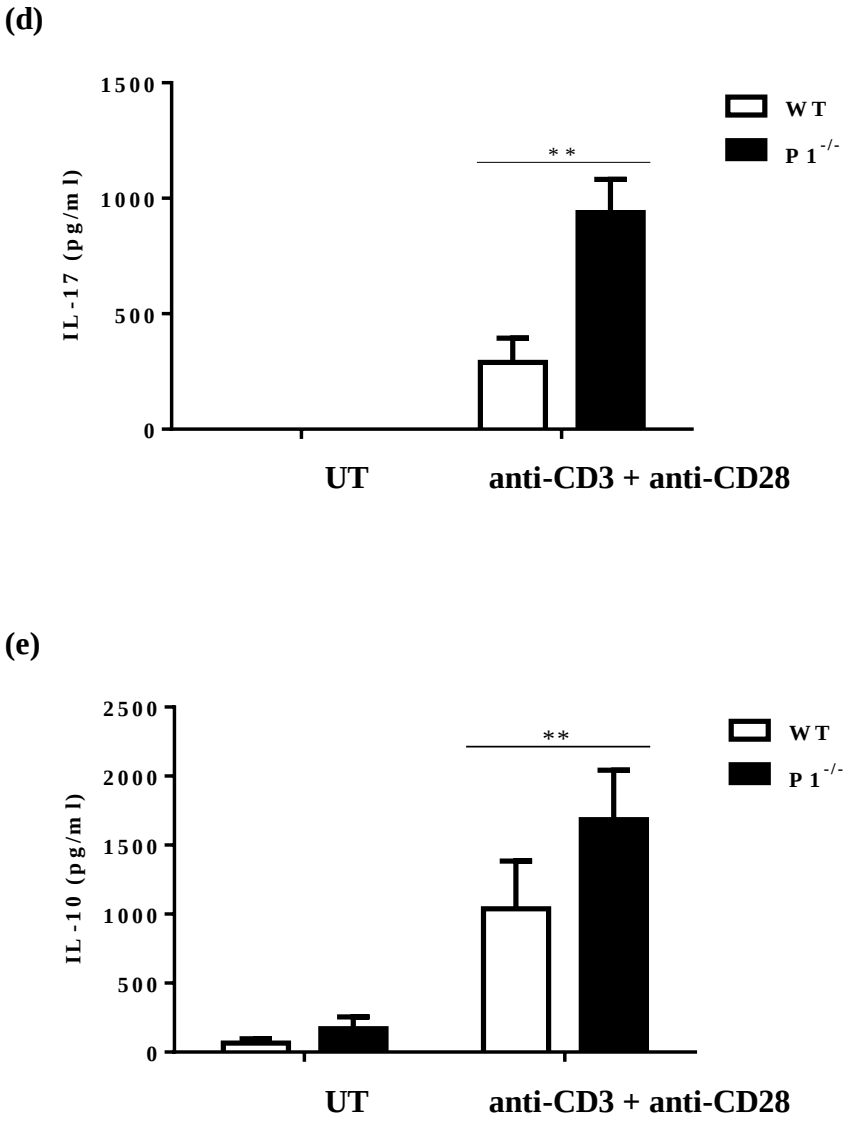

Figure 4.3 Effect of Pellino 1-deficiency on T helper cell differentiation-associated cytokine production in splenocytes

Spleen cells isolated from 8- to 10-week-old WT and Pellino 1-deficient ($P1^{-/-}$) mice were cultured without treatment (UT) or with anti-CD3 (0.5 μg/ml) and anti-CD28 (0.5 μg/ml) over 48 hours. Conditioned media was assayed by ELISA for levels of **(a)** IFN-γ, **(b)** TNF-α, **(c)** IL-4, **(d)** IL-17, and **(e)** IL-10. Data are representative of 4 independent experiments. All error bars are S.E.M. Statistical analysis was performed using two-way ANOVA with statistical significance indicated by $*p \leq 0.05$ and $**p \leq 0.01$.

4.2.3 IL-17 production is unaffected by the loss of Pellino 2, but elevated in the absence of Pellino 3

Pellino 1 has been depicted to confer protection against autoimmune disorders, such as systemic lupus erythematosus (Liu *et al.*, 2018), whereas aberrant IL-17 level is primarily implicated in the pathogenesis of rheumatoid arthritis (Nakae *et al*., 2003). Our data above highlights a striking increase of IL-17 in mice lacking Pellino 1. Based on the relevance of Pellino 1 and IL-17 in autoimmunity, it was intriguing to further explore the regulatory role of other Pellino proteins in controlling IL-17 levels. Spleen cells isolated from WT and *Peli2*$^{-/-}$ or *Peli3*$^{-/-}$ were stimulated for 48 hours with anti-CD3 and anti-CD28 and assessed for IL-17 cytokine levels. While IL-17 levels were unaffected by the absence of Pellino 2 (Fig. 4.4a), IL-17 levels were augmented by Pellino 3-deficiency (Fig. 4.4b). This result highlights the potential of Pellino 3 as a negative regulator of IL-17 and potentially mirrors the effect of Pellino 1 in regulation of IL-17.

To assess potential crosstalk of Pellino proteins in regulating IL-17 production, the above experiment was replicated in Pellino 1 and Pellino 2-double deficient mice (*Peli1/2*$^{-/-}$) or Pellino 1 and Pellino 3-double deficient mice (*Peli1/3*$^{-/-}$). IL-17 production was significantly augmented in both *Peli1/2*$^{-/-}$ (Fig. 4.4a) and *Peli1/3*$^{-/-}$ mice (Fig. 4.4c) compared with WT mice. Together, these results indicate a substantial Pellino 1-specific role in negatively mediating IL-17 production. In other words, secretion level of IL-17 is dictated by the presence of Pellino 1.

(a)

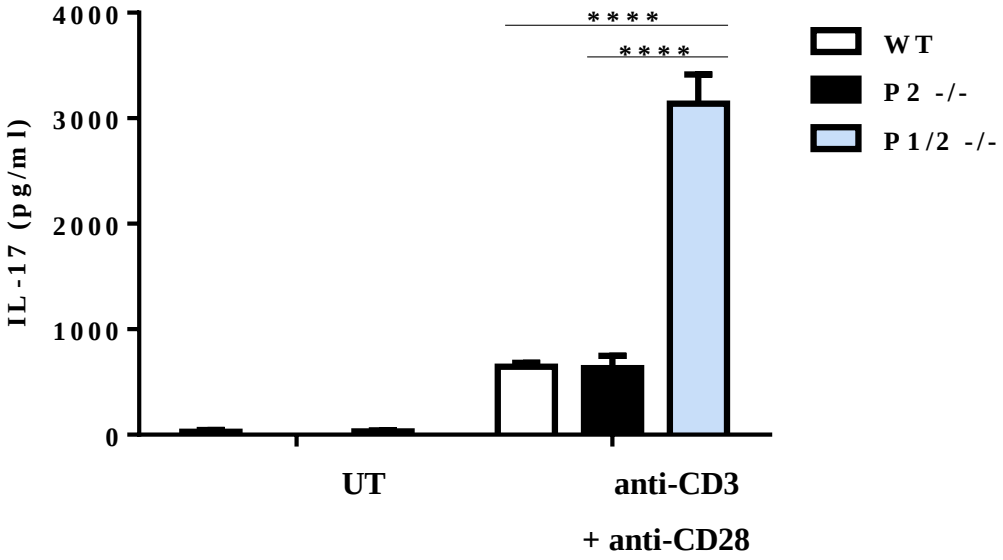
4000
3000
2000
1000
0
IL-17 (pg/ml)
****
****
WT
P2 -/-
P1/2 -/-
UT
anti-CD3
+ anti-CD28

(b)

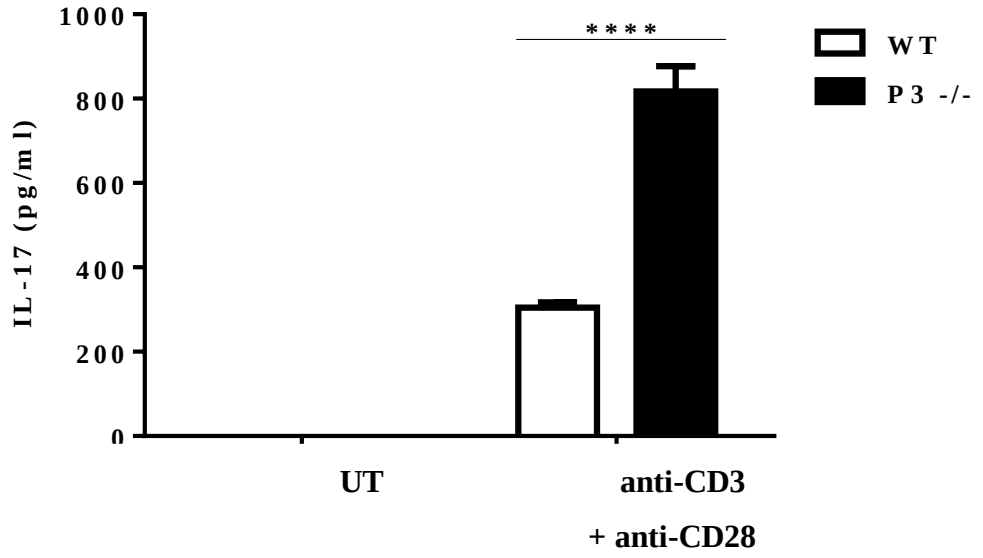
1000
800
600
400
200
0
IL-17 (pg/ml)
****
WT
P3 -/-
UT
anti-CD3
+ anti-CD28

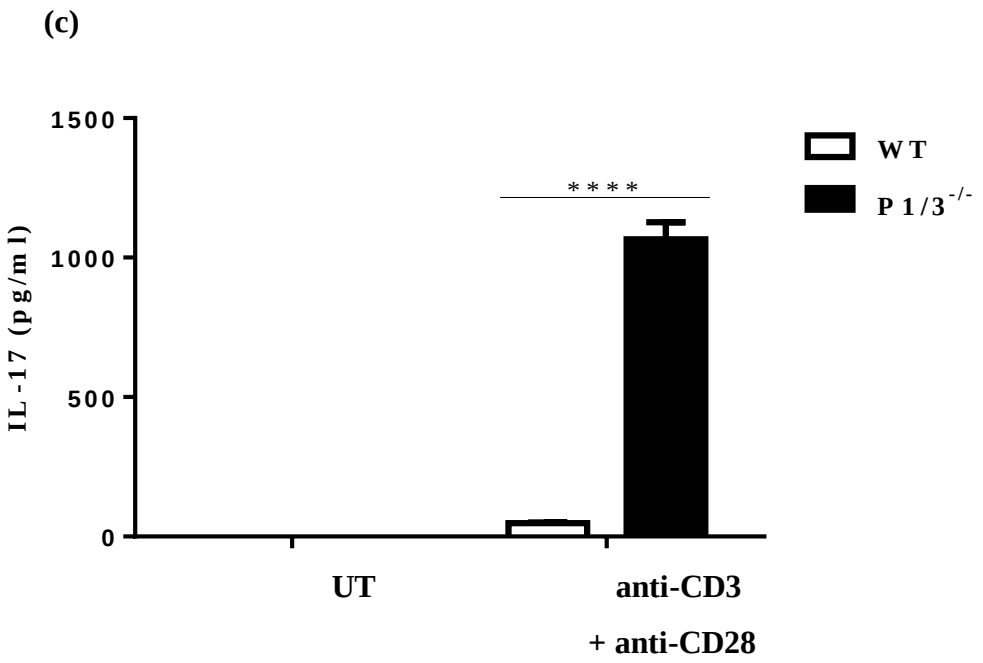

Figure 4.4 Effect of Pellino 2 and Pellino 3 single and double-deficiency on IL-17 production by spleen cells

Spleen cells isolated from 8- to 10-week-old WT and **(a)** Pellino 2-deficient ($P2^{-/-}$) and Pellino 1 and Pellino 2-deficient ($P1/2^{-/-}$) mice or **(b)** Pellino 3-deficient ($P3^{-/-}$) mice were cultured without treatment (UT) or with anti-CD3 (0.5 μg/ml) and anti-CD28 (0.5 μg/ml) over 48 hours. Spleen cells isolated from **(c)** 8-month-old WT and Pellino 1 and Pellino 3-deficient ($P1/3^{-/-}$) mice were cultured without treatment (UT) or with anti-CD3 (0.5 μg/ml) and anti-CD28 (0.5 μg/ml) over 48 hours. Conditioned media was assayed by ELISA for levels of IL-17. Data are shown from an experiment that is representative of **(a, b)** 4 independent experiments and **(c)** an independent experiment. All error bars are S.E.M. Statistical analysis was performed using two-way ANOVA with statistical significance indicated by ****$p \leq 0.0001$.

4.2.4 Loss of Pellino 1 enhances production of IL-17 in Th17 cells

The study above was performed in splenocytes and so we next characterised the T-cell intrinsic role of Pellino1 in controlling IL-17 production by using purified T cell populations. Naïve $CD4^+$ T cells were purified from spleen cells using MACS technology and subjected to T cell activation by co-stimulation with agonistic CD3 and CD28 antibodies for 48 hours. To induce Th17 differentiation, isolated pure naïve $CD4^+$ T cells was stimulated with CD3 and CD28 antibodies in the presence of cytokine combinations that lead to non-pathogenic Th17 (TGF-β and IL-6) and pathogenic Th17 (IL-1β and IL-23) for 96 hours (Lee *et al*., 2012; Shainheit *et al*., 2011). To drive differentiation of naïve $CD4^+$ T cells into Th17 cells and not other Th cells, they were also treated with IFN-γ neutralising antibody and IL-4 neutralising antibody.

Stimulating spleen cells with anti-CD3 and anti-CD28 led to a significantly higher level of IL-17 in *Peli1*$^{-/-}$ mice compared with WT mice (Fig. 4.5a), However, naïve $CD4^+$ T cells purified from the spleen cells produced very low levels of IL-17 in *Peli1*$^{-/-}$ mice relative to splenocytes (Fig. 4.5b). Despite the trivial levels of IL-17 production, a similar trend to spleen cells stimulation was observed in that *Peli1*$^{-/-}$ naïve $CD4^+$ T cells showed some augmentation of IL-17 production relative to naïve $CD4^+$ T cells from WT mice (Fig. 4.5b). Furthermore, naïve $CD4^+$ T cells stimulated with anti-CD3 and anti-CD28 as well as Th17 polarising cytokines, TGF-β and IL-6, induced IL-17 production in WT cells and this was further enhanced in *Peli1*$^{-/-}$ cells (Fig. 4.6). This suggests that Pellino 1 has a T cell-intrinsic regulatory role in controlling non-pathogenic Th17-induced IL-17. When naïve $CD4^+$ T cells were stimulated with anti-CD3, anti-CD28, IL-1β, and IL-23, IL-17 was again released by both WT and *Peli1*$^{-/-}$ mice, but a significantly greater level of IL-17 was driven by the absence of Pellino 1 (Fig. 4.6). The significant increase of IL-17 levels in both non-pathogenic Th17 and pathogenic Th17 cells of Pellino 1-deficient mice further validated the negative regulatory of Pellino 1 in IL-17 production (Fig. 4.6) The difference was more pronounced in non-pathogenic Th17 compared to pathogenic Th17. Overall, these data are consistent with a model in which Pellino 1 negatively regulates IL-17 production in both spleen cells and Th17 cells.

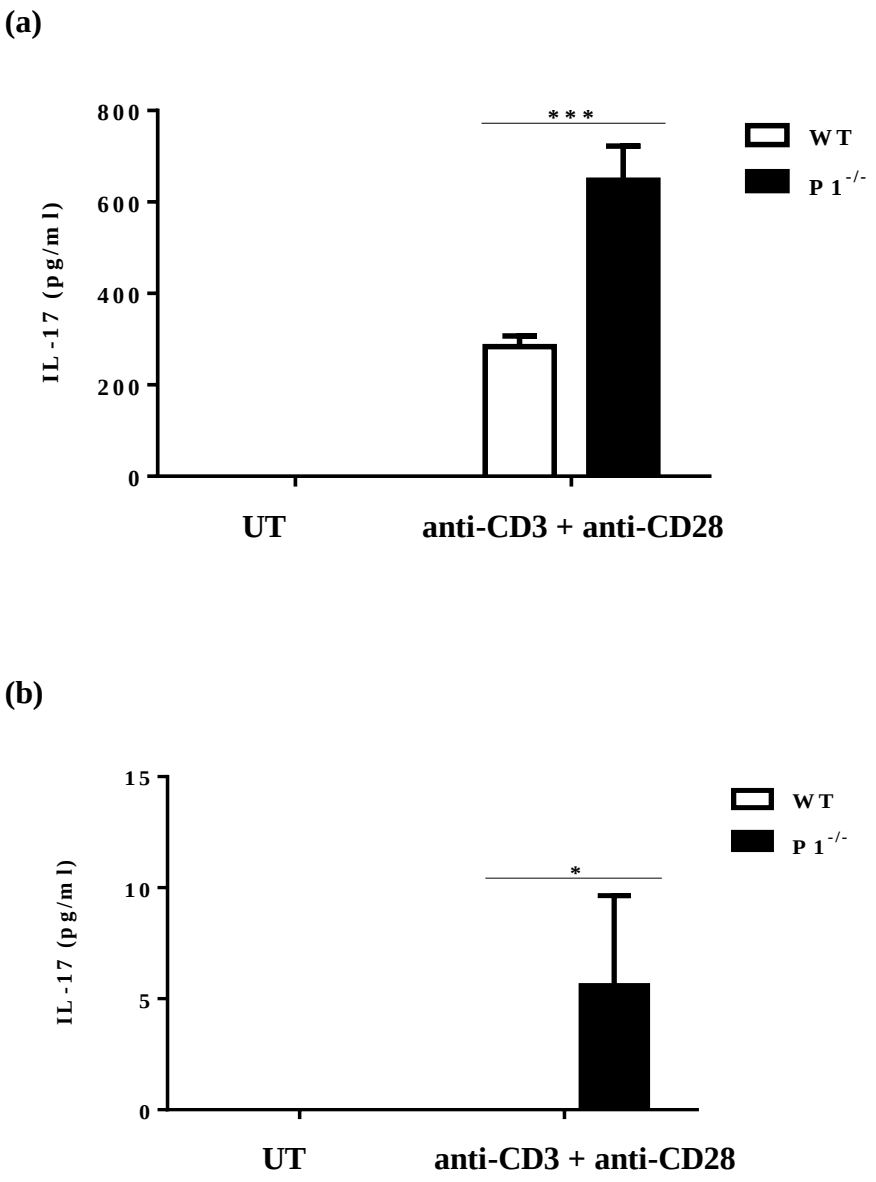

Figure 4.5 Effect of Pellino 1-deficiency on TCR and CD28-induced IL-17 production by spleen cells and naïve CD4$^+$ T cells

(a) Spleen cells and **(b)** naïve CD4$^+$ T cells isolated from the spleens of 8- to 10-week-old WT and Pellino 1-deficient (P1$^{-/-}$) mice were cultured without treatment (UT) or with anti-CD3 (0.5 μg/ml) and anti-CD28 (0.5 μg/ml) over 48 hours. Conditioned media was assayed by ELISA for levels of IL-17. Data are shown from an experiment that is representative of 3 independent experiments. All error bars are S.E.M. Statistical analysis was performed using two-way ANOVA with statistical significance indicated by *$p \leq 0.05$ and ***$p \leq 0.001$.

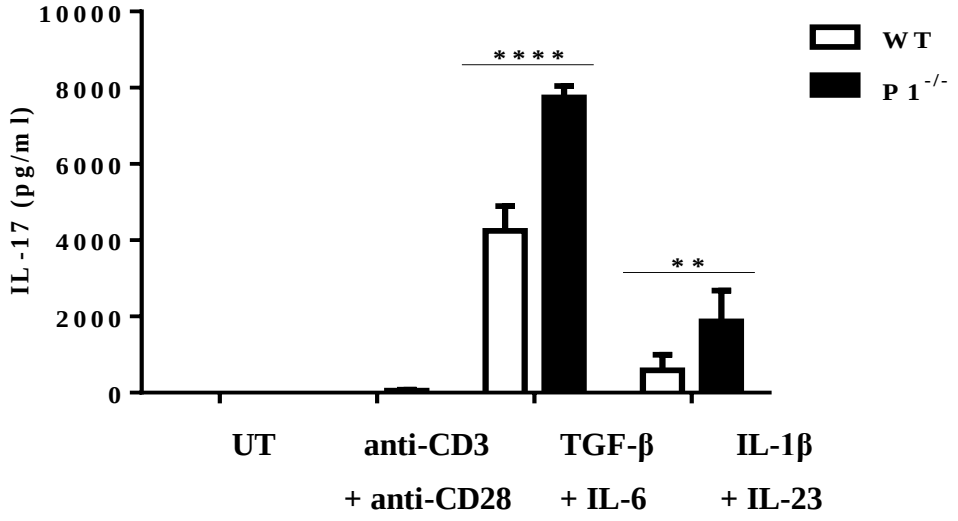

Figure 4.6 Effect of Pellino 1-deficiency on TCR and CD28-induced IL-17 production by Th17 cells

Naïve $CD4^+$ T cells isolated from the spleen of 8- to 10-week-old WT and Pellino 1-deficient ($P1^{-/-}$) mice were cultured without treatment (0) or with anti-CD3 (1 μg/ml) and anti-CD28 (5 μg/ml) over 96 hours. Two groups of stimulated cells were also treated with Th17-polarising cytokines: (i) TGF-β (5 ng/ml) and IL-6 (20 ng/ml), (ii) IL-1β (20 ng/ml) and IL-23 (20 ng/ml), respectively in the presence of IFN-γ neutralising antibody (10 μg/ml) and IL-4 neutralising antibody (10 μg/ml). Conditioned media was assayed by ELISA for levels of IL-17. Data are shown from an experiment that is representative of 3 independent experiments. All error bars are S.E.M. Statistical analysis was performed using two-way ANOVA with statistical significance indicated by **$p \leq 0.01$ and ****$p \leq 0.0001$.

4.2.5 Loss of Pellino 1 augments expression of *il17* mRNA

Having demonstrated a role for Pellino 1 in controlling production of IL-17, we next probed the potential mechanism by which Pellino 1 targets the pathway that controls the levels of IL-17 protein. To this end we examined if Pellino 1 can target the transcription of *il17* genes by measuring *il17* mRNA levels in WT and *Peli1*$^{-/-}$ mice. Since IL-17 represents a family of cytokines, we focused our studies on some members of the *il17* gene family. IL-17A and IL-17F are two of most well described members of the IL-17 family and are encoded by *il17a* and *il17f* , respectively. Sharing 50% sequence overlap at the protein level, they can be secreted as homodimers, IL-17A and IL-17F, or as heterodimer, IL-17A/F (Puşcaş *et al*., 2019). Owing to these characteristics, many analyses have been conducted to find a correlation of both cytokines in inflammatory diseases and psoriasis at gene level (Shao *et al*., 2020; Villalpando-Vargas *et al*., 2021).

Spleen cells stimulated with anti-CD3 and anti-CD28 for 48 hours were harvested and assessed for *il17a* and *il17f* levels by real time PCR. Co-stimulation of WT cells with anti-CD3 and anti-CD28 did promote expression of *il17a* (Fig. 4.7a), but the co-stimuli failed to induce *il17f* (Fig. 4.7b). The expression of *il17a* (Fig. 4.7a) and *il17f* (Fig. 4.7b) was further enhanced in *Peli1*$^{-/-}$ cells stimulated with anti-CD3 and anti-CD28 (Fig. 4.7b). These findings strongly suggest that Pellino 1 targets the pathways that promote transcriptional upregulation of *il17* genes and underlies the regulatory effects of Pellino 1 in tempering the production of IL-17 protein. Together with ELISA data above, Pellino 1-deficiency illustrates an impact on the induction of IL-17 at the mRNA and protein level.

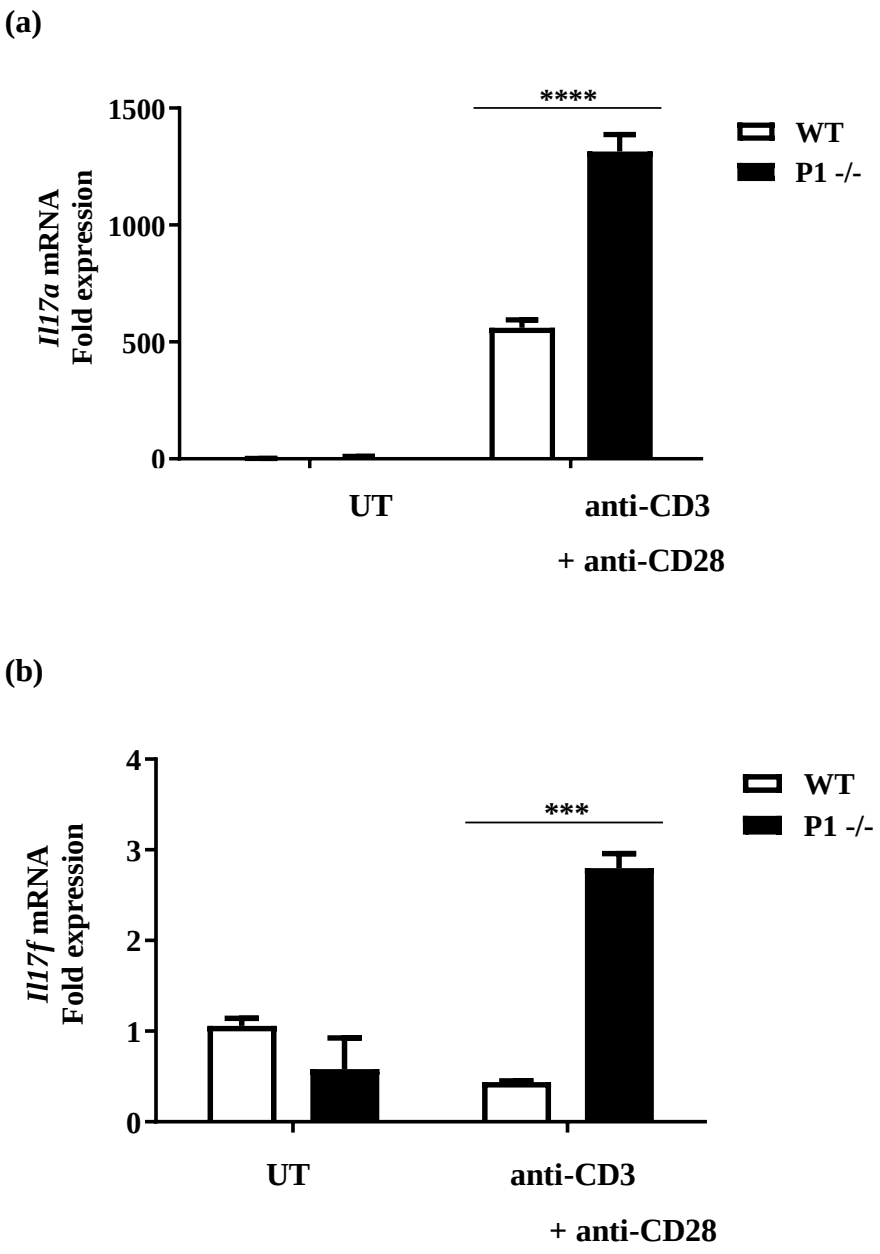

Figure 4.7 Effect of Pellino 1-deficiency on TCR and CD28-induced *il17* mRNA levels

Quantitative RT-PCR of **(a)** *il17a* and **(b)** *il17f* in spleen cells isolated from 8- to 10-week-old WT and Pellino 1-deficient ($P1^{-/-}$) mice cultured without treatment (UT) or with anti-CD3 (0.5 μg/ml) and anti-CD28 (0.5 μg/ml) over 48 hours. mRNA levels are presented as a fold change relative to untreated (UT) WT cells and normalised to HPRT expression. Data are shown from an experiment that is representative of 3 independent experiments. Statistical analysis was performed using two-way ANOVA with statistical significance indicated by ***$p \leq 0.001$ and ****$p \leq 0.0001$.

4.2.6 Myeloid cells are indispensable for regulatory effects of Pellino 1 on expression of IL-17

The composition of a murine spleen includes predominantly T cells, B cells and a variety of innate immune cells (Hensel *et al*., 2019). Given that the T cell response is initiated by antigen presenting cells (APCs), the spleen makes a suitable environment to study the complexity of immune signalling. While our studies above on purified naïve $CD4^+$ T cells is consistent with a T cell-intrinsic role for Pellino 1 in controlling IL-17 production, it was noteworthy that the levels of IL-17 were extremely modest relative to splenocytes. We speculated that the trivial amounts of IL-17 detected in purified naïve $CD4^+$ T cells was caused by the absence of a third signal from the APCs that produce polarising cytokines for Th17 differentiation. To examine this hypothesis, CD3/CD28 induced expression was measured in splenocytes that were depleted of myeloid cells. $CD11b^+$ myeloid cells were depleted from spleen cells using MACS technology and confirmed by flow cytometry (Fig. 4.8a). There was a significant reduction of CD3/CD28-induced IL-17 levels in spleen cells that were depleted of $CD11b^+$ myeloid cells (Fig. 4.8b). This result emphasised the need of myeloid cells acting as APCs to induce Th17 differentiation and immune response and is consistent with the literature (Liu & Janeway, 1992). However, depletion of myeloid cells from splenocytes cultures did not influence the phenotypic augmentation of IL17 that is still apparent in depleted cells from the spleens of *Peli1*$^{-/-}$ mice (Fig. 4.8b). These data are consistent with a T cell-intrinsic role for Pellino1 in regulation of IL-17 and is not mediated by any effects in myeloid cells.

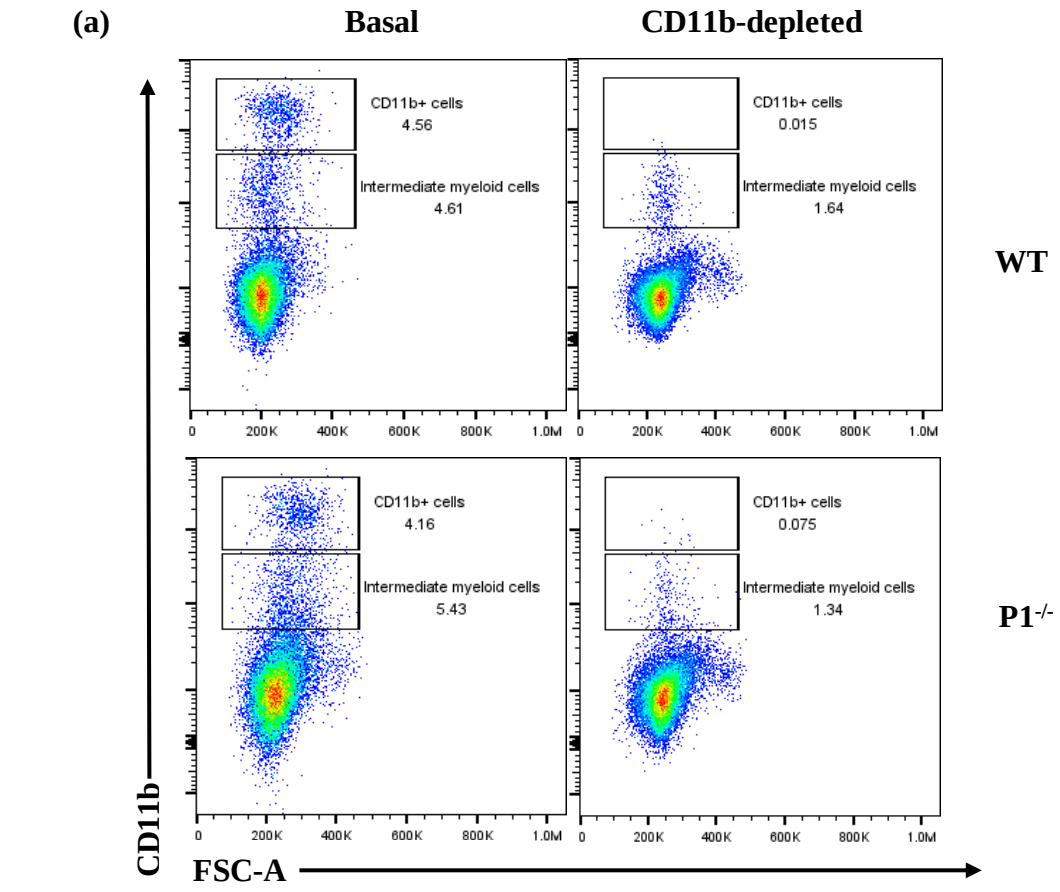
(a)
Basal
CD11b-depleted
CD11b+ cells
4.56
Intermediate myeloid cells
4.61
CD11b+ cells
0.015
Intermediate myeloid cells
1.64
WT
CD11b+ cells
4.16
Intermediate myeloid cells
5.43
CD11b+ cells
0.075
Intermediate myeloid cells
1.34
P1-/-
CD11b
FSC-A
0
200K
400K
600K
800K
1.0M

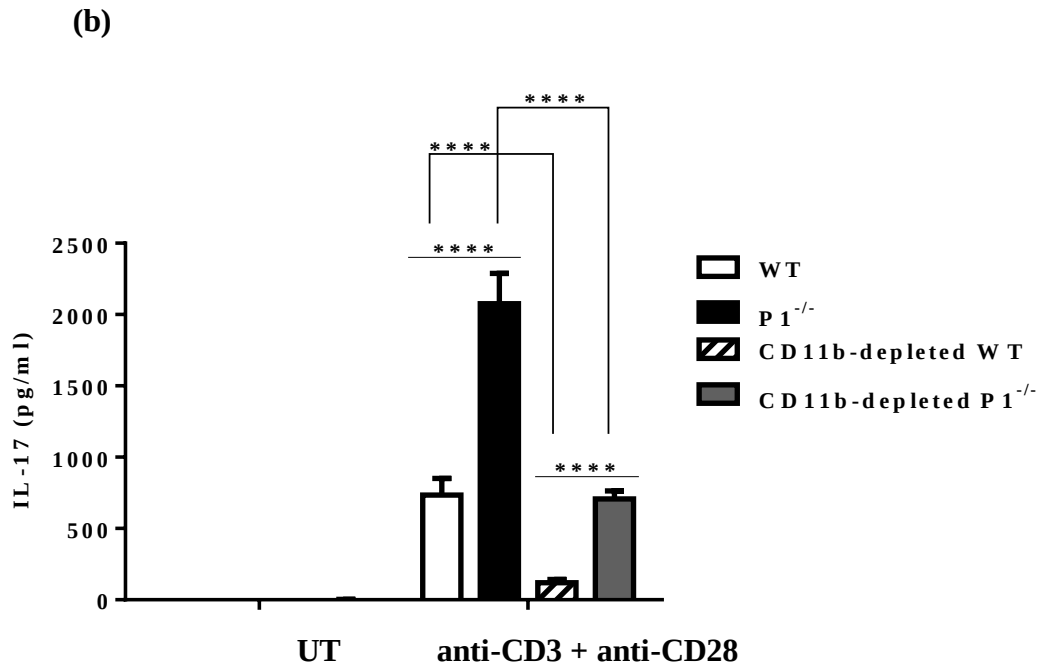
(b)
IL-17 (pg/ml)
2500
2000
1500
1000
500
0
****
****
****
****
WT
P1-/-
CD11b-depleted WT
CD11b-depleted P1-/-
UT
anti-CD3 + anti-CD28

Figure 4.8 Effect of Pellino 1-deficiency on TCR and CD28-induced IL-17 production by spleen cells in the absence and presence of splenic myeloid cells

Spleen cells isolated from 8- to 10-week-old WT and Pellino 1-deficient ($P1^{-/-}$) mice were depleted of CD11b positive myeloid cells by MACS technology and **(a)** depletion was confirmed by flow cytometry. $CD11b^{+}$ myeloid cells were detected on a plot of CD11b vs forward scatter area (FSC-A). Spleen cells with intact or depleted $CD11b^{+}$ myeloid cells were cultured without treatment (UT) or with anti-CD3 (0.5 μg/ml) and anti-CD28 (0.5 μg/ml) over 48 hours. **(b)** Conditioned media was assayed by ELISA for levels of IL-17. Data are shown from an experiment that is representative of 3 independent experiments. All error bars are S.E.M. Statistical analysis was performed using two-way ANOVA with statistical significance indicated by ****$p \leq 0.0001$.

4.2.7 Evaluating the upstream targets for Pellino 1 in mediating deregulated IL-17 generation

Given that Pellino 1 has been implicated in receptor proximal signalling pathways, we next investigated the molecular pathways that may be targeted by Pellino in its regulation of IL-17. As summarised in figure 4.1, Th17 cell differentiation involves signalling pathways through the TCR complex and receptors including TNFR1, IL-6R, IL-21R, and TGF-βR; downstream signalling through these receptors lead to Th17 cell development and subsequent IL-17 production (Zhang *et al*., 2021). To this end, we used pharmacological agents to target these pathways and assess their effects on the enhanced IL-17 production in response to Pellino 1 deficiency.

Spleen cells from WT and *Peli1*$^{-/-}$ mice were stimulated with anti-CD3 and anti-CD28 antibodies for 24 h in the presence of NF-κB inhibitors (BAY 11-7085 and JSH-23), JAK1/2 inhibitor (Ruxolitinib), RORγt inhibitors (GSK805 and (±)-ML 209), TGF-β1R inhibitor (SB-505124), p38α inhibitor (AMG 548), JNK1,2,3 inhibitor (SP 600125), ERK inhibitor (FR 180204), or mTOR inhibitor (Everolimus). BAY 11-7085 inhibits IκBα phosphorylation, whereas JSH-23 disrupts NF-kB nuclear translocation. Moreover, GSK805 is RORγt inhibitor, whereas (±)-ML 209 is a RORγt inverse agonist. Secretion of IL-17 was measured by ELISA.
Each drug impaired IL-17 production in both WT and *Peli1*$^{-/-}$ cells to a different degree (Fig. 4.9). IL-17 production in WT cells was mildly impaired by NF-κB inhibitors, indicating there was a modest involvement of NF-κB in Th17 differentiation. There was very little residual expression of IL-17 in the presence of the JAK1/2 inhibitor (Ruxolitinib), RORγt inhibitors (GSK805 and (±)-ML 209), TGF-β1R inhibitor (SB-505124), p38α inhibitor (AMG 548) or the mTOR inhibitor (Everolimus), indicating critical roles for these pathways in driving production of IL-17. In contrast, the JNK and ERK inhibitors had little or no effect on IL-17 production in WT cells, suggesting that these pathways made little contribution to IL-17 expression. Notably, there was no significant difference in IL-17 production in *Peli1*$^{-/-}$ spleen cells relative to WT cells in the presence of all inhibitors (Fig. 4.9). These data suggest that Pellino 1 does not target any of these pathways to suppress IL-17 production.

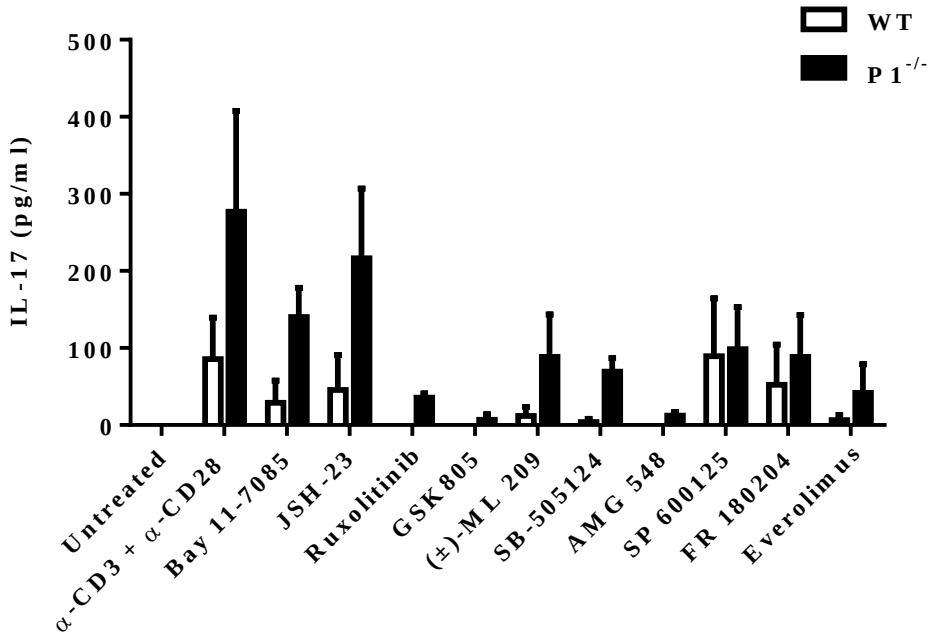

Figure 4.9 Pharmacological targeting of signalling pathways to investigate targets for Pellino 1 in regulating IL-17 production

Spleen cells isolated from 8- to 10-week-old WT and Pellino 1-deficient ($P1^{-/-}$) mice were cultured without treatment (UT) or with anti-CD3 (0.5 μg/ml) and anti-CD28 (0.5 μg/ml) over 24 hours. Conditioned media was assayed by ELISA for IL-17 level upon anti-CD3 and anti-CD28 co-stimulation in the presence of BAY 11-7085 (1 μM), JSH-23 (10 μM), Ruxolitinib (10 μM), GSK805 (10 μM), (±)-ML 209 (10 μM), SB-50512 (10 μM), AMG 548 (10 μM), SP 600125 (10 μM), FR 180204 (10 μM), and Everolimus (1 μM). Data are representative of 2 independent experiments. All error bars are S.E.M. Statistical analysis was performed using two-way ANOVA.

4.2.8 Pellino 1 does not affect the activation of MAPK in T cells

The pharmacological studies above suggested a complex interplay of signalling pathways that regulate IL-17 production in WT and *Peli1*$^{-/-}$ spleen cells. To this end we then investigated the role of Pellino 1 in regulating MAPK activation in T cells. Indeed, it has been previously proposed that the activation of JNK, ERK, and p38 downstream to TNF signalling, activates STAT3, leading to IL-17 secretion (Yang *et al*., 2018).

Naïve CD4^{+} T cells isolated from WT and *Peli1*$^{-/-}$ spleen cells were co-stimulated with CD3 and CD28 antibodies for 20 and 60 minutes to assess the levels of phosphorylated JNK, ERK, and p38 and total levels of JNK, ERK, and p38. Interestingly, co-stimulation with anti-CD3 and anti-CD28 antibodies promoted strong phosphorylation of JNK and ERK but had little or no effect on phosphorylation of p38 MAPK (Fig. 4.10). However, Pellino deficiency did not affect the anti-CD3 and anti-CD28-induced phosphorylation of JNK and ERK suggesting that any regulatory effects of Pellino1 on IL-17 expression that may be mediated by regulation of JNK and/or ERK pathways may be due to targeting of these kinases downstream of their phosphorylation and activation.

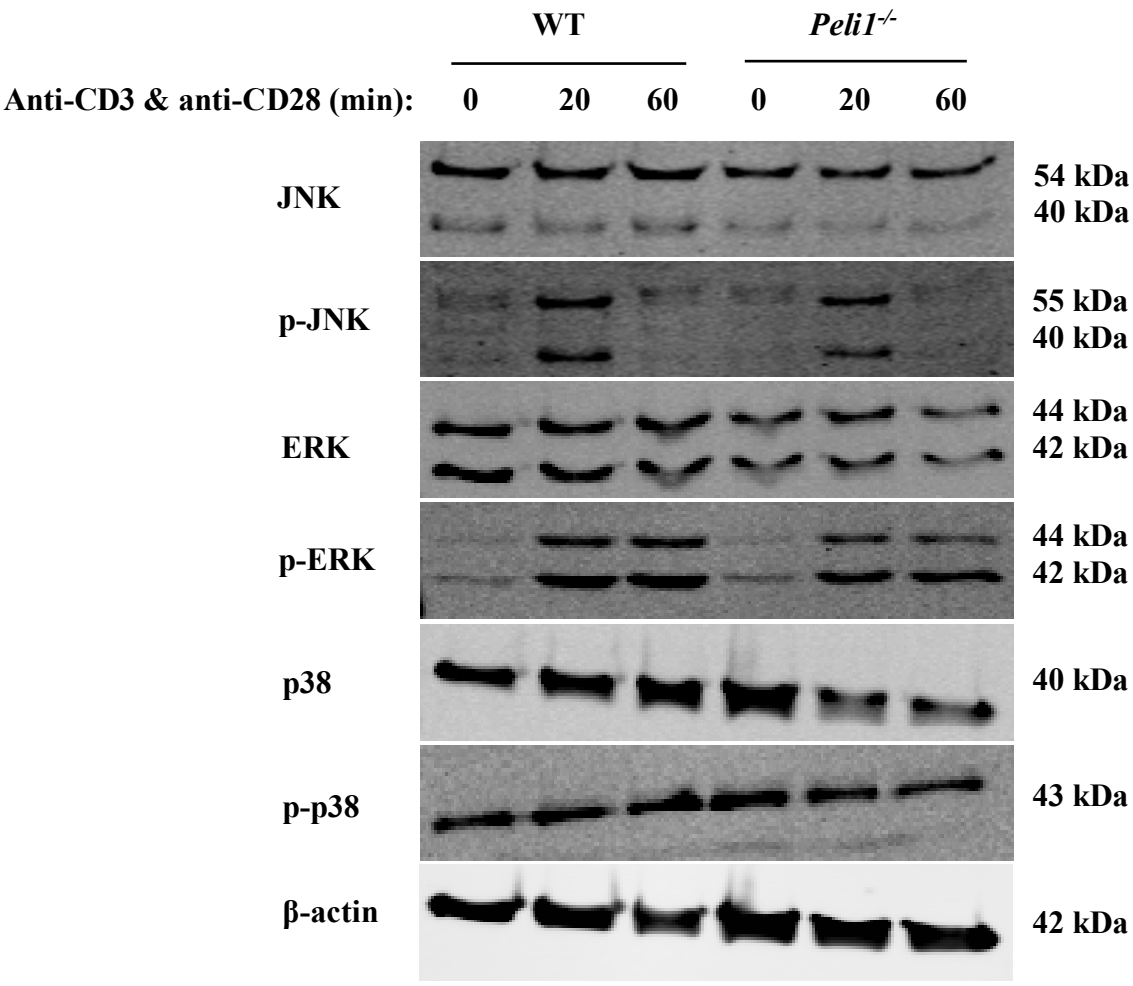

Figure 4.10 Effect of Pellino1-deficiency on CD3 and CD28-induced expression of MAPKs

Naïve $CD4^+$ T cells isolated from the spleen of 8- to 10-week-old WT and *Peli1*$^{-/-}$ mice were cultured without treatment (0) or with anti-CD3 (1μg/ml) and anti-CD28 (1μg/ml) over the indicated time course. Cell lysates were generated and immunoblotted for p-JNK, p-ERK, p-p38 and total levels of JNK, ERK, and p38. β-actin acted as a loading control. Data are shown from an experiment that represents 3 independent experiments.

4.2.9 Effects of Pellino 1 deficiency on expression levels of STAT3, c-Rel, and IRF4 in activated T cells

The various signalling pathways described above tend to converge downstream on transcription factors that regulate transcription of various genes. STAT3 and IRF4 are transcription factors that have been reported to be important positive regulators of IL-17 production (Chen *et al*., 2006; Brüstle *et al*., 2007). In addition, previous work reported the negative role of Pellino 1 in T cell activation by mediating the degradation of the transcription factor c-Rel via K48-linked ubiquitination in NF-κB pathway (Chang *et al*., 2011). We thus measured the levels of the transcription factors STAT3, IRF4 and c-Rel in T cells and compared these levels between WT and *Peli1*$^{-/-}$ cells.

Protein lysates from WT and *Peli1*$^{-/-}$ naïve CD4^{+} T cells with or without anti-CD3 and anti-CD28 stimulation for 20 minutes and 18 hours (Chang *et al*., 2011) were generated and probed with STAT3, c-Rel, IRF-4, and Pellino 1. Co-stimulation with anti-CD3 and anti-CD28 antibodies promoted strong induction of IRF4 and c-Rel but had little effect on levels of STAT3 (Fig. 4.11). However, Pellino deficiency did not affect the anti-CD3 and anti-CD28-induced expression of IRF4 and c-Rel, suggesting that any regulatory effects of Pellino1 on IL-17 expression is not due to direct targeting of these transcription factors.

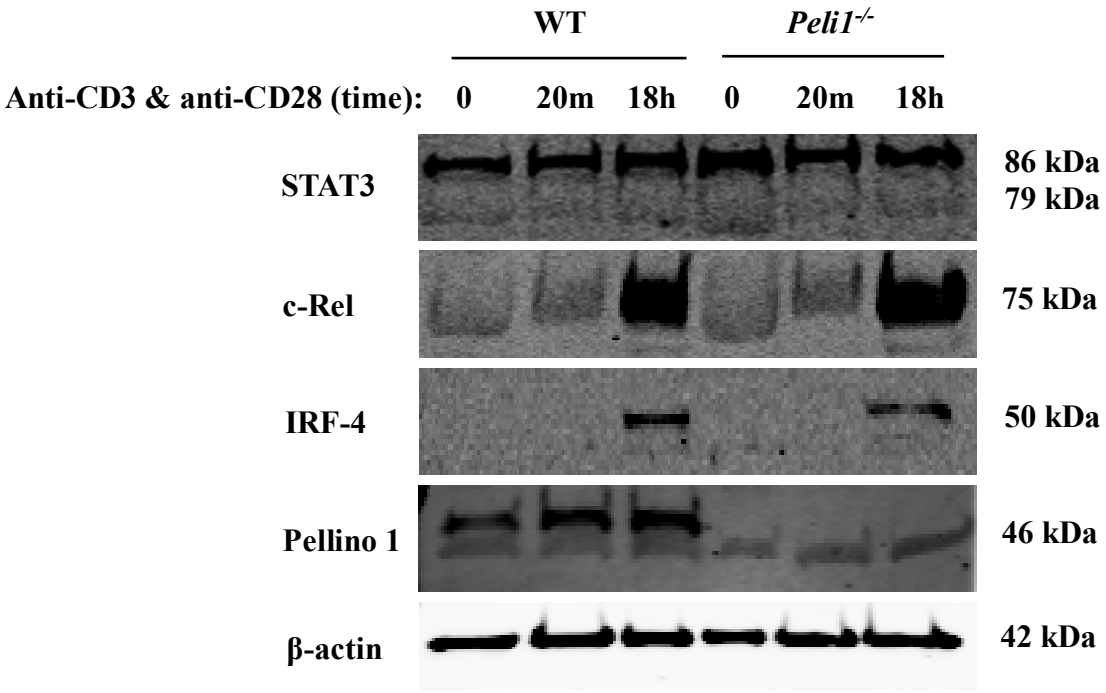

Figure 4.11 Effect of Pellino1-deficiency on CD3 and CD28-induced expression of STAT3, c-Rel, and IRF-4

Naïve $CD4^+$ T cells isolated from the spleen of 8- to 10-week-old WT and *Peli1*$^{-/-}$ mice were cultured without treatment (0) or with anti-CD3 (1μg/ml) and anti-CD28 (1μg/ml) over the indicated time course. Cell lysates were generated and immunoblotted for STAT3, c-Rel, IRF-4, and Pellino 1. β-actin acted as a loading control. Data are shown from an experiment that represents 3 independent experiments

4.2.10 Pellino 1-deficiency has no effect on the TLR-responsive genes in dendritic cells

As part of a comprehensive evaluation of the role for Pellino 1 in controlling T cell activation, we finally assessed its potential regulatory function in controlling activation of antigen presenting cells that are required for T cell stimulation. It should be noted that our strongest phenotypes in Pellino 1 deficient cells were apparent in splenocyte cultures that contain antigen presenting cells and cytokine from the latter can play critical roles in regulating T cell differentiation. For this study, we used bone marrow derived dendritic cells (BMDCs) as a model to investigate possible regulatory functions of Pellino 1 in antigen presenting cells. An initial screening was performed to evaluate the role for Pellino 1 in regulating the expression of pro-inflammatory cytokines through TLR signalling pathways. BMDCs isolated from WT and *Peli1*$^{-/-}$ mice were stimulated for 24 hours with ligands for TLR2/6 (Pam2CSK4), TLR 2/1 (Pam3CSK4), TLR2/Dectin-1 (Zymosan), TLR3 [Poly(I:C)], TLR4 (LPS), TLR5 (Flagelin), TLR8 (Clo75), TLR7/8 (Clo97), and TLR9 (CpG). IL-6 and TNF-α are two common pro-inflammatory cytokines released via TLR signalling that can boost adaptive responses at the effector stages (Medzhitov & Janeway, 1997). Secreted cytokine levels were measured by ELISA. Each TLR ligand induced comparable cytokine protein levels of IL-6 (Fig. 4.12a) and TNF-α (Fig. 4.12b) in dendritic cells from WT mice and *Peli1*$^{-/-}$ mice, suggesting that Pellino 1 does not appear to mediate the expression of TLR-induced pro-inflammatory genes in dendritic cells.

Besides IL-6 and TNF-α, IL-12 p40 and IL-12 p70 can also be released by dendritic cells via TLR signalling (Gautier *et al*., 2005). IL-12 p70 is a pro-inflammatory cytokine consisting of p35 and p40 subunit and contributes to Th1 cell, cytotoxic $CD8^+$ T cell, and NK cell responses (Verma *et al*., 2014). IL-12 p40 was secreted by both WT and *Peli1*$^{-/-}$ BMDCs upon TLR stimulation with the exception of Poly (I:C) (Fig. 4.13c). However, there was no significant difference between WT and *Peli1*$^{-/-}$ BMDCs in producing IL-12 p40 (Fig. 4.12c). On the other hand, IL-12 p70 was secreted at very low levels by both WT and *Peli1*$^{-/-}$ BMDCs upon zymosan, LPS, flagellin, Clo75, and Clo97 challenge (Fig. 4.12d). Like IL-12 p40, BMDCs were

more sensitive towards TLR9 induction when challenged with CpG to generate the cytokine IL-12 p70 (Fig. 4.12c, d). Overall, comparable level was observed between WT and *Peli1*$^{-/-}$ mice in the production of IL-12 p40 and IL-12 p70 (Fig. 4.12c, d), implying that Pellino 1 does not regulate the production of these cytokines in dendritic cells.

After 24 hours of stimulation with a range of TLR ligands, WT and *Peli1*$^{-/-}$ BMDCs were found to only respond to ligands that bind to innate immune receptors responsible for anti-viral protection, including Zymosan, Poly (I:C), LPS, CpG, and to a lesser extent in Clo75 and Clo97 stimulation groups (Fig. 4.13). However, no significant difference was observed in the protein levels of IFN-β between WT and *Peli1*$^{-/-}$ BMDCs (Fig. 4.14). Taken together, Pellino1 lacks a regulatory role in modulating TLR-induced production of pro-inflammatory cytokines (IL-6, TNF-α, IL-12 p40, IL-12 p70) or IFN-β secretion.

Overall, these data are supportive of a model in which the regulatory role of Pellino 1 in T cell differentiation and especially IL-17 production is likely due to T cell-intrinsic effects and not due to modulation of antigen presenting cell function.

(a)

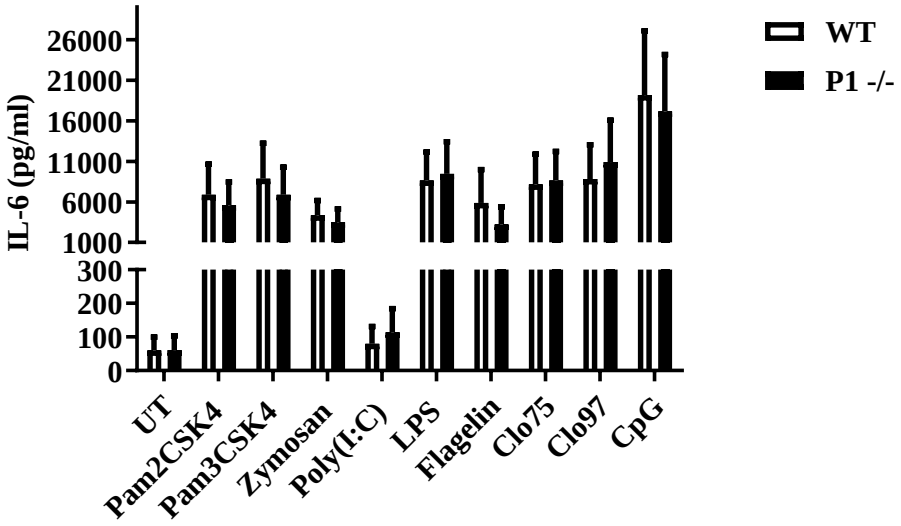
IL-6 (pg/ml)
26000
21000
16000
11000
6000
1000
300
200
100
0
WT
P1 -/-
UT
Pam2CSK4
Pam3CSK4
Zymosan
Poly(I:C)
LPS
Flagelin
Clo75
Clo97
CpG

(b)

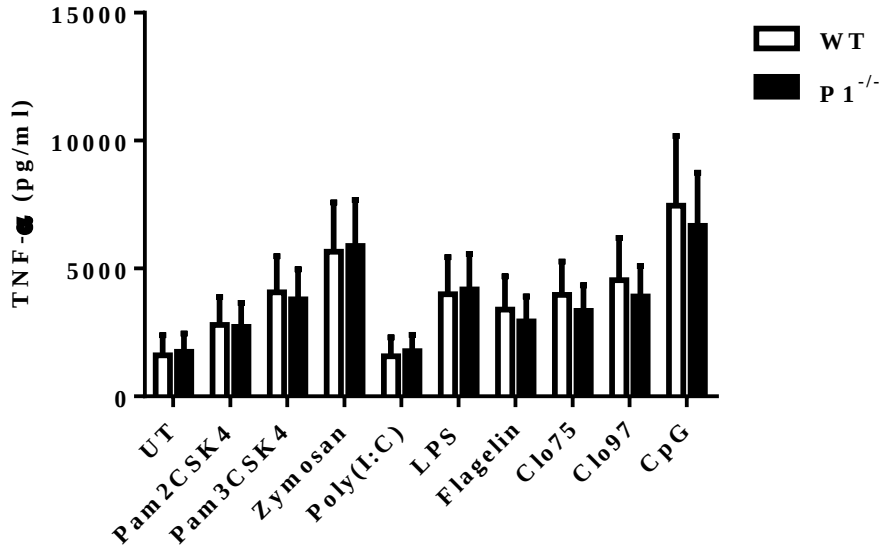
TNF-α (pg/ml)
15000
10000
5000
0
WT
P 1 -/-
UT
Pam2CSK4
Pam3CSK4
Zymosan
Poly(I:C)
LPS
Flagelin
Clo75
Clo97
CpG

(c)

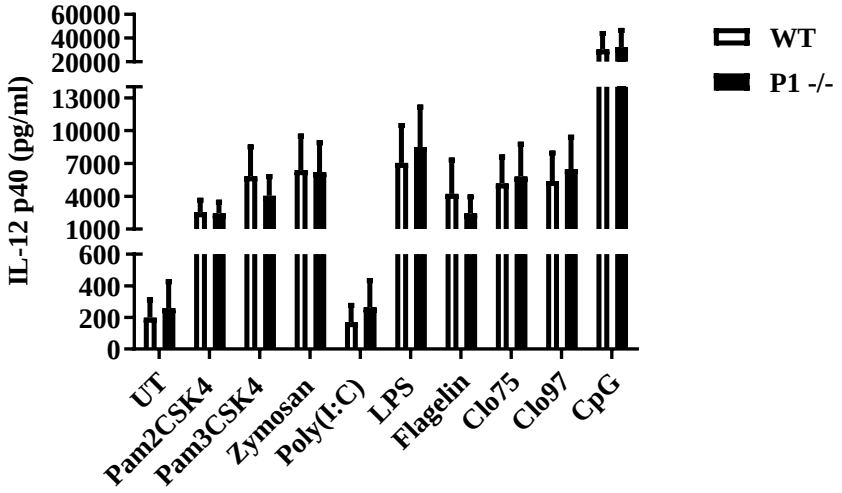

(d)

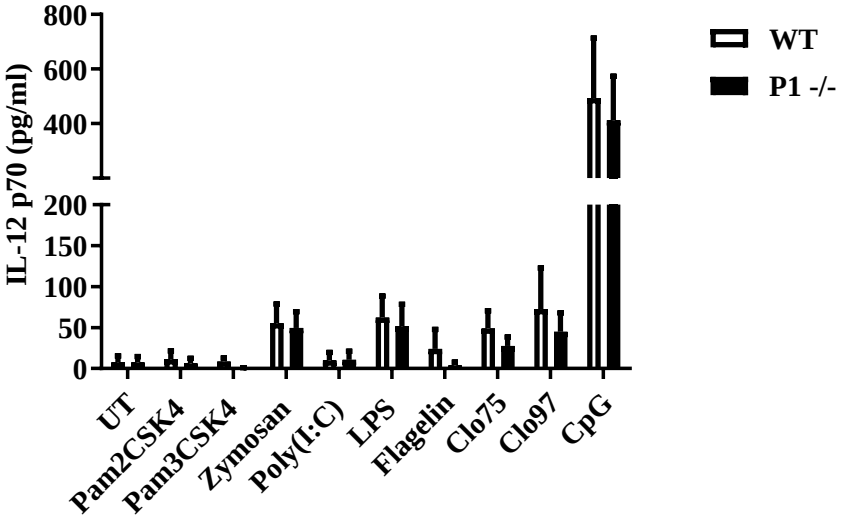

Figure 4.12 Effect of Pellino1-deficiency on TLR-induced expression of pro-inflammatory cytokines

BMDCs from 8- to 10-week-old WT and Pellino 1-deficient ($P1^{-/-}$) mice were cultured without treatment (UT) or treated with Pam2CSK4 (50 ng/ml), Pam3CSK4 (50 ng/ml), Zymosan (1 μg/ml), Poly(I:C) (50 μg/ml), LPS (5 ng/ml), Flagelin (1 μg/ml), Clo75 (1 μg/ml), Clo97 (1 μg/ml), and CpG (1 μg/ml) over 24 hours. Conditioned media was assayed by ELISA for levels of **(a)** IL-6, **(b)** TNF-α, **(c)** IL-12 p40, and **(d)** IL-12 p70. Data are representative of 5 independent experiments. All error bars are S.E.M. Statistical analysis was performed using two-way ANOVA.

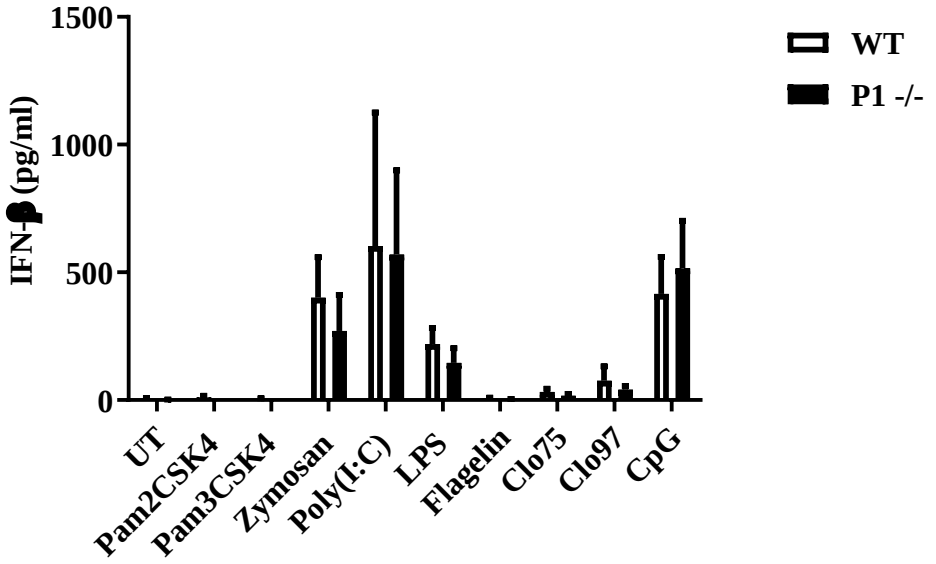

Figure 4.13 Effect of Pellino1-deficiency on TLR-induced expression of IFN-β

BMDCs from 8- to 10-week-old WT and Pellino 1-deficient ($P1^{-/-}$) mice were cultured without treatment (UT) or treated with Pam2CSK4 (50 ng/ml), Pam3CSK4 (50 ng/ml), Zymosan (1 μg/ml), Poly(I:C) (50 μg/ml), LPS (5 ng/ml), Flagelin (1 μg/ml), Clo75 (1 μg/ml), Clo97 (1 μg/ml), and CpG (1 μg/ml) over 24 hours. Conditioned media was assayed by ELISA for levels of IFN-β. Data are representative of 5 independent experiments. All error bars are S.E.M. Statistical analysis was performed using two-way ANOVA.

4.3 Discussion

The functions of all members of the Pellino family have primarily been studied in the context of innate immune signalling, but their functions in adaptive immune system remain ambiguous. Recent reports have shed light on the impact of Pellino 1 in mediating adaptive immune responses. Our comprehensive study of the roles of Pellino proteins in the generation of adaptive immune cell populations also emphasised a role for Pellino 1 in T cell activation. This thesis aimed to further investigate the role of Pellino 1 in mediating T cell activation and downstream T cell effector functions.

The murine spleen is a reservoir of peripheral immune cells with highest prevalence in T cells (38-43%), followed by B cells (18-22%), and a group of immune cells with low frequency ranging from 2% to 5% for each of the following cell types: NK cells, macrophages, monocytes, neutrophils, and dendritic cells (Hensel *et al*., 2019). This heterogenous pool of immune cells creates a microenvironment that allows various immune cells interactions to activate adaptive immune response, making the spleen a favoured secondary lymphoid organ to study the immune system. Indeed, researchers have used the spleen to support learning of the immune system as well as systemic response to inflammation following central nervous system injury (Marcet *et al*., 2017). In this study, we explored the regulatory role of Pellino proteins in adaptive immune system in the splenic environment.

Although Pellino 1 has been identified as a negative regulator of T cell activation (Chang *et al*., 2011), its involvement in controlling T cell effector responses is unknown. We first assessed if Pellino 1 could regulate rates of T cell proliferation. However, rates were comparable in WT and Pellino 1 deficient cells suggesting that the effects of Pellino 1 on T cell activation may be downstream of proliferation. To this end we then investigated its role in T cell differentiation by characterisation of T cell effector cytokines. Our data highlighted novel results that suggest the role of Pellino 1 as a negative regulator in splenic IL-17 and IL-10 production during T cell activation and differentiation. While we also found that Pellino 1 inhibits IFN-γ secretion, this finding is in line with marked elevation of IFN-γ level observed in

splenic $CD4^+$ and $CD8^+$ T cells of *Peli1*$^{-/-}$ mice compared with WT mice (Chang *et al*., 2011). TNF-α level was unaltered, whereas IFN-γ level alone was impacted by the loss of Pellino 1, this indicates that Pellino 1 is partially involved in mediating Th1 cell differentiation, specifically in a pathway that induces IFN-γ production only. Our initial screening also excluded the effect of Pellino 1 on IL-4 generation, but this is inadequate to fully exclude its impact on Th2 and Tfh cell differentiation as these cells are also defined by other effector cytokines, such as IL-5 and IL-13 for Th2 cells and IL-21 for Tfh cells (Swain *et al*., 2012). Similarly, it will be worth measuring IL-17F and IL-22 secretion in mice lacking Pellino 1 to fully elucidate its influence in Th17 cell differentiation. The negative impact of Pellino 1 on IL-10 production in turn indicates that Pellino 1 may negatively affect Treg differentiation and this would be worthy of further investigation. Furthermore, IFN-γ and IL-10 can be produced by other cell types found in the spleen, such as macrophages and NK cells (Bhat *et al*., 2017; Sun *et al*., 2021), making it difficult to clearly elucidate the regulatory function of Pellino 1 on specific effector T cells. Taking the heterogeneity of spleen cells and anti-CD3 and anti-CD28 co-stimulation as a representation of T cell activation into account, this approach to study the effect of Pellino 1 on T cell differentiation is inadequate. Alternatively, the role of Pellino 1 in T cell differentiation can be investigated by the generation of Th cell subsets from naïve $CD4^+$ T cells in response to polarising cytokines specific to each Th cell.

The most pronounced phenotype associated with Pellino 1 deficiency related to augmentation of IL-17 production in T cells and so much of our mechanistic studies focused on this pathway. We were also keen to assess if this role of Pellino 1 was unique in the Pellino family. We thus examined if Pellino 2 and Pellino 3 also play a role in regulating IL-17 production. Our data suggested that Pellino 2 did not have a role in mediating IL-17 secretion, but Pellino 3 participated in IL-17 regulation. Replicating the experiments in Pellino double knockout mice allowed us to explore potential crosstalk of Pellino proteins in IL-17 regulation. It was shown that IL-17 production was positively correlated with the concomitant loss of Pellino 1 and Pellino 2 or Pellino 1 and Pellino 3. A challenge in relation to this part of work was the breeding issue of *Peli1/3*$^{-/-}$ mice that persisted for over a year. Thus, only one *Peli1/3*$^{-/-}$ retired breeder was used to conduct this experiment. The data suggested that Pellino 1 and Pellino 2 did not cross talk or functionally interact in regulation of

IL-17 and that Pellino 1 and Pellino 3 did not work synergistically to control IL-17 generation. However, whether Pellino 1 and Pellino 3 act in redundancy in regulating IL-17 production warrants further evaluation and unfortunately was not feasible to address due to the above breeding issues with mice.

Initial studies focused on splenocyte cultures, but we then progressed to experiments on isolated T cells to explore T cell intrinsic roles of Pellino 1. We thus purified naïve $CD4^+$ T cells and Th17 cells. However, IL-17 production in isolated naïve $CD4^+$ T cells was barely detectable and this may be due to the lack of polarising cytokines from antigen presenting cells in the splenocyte cultures. This is aligned with the literature (Zhang *et al*., 2021) and is further confirmed by impaired IL-17 generation in activated spleen cells without myeloid cells, which consist of APCs, such as dendritic cells and macrophages. Moreover, we tested whether Pellino 1 has a T cell-intrinsic role in mediating IL-17 production by inducing Th17 differentiation from naïve $CD4^+$ T cells with external polarising cytokines stimuli in the absence of APCs. Our data confirm a T-cell intrinsic role for Pellino 1 as it negatively mediated IL-17 secretion by both pathogenic and non-pathogenic Th17 cells. Non-pathogenic Th17 cells are superior in generating IL-17 compared to pathogenic Th17, indicating the overall benefit of IL-17 function outweighs its potential harm in driving autoimmunity. As Pellino 1 can control IL-17 production of both phenotypes, it may turn off response to infection, while confer protection against IL-17 driven pathology. However, further validation in infectious diseases and autoimmune animal models, such as EAE, needs to be carried out to consolidate these findings.

Given the role of Pellino 1 as a negative regulator of IL-17 production, we were keen to investigate the mechanism of its action. The impact of Pellino 1 on secreted IL-17 and *il17a* mRNA expression, which encodes IL-17, suggests that it affects IL-17 production at protein level, as well as transcriptional level. We also provide evidence that the enhanced IL-17 levels did not come from increased number of $CD4^+$ T cells in the spleen as its proliferation was unaffected by Pellino 1, as described above. This corroborates that T-cell intrinsic regulatory role of Pellino 1 on IL-17 production is likely to occur during T cell differentiation upon T cell activation. Hence, a screening experiment was conducted to identify potential target pathways for Pellino 1 in regulating IL-17 production. These studies did not identify a pathway that Pellino 1

may have deployed to suppress IL-17 production since pharmacological inhibition of these pathways did not significantly alter the augmentation of IL-17 level caused by Pellino 1-deficiency. However, whilst co-stimulation of T cells with CD3 and CD28 caused strong activation of the JNK and ERK pathways, based on their increased phosphorylation status, we did not detect any differences in their activation when Pellino 1 was absent. This suggested that any effects of Pellino 1 on these MAPK kinase pathways may be downstream of their phosphorylation and activation. While splenocytes were used for the inhibitor experiments, naïve $CD4^+$ T cells were used for western blot; this inconsistency added complexity to the interpretation of data.

We then focused our efforts on downstream effectors such as the transcription factors STAT3, IRF4, and c-Rel. A previous study reported a role for Pellino 1 as a mediator of K48 polyubiquitination and degradation of c-Rel (Chang *et al*., 2011). IRF4 is critical for Th17 differentiation and maintaining Th17 phenotype (Brüstle *et al*., 2007; Huber *et al*., 2008; Mudter *et al*., 2011). STAT3 has been found to regulate IL-17 transcription through its binding to the promoter regions of IL-17A and IL-17F (Chen *et al*., 2006). However, the levels of these transcription factors were unaffected by Pellino 1 deficiency. STAT3 levels were not affected by co-stimulation of T cells, whereas IRF4 and c-Rel were strongly induced. We were unable to demonstrate a role for Pellino 1 in controlling levels of c-Rel and the reason for this discrepancy is unknown. Although Pellino 1 deficiency has no effect on the levels of IRF4, it is interesting to note that IRF4 requires the cooperation from BATF-JUN family protein complexes to bind to AP1-IRF composite elements in Th17 cells for its transcriptional activity and immunological actions (Li *et al*., 2012). Therefore, it will be interesting to determine whether Pellino 1 has an impact on BATF and JUN proteins to help explain these findings. In addition, these findings from western blot warrant further investigation because of the unknown concentration loaded to wells and differences in thickness of the b-actin band between different groups/timepoints (Fig.4.10 and Fig. 4.11).

Finally, we focused our efforts on investigating the potential regulatory role of Pellino 1 in controlling the function of antigen presenting cells as an indirect means to influence T cell differentiation. It was already reported that Pellino 1 is a mediator of TLR signalling pathways in macrophages and microglial cells (Chang *et al*., 2009;

Xiao *et al*., 2013). However, there is very limited knowledge about the role of Pellino 1 in dendritic cells (DCs). Given the previously described DC-specific role for Pellino 2 in TLR9 signalling pathway (Oleszycka *et al*., 2021), we explored the immunomodulatory function of Pellino 1 in DCs. The secretion of proinflammatory cytokines, such as IL-6, TNF-α, IL-12 p40, and IL-12p70 by BMDCs from WT and Pellino 1-deficient mice were comparable upon challenge with a variety of TLR ligands, indicating that Pellino 1 does not participate in the regulatory pathways of these cytokines within DCs.

It has also been demonstrated that TLR signalling can also contribute to antiviral response. Four main TLR members that play a crucial role in recognising viral genetic materials include TLR3 sensing double-stranded (ds) RNA, TLR7 and TLR8 responding to single-stranded RNA, and TLR9 detecting dsDNA (Alexopoulou *et al*., 2001; Hemmi *et al*., 2000; Diebold *et al*., 2004). Moreover, TLR2 and TLR4 have been described to be activated by measles virus and respiratory syncytial virus, respectively, indicating their involvement in viral recognition (Bieback *et al*., 2002; Kurt-Jones *et al*., 2000). These signalling pathways leads to the production of type I interferon (IFN-α, IFN-β) for antiviral defence (Müller *et al*., 1994). Our data illustrates the ability of TLR2 ligand (Zymosan), TLR3 ligand (Poly (I:C)), TLR4 ligand (LPS), and TLR9 ligand (CpG) to induce IFN-β in BMDCs lacking Pellino 1 that matches the level produced by WT BMDCs. All of these data suggest that it is unlikely that the regulatory effects of Pellino 1 on T cell activation and differentiation are mediated by acting at the level of APCs. Instead, the findings firmly favour a T cell intrinsic role for Pellino 1.

In this chapter, we have described a novel role for Pellino 1 in negatively regulating T cell-derived IL-17 production. This suggests that Pellino 1 may be a promising therapeutic target to ameliorate or prevent IL-17-driven autoimmune diseases. Interestingly, recent studies have highlighted the role of Pellino 1 in exacerbating IL-17-driven skin pathologies, such as psoriasis (Kim *et al*., 2020; Kim *et al*., 2023; Cho *et al*., 2023). However, a gap in our understanding of the precise mechanisms by which Pellino 1 modulates IL-17 secretion remains to exist. We have tried to identify potential molecules/pathways that are involved in shaping this phenotype, but an unambiguous target remains to be identified. Clearly Pellino 1 appears to have a T

cell-intrinsic role in regulating IL-17 production. This could be further investigated by generating conditional knockout mice that are selectively deficient of Pellino 1 in T cells. Such models would allow a delineation of the physiological and pathophysiological relevance of the function of Pellino1 in Th17 differentiation and IL-17 production. This may provide valuable clues to novel pathway that may be amenable to therapeutic exploitation.

Chapter 5: Concluding Remarks

Pellino proteins are E3 ubiquitin ligases that are responsible for post translational modification of target proteins. Ubiquitination induced by Pellino proteins can direct the target proteins for activation of signalling cascades or degradation. As such, members of the Pellino family (Pellino 1, Pellino 2, Pellino 3) have been demonstrated to play important roles in regulating immune responses and diverse cellular processes.

Many studies have delineated the role of Pellino proteins in innate immune signalling. To advance the knowledge of Pellino proteins in mediating adaptive immune system, we performed a novel and comprehensive characterisation of the role of Pellino proteins in producing T and B cell populations. Populations of T and B cell subsets in the spleen of mice lacking individual and different members of the Pellino family were quantified by flow cytometry. The importance of age and gender on these populations was also examined.

Our study revealed a selective role for Pellino 1 in generating activated $CD4^+$ T cells and Tem cells. While Pellino 1 controls T cell activation from a young age, Pellino 2 has an age-dependent role in producing T cell memory. Additionally, there are different roles for Pellino 1 and Pellino 2 in mediating $CD8^+$ T cell compartment. Our findings showed that Pellino 1 and Pellino 2 were capable of negatively modulating the production of Tem and Tcm cells, respectively. This suggests that Pellino 1 may be associated with the cytotoxic capability of Tem cells, whereas Pellino 2 may be able to control systemic infections via Tcm cell function.

This study also presented evidence for a Pellino 1-specific role in mediating B cell function as evidenced by enhanced levels of GC B cells and plasma cells in mice lacking Pellino 1. Uncontrolled production of these B cell subsets has been linked to autoimmunity. Therefore, Pellino 1 may possibly serve as a therapeutic target in the treatment of autoimmune diseases. Our gender evaluation showed enhanced T cell activation in female WT mice. This is aligned with the literature that has reported a higher tendency in female to develop autoimmune diseases which are often linked with aberrant T cell regulation. There was no gender bias related to T cell or B cell activation observed in the absence of Pellino proteins. However, Pellino 1 deficiency posed higher risk of splenomegaly, a sign of autoimmunity, in females.

Given that IL-17 is often implicated in the pathogenesis of autoimmune diseases, we were particularly interested in investigating the functional role of Pellino 1 on IL-17 secretion. When stimulated with anti-CD3 and anti-CD28, both protein and mRNA levels of splenic IL-17 and *il17* respectively increased in the absence of Pellino 1. Loss of Pellino 1 also led to augmented production of both non-pathogenic and pathogenic IL-17 in purified naïve $CD4^+$ T cells stimulated with TGF-β/IL-6 and IL-1β/IL-23 combinations, respectively. These data indicated that Pellino 1 negatively modulates IL-17 production in Th17 cells. Pellino 1-deficiency also did not influence TLR-responsive cytokines secretion in BMDMs. Notably, this regulatory function of Pellino 1 is intrinsic to T cells and not antigen presenting cells.

There are some limitations in our studies. A small sample size of old *Peli1/3*$^{-/-}$ mice was utilised due to challenges associated with breeding these mice that persisted for more than a year. This could have negatively impacted the power of the analysis in relation to this genotype. We were also unable to identify the exact target of Pellino 1 in regulating IL-17 production through our mechanistic studies. Therefore, it is necessary to expand this research in future studies by assessing the potential effect of Pellino 1 on other positive and negative regulators of IL-17. Our study was also limited to *ex vivo* and *in vitro* experiments using spleens from mice. It would have been beneficial to extend our investigation to human models. However, technical problems such as difficulty in knockdown of Pellino 1 using small interfering RNA (siRNA) in human PBMCs and difficulty in collecting skin samples of patients with psoriasis were among the limiting factors to include human models in this work.

IL-17 is an important cytokine in mediating protection against fungal and bacterial infections, but uncontrolled IL-17 expression can promote immunopathology in autoimmune diseases. Consequently, much effort has been made to develop IL-17-targetted therapies such as secukinumab, ixekizumab, and brodalumab for the treatment of psoriasis (Mills, 2023). Nevertheless, adverse effects associated with these biological therapeutics include suicidal thoughts and increased risk of Candida infections in some patients (Schmidt, 2015; Saunte *et al.*, 2017). Small molecule drugs (SMDs) can potentially mitigate biologics-related adverse effects without compromising the protective effects of IL-17 against infection because of their pharmacokinetic profile that do not chronically block IL-17 generation. Additionally,

SMDs have a lower production cost and are easier to be administered to the patients (Mills, 2023). A recent article has also proposed the use of a SMD that targets Src homology 2 domain-containing tyrosine phosphatase (SHP2) to overcome efficacy issue of approved IL-17-targetted therapies for the treatment of psoriasis in other IL-17-associated diseases such as rheumatoid arthritis and multiple sclerosis (Luo *et al.*, 2023).

As generating small molecule regulators of IL-17 have advantages over biologics in combating IL-17-related diseases, the present study points to Pellino 1 as a promising candidate target for this purpose. Our findings shed light on a Pellino 1-specific role in preventing memory formation of T cells and IL-17 production during T cell activation. Targeting Pellino 1 might hold promise for the treatment of IL-17-driven autoimmune diseases. IRAK-1 and IRAK-4 have been described to induce degradation of Pellino proteins (Butler *et al.*, 2007). Hence, a dual IRAK-1 and IRAK-4 inhibitor could be employed to block the degradation of Pellino proteins, enhancing the stability of Pellino 1 to negatively regulate IL-17 production.

Overall, this research expanded into a new avenue to learn about the regulatory role of Pellino proteins in adaptive immune system. Our work has so far assessed the potential molecules and molecular pathways that would contribute to these phenotypes during T cell activation; however, the molecular mechanism remains largely ambiguous. Hence, more work is warranted to study the underlying molecular basis in detail. Moreover, a systematic study is required to characterise Pellino proteins in healthy and disease tissue. This would add important new context in exploring potential therapeutic targeting of Pellino proteins.

Chapter 6: Bibliography

Afkarian, M., Sedy, J.R., Yang, J., Jacobson, N.G., Cereb, N., Yang, S.Y., Murphy, T.L. and Murphy, K.M., 2002. T-bet is a STAT1-induced regulator of IL-12R expression in naive CD4+ T cells. *Nature immunology*, ***3*(6)**, 549-557.

Aggarwal, S., Ghilardi, N., Xie, M.-H., de Sauvage, F.J., Gurney, A.L., 2003. Interleukin-23 Promotes a Distinct CD4 T Cell Activation State Characterized by the Production of Interleukin-17. *The Journal of Biological Chemistry*, **278(3)**, 1910–1914.

Albrecht, J.-C., Nicholas, J., Biller, D., Cameron, K.R., Biesinger, B., Newman, C., Wittmann, S., Craxton, M.A., Coleman, H., Fleckenstein, B., Honess, R.W., 1992. Primary Structure of the Herpesvirus Saimiri Genome. *Journal of Virology*, **66(8)**, 5047–5058.

Alexandre, Y.O. and Mueller, S.N., 2023. Splenic stromal niches in homeostasis and immunity. *Nature Reviews Immunology*, **23(11)**, 705-719.

Alexopoulou, L., Holt, A.C., Medzhitov, R. and Flavell, R.A., 2001. Recognition of double-stranded RNA and activation of NF-κB by Toll-like receptor 3. *Nature*, ***413*(6857)**, 732-738.

Alter-Wolf, S., Blomberg, B.B., Riley, R.L., 2009. Old mice retain bone marrow B1 progenitors, but lose B2 precursors, and exhibit altered immature B cell phenotype and light chain usage. *Mechanisms of Ageing and Development*, **130**, 401–408.

Batalla, A., Coto, E., González-Lara, L., González-Fernández, D., Gómez, J., Aranguren, T.F., Queiro, R., Santos-Juanes, J., López-Larrea, C., Coto-Segura, P., 2015. Association between single nucleotide polymorphisms *IL17RA* rs4819554 and *IL17E* rs79877597 and Psoriasis in a Spanish cohort. *Journal of Dermatological Science*, **80**, 111–115.

Batten, M., Li, J., Yi, S., Kljavin, N.M., Danilenko, D.M., Lucas, S., Lee, J., de Sauvage, F.J., Ghilardi, N., 2006. Interleukin 27 limits autoimmune encephalomyelitis by suppressing the development of interleukin 17-producing T cells. *Nature Immunology*, **7**, 929–936.

Bedoui, S., Gebhardt, T., Gasteiger, G., Kastenmüller, W., 2016. Parallels and differences between innate and adaptive lymphocytes. *Nature Immunology*, **17(5)**, 490–494.

Berg, M., James, S.P., 1990. Human Neutrophils Release the Leu-8 Lymph Node Homing Receptor During Cell Activation. *Blood*, **76(11)**, 2381–2388.

Bettelli, E., Carrier, Y., Gao, W., Korn, T., Strom, T.B., Oukka, M., Weiner, H.L., Kuchroo, V.K., 2006. Reciprocal developmental pathways for the generation of pathogenic effector Th17 and regulatory T cells. *Nature*, **441**, 235–238.

Bhat, N.M., Kantor, A.B., Bieber, M.M., Stall, A.M., Herzenberg, L.A., Teng, N.N.H., 1992. The ontogeny and functional characteristics of human B-1 ($CD5^+B$) cells. *International Immunology*, **4(2)**, 243–252.

Bhat, P., Leggatt, G., Waterhouse, N. and Frazer, I.H., 2017. Interferon-γ derived from cytotoxic lymphocytes directly enhances their motility and cytotoxicity. *Cell death & disease*, **8(6)**, 1–11.

Bieback, K., Lien, E., Klagge, I.M., Avota, E., Schneider-Schaulies, J., Duprex, W.P., Wagner, H., Kirschning, C.J., Ter Meulen, V. and Schneider-Schaulies, S., 2002. Hemagglutinin protein of wild-type measles virus activates toll-like receptor 2 signaling. *Journal of virology*, ***76*(17)**, 8729-8736.

Biswas, P.S., Gupta, S., Chang, E., Song, L., Stirzaker, R.A., Liao, J.K., Bhagat, G., Pernis, A.B., 2010. Phosphorylation of IRF4 by ROCK2 regulates IL-17 and IL-21 production and the development of autoimmunity in mice. *The Journal of Clinical Investigation*, **120(9)**, 3280–3295.

Bleesing, J.J.H., Fleisher, T.A., 2002. Human B Cells Express a CD45 Isoform That Is Similar to Murine B220 and Is Downregulated With Acquisition of the Memory B-Cell Marker CD27. *Cytometry Part B (Clinical Cytometry)*, **51B**, 1–8.

Blevins, H.M., Xu, Y., Biby, S. and Zhang, S., 2022. The NLRP3 inflammasome pathway: A review of mechanisms and inhibitors for the treatment of inflammatory diseases. *Frontiers in aging neuroscience*, **14**, 879021.

Bloch, Y., Bouchareychas, L., Merceron, R., Składanowska, K., Van den Bossche, L., Detry, S., Govindarajan, S., Elewaut, D., Haerynck, F., Dullaers, M. and Adamopoulos, I.E., 2018. Structural activation of pro-inflammatory human cytokine IL-23 by cognate IL-23 receptor enables recruitment of the shared receptor IL-12Rβ1. *Immunity*, ***48*(1)**, 45-58.

Borgulya, P., Kishi, H., Müller, U., Kirberg, J., von Boehmer, H., 1991. Development of the CD4 and CD8 lineage of T cells: instruction versus selection. *The EMBO Journal*, **10(4)**, 913–918.

Bradley, L.M., Atkins, G.G., Swain, S.L., 1992. LONG-TERM $CD4^+$ MEMORY T CELLS FROM THE SPLEEN LACK MEL-14, THE LYMPH NODE HOMING RECEPTOR. *The Journal of Immunology*, **148(2)**, 324–331.

Bradley, L.M., Watson, S.R., Swain, S.L., 1994. Entry of Naïve CD4 T Cells into Peripheral Lymph Nodes Requires L-Selectin. *J. Exp. Med.*, **180**, 2401–2406.

Breitfeld, D., Ohl, L., Kremmer, E., Ellwart, J., Sallusto, F., Lipp, M. and Förster, R., 2000. Follicular B helper T cells express CXC chemokine receptor 5, localize to B cell follicles, and support immunoglobulin production. *The Journal of experimental medicine*, ***192*(11)**, 1545-1552.

Brembilla, N.C., Senra, L., Boehncke, W.-H., 2018. The IL-17 Family of Cytokines in Psoriasis: Il-17A and Beyond. *Front. Immunol.*, **9(1682)**, 1–13.

Brüstle, A., Heink, S., Huber, M., Rosenplänter, C., Stadelmann, C., Yu, P., Arpaia, E., Mak, T.W., Kamradt, T., Lohoff, M., 2007. The development of inflammatory Th-17 cells requires interferon-regulatory factor 4. *Nature Immunology*, **8(9)**, 958–966.

Bryant, V.L., Ma, C.S., Avery, D.T, Li, Y., Good, K.L., Corcoran, L.M., de Waal Malefyt, R., Tangye, S.G., 2007. Cytokine-Mediated Regulation of Human B Cell Differentiation into Ig-Secreting Cells: Predominant Role of IL-21 Produced by CXCR5^{+} T Follicular Helper Cells. *The Journal of Immunology*, **179**, 8180–8190.

Budd, R.C., Cerottini, J.-C., Horvath, C., Bron, C., Pedrazzini, T., Howe, R.C., MacDonald, H.R., 1987. DISTINCTION OF VIRGIN AND MEMORY T LYMPHOCYTES Stable Acquisition of the Pgp-1 Glycoprotein Concomitant with Antigenic Stimulation. *The Journal of Immunology*, **138(10)**, 3120–3129.

Butler, M.P., Hanly, J.A., Moynagh, P.N., 2005. Pellino3 Is a Novel Upstream Regulator of p38 MAPK and Activates CREB in a p38-dependent Manner. *J. Biol. Chem.*, **280**, 27759–27768.

Butler, M.P., Hanly, J.A., Moynagh, P.N., 2007. Kinase-active Interleukin-1 Receptor-associated Kinases Promote Polyubiquitination and Degradation of the Pellino Family DIRECT EVIDENCE FOR PELLINO PROTEINS BEING UBIQUITIN-PROTEIN ISOPEPTIDE LIGASES. *J. Biol. Chem.*, **282**, 29729–29737.

Butterfield, K., Fathman, C.G., Budd, R.C., 1989. A SUBSET OF MEMORY CD4^{+} HELPER T LYMPHOCYTES IDENTIFIED BY EXPRESSION OF Pgp-1. *J. Exp. Med.*, **169**, 1461–1466.

Canté-Barrett, K., Mendes, R.D., Li, Y., Vroegindeweij, E., Pike-Overzet, K., Wabeke, T., Langerak, A.W., Pieters, R., Staal, F.J.T., Meijerink, J.P.P., 2017. Loss of CD44^{dim} Expression from Early Progenitor Cells Marks T-Cell Lineage Commitment in the Human Thymus. *Frontiers in Immunology*, **8(32)**, 1–15.

Cao, Y., Tang, W. and Tang, W., 2019. Immune cell infiltration characteristics and related core genes in lupus nephritis: results from bioinformatic analysis. *BMC immunology*, ***20***, 1-12.

Cao, Z., Henzel, W.J., Gao, X., 1996. IRAK: A Kinase Associated with the Interleukin-1 Receptor. *Science*, **271**, 1128–1131.

Carsetti, R., Köhler, G., Lamers, M.C., 1995. Transitional B Cells Are the Target of Negative Selection in the B Cell Compartment. *J. Exp. Med.*, **181**, 2129–2140.

Casrouge, A., Beaudoing, E., Dalle, S., Pannetier, C., Kanellopoulos, J. and Kourilsky, P., 2000. Size estimate of the αβ TCR repertoire of naive mouse splenocytes. *The Journal of Immunology*, **164(11)**, 5782-5787.

Cesta, M.F., 2006. Normal structure, function, and histology of the spleen. *Toxicologic pathology*, **34(5)**, 455-465.

Chang, M., Jin, W., Chang, J.-H., Xiao, Y., Brittain, G.C., Yu, J., Zhou, X., Wang, Y.-H., Cheng, X., Li, P., Rabinovich, B.A., Hwu, P., Sun, S.-C., 2011. The

ubiquitin ligase Peli1 negatively regulates T cell activation and prevents autoimmunity. *Nat. Immunol.*, **12**, 1002–1009.

Chang, M., Jin, W., Sun, S.-C., 2009. Peli1 facilitates TRIF-dependent Toll-like receptor signaling and proinflammatory cytokine production. *Nat. Immunol.*, **10**, 1089–1095.

Chaplin, D.D., 2010. Overview of the immune response. *J. Allergy Clin. Immunol.*, **125(2)**, S3–S23.

Chen, W., Jin, W., Hardegen, N., Lei, K.J., Li, L., Marinos, N., McGrady, G. and Wahl, S.M., 2003. Conversion of peripheral CD4+ CD25− naive T cells to CD4+ CD25+ regulatory T cells by TGF-β induction of transcription factor Foxp3. *The Journal of experimental medicine*, ***198*(12)**, 1875-1886.

Chen, Z., Laurence, A., Kanno, Y., Pacher-Zavisin, M., Zhu, B.-M., Tato, C., Yoshimura, A., Hennighausen, L., O'Shea, J., 2006. Selective regulatory function of Socs3 in the formation of IL-17 secreting T cells. *PNAS*, **103(21)**, 8137–8142.

Chicooree, N., Connolly, Y., Tan, C.T., Malliri, A., Li, Y., Smith, D.L. and Griffiths, J.R., 2013. Enhanced detection of ubiquitin isopeptides using reductive methylation. *Journal of The American Society for Mass Spectrometry*, **24(3)**, 421-430.

Cho, H., Park, N.J.Y., Ko, J., Lee, C.W., Lee, J.K., Maeng, Y.I. and Go, H., 2023. Pellino-1 expression is associated with epidermal proliferation and enhanced Th17 cell infiltration in psoriatic lesions. *Experimental Dermatology*, **32(9)**, 1476-1484.

Choi, K.-C., Lee, Y.S., Lim, S., Choi, H.K., Lee, C.-H., Lee, E.-K., Hong, S., Kim, I.-H., Kim, S.-J., Park, S.H., 2006. Smad6 negatively regulates interleukin 1-receptor–Toll-like receptor signaling through direct interaction with the adaptor Pellino-1. *Nat. Immunol.*, **7**, 1057–1065.

Chow, J.C., Young, D.W., Golenbock, D. T., Christ, W.J. and Gusovsky, F. (1999). Toll-like Receptor-4 Mediates Lipopolysaccharide-induced Signal Transduction. *The Journal of Biological Chemistry*. **274(16)**, 10689-10692.

Cluxton, D., Petrasca, A., Moran, B. and Fletcher, J.M., 2019. Differential regulation of human Treg and Th17 cells by fatty acid synthesis and glycolysis. *Frontiers in immunology*, ***10***, 115.

Cooper, M.D., Peterson, R.D.A., Good, R.A., 1965. DELINEATION OF THE THYMIC AND BURSAL LYMPHOID SYSTEMS IN THE CHICKEN. *Nature*, **4967**, 143–146.

Cusson-Hermance, N., Khurana, S., Lee, T.H., Fitzgerald, K.A. and Kelliher, M.A., 2005. Rip1 mediates the Trif-dependent toll-like receptor 3-and 4-induced NF-κB activation but does not contribute to interferon regulatory factor 3 activation. *Journal of Biological Chemistry*, **280(44)**, 36560-36566.

Dalton, D.K., Pitts-Meek, S., Keshav, S., Figari, I.S., Bradley, A. and Stewart, T.A., 1993. Multiple defects of immune cell function in mice with disrupted interferon-γ genes. *Science*, ***259*****(5102)**, 1739-1742.

Damasceno, L.E.A., Prado, D.S., Veras, F.P., Fonseca, M.M., Toller-Kawahisa, J.E., Rosa, M.H., Públio, G.A., Martins, T.V., Ramalho, F.S., Waisman, A. and Cunha, F.Q., 2020. PKM2 promotes Th17 cell differentiation and autoimmune inflammation by fine-tuning STAT3 activation. *Journal of Experimental Medicine*, ***217*****(10)**, e20190613.

Davis, C.B., Killeen, N., Crooks, M.E.C., Raulet, D., Littman, D.R., 1993. Evidence for a Stochastic Mechanism in the Differentiation of Mature Subsets of T Lymphocytes. *Cell*, **74**, 237–247.

Diebold, S.S., Kaisho, T., Hemmi, H., Akira, S. and Reis e Sousa, C., 2004. Innate antiviral responses by means of TLR7-mediated recognition of single-stranded RNA. *Science*, ***303*****(5663)**, 1529-1531.

Du, G., Chen, C.Y., Shen, Y., Qiu, L., Huang, D., Wang, R., Chen, Z.W., 2010. TCR Repertoire, Clonal Dominance, and Pulmonary Trafficking of Mycobacterium-Specific $CD4^+$ and $CD8^+$ T Effector Cells in Immunity Against Tuberculosis. *The Journal of Immunology*, **185**, 3940–3947.

D'Souza, L. Bhattacharya, D., 2019. Plasma cells: You are what you eat. *Immunological reviews*, **288(1)**, 161-177.

Enesa, K., Ordureau, A., Smith, H., Barford, D., Cheung, P.C.F., Patterson-Kane, J., Arthur, J.S.C., Cohen, P., 2012. Pellino1 Is Required for Interferon Production by Viral Double-stranded RNA. *J. Biol. Chem.*, **287**, 34825–34835.

Ferretti, S., Bonneau, O., Dubois, G.R., Jones, C.E., Trifilieff, A., 2003. IL-17, Produced by Lymphocytes and Neutrophils, Is Necessary for Lipopolysaccharide-Induced Airway Neutrophilia: IL-15 as a Possible Trigger. *The Journal of Immunology*, **170**, 2106–2112.

Fitzgerald, K.A., McWhirter, S.M., Faia, K.L., Rowe, D.C., Latz, E., Golenbock, D.T., Coyle, A.J., Liao, S.-M. and Maniatis, T., 2003. IKKε and TBK1 are essential components of the IRF3 signaling pathway. *Nature Immunology*. **4(5)**, 491-496.

Fitzgerald, K.A., Palsson-McDermott, E.M., Bowie, A.G., Jefferies, C.A., Mansell, A.S., Brady, G., Brint, E., Dunne, A., Gray, P., Harte, M.T., McMurray, D., Smith, D.E., Sims, J.E., Bird, M.T. and O'Neill, L.A.J., 2001. Mal (MyD88-adapter-like) is required for Toll-like receptor 4 signal transduction. *Nature*. **413**, 78-83.

Frauwirth, K.A., Riley, J.L., Harris, M.H., Parry, R.V., Rathmell, J.C., Plas, D.R., Elstrom, R.L., June, C.H. and Thompson, C.B., 2002. The CD28 signaling pathway regulates glucose metabolism. *Immunity*, ***16*****(6)**, 769-777.

Gallatin, W.M., Weissman, I.L., Butcher, E.C., 1983. A cell-surface molecule involved in organ-specific homing of lymphocytes. *Nature*, **304**, 30–34.

Gao, M., Labuda, T., Xia, Y., Gallagher, E., Fang, D., Liu, Y.C. and Karin, M., 2004. Jun turnover is controlled through JNK-dependent phosphorylation of the E3 ligase Itch. *Science*, ***306*(5694)**, 271-275.

Gautier, G., Humbert, M., Deauvieau, F., Scuiller, M., Hiscott, J., Bates, E.E., Trinchieri, G., Caux, C. and Garrone, P., 2005. A type I interferon autocrine–paracrine loop is involved in Toll-like receptor-induced interleukin-12p70 secretion by dendritic cells. *The Journal of experimental medicine*, ***201*(9)**, 1435-1446.

Gerberick, G.F., Cruse, L.W., Miller, C.M., Sikorski, E.E., Ridder, G.M., 1997. Selective Modulation of T Cell Memory Markers CD62L and CD44 on Murine Draining Lymph Node Cells Following Allergen and Irritant Treatment. *Toxicology and Applied Pharmacology*, **146**, 1–10.

Germain, R.N., 2002. T-CELL DEVELOPMENT AND THE CD4-CD8 LINEAGE DECISION. *Nature Review Immunology*, **2**, 309–322.

Ghoreschi, K., Laurence, A., Yang, X.-P., Tato, C.M., McGreachy, M.J., Konkel, J.E., Ramos, H.L., Wei, L., Davidson, T.S., Bouladoux, N., Grainger, J.R., Chen, Q., Kanno, Y., Watford, W.T., Sun, H.-W., Eberl, G., Shevach, E.M., Belkaid, Y., Cua, D.J., Chen, W., O'Shea, J.J., 2010. Generation of pathogenic Th17 cells in the absence of TGF-β signalling. *Nature*, **467**, 967–971.

Ghosn, E.E.B., Sadate-Ngatchou, P., Yang, Y., Herzenberg, L.A. and Herzenberg, L.A., 2011. Distinct progenitors for B-1 and B-2 cells are present in adult mouse spleen. *Proceedings of the National Academy of Sciences*, **108(7)**, 2879-2884.

Godfrey, D.I., Kennedy, J., Suda, T., Zlotnik, A., 1993. A Developmental Pathway Involving Four Phenotypically and Functionally Distinct Subsets of $CD3^-CD4^-CD8^-$ Triple-Negative Adult Mouse Thymocytes Defined by CD44 and CD25 Expression. *The Journal of Immunology*, **150(10)**, 4244–4252.

Großhans, J., Schnorrer, F., Nüsslein-Volhard, C., 1999. Oligomerisation of Tube and Pelle leads to nuclear localisation of Dorsal. *Mech. Dev.*, **81**, 127–138.

Hägglöf, T., Cipolla, M., Loewe, M., Chen, S.T., Mesin, L., Hartweger, H., Eltanbouly, M.A., Cho, A., Gazumyan, A., Ramos, V., Stamatatos, L., Oliveira, T.Y., Nussenzweig, M.C., Viant, C., 2023. Continuous germinal center invasion contributes to the diversity of the immune response. *Cell*, **186**, 147–161.

Hardy, R.R., Carmack, C.E., Shinton, S.A., Kemp, J.D., Hayakawa, K., 1991. Resolution and Characterization of Pro-N and Pre-Pro-B Cell Stages in Normal Mouse Bone Marrow. *J. Exp. Med.*, **173**, 1213–1225.

Harrington, L.E., Hatton, R.D., Mangan, P.R., Turner, H., Murphy, T.L., Murphy, K.M., Weaver, C.T., 2005. Interleukin 17-producing CD4+ effector T cells develop via a lineage distinct from the T helper type 1 and 2 lineages. *Nature Immunology*, **6(11)**, 1123–1132.

Hasegawa, M., Fujimoto, Y., Lucas, P.C., Nakano, H., Fukase, K., Núñez, G., Inohara, N., 2008. A critical role of RICK/RIP2 polyubiquitination in Nod-induced NF-κB activation. *The EMBO Journal*, **27**, 373–383.

Hayakawa, K., Hardy, R.R., Herzenberg, L.A., Herzenberg, L.A., 1985. PROGENITORS FOR Ly-1 B CELLS ARE DISTINCT FROM PROGENITORS FOR OTHER B CELLS. *J. Exp. Med.*, **161**, 1554–1568.

Haynes, N.M., Allen, C.D., Lesley, R., Ansel, K.M., Killeen, N. and Cyster, J.G., 2007. Role of CXCR5 and CCR7 in follicular Th cell positioning and appearance of a programmed cell death gene-1high germinal center-associated subpopulation. *The Journal of Immunology*, ***179*(8)**, 5099-5108.

Hemmi, H., Takeuchi, O., Kawai, T., Kaisho, T., Sato, S., Sanjo, H., Matsumoto, M., Hoshino, K., Wagner, H., Takeda, K. and Akira, S., 2000. A Toll-like receptor recognizes bacterial DNA. *Nature*, ***408*(6813)**, 740-745.

Hensel, J.A., Khattar, V. and Ponnazhagan, S., 2019. Characterization of immune cell subtypes in three commonly used mouse strains reveals gender and strain-specific variations. *Laboratory Investigation*, **99(1)**, 93-106.

Hershko, A. and Ciechanover, A., 1998. The ubiquitin system. *Annual review of biochemistry*, **67(1)**, 425-479.

Herzog, S., Reth, M., Jumaa, H., 2009. Regulation of B-cell proliferation and differentiation by pre-B-cell receptor signalling. *Nature Reviews Immunology*, **9**, 195–205.

Hochweller, K., Wabnitz, G.H., Samstag, Y., Suffner, J., Hämmerling, G.J., Garbi, N., 2010. Dendritic cells control T cell tonic signaling required for responsiveness to foreign antigen. *PNAS*, **107(13)**, 5931–5936.

Hotta, K., Takahashi, H., Asakura, T., Saitoh, B., Takatori, N., Satou, Y., Satoh, N., 2000. Characterization of Brachyury-Downstream Notochord Genes in the Ciona intestinalis Embryo. *Dev. Biol.*, **224**, 69–80.

Hu, H. and Sun, S.C., 2016. Ubiquitin signaling in immune responses. *Cell research*, ***26*(4)**, 457-483.

Huang, M.-C., Liao, J.-J., Bonasera, S., Longo, D.L., Goetzl, E.J., 2008. Nuclear factor-κB-dependent reversal of aging-induced alterations in T cell cytokines. *FASEB J.*, **22**, 2142–2150.

Huang, W., Na, L., Fidel, P.L., Schwarzenberger, P., 2004. Requirement of Interleukin-17A for Systemic Anti-*Candida albicans* Host Defense in Mice. *The Journal of Infectious Diseases*, **190**, 624–631.

Huber, M., Brüstle, A., Reinhard, K., Guralnik, A., Walter, G., Mahiny, A., von Löw, E. and Lohoff, M., 2008. IRF4 is essential for IL-21-mediated induction, amplification, and stabilization of the Th17 phenotype. *Proceedings of the National Academy of Sciences*, **105(52)**, 20846-20851.

Humphries, F., Bergin, R., Jackson, R., Delagic, N., Wang, B., Yang, S., Dubois, A. V., Ingram, R. J., Moynagh, P.N., 2018. The E3 ubiquitin ligase Pellino2 mediated priming of the NLRP3 inflammasome. *Nature Communications*, **9(1560)**, 1–17.

Humphries, F. and Moynagh, P.N., 2015. Molecular and physiological roles of Pellino E3 ubiquitin ligases in immunity. *Immunological Reviews*, **266(1)**, 93-108.

Huoh, Y.-S., Ferguson, K.M., 2014. The Pellino E3 Ubiquitin Ligases Recognize Specific Phosphothreonine Motifs and Have Distinct Substrate Specificities. *Biochemistry*, **53**, 4946–4955.

Huppler, A.R., Verma, A.H., Conti, H.R., Gaffen, S.L., 2015. Neutrophils Do Not Express IL-17A in the Context of Acute Oropharyngeal Candidiasis. *Pathogens*, **4**, 559–572.

Huster, K.M., Koffler, M., Stemberger, C., Schiemann, M., Wagner, H. and Busch, D.H., 2006. Unidirectional development of CD8+ central memory T cells into protective Listeria-specific effector memory T cells. *European journal of immunology*, **36(6)**, 1453-1464.

Hwang, E.S., Szabo, S.J., Schwartzberg, P.L. and Glimcher, L.H., 2005. T helper cell fate specified by kinase-mediated interaction of T-bet with GATA-3. *Science*, ***307*(5708)**, 430-433.

Ichiyama, K., Yoshida, H., Wakabayashi, Y., Chinen, T., Saeki, K., Nakaya, M., Takaesu, G., Hori, S., Yoshimura, A., Kobayashi, T., 2008. Foxp3 Inhibits RORγt-mediated *IL-17A* mRNA Transcription through Direct Interaction with RORγt. *The Journal of Biological Chemistry*, **283(25)**, 17003–17008.

Ivanov, I.I., McKenzie, B.S., Zhou, L., Tadokoro, C.E., Lepelley, A., Lafaille, J.J., Cua, D.J., Littman, D.R., 2006. The Orphan Nuclear Receptor RORγt Directs the Differentiation Program of Proinflammatory IL-17^{+} T Helper Cells. *Cell*, **126**, 1121–1133.

Ivanyi, J., Murgatroyd, L.B., Lydyard, P.M., 1972. Bursal Origin of Bone Marrow Cells with Competence for Antibody Formation. *Immunology*, **23**, 107–111.

Jensen, L.E., Whitehead, A.S., 2003a. Pellino3, a Novel Member of the Pellino Protein Family, Promotes Activation of c-Jun and Elk-1 and May Act as a Scaffolding Protein. *J. Immunol.*, **171**, 1500–1506.

Jensen, L.E., Whitehead, A.S., 2003b. Pellino2 activates the mitogen activated protein kinase pathway. *FEBS Letters*, **545**, 199–202.

Jiang, Z., Johnson, H.J., Nie, H., Qin, J., Bird, T.A., Li, X., 2003. Pellino 1 Is Required for Interleukin-1 (IL-1)-mediated Signaling through Its Interaction with the IL-1 Receptor-associated Kinase 4 (IRAK4)-IRAK-Tumor Necrosis Factor Receptor-associated Factor 6 (TRAF6) Complex. *J. Biol. Chem.*, **278**, 10952–10956.

Jordan-Williams, K.L., Poston, S., Taparowsky, E.J., 2013. BATF regulates the development and function of IL-17 producing iNKT cells. *BMC Immunology*, **14(16)**, 1–8.

June, C.H., Bluestone, J.A., Nadler, L.M. and Thompson, C.B., 1994. The B7 and CD28 receptor families. *Immunology today*, ***15*(7)**, 321-331.

Kagan, J.C., Su, T., Horng, T., Chow, A., Akira, S. and Medzhitov, R. (2008). TRAM couples endocytosis of Toll-like receptor 4 to the induction of interferon-β. *Nat Immunol*. **9(4)**, 361-368.

Kearney, J.F., Won, W.-J., Benedict, C., Moratz, C., Zimmer, P., Oliver, A., Martin, F., Shu, F., 1997. B Cell Development in Mice. *Intern. Rev. Immunol.*, **15**, 207–241.

Kebir, H., Kreymborg, K., Ifergan, I., Dodelet-Devillers, A., Cayrol, R., Bernard, M., Giuliani, F., Arbour, N., Becher, B., Prat, A., 2007. Human T_H17 lymphocytes promote blood-brain barrier disruption and central nervous system inflammation. *Nature Medicine*, **13(10)**, 1173–1175.

Khan, D. and Ansar Ahmed, S., 2015. Regulation of IL-17 in autoimmune diseases by transcriptional factors and microRNAs. *Frontiers in Genetics*, **6(236)**, 1-9.

Kim, S., Lee, S.Y., Bae, S., Lee, J.K., Hwang, K., Go, H. and Lee, C.W., 2020. Pellino1 promotes chronic inflammatory skin disease via keratinocyte hyperproliferation and induction of the T helper 17 response. *Experimental & Molecular Medicine*, ***52*(9)**, 1537-1549.

Kim, S.H., Oh, J., Roh, W.S., Park, J., Chung, K.B., Lee, G.H., Lee, Y.S., Kim, J.H., Lee, H.K., Lee, H. and Park, C.O., 2023. Pellino-1 promotes intrinsic activation of skin-resident IL-17A–producing T cells in psoriasis. *Journal of Allergy and Clinical Immunology*, ***151*(5)**, 1317-1328.

Kim, T.W., Yu, M., Zhou, H., Cui, W., Wang, J., DiCorleto, P., Fox, P., Xiao, H., Li, X., 2012. Pellino 2 Is critical for Toll-like Receptor/Interleukin-1 Receptor (TLR/IL-1R)-mediated Post-transcriptional Control. *J. Biol. Chem.*, **287**, 25686–25695.

Kleinschek, M.A., Boniface, K., Sadekova, S., Grein, J., Murphy, E.E., Turner, S.P., Raskin, L., Desai, B., Faubion, W.A., de Waal Malefyt, R., Pierce, R.H., McClanahan, T., Kastelein, R.A., 2009. Circulating and gut-resident human Th17 cells express CD161 and promote intestinal inflammation. *J. Exp. Med.*, **206(3)**, 525–534.

Klotz, L., Burgdorf, S., Dani, I., Saijo, K., Flossdorf, J., Hucke, S., Alferink, J., Novak, N., Beyer, M., Mayer, G., Langhans, B., Klockgether, T., Waisman, A., Eberl, G., Schultze, J., Famulok, M., Kolanus, W., Glass, C., Kurts, C., Knolle, P.A., 2009. The nuclear receptor PPARγ selectively inhibits Th17 differentiation in a T cell-intrinsic fashion and suppresses CNS autoimmunity. *JEM*, **206(10)**, 2079–2089.

Korenaga, H., Kono, T., Sakai, M., 2010. Isolation of seven IL-17 family genes from the Japanese pufferfish Takifugu rubripes. *Fish & Shellfish Immunology*, **28**, 809–818.

Kruetzmann, S., Rosado, M.M., Weber, H., Germing, U., Tournilhac, O., Peter, H.-H., Berner, R., Peters, A., Boehm, T., Plebani, A., Quinti, I., Carsetti, R., 2003. Human Immunoglobulin M Memory B Cells Controlling *Streptococcus pneumoniae* Infections Are Generated in the Spleen. *J. Exp. Med.*, **197(7)**, 939–945.

Kumar, B.V., Connors, T.J. and Farber, D.L., 2018. Human T cell development, localization, and function throughout life. *Immunity*, ***48*(2)**, 202-213.

Kumazaki, K., Tirosh, B., Maehr, R., Boes, M., Honjo, T., Ploegh, H.L., 2007. AID$^{-/-}$ μs$^{-/-}$ Mice Are Agammaglobulinemic and Fail to Maintain B220^{-}CD138^{+} Plasma Cells. *The Journal of Immunology*, **178**, 2192–2203.

Kurt-Jones, E.A., Popova, L., Kwinn, L., Haynes, L.M., Jones, L.P., Tripp, R.A., Walsh, E.E., Freeman, M.W., Golenbock, D.T., Anderson, L.J. and Finberg, R.W., 2000. Pattern recognition receptors TLR4 and CD14 mediate response to respiratory syncytial virus. *Nature immunology*, ***1*(5)**, 398-401.

Kurtz, J., 2005. Specific memory within innate immune systems. *TRENDS in Immunology*, **26(4)**, 186–192.

Laidlaw, B.J., Craft, J.E., Kaech, S.M., 2016. The multifaceted role of CD4^{+} T cells in CD8^{+} T cell memory. *Nature Review Immunology*, **16**, 102–111.

Langrish, C.L., Chen, Y., Blumenschein, W.M., Mattson, J., Basham, B.m Sedgwick, J.D., McClanahan, T., Kastelein, R.A., Cua, D.J., 2005. Il-23 drives a pathogenic T cell population that induces autoimmune inflammation. *The Journal of Experimental Medicine*, **201(2)**, 233–240.

Lanier, L., Sun, J., 2009. Do the terms innate and adaptive immunity create conceptual barriers? *Nature Reviews Immunology*, **9**, 302–303.

Laurence, A., Tato, C.M., Davidson, T.S., Kanno, Y., Chen, Z., Yao, Z., Blank, R.B., Meylan, F., Siegel, R., Hennighausen, L. and Shevach, E.M., 2007. Interleukin-2 signaling via STAT5 constrains T helper 17 cell generation. *Immunity*, ***26*(3)**, 371-381.

Lazarevic, V., Chen, X., Shim, J.-H., Hwang, E.-S., Jang, E., Bolm, A.N., Oukka, M., Kuchroo, V.K., Glimcher, L.H., 2011. T-bet represses Th17 differentiation by preventing Runx1-mediated activation of the gene encoding RORγt. *Nature Immunology*, **12(1)**, 96–105.

Lebson, L., Gocke, A., Rosenzweig, J., Alder, J., Civin, C., Calabresi, P.A., Whartenby, K.A., 2010. Cutting Edge: The Transcription Factor Kruppel-Like Factor 4 Regulates the Differentiation of Th17 Cells Independently of RORγt. *The Journal of Immunology*, **185**, 7161–7164.

Lee, J., Ho, W.-H., Maruoka, M., Corpuz, R.T., Baldwin, D.T., Foster, J.S., Goddard, A.D., Yansura, D.G., Vandlen, R.L., Wood, W.I., Gurney, A.L., 2001. IL-17E, a Novel Proinflammatory Ligand for the IL-17 Receptor Homolog IL-17Rh1. *The Journal of Biological Chemistry*, **276(2)**, 1660–1664.

Lee, J.S., Tato, C.M., Joyce-Shaikh, B., Gulen, M.F., Cayatte, C., Chen, Y., Blumenschein, W.M., Judo, M., Ayanoglu, G., McClanahan, T.K., Li, X., Cua, D.J., 2015. *Immunity*, **43**, 727–738.

Lee, Y., Awasthi, A., Yosef, N., Quintana, F.J., Xiao, S., Peters, A., Wu, C., Kleinewietfeld, M., Kunder, S., Hafler, D.A., Sobel, R.A., Regev, A., Kuchroo, V.K., 2012. Induction and molecular signature of pathogenic Th17 cells. Interleukin-23-Independent IL-17 Production Regulates Intestinal Epithelial Permeability. *Nature Immunol*ogy, **13(10)**, 991–999.

Lertmemongkolchai, G., Cai, G., Hunter, C.A., Bancroft, G.J., 2001. Bystander Activation of $CD8^+$ T cells Contributes to the Rapid Production of IFN-γ in Response to Bacterial Pathogens. *J. Immunol.*, **166(2)**, 1097–1105.

Li, H., Chen, J., Huang, A., Stinson, J., Heldens, S., Foster, J., Dowd, P., Gurney, A.L., Wood, W.I., 2000. Cloning and characterization of IL-17B and IL-17C, two new members of the IL-17 cytokine family. *PNAS*, **97(2)**, 773–778.

Li, P., Spolski, R., Liao, W., Wang, L., Murphy, T.L., Murphy, K.M. and Leonard, W.J., 2012. BATF–JUN is critical for IRF4-mediated transcription in T cells. *Nature*, **490(7421)**, 543-546.

Li, S., Strelow, A., Fontana, E.J. and Weshe, H., 2002. IRAK-4: A novel member of the IRAK family with the properties of an IRAK-kinase. *PNAS*. **99(8)**, 5567-5572.

Liang, S.C., Tan, X.-Y., Luxenberg, D.P., Karim, R., Dunussi-Joannopoulos, K., Collins, M., Fouser, L.A., 2006. Interleukin (IL)-22 and IL-17 are coexpressed by Th17 cells and cooperatively enhance expression of antimicrobial peptides. *The Journal of Experimental Medicine*, **203(10)**, 2271–2279.

Lighvani, A.A., Frucht, D.M., Jankovic, D., Yamane, H., Aliberti, J., Hissong, B.D., Nguyen, B.V., Gadina, M., Sher, A., Paul, W.E. and O'Shea, J.J., 2001. T-bet is rapidly induced by interferon-γ in lymphoid and myeloid cells. *Proceedings of the National Academy of Sciences*, ***98*(26)**, 15137-15142.

Lin, C.-C., Huoh, Y.-S., Schmitz, K.R., Jensen, L.E., Ferguson, K.M., 2008. Pellino Proteins Contain a Cryptic FHA Domain that Mediates Interaction with Phosphorylated IRAK1. *Structure*, **16**, 1806–1816.

Liu, J., Huang, X., Hao, S., Wang, Y., Liu, M., Xu, J., Zhang, X., Yu, T., Gan, S., Dai, D., Luo, X., Lu, Q., Mao, C., Zhang, Y., Shen, N., Li, B., Huang, M., Zhu, X., Jin, J., Cheng, X., Sun, S.-C., Xiao, Y., 2018. Peli1 negatively regulates noncanonical NF-κB signaling to restrain systemic lupus erythematosus. *Nature Communications*, **9(1136)**, 1–13.

Liu, Y. and Janeway Jr, C.A., 1992. Cells that present both specific ligand and costimulatory activity are the most efficient inducers of clonal expansion of normal CD4 T cells. *Proceedings of the National Academy of Sciences*, ***89*(9)**, 3845-3849.

Liu, Y., Dong, W., Chen, L., Xiang, R., Xiao, H., De, G., Wang, Z., Qi, Y., 2004. BCL10 Mediates Lipopolysaccharide/Toll-like Receptor-4 Signaling through Interaction with Pellino2. *J. Biol. Chem.*, **279**, 37436–37444.

Loder, F. Mutschler, B., Ray, R.J., Paige, C.J., Sideras, P., Torres, R., Lamers, M.C., Carsetti, R., 1999. B Cell Development in the Spleen Takes Place in Discrete Steps and Is Determined by the Quality of B Cell Receptor-derived Signals. *J. Exp. Med.*, **190(1)**, 75–89.

Lowes, M.A., Kikuchi, T., Fuentes-Duculan, J., Cardinale, I., Zaba, L.C., Haider, A.S., Bowman, E.P., Kruger, J.G., 2008. Psoriasis Vulgaris Lesions Contain Discrete Populations of Th1 and Th17 T Cells. *Journal of Investigative Dermatology*, **128**, 1207–1211.

Lu, Y.-J., Gross, J., Bogaert, D., Finn, A., Bagrade, L., Zhang, Q., Kolls, J.K., Srivastava, A., Lundgren, A., Forte, S., Thompson, C.M., Harney, K.F., Anderson, P.W., Lipsitch, M., Malley, R., 2008. Interleukin-17A Mediates Acquired Immunity to Pneumococcal Colonization. *PLoS Pathogens*, **4(9)**, 1–11.

Luckheeram, R.V., Zhou, R., Verma, A.D., Xia, B., 2012. $CD4^+$ T Cells: Differentiation and Functions. *Clinical and Developmental Immunology*, **2012(925135)**, 1–12.

Lugo-Villarino, G., Maldonado-Lopez, R., Possemato, R., Penaranda, C. and Glimcher, L.H., 2003. T-bet is required for optimal production of IFN-γ and antigen-specific T cell activation by dendritic cells. *Proceedings of the National Academy of Sciences*, ***100*(13)**, 7749-7754.

Luo, Q., Liu, Y., Shi, K., Shen, X., Yang, Y., Liang, X., Lu, L., Qiao, W., Chen, A., Hong, D. and Sun, Y., 2023. An autonomous activation of interleukin-17 receptor signaling sustains inflammation and promotes disease progression. *Immunity*, **56(9)**, 2006-2020.

Luzza, F., Parrello, T., Monteleone, G., Sebkova, L., Romano, M., Zarrilli, R., Imeneo, M., Pallone, F., 2000. Up-Regulation of IL-17 Is Associated with Bioactive IL-8 Expression in *Helicobacter pylori*-Infected Human Gastric Mucosa. *The Journal of Immunology*, **165**, 5332–5337.

Mackay, C.R., Marston, W.L., Dudler, L., 1990. NAÏVE AND MEMORY T CELLS SHOW DISTINCT PATHWAYS OF LYMPHOCYTES RECIRCULATION. *J. Exp. Med.*, **171**, 801–817.

MacLennan, I.C.M., Toellner, K.-M., Cunningham, A.F., Serre, K., Sze, D.M.-Y., Zúñiga, E., Cook, M.C., Vinuesa, C.G., 2003. Extrafollicular antibody responses. *Immunological Reviews*, **194**, 8–18.

Maclver, N.J., Michalek, R.D. and Rathmell, J.C., 2013. Metabolic regulation of T lymphocytes. *Annual review of immunology*, **31**, 259-283.

Majumder, S., McGeachy, M.J., 2021. IL-17 in the Pathogenesis of Disease: Good Intentions Gone Awry. *Annu. Rev. Immunol.*, **39**, 537–56.

Marcet, P., Santos, N. and Borlongan, C.V., 2017. When friend turns foe: central and peripheral neuroinflammation in central nervous system injury. *Neuroimmunology and neuroinflammation*, **4**, 82.

Marks, B.R., Nowyhed, H.N., Choi, J.-Y., Poholek, A.C., Odegard, J.M., Flavell, R.A., Craft, J., 2009. Thymic self-reactivity selects natural interleukin 17-producing T cells that can regulate peripheral inflammation. *Nature Immunology*, **10(10)**, 1125–1132.

Martin, M.D. and Badovinac, V.P., 2018. Defining memory CD8 T cell. *Frontiers in immunology*, **9(2692)**,1-10.

Martínez-Riaño, A., Delgado, P., Tercero, R., Barrero, S., Mendoza, P., Oeste, C.L., Abia, D., Rodríguez-Bovolenta, E., Turner, M., Alarcón, B, 2023. Recreation of an antigen-driven germinal center in vitro by providing B cells with phagocytic antigen. *Communications Biology*, **6(437)**, 1–18.

Martinez, G.J., Zhang, Z., Chung, Y., Reynolds, J.M., Lin, X., Jetten, A.M., Feng, X.H. and Dong, C., 2009. Smad3 differentially regulates the induction of regulatory and inflammatory T cell differentiation. *Journal of Biological Chemistry*, ***284*(51)**, 35283-35286.

Mason, K.D., Juneja, S.K. and Szer, J., 2006. The immunophenotype of acute myeloid leukemia: is there a relationship with prognosis?. *Blood reviews*, **20(2)**, 71-82.

Matusevicius, D., Kivisäkk, P., He, B., Kostulas, N., Özenci, V., Fredrikson, S., Link, H., 1999. Interleukin-17 mRNA expression in blood and CSF mononuclear cells is augmented in multiple sclerosis. *Multiple Sclerosis*, **5**, 101–104.

McGeachy, M.J., Cua, D.J., Gaffen, S.L., 2019. The IL-17 Family of Cytokines in Health and Disease. *Immunity*, **50**, 892–906.

Mebius, R.E., Kraal, G., 2005. STRUCTURE AND FUNCTION OF THE SPLEEN. *Nature Reviews Immunology*, **5**, 606–616.

Medzhitov, R. and Janeway Jr, C.A., 1997. Innate immunity: impact on the adaptive immune response. *Current opinion in immunology*, **9(1)**, 4-9.

Mills, K.H.G., 2023. IL-17 and IL-17-producing cells in protection versus pathology. *Nature Reviews Immunology*, **23**, 38–54.

Miquel, C.H., Faz-Lopez, B. and Guéry, J.C., 2023. Influence of X chromosome in sex-biased autoimmune diseases. *Journal of Autoimmunity*, **137**, 102992.

Miyake, K., Medina, K.L., Hayashi, S.-I., Ono, S., Hamaoka, T., Kingade, P.W., 1990. MONOCLONAL ANTIBODIES TO Pgp-1/CD44 BLOCK LYMPHO-HEMOPOIESIS IN LONG-TERM BONE MARROW CULTURES. *J. Exp. Med.*, **171**, 477–488.

Moisan, J., Grenningloh, R., Bettelli, E., Oukka, M., Ho, I-C., 2007. Ets-1 is a negative regulator of Th17 differentiation. *The Journal of Experimental Medicine*, **204(12)**, 2825–2835.

Monin, L., Gaffen, S., 2018. Interleukin 17 Family Cytokines: Signaling Mechanisms, Biological Activities, and Therapeutic Implications. *Cold Spring Harb. Perspect. Biol*., **10:a028522**, 1–20.

Moynagh, P.N., 2005. The NF-κB pathway. *Journal of cell science*, **118(20)**, 4589-4592.

Moynagh, P.N., 2014. The roles of Pellino E3 ubiquitin ligases in immunity. *Nature Reviews Immunology*, **14(2)**, 122-131.

Mudter, J., Yu, J., Zufferey, C., Brüstle, A., Wirtz, S., Weigmann, B., Hoffman, A., Schenk, M., Galle, P.R., Lehr, H.A. and Mueller, C., 2011. IRF4 regulates IL-17A promoter activity and controls RORγt-dependent Th17 colitis in vivo. *Inflammatory bowel diseases*, **17(6)**, 1343-1358.

Müller, U., Steinhoff, U., Reis, L.F., Hemmi, S., Pavlovic, J., Zinkernagel, R.M. and Aguet, M., 1994. Functional role of type I and type II interferons in antiviral defense. *Science*, **264(5167)**, 1918-1921.

Nakae, S., Nambu, A., Sudo, K., Iwakura, Y., 2003. Suppression of Immune Induction of Collagen-Induced Arthritis in IL-17-Deficient Mice. *The Journal of Immunology*, **171**, 6173–6177.

Nakajima, Y., Chamoto, K., Oura, T., Honjo, T., 2021. Critical role of the $CD44^{low}CD62L^{low}$ $CD8^{+}$ T cell subset in restoring antitumor immunity in aged mice. *PNAS*, **118(23)**, 1–10.

Naramura, M., Jang, I.K., Kole, H., Huang, F., Haines, D. and Gu, H., 2002. c-Cbl and Cbl-b regulate T cell responsiveness by promoting ligand-induced TCR down-modulation. *Nature immunology*, ***3*(12)**, pp.1192-1199.

Newton, H.S. and Dobrovolskaia, M.A., 2022. Immunophenotyping: Analytical approaches and role in preclinical development of nanomedicines. *Advanced drug delivery reviews*, **185**, 1-11.

Nishihara, M., Ogura, H., Ueda, N., Tsuruoka, M., Kitabayashi, C., Tsuji, F., Aono, H., Ishihara, K., Huseby, E., Betz, U.A. and Murakami, M., 2007. IL-6–

gp130–STAT3 in T cells directs the development of IL-17+ Th with a minimum effect on that of Treg in the steady state. *International immunology*, ***19*(6)**, 695-702.

Nishimoto, N., Kubagawa, H., Ohno, T., Gartland, G.L., Stankovic, A.K., Cooper, M.D., 1991. Normal pre-B cells express a receptor complex of μ heavy chains and surrogate light-chain proteins. *Proc. Natl. Acad. Sci. USA*, **88**, 6284–6288.

Novatchkova, M., Leibbrandt, A., Werzowa, J., Neubüser, A., Eisenhaber, F., 2003. The STIR-domain superfamily in signal transduction, development and immunity. *TRENDS in Biochemical Sciences*, **28(5)**, 226–229.

Nurieva, R., Yang, X.O., Martinez, G., Zhang, Y., Panopoulos, A.D., Ma, L., Schluns, K., Tian, Q., Watowich, S.S., Jetten, A.M. and Dong, C., 2007. Essential autocrine regulation by IL-21 in the generation of inflammatory T cells. *Nature*, **448(7152)**, 480-483.

Nurieva, R.I., Chung, Y., Hwang, D., Yang, X.O., Kang, H.S., Ma, L., Wang, Y.H., Watowich, S.S., Jetten, A.M., Tian, Q. and Dong, C., 2008. Generation of T follicular helper cells is mediated by interleukin-21 but independent of T helper 1, 2, or 17 cell lineages. *Immunity*, ***29*(1)**, 138-149.

Nurieva, R.I., Chung, Y., Martinez, G.J., Yang, X.O., Tanaka, S., Matskevitch, T.D., Wang, Y.H. and Dong, C., 2009. Bcl6 mediates the development of T follicular helper cells. *Science*, **325(5943)**, 1001-1005.

Ogura, H., Marukami, M., Okuyama, Y., Tsuruoka, M., Kitabayashi, C., Kanamoto, M., Nishihara, M., Iwakura, Y., Hirano, T., 2008. Interleukin-17 Promotes Autoimmunity by Triggering a Positive-Feedback Loop via Interleukin-6 Induction. *Immunity*., **29**, 628–636.

Ohtake, F., Saeki, Y., Sakamoto, K., Ohtake, K., Nishikawa, H., Tsuchiya, H., Ohta, T., Tanaka, K. and Kanno, J., 2015. Ubiquitin acetylation inhibits polyubiquitin chain elongation. *EMBO reports*, ***16*(2)**, 192-201.

Oleszycka, E., Rodgers, A.M., Xu, L. and Moynagh, P.N., 2021. Dendritic Cell–Specific Role for Pellino2 as a Mediator of TLR9 Signaling Pathway. *The Journal of Immunology*, **207(9)**, 2325-2336.

O'Neill LA, Golenbock D, Bowie AG, 2013. The history of Toll-like receptors – redefining innate immunity. *Nat Rev Immunol*, **13**, 453–460.

Onishi, R.M., Gaffen, S.L., 2010. Interleukin-17 and its target genes: mechanisms of interleukin-17 function in disease. *Immunol*ogy, **129**, 311–321.

Oppmann, B. Lesley, R., Blom, B., Timans, J.C., Xu, Y., Hunte, B., Vega, F., Yu, N., Wang, J., Singh, K., Zonin, F., Vaisberg, E., Churakova, T., Liu, M.-r., Gorman, D., Wagner, J., Zurawski, S., Liu, Y.-J., Abrams, J.S., Moore, K.W., Rennick, D., de Waal-Malefyt, R., Hannum, C., Bazan, J.F., Kastelein, R.A., 2000. Novel p19 Protein Engages IL-12p40 to Form a Cytokine, IL-23, with

Biological Activites Similar as Well as Distinct from IL-12. *Immunity*, **13**, 715–725.

Ouyang, X., Zhang, R., Yang, J., Li, Q., Qin, L., Zhu, C., Liu, J., Ning, H., Shin, M.S., Gupta, M., Qi, C.-F., He, J.C., Lira, S.A., Morse III, H.C., Ozato, K., Mayer, L., Xiong, H., 2011. Transcription factor IRF8 directs a silencing programme for Th17 cell differentiation. *Nature Communications*, **2(314)**, 1–12.

Overman, M.J., Pozadzides, J., Kopetz, S., Wen, S., Abbruzzese, J.L., Wolff, R.A. and Wang, H., 2010. Immunophenotype and molecular characterisation of adenocarcinoma of the small intestine. *British journal of cancer*, **102(1)**, 144-150.

Palmer, E.M., Holbrook, B.C., Arimilli, S., Parks, G.D., Alexander-Miller, M.A., 2010. IFN-γ-producing, virus-specific $CD8^+$ effector cells acquire the ability to produce IL-10 as a result of entry into the infected lung environment. *Virology*, **404**, 225–230.

Park, J.-S., Lee, J., Lim, M.-A., Kim, E.-K., Kim, S.-M., Ryu, J.-G., Lee, J.H., Kwok, S.-K., Park, K.-S., Kim, H.-Y., Park, S.-H., Cho, M.-L., 2014. JAK2-STAT3 Blockade by AG490 Suppresses Autoimmune Arthritis in Mice via Reciprocal Regulation of Regulatory T Cells and Th17 Cells. *The Journal of mmunology*, **192**, 4417–4424.

Parker, M.J., Licence, S., Erlandsson, L., Galler, G.R., Chakalova, L., Osborne, C.S., Morgan, G., Fraser, P., Jumaa, H., Winkler, T.H., Skok, J., Mårtensson, I-L., 2005. The pre-B-cell receptor induces silencing of VpreB and λ5 transcription. *The EMBO Journal*, **24**, 3895–3905.

Parsonage, G., Filer, A., Bik, M., Hardie, D., Lax, S., Howlett, K., Church, L.D., Raza, K., Wong, S.-H., Trebilcock, E., Scheel-Toellner, D., Salmon, M., Lord, J.M., Buckley, C.D., 2008. Prolonged, granulocyte-macrophage colony-stimulating factor-dependent, neutrophil survival following rheumatoid synovial fibroblast activation by IL-17 and TNFalpha. *Arthritis Research & Therapy*, **10**, 1–12.

Patel, D.D., Kuchroo, V.K., 2015. Th17 Cell Pathway in Human Immunity: Lessons from Genetics and Therapeutics Interventions. *Immunity*, **43**, 1040–1051.

Peng, J., Schwartz, D., Elias, J.E., Thoreen, C.C., Cheng, D., Marsischky, G., Roelofs, J., Finley, D. and Gygi, S.P., 2003. A proteomics approach to understanding protein ubiquitination. *Nature biotechnology*, **21(8)**, 921-926.

Picker, L.J., Treer, J.R., Ferguson-Darnell, B., Collins, P.A., Buck, D., Terstappen, L.W.M.M., 1993. Control of Lymphocyte Recirculation in Man. *The Journal of Immunology*, **150(3)**, 1105–1121.

Pockley, A.G., Foulds, G.A., Oughton, J.A., Kerkvliet, N.I. and Multhoff, G., 2015. Immune cell phenotyping using flow cytometry. *Current protocols in toxicology*, **66(1)**, 1-34.

Prieto, J.M.B., Felippe, M.J.B., 2017. Development, phenotype, and function of non-conventional B cells. *Comparative Immunology, Microbiology and Infectious Diseases*, **54**, 38–44.

Puel, A., Cypowyj, S., Bustamante, J., Wright, J.F., Liu, L., Lim, H.K., Migaud, M., Israel, L., Chrabieh, M., Audry M., Gumbleton, M., Toulon, A., Bodemer, C., El-Baghdadi, J., Whitters, M., Paradis, T., Brooks, J., Collins, M., Wolfman, N.M., Al-Muhsen, S., Galicchio, M., Abel, L., Picard, C., Casanova, J.-M., 2011. Chronic Mucocutaneous Candidiasis in Humans with Inborn Errors of Interleukin-17 Immunity. *Science*, **332(6025)**, 65–68.

Pușcaș, A.D., Cătană, A., Pușcaș, C., Roman, I.I., Vornicescu, C., Șomlea, M. and Orăsan, R.I., 2019. Psoriasis: Association of interleukin-17 gene polymorphisms with severity and response to treatment. *Experimental and Therapeutic Medicine*, ***18*(2)**, 875-880.

Rahighi, S., Ikeda, F., Kawasaki, M., Akutsu, M., Suzuki, N., Kato, R., Kensche, T., Uejima, T., Bloor, S., Komander, D. and Randow, F., 2009. Specific recognition of linear ubiquitin chains by NEMO is important for NF-κB activation. *Cell*, **136(6)**, 1098-1109.

Raskov, H., Orhan, A., Christensen, J.P. and Gögenur, I., 2021. Cytotoxic CD8+ T cells in cancer and cancer immunotherapy. *British journal of cancer*, ***124*(2)**, 359-367.

Reinhardt, R.L., Liang, H.-E., Locksley, R.M., 2009. Cytokine-secreting follicular T cells shape the antibody repertoire. *Nature Immunology*, **10(4)**, 385–393.

Resch, K., Jockusch, H., Schmitt-John, T., 2001. Assignment of homologous genes, Peli1/PELI1 and Peli2/PELI2, for the Pelle adaptor protein Pellino to mouse chromosomes 11 and 14 and human chromosomes 2p13.3 and 14q21, respectively, by physical and radiation hybrid mapping. *Cytogenet. Cell Genet.*, **92**, 172–174.

Reth, M., Petrac, E., Wiese, P., Lobel, L., Alt, F.W., 1987. Activation of Vκ gene arrangement in pre-B cells follows the expression of membrane-bound immunoglobulin heavy chains. *The EMBO Journal*, **6(11)**, 3299–3305.

Ribot, J.C., Lopes, N. and Silva-Santos, B., 2021. γδ T cells in tissue physiology and surveillance. *Nature Reviews Immunology*, ***21*(4)**, 221-232.

Rich, T., Allen, R.L., Lucas, A.-M., Stewart, A., Trowsdale, J., 2000. Pellino-related sequences from Caenorhabditis elegans and Homo sapiens. *Immunogenetics*, **52**, 145–149.

Rickert, R.C., 2013. New insights into pre-BCR and BCR signalling with relevance to B cell malignancies. *Nature Reviews Immunology*, **13(8)**, 578-591.

Roulland, S., Suarez, F., Hermine, O., Nadel, B., 2007. Pathophysiological aspects of memory B-cell development. *TRENDS in Immunology*, **29(1)**, 25–33.

Rouvier, E., Luciani, M.-F., Mattéi, M.-G., Denizot, F., Golstein, P., 1993. CTLA-8, Cloned from an Activated T Cell, Bearing AU-Rich Messenger RNA Instability Sequences, and Homologous to a Herpesvirus Saimiri Gene. *The Journal of Immunology*, **150**, 5445–5456.

Rowe, D.C., McGettrick, A.F., Latz, E., Monks, B.G., Gay, N.J., Yamamoto, M., Akira, S., O'Neill, L.A., Fitzgerald, K.A. and Golenbock, D.T., 2006. The myristoylation of TRIF-related adaptor molecule is essential for Toll-like receptor 4 signal transduction. *Proceedings of the National Academy of Sciences*, **103(16)**, 6299-6304.

Ruan, Q., Kameswaran, V., Zhang, Y., Zheng, S., Sun, J., Wang, J., DeVirgiliis, J., Liou, H.-C., Beg, A.A., Chen, Y.H., 2011. The Th17 immune response is controlled by the Rel-RORγ-RORγT transcriptional axis. *J. Exp. Med.*, **208(11)**, 2321–2333.

Rubino, S.J., Selvanantham, T., Giradin, S.E., Philpott, D.J., 2012. Nod-like receptors in the control of intestinal inflammation. *Current Opinion in Immunology*, **24**, 1–7.

Sallusto, F., Geginat, J., Lanzavecchia, A., 2004. CENTRAL MEMORY AND EFFECTOR MEMORY T CELL SUBSETS: Function, Generation, and Maintenance. *Annu. Rev. Immunol.*, **22**, 745–763.

Saravia, J., Chapman, N.M., Chi, H., 2019. Helper T cell differentiation. *Cellular & Molecular Immunology*, **16**, 634–643.

Sato, K., Suematsu, A., Okamoto, K., Yamaguchi, A., Morishita, Y., Kadono, Y., Tanaka, S., Kodama, T., Akira, S., Iwakura, Y., Cua, D.J., Takayanagi, H., 2006. Th17 functions as an osteoclastogenic helper T cell subset that links T cell activation and bone destruction. *The Journal of Experimental Medicine*, **203(12)**, 2673–2682.

Saunte, D.M., Mrowietz, U., Puig, L. and Zachariae, C., 2017. Candida infections in patients with psoriasis and psoriatic arthritis treated with interleukin-17 inhibitors and their practical management. *British Journal of Dermatology*, **177(1)**, 47-62.

Saurin, A.J., Borden, K.L., Boddy, M.N. and Freemont, P.S., 1996. Does this have a familiar RING?. *Trends in biochemical sciences*, **21(6)**, 208-214.

Schauvliege, R., Janssens, S., Beyaert, R., 2006. Pellino proteins are more than scaffold proteins in TLR/IL-1R signalling: A role as novel RING E3–ubiquitin-ligases. *FEBS Lett.*, **580**, 4697–4702.

Schmidt, C., 2015. Suicidal thoughts end Amgen's blockbuster aspirations for psoriasis drug. *Nature biotechnology*, **33(9)**, 894-895.

Schroder, K., Zhou, R. & Tschopp, J., 2010. The NLRP3 inflammasome: a sensor for metabolic danger? *Science*, **327**, 296–300.

Shah, K., Al-Haidari, A., Sun, J., Kazi, J.U., 2021. T cell receptor (TCR) signaling in health and disease. *Signal Transduction and Targeted Therapy*, **6(412)**, 1–26.

Shainheit, M.G., Lasocki, K.W., Finger, E., Larkin, B.M., Smith, P.M., Sharpe, A.H., Dinarello, C.A., Rutitzky, L.I. and Stadecker, M.J., 2011. The pathogenic Th17 cell response to major schistosome egg antigen is sequentially dependent on IL-23 and IL-1β. *The Journal of Immunology*, ***187*(10)**, 5328-5335.

Shao, M., Xu, S., Yang, H., Xu, W., Deng, J., Chen, Y., Gao, X., Guan, S., Xu, S., Shuai, Z. and Pan, F., 2020. Association between IL-17A and IL-17F gene polymorphism and susceptibility in inflammatory arthritis: A meta-analysis. *Clinical Immunology*, ***213***, 108374.

Sharma, S., TenOever, B.R., Grandvaux, N., Zhou, G.P., Lin, R. and Hiscott, J., 2003. Triggering the interferon antiviral response through an IKK-related pathway. *Science*, **300(5622)**, 1148-1151.

Shi, L.Z., Wang, R., Huang, G., Vogel, P., Neale, G., Green, D.R. and Chi, H., 2011. HIF1α–dependent glycolytic pathway orchestrates a metabolic checkpoint for the differentiation of TH17 and Treg cells. *Journal of experimental medicine*, ***208*(7)**, 1367-1376.

Shirota, H., Gursel, M. and Klinman, D.M., 2004. Suppressive oligodeoxynucleotides inhibit Th1 differentiation by blocking IFN-γ-and IL-12-mediated signaling. *The Journal of Immunology*, **173(8)**, 5002-5007.

Siednienko, J., Jackson, R., Mellett, M., Delagic, N., Yang, S., Wang, B., Tang, L.S., Callanan, J.J., Mahon, B.P., Moynagh, P.N., 2012. Pellino3 targets the IRF7 pathway and facilitates autoregulation of TLR3- and viral-induced expression of type I interferons. *Nature Immunology*, **13(11)**, 1055–1062.

Silva-Santos, B., Serre, K. and Norell, H., 2015. γδ T cells in cancer. *Nature reviews immunology*, ***15*(11)**, 683-691.

Sims, G.P., Ettinger, R., Shirota, Y., Yarboro, C.H., Illei, G.G. and Lipsky, P.E., 2005. Identification and characterization of circulating human transitional B cells. *Blood*, **105(11)**, 4390-4398.

Skepner, J., Ramesh, R., Trocha, M., Schmidt, D., Baloglu, E., Lobera, M., Carlson, T., Hill, J., Orband-Miller, L.A., Barnes, A., Boudjelal, M., Sundrud, M., Ghosh, S., Yang, J., 2014. Pharmacologic Inhibition of RORγt Regulates Th17 Signature Gene Expression and Supresses Cutaneous Inflammation In Vivo. *The Journal of Immunology*, **192**, 2564–2575.

Starnes, T., Broxmeyer, H.E., Robertson, M.J., Hromas, R., 2002. Cutting Edge: IL-17D, a Novel Member of the IL-17 Family, Stimulates Cytokine Production and Inhibits Hemopoiesis. *J. Immunol*., **169(2)**, 642–646.

Starnes, T., Robertson, M.J., Sledge, G., Kelich, S., Nakshatri, H., Broxmeyer, H.E., Hromas, R., 2001. Cutting Edge: IL-17F, a Novel Cytokine Selectively

Expressed in Activated T Cells and Monocytes, Regulates Angiogenesis and Endothelial Cell Cytokine Production. *J. Immunol*., **167(8)**, 4137–4140.

Strelow, A., Kollewe, C., Wesche, H., 2003. Characterization of Pellino 2, a substrate of IRAK1 and IRAK3. *FEBS Letters*, **547**, 157–161.

Strickson, S., Emmerich, C.H., Goh, E.T., Zhang, J., Kelsall, I.R., Macartney, T., Hastie, C.J., Knebel, A., Peggie, M., Marchesi, F. and Arthur, J.S.C., 2017. Roles of the TRAF6 and Pellino E3 ligases in MyD88 and RANKL signaling. *Proceedings of the National Academy of Sciences*, ***114*(17)**, E3481-E3489.

Stritesky, G.L., Muthukrishnan, R., Sehra, S., Goswami, R., Pham, D., Travers, J., Nguyen, E.T., Levy, D.E. and Kaplan, M.H., 2011. The transcription factor STAT3 is required for T helper 2 cell development. *Immunity*, ***34*(1)**, 39-49.

Sun, H., Wu, Y., Zhang, Y. and Ni, B., 2021. IL-10-Producing ILCs: Molecular mechanisms and disease relevance. *Frontiers in Immunology*, **12**, p.650200.

Sun, L., Deng, L., Ea, C.K., Xia, Z.P. and Chen, Z.J., 2004. The TRAF6 ubiquitin ligase and TAK1 kinase mediate IKK activation by BCL10 and MALT1 in T lymphocytes. *Molecular cell*, ***14*(3)**, 289-301.

Suzuki, H., Punt, J.A., Granger, L.G., Singer, A., 1995. Asymmetric Signaling Requirements for Thymocyte Commitment to the $CD4^+$ versus $CD8^+$ T Cell Lineages: A New Perspective on Thymic Commitment and Selection. *Immunity*, **2**, 413–425.

Suzuki, N., Suzuki, S., Duncan, G.S., Millar, D.G., Wada, T., Mirtsos, C., Takada, H., Wakeham, A., Itie, A., Li, S. and Penninger, J.M., 2002. Severe impairment of interleukin-1 and Toll-like receptor signalling in mice lacking IRAK-4. *Nature*, **416(6882)**, 750-754.

Swain, S.L., McKinstry, K.K., Strutt, T.M., 2012. Expanding roles for $CD4^+$ T cells in immunity to viruses. *Nature Reviews Immunology*, **12**, 136–148.

Takimoto, T., Wakabayashi, Y., Sekiya, T., Inoue, N., Morita, R., Ichiyama, K., Takahashi, R., Asakawa, M., Muto, G., Mori, T. and Hasegawa, E., 2010. Smad2 and Smad3 are redundantly essential for the TGF-β–mediated regulation of regulatory T plasticity and Th1 development. *The Journal of immunology*, ***185*(2)**, 842-855.

Tikhonova, A.N., Van Laethem, F., Hanada, K., Lu, J., Pobezinsky, L.A., Hong, C.m Guinter, T.I., Jeurling, S.K., Bernhardt, G., Park, J.-H., Yang, J.C., Sun, P.D., Singer, A., 2012. αβ T Cell Receptors that Do Not Undergo Major Histocompatibility Complex-Specific Thymic Selection Possess Antibody-like Recognition Specificities. *Immunity*, **36**, 79–91.

Tzieply, N., Kuhn, A.-M., Morbitzer, D., Namgaladze, D., Heeg, A., Schaefer, L., von Knethen, A., Jensen, L.E., Brüne, B., 2012. OxLDL inhibits LPS-induced IFNβ expression by Pellino3- and IRAK1/4-dependent modification of TANK. *Cellular Signalling*, **24**, 1141–1149.

Usui, T., Nishikomori, R., Kitani, A. and Strober, W., 2003. GATA-3 suppresses Th1 development by downregulation of Stat4 and not through effects on IL-12Rβ2 chain or T-bet. *Immunity*, ***18*****(3)**, 415-428.

Van der Fits, L., Mourits, S., Voerman, J.S.A., Kant, M., Boon, L., Laman, J.D., Cornelissen, F., Mus, A.-M., Florencia, E., Prens, E.P., Lubberts, E., 2009. Imiquimod-Induced Psoriasis-Like Skin Inflammation in Mice Is Mediated via the IL-23/IL-17 Axis. *The Journal of Immunology*, **182**, 5836–5845.

Vantourout, P. and Hayday, A., 2013. Six-of-the-best: unique contributions of γδ T cells to immunology. *Nature Reviews Immunology*, ***13*****(2)**, 88-100.

Verma, N.D., Hall, B.M., Plain, K.M., Robinson, C.M., Boyd, R., Tran, G.T., Wang, C., Bishop, G.A. and Hodgkinson, S.J., 2014. Interleukin-12 (IL-12p70) promotes induction of highly potent Th1-like CD4+ CD25+ T regulatory cells that inhibit allograft rejection in unmodified recipients. *Frontiers in immunology*, ***5***, 190.

Viallard, J.F., Parrens, M., Blanco, P., Moreau, J.F., Oksenhendler, E. and Fieschi, C., 2024. Influence of Splenomegaly and Splenectomy on the Immune Cell Profile of Patients with Common Variable Immunodeficiency Disease. *Journal of Clinical Immunology*, ***44*****(2)**, 46.

Villalpando-Vargas, F.V., Rivera-Valdés, J.J., Alvarado-Navarro, A., Huerta-Olvera, S.G., Macías-Barragán, J., Martínez-López, E. and Graciano-Machuca, O., 2021. Association between IL-17A, IL-17F and IL-17RA gene polymorphisms and susceptibility to psoriasis and psoriatic arthritis: a meta-analysis. *Inflammation Research*, ***70***, 1201-1210.

Villanova, F., Flutter, B., Tosi, I., Grys, K., Sreeneebus, H., Perera, G.K., Chapman, A., Smith, C.H., Meglio, P.D., Nestle, F.O., 2014. Characterization of Innate Lymphoid Cells in Human Skin and Blood Demonstrates Increase of NKp44+ ILC3 in Psoriasis. *Journal of Investigative Dermatology*, **134**, 984–991.

Vivarelli, M.S., McDonald, D., Miller, M., Cusson, N., Kelliher, M., Geha, R.S., 2004. RIP links TLR4 to Akt and is essential for cell survival in response to LPS stimulation. *J. Exp. Med.* **200**, 399–404.

Vivier, E., Raulet, D.H., Moretta, A., Caligiuri, M.A., Zitvogel, L., Lanier, L.L., Yokoyama, W.M., Ugolini, S., 2011. Innate or Adaptive Immunity? The Example of Natural Killer Cells. *SCIENCE*, **331**, 44–49.

Waldschmidt, T.J., Conrad, D.H., Lynch, R.G., 1988. THE EXPRESSION OF B CELL SURFACE RECEPTORS I. The ontogeny and Distribution of the Murine B Cell IgE Fc Receptor. *The Journal of Immunology*, **140(7)**, 2148–2154.

Wang, C., Deng, L., Hong, M., Akkaraju, G.R., Inoue, J.I. and Chen, Z.J., 2001. TAK1 is a ubiquitin-dependent kinase of MKK and IKK. *Nature*, **412(6844)**, 346-351.

Wang, H.Y., Altman, Y., Fang, D., Elly, C., Dai, Y., Shao, Y. and Liu, Y.C., 2001. Cbl promotes ubiquitination of the T cell receptor ζ through an adaptor function of Zap-70. *Journal of Biological Chemistry*, ***276*****(28)**, pp.26004-26011.

Wang, K., Wei, G., Liu, D., 2012. CD19: a biomarker for B cell development, lymphoma diagnosis and therapy. *Experimental Hematology & Oncology*, **1(36)**, 1–7.

Weller, S., Braun, M.C., Tan, B.K., Rosenwald, A., Cordier, C., Conley, M.E., Plebani, A., Kumararatne, D.S., Bonnet, D., Tournilhac, O., Tchernia, G., Steiniger, B., Staudt, L.M., Casanova, J.-L., Reynaud, C.-A., Weill, J.-C., 2004. Human blood IgM "memory" B cells are circulating splenic marginal zone B cells harboring a prediversified immunoglobulin repertoire. *Blood*, **104(12)**, 3647–3654.

Wherry, E.J., Teichgräber, V., Becker, T.C., Masopust, D., Kaech, S.M., Antia, R., Von Andrian, U.H. and Ahmed, R., 2003. Lineage relationship and protective immunity of memory CD8 T cell subsets. *Nature immunology*, ***4*****(3)**, 225-234.

Whibley, N., Tritto, E., Traggiai, E., Kolbinger, F., Moulin, P., Brees, D., Coleman, B.M., Mamo, A.J., Garg, A.V., Jaycox, J.R., Siebenlist, U., Kammüller, M., Gaffen, S.L., 2016. Antibody blockade of IL-17 family cytokines in immunity to acute murine oral mucosal candidiasis. *Journal of Leukocyte Biology*, **99**, 1–12.

Woś, I. and Tabarkiewicz, J., 2021. Effect of interleukin-6,-17,-21,-22, and-23 and STAT3 on signal transduction pathways and their inhibition in autoimmune arthritis. *Immunologic Research*, **69(1)**, 26-42.

Xia, F., Qian, C.-R., Xun, Z., Hamon, Y., Sartre, A.-M., Formisano, A., Mailfert, S., Phelipot M.-C., Billaudeau, C., Jaeger, S., Nunès, J.A., Guo, X.-J., He, H.-T., 2018. TCR and CD28 Concomitant Stimulation Elicits a Distinctive Calcium Response in Naive T Cells. *Frontiers in Immunology*, **9(2864)**, 1–12.

Xiao, H., Qian, W., Staschke, K., Qian, Y., Cui, G., Deng, L, Ehsani, M., Wang, X., Qian, Y.-W., Chen, Z.J., Gilmour, R., Jiang, Z., Li, X., 2008. Pellino 3b Negatively Regulates Interleukin-1-induced TAK1-dependent NKκB Activation. *The Journal of Biological Chemistry*, **283(21)**, 14654–14664.

Xiao, Y., Jin, J., Chang, M., Chang, J.-H., Hu, H., Zhou, X., Brittain, G.C., Stansberg, C., Torkildsen, Ø., Wang, X., Brink, R., Cheng, X., Sun, S.-C., 2013. Peli1 promotes microglia-mediated CNS inflammation by regulating Traf3 degradation. *Nat. Med.*, **19**, 595–602.

Xing, E., Billi, A.C. and Gudjonsson, J.E., 2022. Sex bias and autoimmune diseases. *Journal of Investigative Dermatology*, **142(3)**, 857-866.

Yamamoto, M., Sato, S., Hemmi, H., Uematsu, S., Hoshino, K., Kaisho, T., Takeuchi, O., Takeda, K. and Akira, S., 2003. TRAM is specifically involved

in the Toll-like receptor 4 mediated MyD88-independent signaling pathway. *Nature Immunology*. **4(11)**, 1144-1150.

Yang, S., Wang, B., Humphries, F., Hogan, A.E., O'Shea, D., Moynagh, P.N., 2014. The E3 Uniquitin Ligase Pellino3 Protects against Obesity-Induced Inflammation and Insulin Resistance. *Immunity*, **41**, 973–987.

Yang, S., Wang, B., Humphries, F., Jackson, R., Healy, M.E., Bergin, R., Aviello, G., Hall, B., McNamara, D., Darby, T., Quinlan, A., Shanahan, F., Melgar, S., Fallon, P.G., Moynagh, P.N., 2013a. Pellino3 ubiquitinates RIP2 and mediates Nod2-induced signaling and protective effects in colitis. *Nature Immunology*, **14(9)**, 927–936.

Yang, S., Wang, B., Tang, L.S., Siednienko, J., Callanan, J.J., Moynagh, P.N., 2013b. Pellino3 targets RIP1 and regulates the pro-apoptotic effects of TNF-α. *Nature Communications*, **4(2583)**, 1–19.

Yang, S., Wang, J., Brand, D.D. and Zheng, S.G., 2018. Role of TNF–TNF receptor 2 signal in regulatory T cells and its therapeutic implications. *Frontiers in immunology*, ***9***, 784.

Yang, X.O., Panopoulos, A.D., Nurieva, R., Chang, S.H., Wang, D., Watowich, S.S. and Dong, C., 2007. STAT3 regulates cytokine-mediated generation of inflammatory helper T cells. *Journal of Biological Chemistry*, ***282*(13)**, 9358-9363.

Yang, Y., Wang, H., Kouadir, M., Song, H. and Shi, F., 2019. Recent advances in the mechanisms of NLRP3 inflammasome activation and its inhibitors. *Cell death & disease*, **10(128)**, 1-11.

Yao, Z., Fanslow, W.C., Seldin, M.F., Rousseau, A.-M., Painter, S.L., Comeau, M.R., Cohen, J.I., M., Spriggs, 1995a. Herpesvirus Saimiri Encodes a New Cytokine, IL-17, Which Binds to a Novel Cytokine Receptor. *Immunology*, **3**, 811–821.

Yao, Z., Painter, S.L., Fanslow, W.C., Ulrich, D., Macduff, B.M., Spriggs, M.K., Armitage, R. J., 1995b. Human IL-17: A Novel Cytokine Derived from T Cells. *The American Association of Immunologists*, **155**, 5483–5486.

Ye, P., Rodriguez, F.H., Kanaly, S., Stocking, K.L., Schurr, J., Schwarzenberger, P., Oliver, P., Huang, W., Zhang, P., Zhang, J., Shellito, J.E., Bagby, G.J., Nelson, S., Charrier, K., Peschon, J.J., Kolls, J.K., 2001. Requirement of Interleukin 17 Receptor Signaling for Lung CXC Chemokine and Granulocyte Colony-stimulating Factor Expression, Neutrophil Recruitment, and Host Defense. *J. Exp. Med.*, **194(4)**, 519–527.

Yen, D., Cheung, J., Scheerens, H., Poulet, F., McClanahan, T., Mckenzie, B., Kleinschek, M.A., Owyang, A., Mattson, J., Blumenschein W., Murphy, E., Sathe, M., Cua, D.J., Kastelein, R.A., Rennick, D., 2006. IL-23 is essential for T cell-mediated colitis and promotes inflammation via IL-17 and IL-6. *The Journal of Clinical Investigation*, **116(5)**, 1310–1316.

Yu, K.-Y., Kwon, H.-J., Norman, D.A.M., Vig, E., Goebl, M.G., Harrington, M.A., 2002. Cutting Edge: Mouse Pellino-2 Modulates IL-1 and Lipopolysaccharide Signaling. *J. Immunol.*, **169**, 4075–4078.

Zhang, F., Meng, G., Strober, W., 2008. Interactions among the transcription factors Runx1, RORγt and Foxp3 regulate the differentiation of interleukin 17-producing T cells. *Nature Immunology*, **9(11)**, 1297–1306.

Zhang, N., Bevan, M.J., 2011. $CD8^+$ T Cells: Foot Soldiers of the Immune System. *Immunity*, **35**, 161–168.

Zhang, S., 2018. The role of transforming growth factor β in T helper 17 differentiation. *Immunology*, ***155*(1)**, 24-35.

Zhang, S., Takaku, M., Zou, L., Gu, A.D., Chou, W.C., Zhang, G., Wu, B., Kong, Q., Thomas, S.Y., Serody, J.S. and Chen, X., 2017. Reversing SKI–SMAD4-mediated suppression is essential for TH17 cell differentiation. *Nature*, ***551*(7678)**, 105-109.

Zhang, S., Zhang, G. and Wan, Y.Y., 2019. SKI and SMAD4 are essential for IL-21-induced Th17 differentiation. *Molecular immunology*, ***114***, 260-268.

Zhang, W., Liu, X., Zhu, Y., Liu, X., Gu, Y., Dai, X. and Li, B., 2021. Transcriptional and posttranslational regulation of Th17/Treg balance in health and disease. *European Journal of Immunology*, ***51*(9)**, 2137-2150.

Zhao, Y., Niu, C., Cui, J., 2018. Gamma-delta (γδ) T cells: friend or foe in cancer development? *J. Transl. Med.*, **16(3)**, 1–13.

Zheng, B., Yang, Y., Chen, L., Wu, M. and Zhou, S., 2022. B-cell receptor repertoire sequencing: Deeper digging into the mechanisms and clinical aspects of immune-mediated diseases. *Iscience*, **25(10)**, 1-13.

Zhou, L., Ivanov, I.I., Spolski, R., Min, R., Shenderov, K., Egawa, T., Levy, D.E., Leonard, W.J., Littman, D.R., 2007. IL-6 programs Th-17 cell differentiation by promoting sequential engagement of the IL-21 and IL-23 pathways. *Nature Immunol*ogy, **8(9)**, 967–974.

Zhu, J., Cote-Sierra, J., Guo, L. and Paul, W.E., 2003. Stat5 activation plays a critical role in Th2 differentiation. *Immunity*, ***19*(5)**, 739-748.

Zhu, J., Guo, L., Watson, C.J., Hu-Li, J. and Paul, W.E., 2001. Stat6 is necessary and sufficient for IL-4's role in Th2 differentiation and cell expansion. *The Journal of Immunology*, ***166*(12)**, 7276-7281.

Zhu, J., Min, B., Hu-Li, J., Watson, C.J., Grinberg, A., Wang, Q., Killeen, N., Urban, J.F., Guo, L. and Paul, W.E., 2004. Conditional deletion of Gata3 shows its essential function in TH1-TH2 responses. *Nature immunology*, ***5*(11)**, 1157-1165.

Zhu, J., Yamane, H. and Paul, W.E., 2009. Differentiation of effector CD4 T cell populations. *Annual review of immunology*, ***28***, 445-489.

Zhu, J., Yamane, H., Cote-Sierra, J., Guo, L. and Paul, W.E., 2006. GATA-3 promotes Th2 responses through three different mechanisms: induction of Th2 cytokine production, selective growth of Th2 cells and inhibition of Th1 cell-specific factors. *Cell research*, ***16*****(1)**, 3-10.